Studies on 3-substituted isoquinolin-1(2H)-ones designed as inhibitors of poly(ADP-ribose) polymerase

Woon, Esther Chue Yen

Award date:
2004

Awarding institution:
University of Bath

Studies on 3-Substituted Isoquinolin-1(2*H*)-ones Designed as Inhibitors of Poly(ADP-ribose) Polymerase

submitted by

Esther Chue Yen Woon

for the degree of PhD

of the University of Bath

2004

The research work in this thesis has been carried out in the Department of Pharmacy and Pharmacology, under the supervision of Dr Michael D. Threadgill.

Esther CYWoon

19th May '2004

19th May '2004

ProQuest LLC
789 East Eisenhower Parkway
P.O. Box 1346
Ann Arbor, MI 48106-1346

Abstract

Poly(ADP-ribose) polymerase-1 (PARP-1) is a nuclear enzyme that catalyses the synthesis of ADP-ribose polymers from NAD^+ in response to DNA strand breaks. It plays a major role in controlling the repair of damaged DNA and has been implicated in the pathogenesis of a great variety of human diseases, such as cancer, ischaemia-reperfusion injury and inflammatory disorders where massive, oxidative stress-induced damage to DNA resulted in PARP-1 overactivation, leading to cellular NAD^+ depletion and cell death. However, this series of events may be prevented through pharmacological inhibition of NAD^+ cleavage by PARP-1. Accordingly, PARP-1 inhibitor provides an exciting, novel therapeutic approach to a wide range of diseases. We have recently identified 5-aminoisoquinolin-1(2*H*)-one hydrochloride (5AIQ.HCl) as a potent, water-soluble PARP-1 inhibitor that exhibited outstanding therapeutic benefits in a wide range of diseases *in vivo*. It appeared that 5AIQ.HCl gained much of its advantage through its excellent biopharmaceutical properties, such as water-solubility and biodistribution, which were severely lacking in most currently known PARP-1 inhibitors. Thus, we decided to exploit this discovery by designing and synthesising a series of related compounds which bear substituents at the 3- and 4-position of 5AIQ, with major emphasis on the former.

In this thesis, various chemical approaches to these targets have been investigated and a reliable, efficient and versatile synthetic route for the synthesis of the 3-substituted targets has been developed, based on the Hurtley reaction. Attempts to effect synthesis *via* organometallic approaches, such as Sonogashira coupling, Castro-Stephens coupling, Negishi coupling and Heck coupling, revealed some of the limitations associated with the use of these protocols in sterically challenged and electron-deficient systems. The presence of a nitro function also gave rise to many interesting observations with regards to regioselectivity, in particular the propensity for 6-endo-dig ring closure to give the desired isocoumarin, rather than phthalide (*via* 5-exo-dig cyclisation), which was formed in the non-nitrated analogue. A novel synthesis of the lead compound, 5AIQ, *via* the reductive cyclisation of methyl

2-cyanomethyl-3-nitrobenzoate has also been realised and this strategy could potentially be extended to the synthesis of the 4-substituted targets.

The successful synthesis of a series of 3-substituted targets allows, for the first time, a systematic investigation of their structure-activity relationship. All the members in this series demonstrated good water-solubility and excellent PARP-1 inhibitory activity *in vitro*, with IC_{50} values in low micromolar range. The 3-substituents were generally well tolerated by the active site and they resulted in a significant enhancement of PARP-1 inhibitory potency with respect to 5AIQ, the most potent inhibitors being 5-amino-3-methylisoquinolin-1(2*H*)-one (**94**) (IC_{50} 0.23 μM), which is *ca.* 7-fold more active than 5AIQ. Additional interactions between the 3-substituents and a deep hydrophobic pocket within the active site, as well as a putative, water-mediated hydrogen bond between the 5-amino group and Glu988 probably accounts for their outstanding potencies. Thus, we have invented a novel, water-soluble and potent class of PARP-1 inhibitors. Their highly encouraging *in vivo* profiles and favourable physical properties made them attractive candidates for preclinical development.

Acknowledgements

I thank God for sending so many beautiful people in my path to help me and to teach me the things of science and life, and for making my PhD such an enriching experience.

I am indeed indebted to my supervisor, Dr Mike Threadgill, without whom my PhD would not have been possible. I wish to thank him for his tremendous insight, ceaseless enthusiasm and patient guidance throughout my PhD, especially during times of journeying without answers and when the end seemed distant.

I would also like to thank Dr Steve Black for his NMR services, Mr Chris Cryer for the provision of Mass Spectra and Mr Alan Carver for Microanalysis data. Thanks also to Dr Andy Thompson for his much appreciated assistance in molecular modelling, and to KuDOS Pharmaceuticals Ltd. for kindly conducting the biological assays.

I acknowledge the friendship, support and advice of Dr Chris Upton and all the medicinal chemistry postgraduates and post-doctorals, in particular my colleagues in lab 3.5 (Christian, Claire, Ghadeer, Joey and Mervat).

Finally I wish to express my deepest gratitude to my family (my mum and dad, Sin Yong, Guat Yong and Prisy) and friends (Lisa, Yee May, Wing...), for the love they have demonstrated to me through their prayers, encouraging words and for cheering me on when the problems were great, answers were few and faith was little. For this reason, I gratefully and affectionately dedicate this thesis to them.

Contents

List of Figures, Schemes and Tables

Figures

Schemes

Tables

Abbreviations

3AB	3-aminobenzamide
5AIQ	5-aminoisoquinolin-1(2*H*)-one
ADP	adenosine diphosphate
ATP	adenosine triphosphate
BRCT	breast cancer susceptibility protein, BRCA1, C-terminus
CI	chemical ionisation
COSY	correlation spectroscopy
DBD	DNA binding domain
DCM	dichloromethane
DEVD	Asp-Glu-Val-Asp
DIBAL-H	diisobutylaluminium hydride
DIPA	diisopropylamine
DMADMA	dimethylacetamide dimethyl acetal
DMBDMA	dimethylbenzamide dimethyl acetal
DMF	*N,N*-dimethylformamide
DMFDMA	dimethylformamide dimethyl acetal
DMSO	dimethyl sulphoxide
DNA	deoxyribonucleic acid
EI	electron-impact
FAB	fast atom bombardment
HIV-1	human immunodeficiency virus-1
HMQC	heteronuclear multiple quantum coherence
I/R	ischaemia reperfusion
IC_{50}	concentration required for 50% inhibition of activity
ICAM-1	intracellular adhesion molecule-1
***i*NOS**	inducible nitric oxide synthase
IR	infrared
LHMDS	lithium hexamethyldisilazide
MNNG	*N*-methyl-*N'*-nitro-*N*-nitrosoguanidine

MS	mass spectrum
NAD^+	nicotinamide adenine dinucleotide
NLS	nuclear localisation signal
NMR	nuclear magnetic resonance
NOESY	nuclear Overhauser enhancement spectroscopy
p.p.m.	parts per million
PARG	poly(ADP-ribose) glycohydrolase
PARP	poly(ADP-ribose) polymerase
R_f	retention factor
RNA	ribonucleic acid
SAR	structure activity relationship
TANK	tankyrase
THF	tetrahydrofuran
TLC	thin layer chromatography
TMSA	trimethylsilylacetylene
TNF	tumour necrosis factor
UV	ultraviolet
vPARP	vault poly(ADP-ribose) polymerase

Introduction

1.1 Poly(ADP-ribose) polymerase-1

Poly(ADP-ribose) polymerase-1 (PARP-1) [EC 2.4.2.30], also known as poly(ADP-ribose) synthetase (PARS) or poly(ADP-ribose) transferase (pADPRT), is a multifunctional enzyme that is selectively activated by DNA strand breaks. It catalyses **poly(ADP-ribosyl)ation**, which is the synthesis of long homopolymers of ADP-ribose through sequential attachment of ADP-ribosyl moieties from its substrates nicotinamide adenine dinucleotide (NAD^+) **(1)** to a variety of acceptor proteins[1]. This enzyme is present in great abundance in most eukaryotic cells (with the notable exception of yeasts) and is located predominantly within the nucleus where it is tightly bound to the chromatin[2].

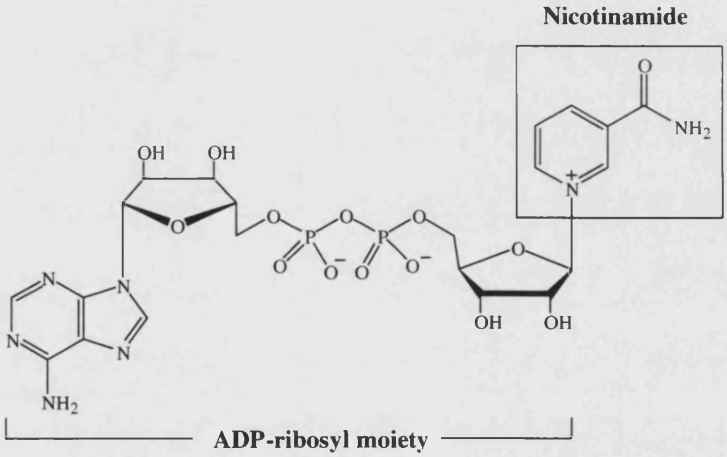

Nicotinamide Adenine Dinucleotide (NAD^+) (1)

Though its exact biological function remains highly debatable, there is now a great body of evidence indicating that PARP-1 plays a major role in controlling the repair of damaged DNA and the maintenance of genomic integrity[3,4]. Current research has also thrown light into the possible involvement that PARP-1 may have in cellular proliferation[5], differentiation[6], gene transcription[7] and cell death[8]. Whatever its precise physiological roles may be, great therapeutic benefits in a diverse range of diseases such as rheumatoid arthritis[9], neurodegenerative disorders[10], retroviral infection[11] and ischaemia-reperfusion injury[12] secondary to stroke, cardiac infarction

and haemorrhagic shock has recently been demonstrated through an inhibition of this enzyme. In view of such enormous therapeutic potentials, this enzyme rapidly became the target for drug development and is currently the subject of significant research. PARP, which was little more than a biochemical curiosity for almost three decades following its discovery, has finally gained its much-deserved attention.

1.2 The molecular structure of human PARP-1

The human PARP-1 is a 116 kDa protein consisting of a single polypeptide chain of 1014 amino acid residues[13]. It is found in the nuclei of all organs of the human body and is encoded by a single copy gene which is localised on chromosome 1 at position q41-q42--- a gene consisting of 23 exons, spanning 43 Kb[14]. Three distinct functional domains were identified following limited proteolysis of the pure enzyme with papain and/ or α-chymotrypsin[15].

- A 42 kDa N-terminal fragment, which includes the **DNA-binding domain**.
- A 22 kDa central fragment containing the **automodification domain**.
- A 52 kDa C-terminal fragment bearing the **catalytic domain**.

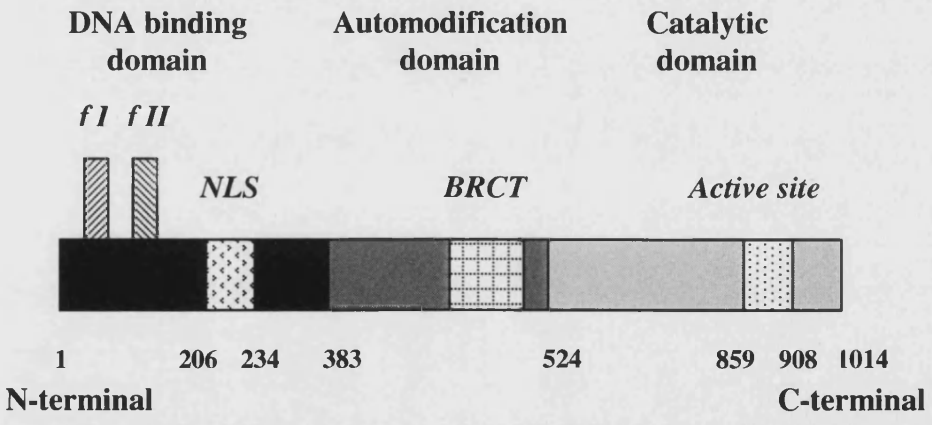

Figure 1. *Schematic representation of the three functional domains of hPARP-1*[18].

1.2.1 The DNA-binding domain (DBD)

The DNA-binding domain consists of two zinc finger motifs and a nuclear localisation signal (NLS). The zinc fingers are loops in the polypeptide chain formed as a result of a zinc ion coordinating to four amino acid residues (two cysteine and two histidine residues). The two zinc fingers are about 28-30 amino acid residues apart[16]. They are differentially required for the recognition of single- and double-stranded DNA breaks and the consequent activation of the enzyme. In particular, a deletion or mutation of the first finger (f I) resulted in a total abolition of enzymatic activity, whatever the nature of DNA break. Destruction of the second finger (f II), on the other hand, only abolishes the activation of enzyme by DNA containing single strand breaks[16]. These classical zinc finger motifs are common in many other DNA regulatory proteins that showed preferential binding at DNA single-strand break, for example the amino-terminal region of human DNA ligase III and the carboxy-terminal region of DNA polymerase ε[17]. The DBD also contains an NLS which is essential for effective translocation of PARP-1 into the nucleus. Within the NLS is a caspase-cleavage site, DEVD[17].

1.2.2 The automodification domain

The automodification domain is located in the central region of PARP-1, between the DBD and the catalytic domains. It contains a leucine zipper motif, which may be involved in protein-protein interaction and a BRCT motif (*br*east cancer susceptibility protein, BRCA1, *C-t*erminus), which is common in many proteins that function in DNA repair or in cell-cycle checkpoints[17]. In addition, there are fifteen highly conserved glutamate residues which are the presumed target for auto-poly(ADP-ribosyl)ation. Although found largely in the automodification domain, further sites for automodification also exist in the DBD and catalytic domains.

1.2.3 The catalytic domain

The catalytic domain is the most conserved region of the PARP-1 molecule. It contains a block of 50 amino acids (residues 859-908) which are strictly conserved among the vertebrates (100%) and among different species (92%) such as mouse, cow, chicken, *Xenopus* and *Drosophilia*[18]. As such, this part of the protein is often referred to as the "PARP-1 signature". This domain alone is responsible for all the catalytic functionality of the full length enzyme namely; NAD^+ hydrolysis, initiation, elongation and branching of ADP-ribose polymer synthesis[17]. Such basal activity is independent of the presence of DNA strand-breaks but lacks specificity. The specificity of PARP-1 for damaged DNA is absolutely dependent on the integrity of the zinc finger domain[19]. Another functionally important feature in this domain is the presence of Glu988, a highly conserved amino acid residue that is directly involved in the catalysis of the ADP-ribose transfer reaction.

1.3 The PARP super family

For over three decades, it was assumed that PARP activity resulted from the function of a single enzyme. This assumption was challenged recently with the discovery of two structurally different PARP proteins, both possessing DNA-dependent poly(ADP-ribosyl)ating activities, in two higher plants (*Arabidopsis thaliana* and maize)[20]. Subsequently, it has been reported that embryonic fibroblasts derived from PARP-1 knockout mice were surprisingly able to synthesise ADP-ribose polymers in response to DNA damage caused by *N*-methyl-*N'*-nitro-*N*-nitrosoguanidine (MNNG)[21], a genotoxic agent. There was, nevertheless, an observed 90% decline in overall PARP activity and both the amount and length of ADP-ribose polymers were decreased in these cells. These findings suggested that some previously unreported enzyme(s) that are capable of producing ADP-ribose polymers might be present in these PARP knockout mice.

Intensive research in the last two years has begun to identify many new forms of human PARP, such as PARP-2[22], PARP-3[23], vault PARP (vPARP)[24] and tankyrases[25], with the founding member of the PARP family (previously known as "PARP") now designated as PARP-1. The huge decline in PARP activity following PARP-1 knockout indicates that PARP-1 is the principal member of the family and is responsible for majority of the poly(ADP-ribosyl)ating activities. The existence of a family of PARP proteins in human and other species raises a number of important questions with regards to their specific functions and their specific targets. Although research on the biological role of these novel PARP homologues is still in the embryonic stage, interesting differences in domain structure (summarised in Figure 2), subcellular localization, tissue distribution and their ability to bind to DNA have already been established.

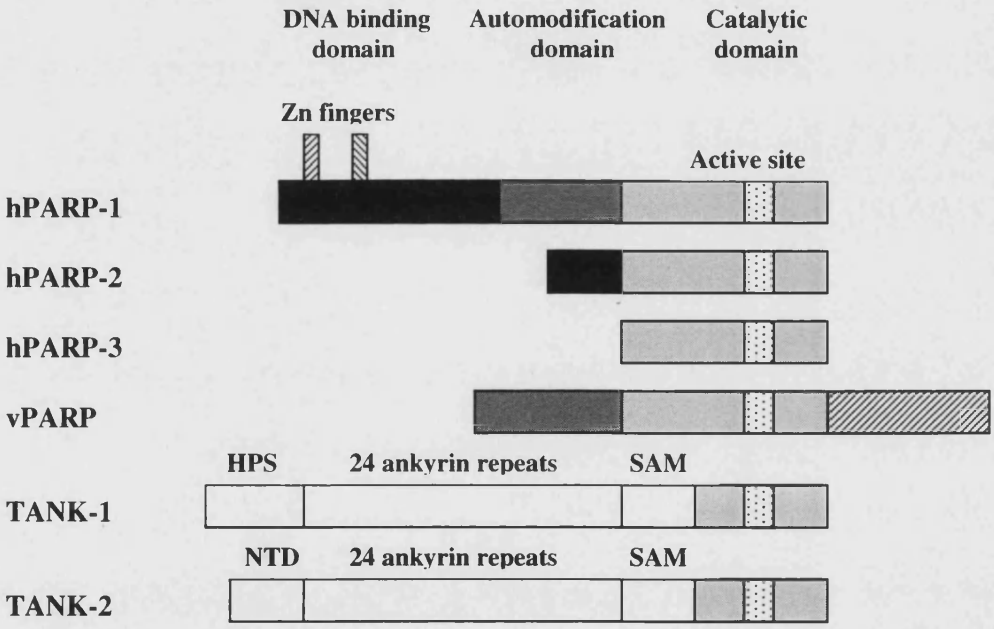

Figure 2. *Comparison of the domain structures of six PARP enzymes*[29].

HPS: histidine-, proline- and serine-rich region

SAM: sterile alpha motif

NTD: N-terminal domain

1.3.1 PARP-2 and PARP-3

Among the currently identified members of PARP family, PARP-2, (62 kDa) bears the strongest resemblance to PARP-1 and PARP-3 (60 kDa) is the smallest PARP characterised[22,23]. They are encoded by chromosome 14q11.2-q12 and 3p21.1-p22.2 respectively, which are distinct from PARP-1 gene loci. Both PARP-2 and -3 are characterized by a short, basic N-terminal domain of variable length and a highly conserved catalytic domain which shares considerable homology (40% and 31% sequence identity respectively) with the catalytic domain of PARP-1[22,23]. Their major structural differences with PARP-1 includes a smaller size and the following structural features:

- Absence of the nuclear localisation signal (NLS).
- Absence of the automodification domain.
- While the DNA binding domain (DBD) of PARP-2 lacks the zinc finger motif, this domain is absent altogether in PARP-3.

Interestingly, despite the lack of the classic zinc finger motif which acts as a nick sensor in PARP-1, both PARP-2 and -3 are nevertheless capable of binding to DNA that has been treated with DNase I and to catalyse the formation of poly(ADP-ribose) polymers in a DNA-dependent manner[26]. Furthermore, they are also capable of efficient automodification processes despite the absence of an automodification domain. This interaction could be driven by some other mechanisms involving binding modules that have yet to be discovered. While the catalytic function is structurally and mechanistically conserved between these two enzymes, their functional specificity is presumably determined by their variable N-terminal modules.

1.3.2 Vault PARP

Vault PARP (vPARP) is a 193 kDa cytoplasmic PARP that has been found associated with vaults, barrel-shaped ribonucleoprotein particles of arched morphology reminiscent of the vaulted ceilings of cathedrals[24]. Unlike PARP-1, -2 or -3, vPARP does not require DNA for activity and therefore, understandably, does not contain a DBD. Its N-terminal is occupied by a BRCT motif while its C-terminal contains the NLS. The functional significance of vPARP is as elusive as the full biological role of vaults. Since vaults are implicated in cellular transport, the identification of vPARP as a component of the vault ribonucleoprotein complex suggest a role for vPARP in regulating the transport of molecules, possibly through poly(ADP-ribosyl)ation of the major vault protein[24].

1.3.3 Tankyrases

As with vPARP, tankyrases do not require DNA for activity and they are localised to human telomeres---proteins situated at the end of eukaryotic chromosomes that are essential for chromosome maintenance and stability. Tankyrase-1 (TANK-1) is a 142 kDa protein containing 24 ankyrin repeats, a sterile alpha motif (SAM), and a catalytic domain[25]. Its N-terminal has a histidine-, proline-, and serine-rich (HPS) region. TANK-1 probably binds to and poly(ADP-ribosyl)ates telomere repeat-binding factor 1 (TRF1), thereby causing the latter to be released from telomeres, allowing access of telomerase, a specialised reverse transcriptase that restores telomeric sequences lost during cell division. In this way, TANK-1 acts as a positive regulator for telomere length[25]. An inference from this finding is that tankyrase-specific inhibitors might prove useful in anti-cancer therapies, since telomere maintenance is required for the continued growth of tumour cells[19].

Tankyrase-2 (TANK-2), apart from having a unique N-terminal domain (NTD), shows 85% homology to TANK-1 at the amino acid level[25]. The function of this perinuclear enzyme is not yet known but is probably different from that of TANK-1, since overexpression of TANK-1 induces progressive telomere elongation, while TANK-2 overexpression results in rapid cell death by necrosis[27].

This list of PARP enzymes is far from complete. Molecular cloning and sequence analysis are beginning to add new siblings to the PARP family. Already, de Murcia's laboratory has very recently cloned a total of 16 PARP cDNA sequences encoding 16 novel PARP homologues[28] and there is no doubt that this family is still expanding, giving rise to what he described as the "expanding universe of PARP proteins". PARP research now faces a stimulating challenge in elucidating the distinct (or sometimes overlapping) biological roles of these new members of the PARP family. This requires further studies using selective PARP inhibitors and modern molecular biological approaches. Cells and animals models that are deficient in the expression of specific PARP homologues as well as multiple gene knockouts that completely lack poly(ADP-ribosyl)ation will form the basis for future studies. Until then, the potentials of these new forms of PARP as drug targets remain to be defined. The subsequent sections deal primarily with PARP-1, the most studied and understood member of the family, as a therapeutic target.

1.4 Mechanism of action of PARP-1

The activation of PARP-1 and the ensuing poly(ADP-ribosyl)ation is one of the earliest eukaryotic responses to DNA strand breakage. Though PARP-1 can bind to undamaged DNA, it displays negligible activity in the absence of DNA strand breaks. The obligatory triggers of PARP-1 activation are nicks and breaks in the DNA[30], which can be induced by a variety of environmental stimuli and oxidants/ free radicals[31]. This includes hydroxyl radical, peroxynitrite, ionizing radiation and genotoxic agents such as MNNG.

Electron microscopy has shown that the introduction of a break in one strand of the DNA duplex induced flexibility at the nicked site. This caused the two DNA duplexes to come into close proximity with each other at an angle, forming a characteristic V-shape conformation which is recognisable by PARP-1[18]. PARP-1, upon detection of such conformational changes, binds rapidly and specifically mainly through its second zinc-finger to the centre of the V covering 7±1 base pairs symmetrically on each side of the break[18].

This in turn led to the recruitment of a second PARP-1 molecule which forms a homodimer with the first PARP-1 molecule, possibly through the leucine zipper motif in the automodification domain[32]. The second PARP-1 molecule is believed to serve as a polymer acceptor during subsequent ADP-ribose polymer synthesis by the first PARP-1 molecule. The idea that PARP-1 functions as a dimer is supported by Uchida *et al*[32] where they showed that addition of a single molecule of PARP-1 to damaged DNA only resulted in binding of the PARP-1 molecule to DNA without any detectable polymerase activity. This PARP-1 molecule remained "inactive" until a second molecule of PARP-1 was added. Figure 3 summarises the series of events that leads to the recognition and binding of PARP-1 to DNA single strand break.

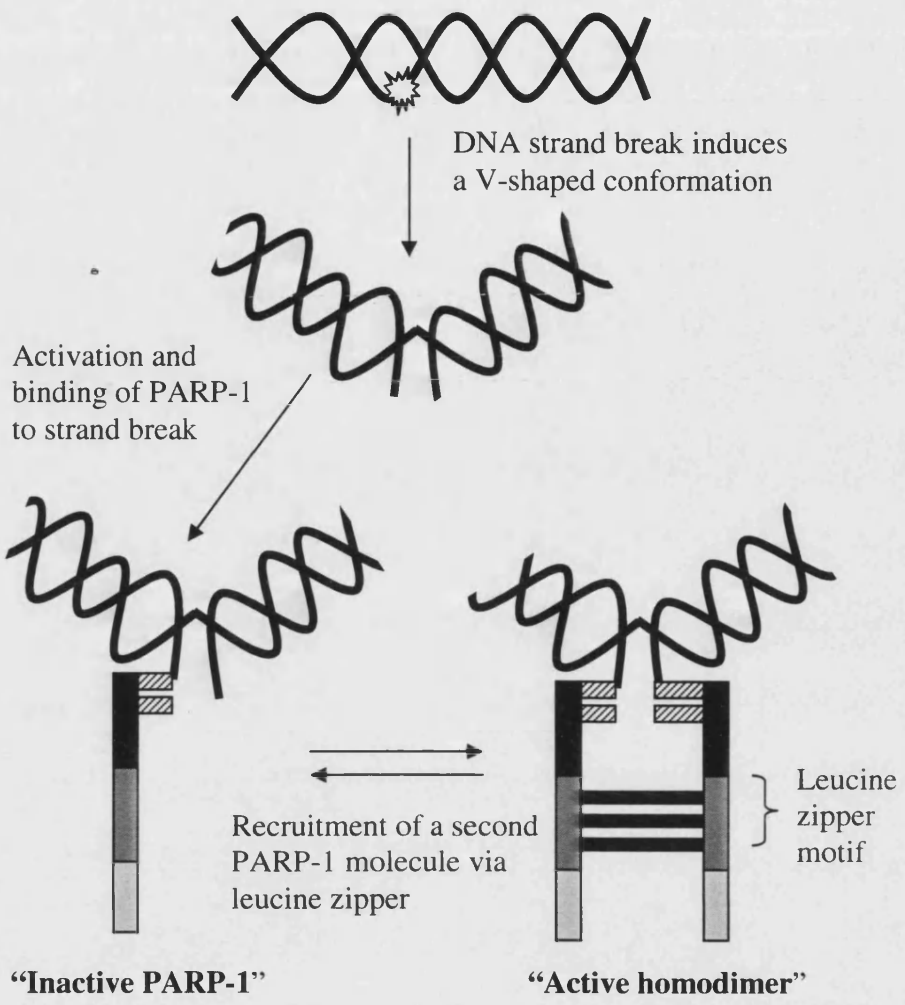

Figure 3. *Model for recognition and binding of PARP-1 to DNA single strand breaks*[18].

The binding of PARP-1 to damaged DNA also brings about a marked activation of its catalytic domain (of up to 500 times)[33] and subsequent poly(ADP-ribosyl)ation. As in many other cellular processes such as acetylation and phosphorylation, poly(ADP-ribosyl)ation brings about covalent post-translational modifications of nuclear proteins, a process that is crucial for the regulation of activities within the cell[34]. By mechanisms that are not altogether clear, it was believed that poly(ADP-ribosyl)ation of nuclear proteins at the sites of DNA damage produces intracellular signals that initiate DNA repair and cell survival programs. ADP-ribose polymer formation is subjected to very complex regulatory mechanisms and consists of three main reactions: **initiation, elongation** and **branching**.

1.4.1 Initiation

During initiation, PARP-1 binds to its substrate, NAD^+ (**1**), at the NAD^+ binding domain and catalyses the cleavage of the nicotinamide-ribose bond in NAD^+. This is followed by the transfer of the resulting ADP-ribosyl moiety to the nucleophilic centre (invariably a Glutamate residue) of an appropriate protein acceptor. The protein acceptors may be nuclear proteins that are involved in DNA repair, DNA metabolism or chromatin architecture (**heteromodification**), for instance histones[35], high mobility group (HMG) proteins[35] and DNA enzymes such as DNA topoisomerases I and II[36], DNA polymerase α and β[37] and DNA ligases[38]. However the main protein to be poly(ADP-ribosyl)ated is PARP-1 itself[39], in a process known as **automodification** where the ADP-ribose moiety is being attached to the glutamate acid residues in the automodification domain of PARP-1.

The cleavage of the nicotinamide-ribose bond in NAD^+ has an S_N1 character and is probably facilitated by an adjacent ribose oxygen lone pair, leading to an intermediate oxocarbenium ion[40] (mechanism outlined in figure 4). The highly conserved Glu988 residue within the active site of PARP-1 helps catalysis in two respects. It binds to and polarises both the attacking nucleophile (the anchor point for ADP-ribose polymer synthesis) and NAD^+, thereby increasing the nucleophilicity of the nucleophile and stabilising the oxycarbenium intermediate respectively. Nicotinamide is released during the process. Polymerisation reactions (**chain elongation** and **branching**) then follow.

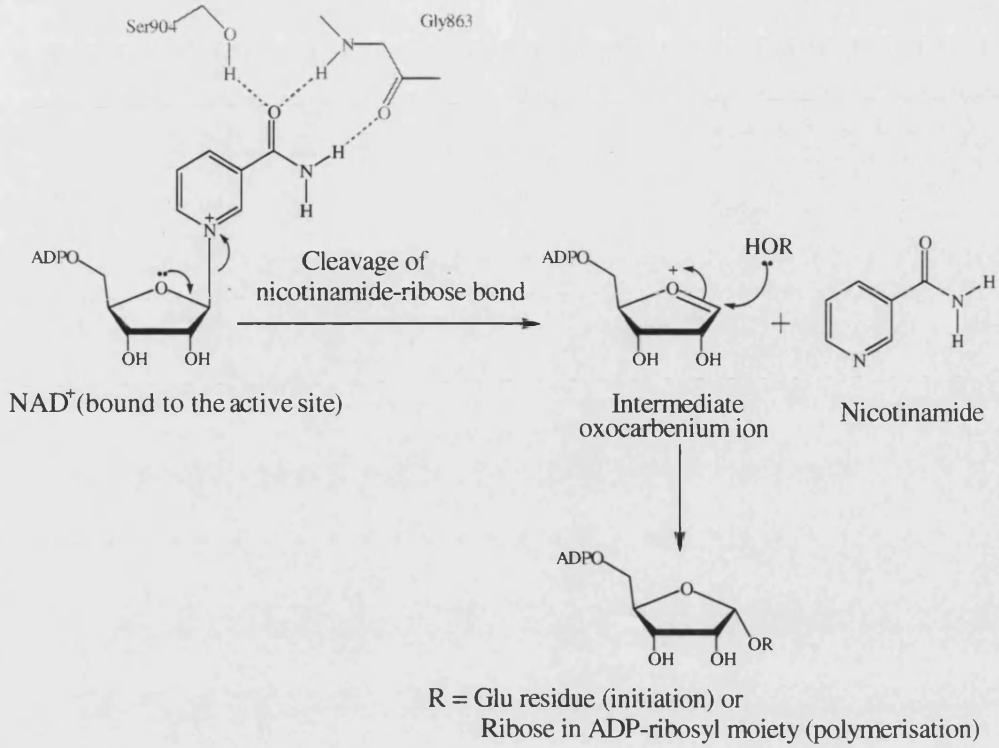

Figure 4: *Proposed mechanism for poly(ADP-ribosyl)ation by PARP-1*[40].

1.4.2 Elongation

In elongation, an α(1″→2′) glycosidic bond is formed between C-1 of the nicotinamide ribose and the 2-OH of the adenine ribose of the preceding ADP-ribose unit (Figure 5). This leads to the formation of linear polymers which may be up to 200 residues long.

1.4.3 Branching

Branching occurs when the C-1 of the nicotinamide ribose is joined with the 2-OH of the nicotinamide ribose of another ADP-ribose polymer via a 1‴→2″ glycosidic bond (Figure 5). The frequency of occurrence is one every 30 to 50 ADP-ribose units polymerised[41].

1.4.4 Termination

Automodification of PARP-1 eventually causes the enzyme to be detached from the damaged DNA due to electrical repulsion between the highly negatively charged ADP-ribose chains (two negative charges per monomer) and the negative charges in DNA molecule. Separation of PARP-1 from DNA presumably allows access of DNA repair enzymes such as DNA polymerase and DNA ligase to the site of damage[42], setting off a series of DNA repair processes. The detachment of PARP-1 from the DNA also terminates its own catalytic activity. Hence, automodification represents a major regulatory mechanism for PARP-1 resulting in the down-regulation of the enzyme and the cessation of further ADP-ribose polymer synthesis.

1.5 Catabolism of ADP-ribose polymers

Poly(ADP-ribosyl)ation is a dynamic process, as indicated by the very short half-life (less than 1 minute)[43] of the polymer *in vivo*. The transient nature of the polymer is attributable to its fast degradation by at least two types of enzymes: **poly(ADP-ribose) glycohydrolase (PARG)** and **ADP-ribosyl protein lyase**[44]. Once the ADP-ribose polymer is formed, it is almost immediately hydrolysed by the constitutively active PARG, which cleaves the ribose-ribose linkage in the linear ($1''\rightarrow2'$ glycosidic bond) and branched ($1'''\rightarrow2''$ glycosidic bond) portion of the polymer to produce ADP-ribose monomers[44]. Because the K_m value of PARG is about 100 times lower for larger ADP-ribose polymers than for smaller ones[45], the enzyme probably hydrolyses bigger fragments first, then switches to removal of ADP-ribose units one by one. Despite the many new PARP genes that were described, so far there is still only one PARG enzyme. As with PARP-1, PARG is localised to the nucleus[46]. It is about 13-50 fold less abundant than PARP-1 but its specific catalytic activity is about 50-70 fold higher. Hence there is no kinetic constraint in its ability to cope with large amount of ADP-ribose polymer being formed by PARP-1 during DNA damage[47].

ADP-ribosyl protein lyase then removes the remaining proximal ADP-ribose moiety from the acceptor proteins by breaking the ADP-ribose glutamate ester bond[44]. This yields a dehydrated form of ADP-ribose, 5-ADP-3-deoxypent-2-enofuranose (**2**), and releases the acceptor proteins, allowing them to resume their activities. The rapid biosynthesis and degradation of ADP-ribose polymer constitute a cycle (figure 5), the regulation of which appears to be absolutely necessary for normal growth of all poly(ADP-ribose) producing cells[48].

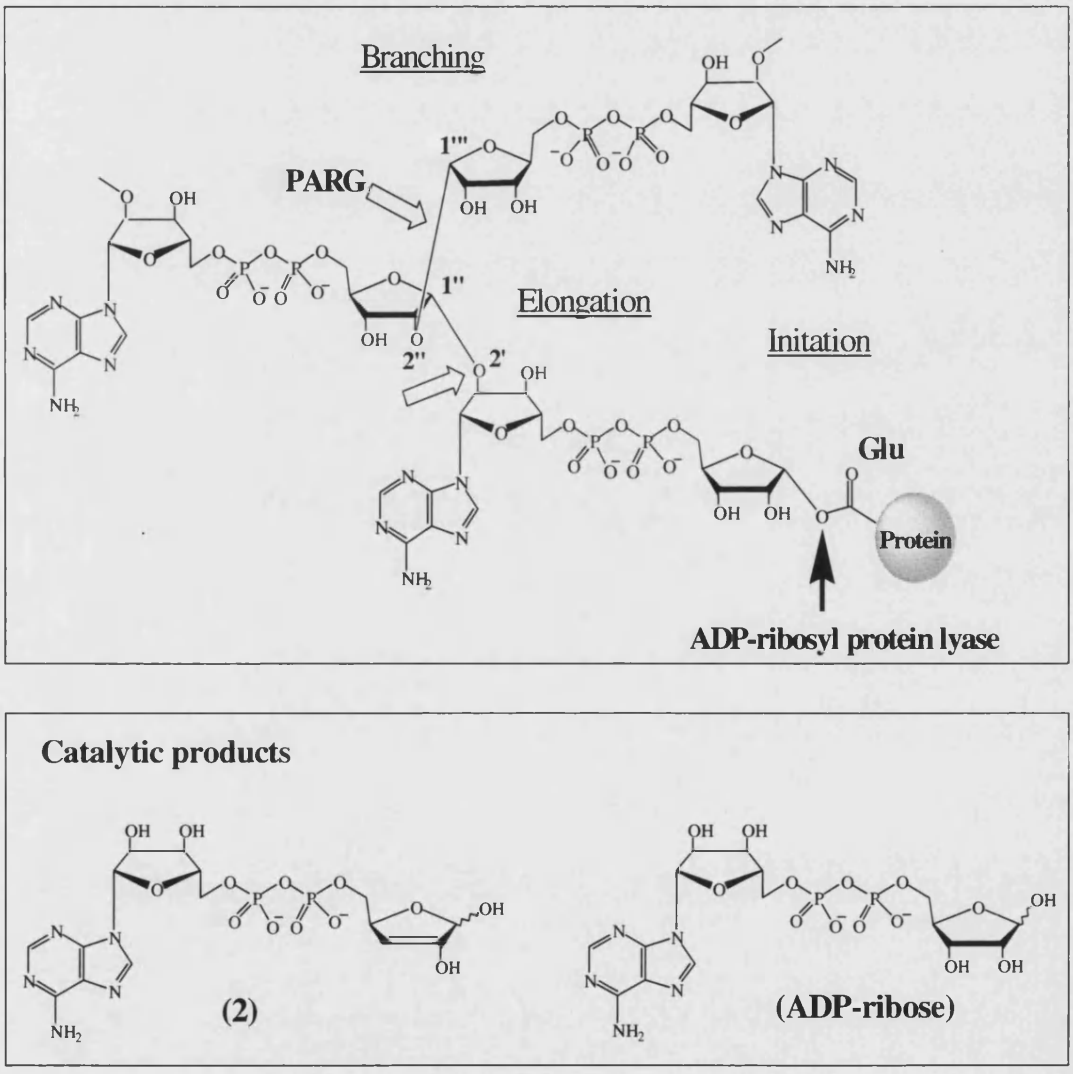

Figure 5. *Biosynthesis and degradation of ADP-ribose polymers. Catalytic activities of ADP-ribosyl protein lyase (indicated by black arrow) and PARG (white arrows) lead to formation of* (**2**) *and ADP-ribose respectively*[48].

1.6 PARP-1: The "guardian angel" of the genome

It has been estimated that there are about one million PARP-1 molecules per cell, in another word one PARP-1 molecule for each 1000 base pairs of DNA[49]. Considering such great abundance, this enzyme must serve some important physiological function(s). One such physiological role has clearly been identified to be the cytoprotective effect of PARP-1 with regard to cell survival and maintenance of genomic stability under genotoxic stress[3,4]. It is also generally believed that PARP-1 is involved in the regulation of other DNA plasticity-related phenomena[5-8], such as DNA replication, cellular proliferation and differentiation, gene transcription, chromatin remodelling, gene expression and cell death.

1.6.1 PARP-1 in DNA repair and maintenance of genomic integrity

PARP-1 has long been implicated in DNA repair, since it is activated by DNA strand breaks[3]. Such activation is immediate and can be elicited by a very small amount of DNA damage. Indeed many studies have now clearly indicated that PARP-1 plays a pivotal role in controlling DNA base-excision repair and is part of an intricate DNA surveillance network that protect the cell genome from the deleterious consequences of accumulated unrepaired or misrepaired lesions. These studies collectively demonstrated that PARP-1 knockout mice show normal foetal and postnatal development but have inherent genomic instability as evidenced by an increased number of micronuclei[26,50] (chromatin fragments indicating chromosomal damage). They are also severely hypersensitive to DNA damage induced by ionising radiation and monofunctional alkylating agents[51,52]. A substantial delay in DNA base excision repair and a high frequency of sister chromatid exchange was also observed. The involvement of PARP-1 in genomic housekeeping is further indicated by the interaction of PARP-1 with other nick sensors such as DNA ligase III and DNA repair effectors, such as DNA polymerase[53]. Hence, although PARP-1 appears to be dispensable for normal cellular activities such as growth, development or differentiation, it should be considered an essential survival factor for recovery following DNA damage. The exact mechanism by which the poly(ADP-ribosyl)ating

activities of PARP-1 facilitates DNA repair has not been clearly defined. It is postulated that these polymers play structural and functional roles in the DNA repair process.

1.6.1.1 Structural roles

In regards to a possible structural role, rapid synthesis of a large number of negatively charged polymers provides a mechanism to prevent the damaged DNA from associating with the recombination systems and helps to repel other DNA molecules[54]. It also causes a relaxation of the chromatin superstructure as will be explained in section 1.6.3. Detachment of PARP-1, on the other hand, allows access of DNA repair enzymes such as DNA polymerase and DNA ligase to the site of damage[42]. It is believed that the timing of PARP-1 attachment to and release from the DNA strand break may help to synchronise the whole repair process. Once the repair is completed, there will be no more strand break to stimulate PARP-1 and hence synthesis of ADP-ribose chains stops. Remaining polymer molecules will then be rapidly degraded by PARG and ADP-ribosyl protein lyase, allowing the DNA molecule to restore its pre-damaged primary structure[44].

1.6.1.2 Functional roles

It is also possible that the ADP-ribose polymer has a more direct functional role in DNA repair. Poly(ADP-ribosyl)ation has different regulatory effects on the various acceptor proteins[55]. For instance, it inhibits DNA polymerase α and β, topoisomerase I and II, Ca^{2+}/Mg^{2+} endonucleases and DNA ligase II. It is possible that, through poly(ADP-ribosyl)ation of these proteins, PARP-1 controls and coordinates the various enzymatic processes that are involved in DNA repair, thereby responding as a general director of the crisis situation that exists in DNA damage.

1.6.2 PARP-1 in DNA replication and cellular differentiation

A wealth of information has now been gathered that seems to indicate the possible involvement of PARP-1 in the regulation of DNA replication. Several research groups have reported on separate occasions the observation that ADP-ribose polymer metabolism is accelerated in the nuclei of proliferating cells[56-58]. PARP-1 was also found to co-purify with key components of multiprotein replication complex (MRC), many replication factors and centromere proteins[59,60]. In addition, various experimental models using PARP-1 knockout cells and pharmacological inhibition have demonstrated an inhibition of DNA replication and cell proliferation[61], hence suggesting a possible role of PARP-1 in regulating these two processes.

Given that replication and differentiation are closely coupled processes, it is not surprising that PARP-1 may also be involved in the regulation of cellular differentiation. This is an important process where cells undergo a series of proliferative steps during which they gain new functions and lose others in order to fulfil certain tasks. Examples of such highly specialized cells include hepatocytes, neurons and renal tubular cells. Differentiation is a strictly controlled process, requiring concerted gene activation and repression. The idea that PARP-1 may regulate this process is supported by the findings that PARP-1 inhibitors were found to inhibit differentiation of human granulocyte-macrophage progenitor cells to the macrophage lineage[62]. Overexpression of PARP-1 also arrests NB4 cells and blocks all trans-retinoic acid-induced terminal neutrophilic differentiation[63].

1.6.3 PARP-1 in gene transcription and chromatin remodelling

The frequent association of PARP-1 with transcriptionally active regions of chromatin[34,42] suggests yet another possible role for this enzyme, *i.e.* the regulation of transcription. One component of the transcription-regulating activity of PARP-1 may be the regulation of chromatin structure and function through poly(ADP-ribosyl)ation of histones (the next major protein acceptors of poly(ADP-ribose) after PARP-1). These are the principal structural proteins of

eukaryotic chromosomes that help to hold the nucleotide together and condense the chromatin. Their positive charges, due to high proportion of lysine and arginine residues, enable them to bind tightly to DNA. Poly(ADP-ribosyl)ation of histones confers negative charge to the latter, leading to electrostatic repulsion with DNA molecules and consequently, decondensation and relaxation of chromatin[64]. Such loosening of the chromatin structure makes genes more accessible for the transcriptional machinery. This mechanism has also been implicated in DNA repair, DNA replication and chromatin remodelling[42].

1.6.4 PARP-1 in gene expression

There was recently a remarkable observation that PARP-1 may help regulate the expression of various proteins at the transcriptional level[65]. Of special importance is the regulation by PARP-1 of the production of inflammatory mediators. Although details for this mechanism are still far from clear, it appears to involve interaction of PARP-1 with nuclear factor B (NF-κB), a key transcription factor regulating the expression of several elements of inflammation[66], such as cytokines, chemokines, intercellular adhesion molecule-1 (ICAM-1) and inflammatory mediators, such as inducible form of nitric oxide synthase (*i*NOS) and cyclooxygenase. Studies have showed that PARP-1 deficient cells were defective in NF-κB dependent transcription activation in response to tumour necrosis factor (TNF)[67]. Treating mice with bacterial lipopolysaccharide (LPS), an endotoxin, resulted in the rapid activation of NF-κB in macrophages from PARP-1 but not from PARP-1 knockout mice. In fact, PARP-1-deficient mice were extremely resistant to LPS-induced endotoxic shock[67].

Continuous efforts by research groups worldwide have led to a better understanding of the biochemistry of PARP-1 and, as more of its secrets get unlocked, more physiological functions emerge. In addition to those already discussed above, this protein is currently also implied in an array of other functions such as the regulation of cytoskeletal organisation[68], the control of the ageing process[69] and viral replication[70].

1.7 PARP-1: The "Janus-faced" enzyme

1.7.1 Cellular energy dynamics

Paradoxically, despite PARP-1 having the cytoprotective, "guardian angel" functions discussed above, its over-activation can actually induce cell death. It seems that the PARP-1 directed DNA repair process is a highly inefficient and energy-consuming process. With the formation of each ADP-ribose polymer, PARP-1 consumes up to 200 molecules of NAD^+. In addition, the rate of turnover of nuclear NAD^+ in a normal intact cell is estimated to be at least 100-fold less than the poly(ADP-ribosyl)ating activity of PARP-1[71], the actual rate of which depends on the degree of DNA damage in a dose-dependent manner. As a result, over-activation of PARP-1, consequent to massive DNA damage, may actually lead to a crisis situation where there is rapid (within only a few minutes) and severe depletion of intracellular NAD^+ level.

NAD^+ is an important respiratory coenzyme that regulates an array of vital cellular processes, such as glycolysis and mitochondria respiration, thereby providing ATP for most cellular processes[72]. It also serves as the precursor for nicotinamide adenine dinucleotide phosphate (NADP), which acts as a cofactor for the pentose shunt, and is involved in the maintenance of reduced glutathione pools[73]. The result of massive NAD^+ usage is a decline in the rate of all these vital processes, leading to cellular dysfunction and ultimately cell death. Moreover, under these precarious conditions, phosphoribosyl pyrophosphate synthetase and nicotinamide mononucleotide adenylyl transferase consume ATP in an effort to replenish the cellular NAD^+ store[55], further worsening the energy shortage and leading to a pronounced reduction of several crucial energy-dependent processes, such as DNA, RNA and protein synthesis[74].

1.7.2 The "suicide hypothesis"

PARP-1 then appears to be a "Janus-faced" enzyme that performs two seemingly contradictory functions---DNA repair that enables the cell to survive or NAD^+ depletion that leads to cell death. Based on this observation, Berger[55] proposed a hypothesis postulating that the activation of PARP-1 by massive levels of DNA damage is actually a suicide response since it results in a rapid depletion of NAD^+ and ATP and the cells die before there is any opportunity to repair the damage. This cell death is presumably nature's way of preventing gravely damaged cells from attempting to repair themselves, as such cells tends to have high mutation frequency and can undergo potentially malignant transformation. PARP-1 activation then served as a safety mechanism whereby massively damaged cells are removed from the population. The profound depletion of NAD^+ and ATP associated with PARP-1 activation also raised the possibility that even with milder activation of the enzyme associated with physiological DNA repair, the partial energy depletion provided by PARP-1 activation may prevent the cells from "over-exerting" themselves until DNA repair is completed[71].

1.7.3 The "molecular switch hypothesis"

The "suicide hypothesis" is controversial because it was never established whether an extensively damaged cell dies because of a depleted NAD^+/ ATP pool or from the DNA damage itself. Nevertheless, it is currently accepted that PARP-1 is involved in the two main pathways of cell death: apoptosis and necrosis, the actual mode of cell death being determined chiefly by the level of NAD^+ and ATP[75]. It was therefore plausible to hypothesise that PARP-1, being a NAD^+-catabolizing enzyme, may serve as a molecular switch between apoptosis and necrosis[76]. According to this hypothesis, cells exposed to DNA-damaging agents (especially oxidative insults) can enter three different routes as determined by the severity of DNA damage (Figure 6):

1) PARP-1 activated by mild genotoxic stimuli facilitates **DNA repair** by signalling cell-cycle arrest and by interacting with DNA repair enzymes and DNA-dependent protein kinase. As a result, DNA damage is repaired, and cells survive without the risk of passing on mutated genes.

2) More severe DNA damage induces **apoptotic cell death** during which caspases, the main executor enzymes of the apoptotic process, inactivate PARP-1 by cleaving it into two fragments (p89 and p24) at the DEVD motif in the nuclear localization signal of PARP-1[77]. Cleavage at this site separates the DNA binding domain from the catalytic domain, resulting in inactivation of the enzyme. The cleavage fragments further contribute to the suppression of PARP-1 activity through inhibition of dimerisation and DNA binding of intact PARP-1 by p89 and p24 respectively[78]. This pathway allows cells with irreparable DNA damage to be eliminated in a safe way *i.e. via* ingestion by macrophages. Cleavage of PARP-1 is believed to aim at preventing the activation of PARP-1 (by the ensuing DNA fragmentation) and thereby preventing cells from the pathological sequel of the third route in which cells die by necrosis, a less controlled mechanism posing danger for bystander cells.

3) The third route, **necrotic cell death**, is induced by extensive DNA breakage that is usually triggered by a massive degree of oxidative stress (hydroxyl radical, peroxynitrite). The overactivation of PARP-1 depletes the intracellular stores of NAD^+ and consequently ATP level. This severely compromised cellular energetic state prevents cell death via the apoptotic pathway because many steps of apoptosis are known to depend on ATP[79]. Necrosis represents a more severe form of cell demise compared with apoptosis. In addition to numerous biochemical and morphological differences between apoptosis and necrosis, probably the most distinctive feature of necrosis is the disintegration of the plasma membrane[80]. Consequent leakage of cellular content from necrotic cells into the surrounding tissue may contribute to inflammatory responses and further injuries.

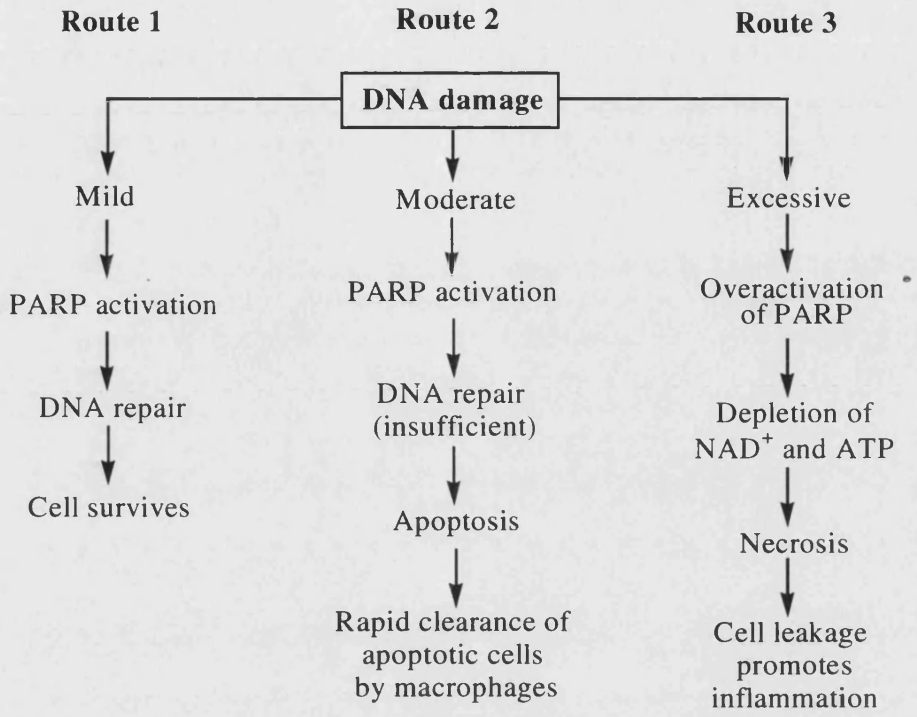

Figure 6. *Responses of PARP-1 to different severity of DNA damage*[81].

Research into the "suicidal" role of PARP-1 gained new momentum over the last decade with the important discoveries that DNA damage and DNA repair are not confined to a few relatively uncommon genetic disorders and that a great variety of human diseases, such as cancer, ischaemia-reperfusion injury, inflammatory disorders and neurodegenerative diseases involve damage to DNA as a crucial element to their pathogenesis. Most of these damages are caused by oxidative stress where PARP-1 is very much involved as the final mediator of cellular injury and death. PARP-1 inhibition, therefore, provides an exciting, novel therapeutic approach to a wide range of diseases. Many pharmaceutical companies have seized upon this possibility and are already actively making pharmacologically useful PARP-1 inhibitors. There has never been a more exciting time than now in this field. The next two sections are devoted to the discussion of the therapeutic effects of PARP-1 inhibitors in various disease models and the development of PARP-1 inhibitors.

1.8 Therapeutic potential of PARP-1 inhibition

1.8.1 The concept of ischaemia-reperfusion injury

Clinically, when there is a substantial reduction of blood flow to the tissues, the cells are said to be ischaemic. Ischaemia is a common condition during surgery and in many diseases, such as myocardial infarction, stroke and haemorrhage. Without question, early reperfusion is an absolute prerequisite for the survival of ischaemic tissues. However, that is not without hazard. Reperfusion has often been observed to exacerbate the injury sustained by the ischaemic tissues and lethally damage the organs (**ischaemia-reperfusion injury**)[82]. The damage, which occurred during the early minutes of reperfusion, appeared to be far greater than would have occurred if the ischaemia has been maintained.

Recent studies confirmed this "oxygen paradox" and suggested that reperfusion could trigger sudden metabolic and physiological changes, most notably, an outburst of oxidants and free radical production, in particular, hydrogen peroxide, hydroxyl radical, superoxide anion, nitric oxide and peroxynitrite[31] (Table 1). These are believed to be the major contributing factors in the origin and progression of reperfusion injuries. Not only are they capable of exerting cytotoxic effects, independently or synergistically, via a number of mechanisms, both hydroxyl radical and peroxynitrite (a highly reactive oxidant produced from the reaction between nitric oxide and superoxide) can also trigger massive DNA single strand break, leading to PARP-1 over-activation[83]. As described earlier in section 1.7.1, over-activation of PARP-1 depletes intracellular NAD^+ reservoir and consequently ATP store, culminating in cell dysfunction or necrosis[45-47]. Over-activation of PARP-1 also induces the expression of a number of genes that are essential for inflammatory responses (overviewed in section 1.6.4)[66,67]. For instance, it potentiates NF-κB activation, resulting in a greater expression of NF-κB-dependent inflammatory elements, such as cytokines, chemokines, *i*NOS, ICAM-1 and TNF. Both cytokines and chemokines can trigger free-radical formation through many different pathways, for example by stimulating xanthine oxidase activity and by

recruiting activated neutrophils. In addition, the level of production of nitric oxide is increased due to *de novo* *i*NOS expression. These events further worsen the oxidant stress, producing even greater PARP-1 activation and cell dysfunction (Figure 7).

Reactive oxygen or nitrogen species	**Main cellular sources**	**Comments**
Superoxide anion (O_2^-)	• Mitochondrial respiratory chain • Activated neutrophils, macrophages • Xanthine oxidase • Lipid peroxidation • Catechol auto-oxidation • Redox cycling	Does not induce DNA single strand break or PARP activation Relatively mild oxidant
Hydrogen peroxide (H_2O_2)	• Mitochondrial respiratory chain • Xanthine oxidase • Catechol auto-oxidation • Redox cycling	Potent trigger of DNA single strand break, activates PARP Potent oxidant
Hydroxyl radical (OH·)	• From hydrogen peroxide (*via* Fenton reaction) • Monoamine oxidase (in response to ionising radiation) • Catechol auto-oxidation • Redox cycling	Potent trigger of DNA single strand break, activates PARP Potent oxidant
Nitric oxide (NO·)	• Nitric oxide synthases	Does not induce DNA single strand break or PARP activation Relatively mild oxidant
Peroxynitrite ($ONOO^-$)	• Reaction of nitric oxide and superoxide	Potent trigger of DNA single strand break, activates PARP Potent oxidant

Table 1. *Pathophysiologically relevant sources of oxidant and free radical species*[81].

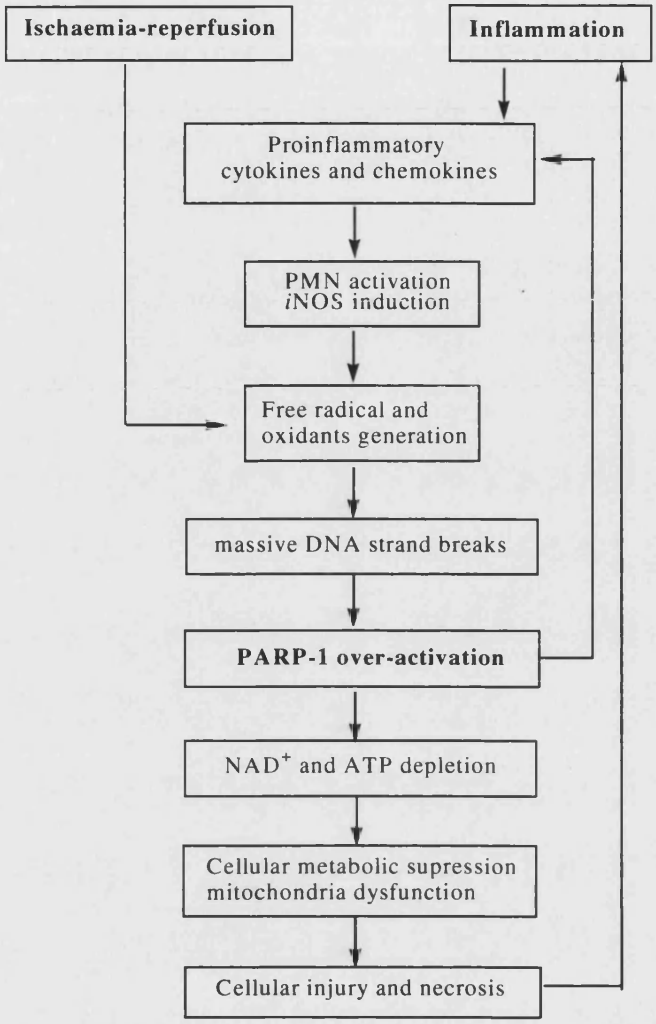

Figure 7. *The involvement of PARP-1 in the chain of events leading to pathophysiological changes in response to various insults.*

1.8.2 PARP-1 inhibition in ischaemia-reperfusion injury

It follows that pharmacological inhibition of PARP-1 will have two beneficial effects in ischaemia-reperfusion injury:

1. Preserving intracellular NAD^+ and ATP pools in oxidatively stressed cells, thereby increasing the survival of ischaemic tissues
2. Abating the inflammatory response.

Zingarelli *et al*[84] evaluated the role of PARP-1 in an acute model of myocardial reperfusion injury in the rat. Surgical occlusion of myocardial blood flow followed by reperfusion resulted in a marked cellular injury and development of a large infarct area. Pharmacological inhibition of PARP with 3-aminobenzamide (3AB) significantly improved the outcome of myocardial dysfunction, as evidenced by a reduction in creatine phosphokinase levels, diminished infarct size, and preserved ATP pools. Other investigators[85-89] confirmed their results using different animal models of myocardial infarction (rabbit and pig) and different PARP-1 inhibitors (nicotinamide, 5AIQ, PJ34). The results are summarised in Table 2.

Neural damage following stroke is thought to be elicited in large part by a massive release of the excitatory neurotransmitter glutamate acting upon *N*-methyl-D-aspartate (NMDA) and other excitatory receptors[90]. Stimulation of NMDA activates the production of nitric oxide by neuronal nitric oxide synthase (nNOS), which ultimately accounts for reperfusion injury in the central nervous system. In PARP-1 knockout mice, a markedly reduced infarct volume is observed after transient middle cerebral artery occlusion[91]. Several PARP-1 inhibitors have also been shown to reduce infarct size and improve neurological status in cerebral ischaemia-reperfusion[92-94].

The role of PARP-1 activation in ischaemia-reperfusion is not confined to the heart and brain. Recent reports have demonstrated that the inhibition of PARP-1 provides protective effects in many other reperfused organs such as gut[95-97], skeletal muscle[87], liver[98], kidney[99] and retina[100]. It also improves the outcome of heart transplantation[101] and protects against multiple organ damage secondary to haemorrhagic shock[102,103].

Experimental model	PARP-1 inhibitors	Effects of PARP-1 inhibition
Myocardial I/R		
Rat	3AB[84,85] 5AIQ[86]	Preserve myocardial ATP stores, decrease in infarct size, reduce left ventricle (LV) dysfunction, reduce neutrophil infiltration
Rabbit	3AB & Nicotinamide[87]	Reduce infarct size
Pig	3AB[88] PJ34[89]	Decrease infarct size, improve LV function
Cerebral I/R		
Rat	3AB & Nicotinamide[92]	Reduce infarct size, improve neurological status; become detrimental at high doses
Rat	DPQ[93]	Reduce infarct size, improve neurological status; loses protective effect at high doses
Rat	PJ34[94]	Reduce infarct size, improve neurological status
Mesenteric I/R		
Rat	3AB[95] GPI-6150[96] PJ34[97]	Protect against histological damage, neutrophil infiltration and mucosal barrier failure
Skeletal muscle I/R		
Rabbit	3AB[87]	Reduce infarct size
Liver I/R		
Rat	5AIQ[98]	Reduce rise in serum level of transaminases, lactate dehydrogenase and γ-glutamyl transferase.
Renal I/R		
Rat	3AB[99] 5AIQ[156]	Accelerate recovery of normal renal function. Reduce serum creatinine and blood urea nitrogen.
Retina I/R		
Rat	3AB[100]	Reduce I/R-induced injury
Heart transplantation		
Rat	5AIQ & PJ34[101]	Improve contractile function and reduce ICAM-1 expression
Hemorrhagic shock		
Pig Rat	3AB[102] 5AIQ[103]	Improve haemodynamics. Abolish multiple organ injury and dysfunction.

Table 2. *Effects of PARP-1 inhibitors in animal models of ischaemia-reperfusion injury.*

I/R: ischaemia-reperfusion; **3AB**: 3-aminobenzamide; **5AIQ**: 5-aminoisoquinolin-1-one

PJ34: *N*-(6-oxo-5,6-dihydro-phenanthridin-2-yl)-*N*,*N*-dimethylacetamide

DPQ: 3,4-dihydro-5-[4-(1-piperidinyl)butoxy]-1(2*H*)-isoquinolinone

GPI-6150: 2,3-dihydrobenzopyrano[4,3,2-*de*]isoquinolin-1-one

1.8.3 PARP-1 inhibition in inflammatory diseases

In view of the role that PARP-1 has in inflammatory signal transduction and the observation that a high level of inflammatory responses also elicit PARP-1 mediated cell death, one may anticipate PARP-1 inhibitors to protect against inflammation related cellular injuries. Indeed, the earliest implication of PARP-1 in the pathophysiology of inflammatory diseases was related to pancreatic islet cell injury and diabetes. Yamamoto *et al*[104] demonstrated that in streptozotocin-treated islet cells, inhibition of PARP-1 with 3-aminobenzamide prevented NAD^+ depletion and the suppression of pro-insulin synthesis without modifying the extent of DNA damage. Subsequent experiments *in vivo* demonstrated that such inhibition delays the onset of streptozotocin- and alloxan-induced diabetes[105,106].

More recent studies have implicated PARP-1 in a wide range of other local or systemic inflammatory conditions (summarised in Table 3). Inhibition of PARP-1 suppresses the development of rheumatoid arthritis[107], colitis[108] and respiratory inflammation[109-111] in rodent or mice models. Systemic inflammatory conditions, such as various forms of circulatory shock are associated with a reduced responsiveness of blood vessels to vasoconstrictor agents (a result of nitric oxide and peroxynitrite production), myocardial dysfunction and impaired intracellular energetic processes, culminating in multiple organ failure. Inhibition of PARP-1 significantly improves the survival rate of mice which have been injected with a high dose of endotoxin[97,112] and in septic shock induced by *E. coli*[113].

Experimental model	PARP-1 inhibitors	Effects of PARP-1 inhibition
Diabetes		
Rat	Nicotinamide & 3AB[105,106]	Pretreatment protects against alloxan- or streptozotocin-induced decrease in proinsulin synthesis
Arthritis		
Rodent	Nicotinamide[107]	Protection from potassium peroxochromate-induced arthritis
Colitis		
Mice (IL-10 gene-deficient: Crohn's disease model)	3AB[108]	Normalises colonic permeability, reduces tumour necrosis factor-α and interferon-γ secretion, reduces inducible nitric-oxide synthase expression, reduces nitrotyrosine levels, significantly attenuates inflammation.
Pulmonary inflammation		
Rodent	Benzamide[109] PJ34[110] 5AIQ[111]	Suppress NMDA receptor-mediated lung edema formation and endotoxin-induced or zymosan-activated plasma-induced lung injury
Endotoxin shock		
Rat	3AB[112] PJ34[97]	Significantly reduce the lipopolysaccharide-induced hyperpermeability in both organs, without affecting neutrophil deposition
Septic shock		
Pig (LD100 sepsis model)	PJ34[113]	Improve survival and maintain cardiac function

Table 3. *Effects of PARP-1 inhibitors in animal models of inflammatory-related diseases.*

3AB: 3-aminobenzamide

5AIQ: 5-aminoisoquinolin-1-one;

PJ34: *N*-(6-oxo-5,6-dihydro-phenanthridin-2-yl)-*N*,*N*-dimethylacetamide

1.8.4 PARP-1 inhibition in cancer treatment

Most anti-tumour agents and radiotherapy eliminate fast-growing tumour cells by disrupting DNA replication and halting the cell cycle. However the effectiveness of these treatments is often limited by the lack of selectivity for cancer cells. As a result, many rapidly dividing normal cells, such as bone marrow, gastrointestinal epithelial cells and endothelial cells, are damaged along with the tumour cells. As such, selective sensitisation of tumour cells to the cytotoxic effects of these agents is necessary. The rationale for the use of PARP-1 inhibitors as chemo- and radio-sensitisers comes from the observation that PARP-1 is important for DNA base-excision repair and its inhibition caused a significant delay in the DNA repair processes. Accordingly, PARP-1 inhibitors, by preventing tumour cell from repairing its DNA, would potentiate the cytotoxic effects of both chemo- and radio-therapeutic agents used in the treatment of cancer. Indeed, several lines of evidence now indicate that tumour cells can be sensitised by PARP inhibitors to *N*-methyl-*N*-nitrosourea, bleomycin, campthotecin, and ionising radiation-induced cytotoxicity[114-116]. The results are summarised in Table 4.

Many anti-tumour drugs can also induce oxidative stress in several tissues and trigger PARP-1-mediated cell dysfunction and organ injuries[117,118]. The use of PARP-1 inhibitors in combination with chemotherapeutic agents provides further advantage of attenuating their adverse effects without compromising their anti-tumour efficacy. For instance, PARP-1 inhibitors such as PJ34 and BGP-15 have demonstrated efficacy in counteracting doxorubicin-induced cardiotoxicity[117] and cisplatin-induced nephrotoxicity[118], respectively.

1.8.5 PARP-1 inhibition in HIV-1 infection

There is an increasing body of evidence suggesting the involvement of PARP-1 in HIV-1 infection. During the life cycle of the HIV-1 virus within the infected cell, the RNA genome of the virus is reverse-transcribed into double-stranded DNA by reverse transcriptase[119]. The proviral DNA, in turn, enters the nucleus, where the virion-associated viral enzyme, integrase, catalyses the integration of the viral double-stranded DNA into the host genome. This process requires nicking of both DNA strands and may therefore lead to PARP-1 activation. Indeed, increased PARP-1 activity of HIV-1-infected cells has been reported by Furlini *et al*[120], indicating that the HIV-1 life cycle may require poly(ADP-ribosyl)ation. Furthermore, two studies[121,122] independently showed that benzopyrone derivatives, benzamides and nicotinamide possessed potent antiviral effects in HIV-infected cells. At present, it seems that PARP-1 regulates HIV infection at two levels: integration and transcription[119] and PARP-1 inhibition may be a viable strategy in controlling HIV-1 infection.

1.8.6 Other diseases

Preliminary data also indicate the beneficial effects of PARP-1 inhibitors in a variety of other diseases including Parkinson's disease[123], Alzheimer's disease[124], endothelial dysfunction associated with ageing and hypertension[125], acetaminophen-induced hepatotoxicity[126] and UV radiation-induced dermal necrosis[127] (summarised in Table 4). The causative role of PARP-1 in these conditions has yet to be addressed in detail.

Experimental model	PARP-1 inhibitors	Effects of PARP-1 inhibition
Cancer treatment		
Gamma radiation	3AB[114] PND[115]	Enhance cytotoxicity of lymphoma cells
N-methyl-N-nitrosourea	3AB[114]	Potentiate cytotoxicity
Temozolamide	3AB, Benzamide, PD128763 & NU1025[116]	Potentiate cytotoxicity of murine leukaemia L1210 cells
Counteract side effects of cytotoxic drugs		
Doxorubicin	PJ34[117]	Prevent depression of left ventricular function
Cisplatin	BGP-15[118]	Prevent kidney dysfunction
HIV-1 infection	6ABP & INH2BP[121] Benzamides & Nicotinamide[122]	Inhibition of HIV-1 replication
Parkinson's disease	Benzamide[123] 3AB	Protect against MPTP-induced depletion of striatal dopamine and cortical noradrenaline
Diabetic endothelial dysfunction	PJ34[125]	Prevent diabetic endothelial dysfunction
Hepatotoxicity	Nicotinamide Benzamide[126]	Suppress acetaminophen-induced liver damage
Photodamage in skin	BPG-15[127]	Topical application reduce UV radiation-induced skin damage

Table 4. *Effects of PARP-1 inhibitors in cancer therapy, HIV-1 infection and other diseases.*

MPTP: 1-methyl-4-phenyl-1,2,3,6-tetrahydropyridine; **3AB**: 3-aminobenzamide;

PND: 6(5*H*)-phenanthridinone; **PD128763**: 3,4-dihydro-5-methylisoquinolin-1(2*H*)-one;

NU1025: 8-hydroxy-2-methylquinozolin-4(3*H*)-one;

PJ34: *N*-(6-oxo-5,6-dihydro-phenanthridin-2-yl)-*N*,*N*-dimethylacetamide;

BPG-15: *O*-(3-piperidino-2-hydroxy-1-propyl) pyridine-3-carboxylic acid amidoxime monohydrochloride; **6ABP**: 6-amino-1,2-benzopyrone;

INH2BP: 5-iodo-6-amino-1,2-benzopyrone

1.9 Possible side effects of PARP-1 inhibitors

The remarkable cytoprotective effects of PARP-1 inhibitors observed over a wide range of human diseases is very encouraging. However, before potent PARP-1 inhibitors can be used in humans, crucial safety issues must be addressed. It is noteworthy that human clinical trials with nicotinamide in Type I diabetic patients[128] represent the only example to date where a PARP-1 inhibitor has been administered to a human being. This is possible as nicotinamide is a vitamin (Vitamin B3), with an established safety profile in humans. Although several small Phase II trials gave promising results, one is unable to fully ascertain its effect in Phase III trial due to its low potency.

On the negative side is the pioneering work of Okamoto *et al*[104] who was the first group to point out that, since PARP-1 has been implicated in DNA repair and maintenance of genomic integrity, one possible risk associated with long-term PARP-1 inhibition might be an increase in mutation rate and cancer formation. In an elegant experiment, they showed that PARP inhibitors could prevent the onset of diabetes but the result of this intervention was the appearance of pancreatic tumours. However, Ménissier-de Murcia *et al*[129] did not find an excess of tumours in the PARP-1 deficient mice that they have constructed, indicating that whilst general inhibition of PARP lead to untoward effects, selective PARP-1 inhibition is relatively well tolerated.

PARP-1 inhibitors, in theory, may also interfere with the binding of NAD^+ to other enzymes that require NAD^+ for their functions, leading to various adverse effects. In addition, many of the PARP-1 inhibitors are planar cyclic systems (Figure 8). Such molecules are prone to DNA intercalation and may be associated with an increased risk of genotoxic effects. These possibilities further highlight the importance for the development of PARP-1 selective inhibitors.

1.10 Development of PARP-1 inhibitors

Intensive research, especially over the last decade, by both academic and pharmaceutical laboratories, has yielded multiple classes of PARP-1 inhibitors with hundreds of compounds, the vast majority of which bind to the nicotinamide binding domain of the enzyme and act as competitive, reversible inhibitors with respect to NAD^+, the natural substrate for PARP-1.

1.10.1 Nicotinamide and NAD^+-related compounds

The earliest compounds that were shown to inhibit PARP-1 bear structural similarities to NAD^+; these include nicotinamide **(3),** purine analogues [*e.g.* theophylline **(4)**] and pyrimidine analogues [e.g. 5-bromouridine **(5),** thymidine **(6)**][130]. However, it was quickly realised that these compounds were not very selective in their actions and many of them interfere with other cellular processes. Nicotinamide, for instance, served as substrates for NAD^+ metabolising enzymes such as nicotinamide-N-methyltransferase deaminase and phosphoribosyl transferase[131]. Thymidine, on the other hand, inhibits DNA synthesis *via* depletion of cellular dCTP level[130].

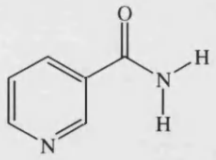

(3) IC_{50} 210 μM

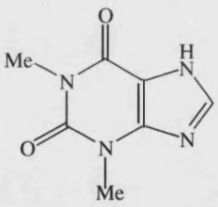

(4)

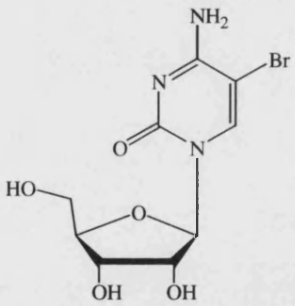

(5)

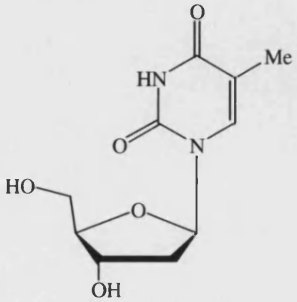

(6) IC_{50} 180 μM

1.10.2 Benzamide and 3-subsitiuted benzamides

Clearly, more selective PARP-1 inhibitors are required if they are to have any therapeutic application. This led to the discovery of benzamide (**7**), a close structural analogue of nicotinamide, by Shall in 1975[132]. Benzamide is more specific in its action because it lacks the ring nitrogen in nicotinamide and, therefore, cannot be metabolised by NAD^+ biosynthetic enzymes. However it suffers from poor water-solubility, given the hydrophobic nature of its structure. Good water solubility is a desirable feature in PARP-1 inhibitors because it facilitates their *in vivo* administration. Compounds that lack water solubility require other biocompatible vehicles. Often, dimethylsulphoxide (DMSO) is used; however, it is a potent scavenger of hydroxyl radicals and recent study also indicates that it inhibits PARP-1 activity[133]. This causes substantial problems in the experiment and makes any interpretation of results very difficult.

In an attempt to improve the aqueous solubility of benzamide, Purnell and Whish substituted the 3-position of benzamide with polar substituents[134]. This position corresponds to the location of the ring nitrogen in nicotinamide and, at this position, it is likely to bind with the ribose nucleoside-binding domain where they function as competitive inhibitors due to the lack of a cleavable C-N bond[135]. The 3-substituted benzamides, namely 3-aminobenzamide (**8**), 3-methoxybenzamide (**9**) and 3-hydroxybenzamide (**10**), were found to combine reasonably good water solubility with moderate PARP-1 inhibitory activity[136]. Although unlikely as drug candidates, they serve as powerful experimental tools in elucidating the biological role of PARP-1. They have also become the benchmark compounds against which all potential PARP-1 inhibitors were compared.

Benzamides

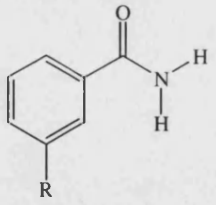

Code	R	IC_{50} (μM)
(7)	H	22.0
(8) [3AB]	NH_2	9.0
(9)	OMe	17.0
(10)	OH	9.10

Table 5. *PARP-1 inhibitory activity of benzamide and various 3-substituted benzamides*[136].

1.10.3 Structure activity relationship of PARP-1 inhibitors

The emergence of 3-substituted benzamides as prototype PARP-1 inhibitors has stimulated considerable interest in the structure activity relationship (SAR) of this class of compounds and a number of very detailed investigations by research groups working independently have been undertaken[136-139]. Inevitably, different assay methods and conditions have been utilised by different research groups in their evaluation of PARP-1 inhibitory activities and this caused considerable variations in the inhibition constants (IC_{50}, K_i, EC_{50}). As such, any direct comparison of the results is difficult and has left more or less inconclusiveness to the studies. In an attempt to account for such discrepancies, Banasik *et al*[136] conducted one of the most comprehensive evaluations to date where they compared more than 170 compounds from a variety of structural classes for their ability to inhibit PARP-1 using standardised assay methods. They found that all the strong PARP-1 inhibitors have a common structural motif: the **benzamide pharmacophore** (outlined in red, Figure 8) which mimics the nicotinamide portion of NAD^+ (1). This pharmacophore is thought to occupy the nicotinamide-binding site of PARP-1 and it consists of two important structural features: a **carboxamide function** and an **aromatic ring**.

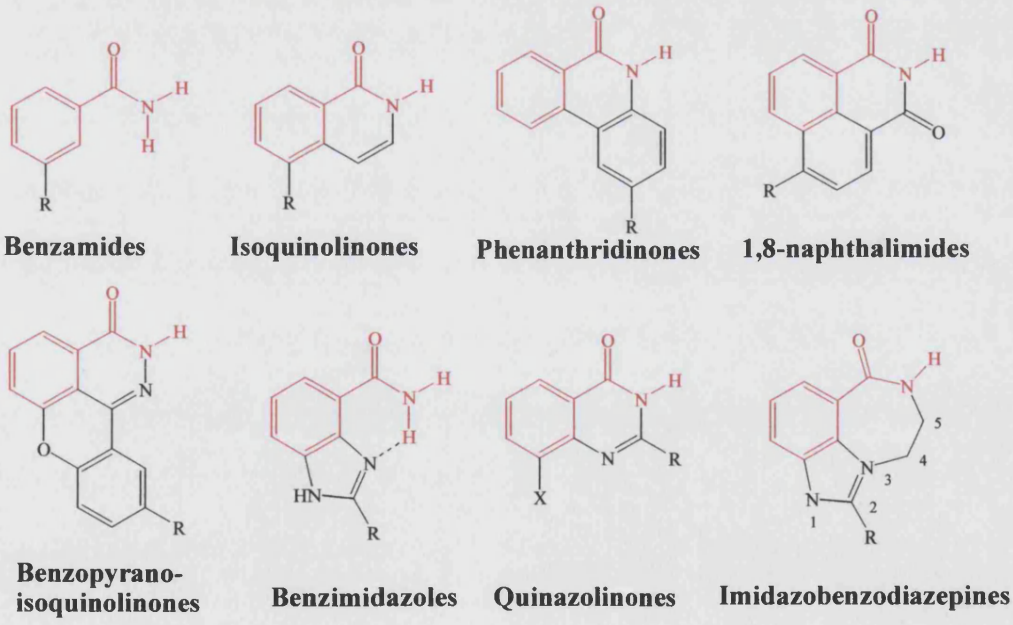

Figure 8. *The benzamide pharmacophore for PARP-1 inhibition.*

1.10.3.1 The carboxamide function

The presence of an unsubstituted carboxamide group was found to be an essential pre-requisite for significant activity. Removal or alteration of this amide moiety resulted in abrogation of activity in almost every instance. For example, replacement of the amide group in benzamide with a carboxylate **(11)**, a sulphonamide **(12)** or a thioamide group **(13)** resulted in a dramatic loss of activity[140], as did N-alkylation **(14)**[134]. The position of the carboxamide function, however, was less critical, with pyridine-2-carboxamide **(15)** and pyridine-4-carboxamide **(16)** both exhibiting activity comparable to that of nicotinamide **(3)**[137].

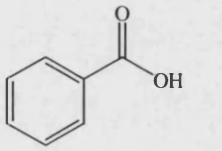

(11)

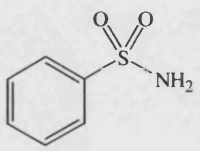

(12)

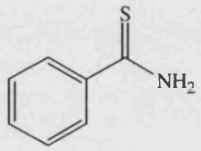

(13)

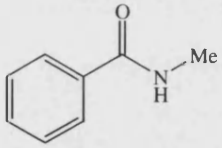

(14)

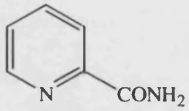

(15)

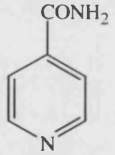

(16)

It is believed that the carboxamide forms hydrogen-bonds with the amino acid residues in the active site, which are crucial in holding the molecule in place within the domain. For such interaction to occur, the carboxamide group must be at the right conformation. In a compelling and elegant experiment to identify the active conformation, Suto *et al*[138] made a series of rigid benzamide analogues, the 3,4-dihydroisoquinolinones, by closing the amide nitrogen upon the benzene ring with an ethane bridge. They found that the 5-substituted dihydroisoquinolin-1-ones **(17a-d)**, where the carboxamide is in the *anti*-orientation, were 50 to 75 fold more potent than the 7-substituted *syn*-analogues **(18a-d)**. They were also significantly more potent than the unconstrained 3-aminobenzamide **(8)** (IC_{50} 9.0 μM) where equal population of both rotamers exist. To provide further evidence, they then synthesised a series of 2,3-disubstituted benzamides. These compounds had either a

hydroxyl or a methoxy group in the 3-position and various alkyl groups in the 2-position. All were found to be completely inactive except for 3-hydroxy-2-methylbenzamide which has only very weak activity (IC_{50} 590 μM). Energy calculation revealed that the presence of a 2-substituent restricts the rotation of the amide, causing them to exist predominantly in the less hindered, nevertheless inactive *syn*-conformation. Hence Suto clearly demonstrated that the biologically active conformation is one where the carboxamide group is orientated in such a way that the carbonyl group is anti to the 1,2-bond of the ring i.e. *anti*-conformation.

Dihydroisoquinolinone derivatives

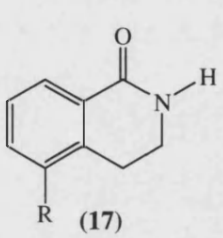

(17)

Active *anti*-conformation

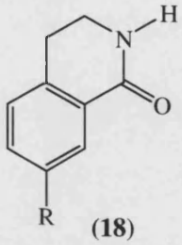

(18)

Inactive *syn*-conformation

Code	R	IC_{50} (μM)
17a	NO_2	3.2
18a	NO_2	13
17b	OMe	0.42
18b	OMe	120
17c	NH_2	0.41
18c	NH_2	8.0
17d	OH	0.10
18d	OH	9.5

2,3-Disubstituted benzamides

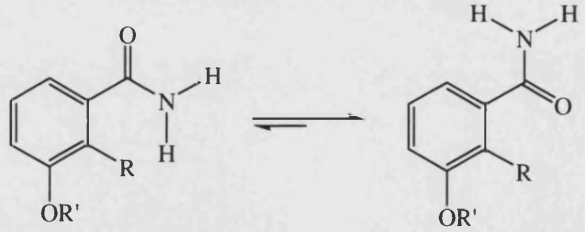

Active *anti*-conformation

Inactive *syn*-conformation
Preferred conformation

R = Me, Et, Propyl
R' = H or Me

Figure 9. *Conformational study on dihydroisoquinolinone and benzamide PARP-1 inhibitors*[138].

1.10.3.2 The aromatic ring

The aromatic ring is also crucial for PARP-1 inhibitory activity. Whilst the saturated analogue of benzamide, cyclohexanecarboxamide, was found to be devoid of activity, addition of a ring nitrogen was well tolerated, with pyrazinamide displaying similar inhibitory potency to that of nicotinamide **(3)** (IC_{50} 210 μM)[137]. In contrast to earlier reports which showed that replacement of the benzene ring with a thiophene ring in thiophene-3-carboxamide reduced the inhibitory potency, a recent study by Shinkwin *et al*[157] demonstrated that the isomeric thiophene-2-carboxamide displayed good PARP-1 inhibition, with potency of the same order of magnitude as benzamide. Similar inhibitory activity was also observed for thieno[3,4-*c*]pyridin-4(5*H*)-ones **(19)** and thieno[3,4-*d*]pyrimidin-4(3*H*)-ones **(20)**, which are heterocyclic analogues of isoquinolin-1(2*H*)-ones **(23)** and quinazolin-4-ones **(31)** respectively, thus demonstrating that the heterocyclic ring can indeed substitute for the benzene ring without significant loss in PARP inhibitory potency.

It was postulated that the presence of an electron-rich aromatic ring enhanced the ability of the carbonyl group to participate in hydrogen-bonding within the active site[40]. In addition, there is also non-polar interaction between the aromatic ring and the active site. Such interaction might contribute to the increased activity of the larger, planar fused ring molecule such as isoquinolinones[40].

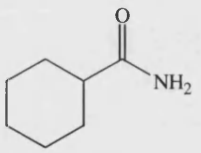

cyclohexanecarboxamide

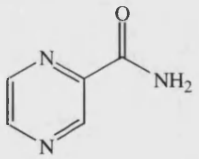

pyrazinamide

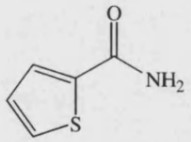

thiophene-2-carboxamide

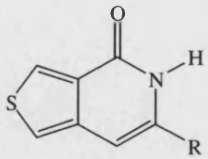

(19)

R = Me or Ph

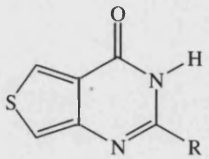

(20)

R = Me or Ph

The positioning of the substituents on the benzene ring was also found to be critical for optimal activity. When the substituent in 5-substituted dihydroisoquinolinones was moved to the 6, 7 or 8 position (which corresponds to position 4, 5 and 6 of benzamides respectively), activity was decreased[138] (Table 6). It was believed that substituents at the 5-position (or 3-position of benzamides) was accommodated within the ribose-nucleoside binding domain. In contrast to the substrates NAD^+, these compounds are incapable of undergoing analogous C-N bond cleavage, thus serving as competitive inhibitors.

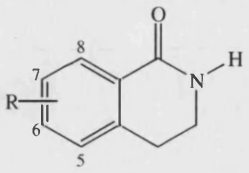

R	IC_{50} (μM)
5-OH (**17d**)	0.10
6-OH	2.0
7-OH	9.5
8-OH	11
5-OMe (**17b**)	0.42
6-OMe	39
7-OMe	120

Table 6. *Effects of substituents on various positions of the aromatic ring*[138].

In summary, the following structural features are essential for PARP-1 inhibition (Figure 10):

1. An unsubstituted aromatic or polyaromatic heterocyclic system.
2. A carboxamide group which is restricted into the *anti*-conformation.
3. Presence of at least one amide proton.
4. A non-cleavable bond at the position corresponding to the 3-position of benzamides.

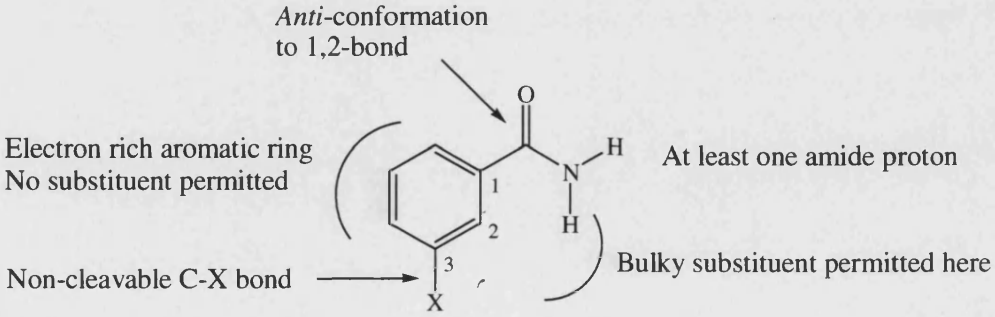

Figure 10. *Structure activity relationship for inhibitors of PARP-1*[40].

The availability of X-ray crystallographic structures of the catalytic fragment of PARP-1, and those crystallised with competitive inhibitors, such as PD128763 (**22f**), NU1025 (**31d**) and 3-methoxybenzamide (**9**) have helped confirmed the above SAR scheme and enabled us to rationalise it on a structural basis[141-143]. It was found that in all the above PARP-1-inhibitor crystal structures, the position of binding is similar *i.e.* in the nicotinamide sub-site of the NAD^+-binding domain of PARP-1. This is represented by the motif found for PD128763 (Figure 11). The carboxamide group invariably forms three important hydrogen-bonds: The inhibitor carbonyl oxygen accepts two hydrogen bonds, one from the side chain of Ser904, the other from Gly863 polypeptide amide NH. The third hydrogen-bond is formed between the carboxamide NH and Gly863 carbonyl oxygen. In addition, a parallel tyrosine residue (Tyr907) within the active site interacts with the planar aromatic portions of the inhibitors, presumably through π-π interactions, forming a "π-electron sandwich". This accounts for the propensity for planar aromatic compounds to bind to the active site.

Additional interactions between the inhibitors and the active sites were also observed and these were specific for specific classes of inhibitors, accounting for greater potencies. For instance, interaction between Glu988 and the methyl carbon atom of PD128763 (**22f**) was observed[142]. This glutamate catalyses PARP-1 activity by serving as a general base which activates the acceptor protein for nucleophilic attack at the C-1 of the nicotinamide ribose. It also stabilises the intermediate oxocarbenium ion formed from the cleavage of ribose-nicotinamide bond of NAD^+ (Section 1.4.1).

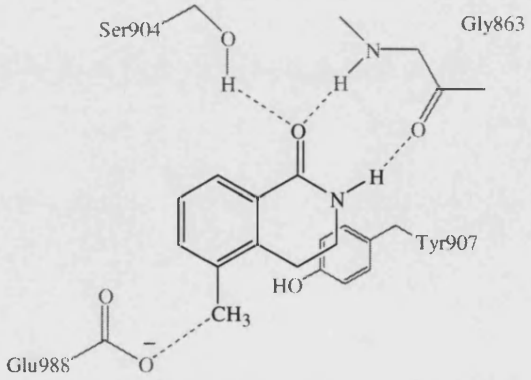

Figure 11. *Enzyme-inhibitor interaction between PARP-1 catalytic fragment and PD128763 (**22f**)*[143].

1.10.4 Dihydroisoquinolinones and isoquinolinones

As a result of Suto's studies, numerous structural modifications have been made to the parent dihydroisoquinolinone and isoquinolinone, giving rise to a great number of highly potent and selective PARP-1 inhibitors. The most potent inhibitor identified in these two classes of compounds are DPQ (**22g**) [91,93,144], which was recently patented by Guilford Pharmaceuticals, and 5-hydroxyisoquinolin-1-one (**23e**)[138] respectively. It was believed that the structurally flexible butoxy-piperidine side chain at the 5-position of DPQ favours its insertion into the hydrophobic pocket within the active site, thereby increasing its potency tremendously. Other compounds of great therapeutic interest are PD128763 (**22f**)[116,145,146] and 5AIQ (**23d**)[86,98,101,103,111].

Dihydroisoquinolinones (22)

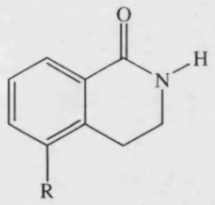

Code	R	IC_{50} (μM)[1]
17a	NO_2	3.2
(a) [DHIQ]	H	1.5
17b	OMe	0.42
17c	NH_2	0.41
(f) [PD128763]	Me	0.14
17d	OH	0.10
(g) [DPQ]	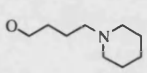	0.04

Isoquinolinones (23)

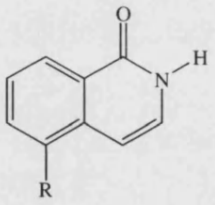

Code	R	IC_{50} (μM)
(a)	H	6.2
(b)	NO_2	3.2
(c)	OMe	0.58
(d) [5AIQ]	NH_2	0.24
(e)	OH	0.14

Table 7. *PARP-1 inhibitory activity of various 5-substituted dihydroisoquinolinones and isoquinolinones*[138].

1.10.5 Isoquinolinones-related compounds

The isoquinolinone core is also present in various tricyclic and tetracyclic compounds such as phenanthridinones (**24a-c**), thieno[2,3-c]isoquinoline (**25a-d**) (SKB), 1,8-naphthalamide (**26a & b**)[136] and benzopyrano[4,3,2-de]isoquinolinones (**27, 28a-c**). Among these compounds, PJ34 (**24c**)[89,94,97,101,110,113,117,125] (INOTEK Pharmaceuticals) and GPI-6150 (**27**)[96,147] (Guilford Pharmaceuticals) have been extensively studied and published.

Phenanthridinones (24)

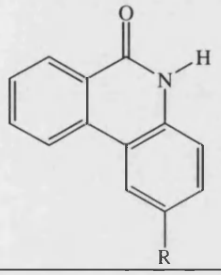

Code	R	IC_{50} (μM)
(a) [PND]	H	0.30
(b)	NO_2	0.35
(c) [PJ34]	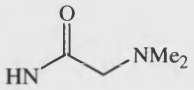	0.04 (EC_{50})

Thieno[2,3-c]isoquinolines (25)

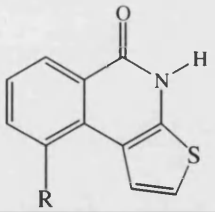

Code	R	IC_{50} (μM)
(a)	H	0.30
(b)	OMe	0.30
(c)	OH	0.10
(d)	NH_2	0.05

1,8-Naphthalamides (26)

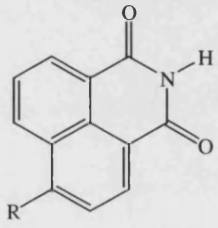

Code	R	IC_{50} (μM)
(a)	H	1.4
(b)	NH_2	0.18

Benzopyrano[4,3,2-de]isoquinolinones

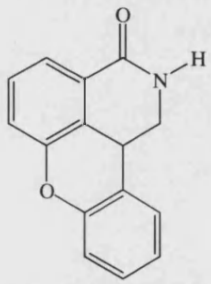

(27) [GPI-6150]
IC_{50} = 0.060 μM

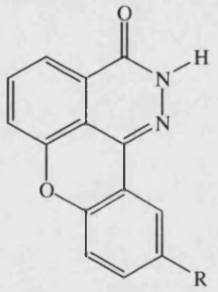

(28)

Code	R	IC_{50} (μM)
(a)	H	0.080
(b)	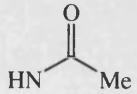	0.038
(c)		0.028

Table 8. *PARP-1 inhibitory activity of isoquinolinone-related compounds.*

1.10.6 Benzoxazoles and benzimidazoles

On the basis of currently accepted structural requirements for PARP-1 inhibition, in particular the need for an *anti* disposition of the amido moiety, researchers at the University of Newcastle-upon-Tyne designed a series of benzoxazole-4-carboxamides[135] and benzimidazole-4-carboxamides[148] compounds that elegantly favoured the active *anti*-conformation by means of an intramolecular H-bonding between the amide proton and the cyclic nitrogen. These compounds possess good donor properties by virtue of the electron-rich heterocycle and they exhibit potencies superior to those usually shown by monocyclic carboxamides, with IC_{50} values ranging from 1 to 10 μM. In general, benzimidazole analogues are a few times more potent than the corresponding benzoxazoles. Compounds with substituted phenyl group at 2-position, such as **(29b)**, **(30e)** and **(30f)** are the most potent examples in these classes of inhibitors.

Benzoxazole-4-carboxamides (29)

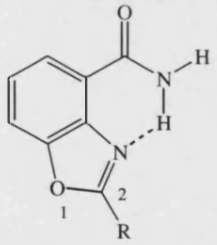

Code	R	IC_{50} (μM)
(a)	Me	9.5
(b)	Ph	0.44

Benzimidazoles-4-carboxamides (30)

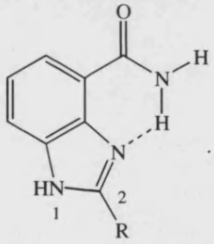

Code	R	K_i (nM)
(a)	H	95
(b) **[NU1064]**	Me	99 (IC_{50} 1.0 μM)
(c)	Ph	15
(d)	4-CF_3-Ph	350
(e)	4-Cl-Ph	3
(f)	4-CH_2OH-Ph	1.6

Table 9. *PARP-1 inhibitory activity of benzoxazole-4-carboxamides and benzimidazole-4-carboxamides.*

1.10.7 Quinazolinones and phthalazinones

During initial attempts at the synthesis of benzoxazole-4-carboxamides, an unexpected rearrangement, which resulted in the formation of quinazolinone derivatives, occurred[149]. These compound were then assayed for inhibitory activities against PARP-1 and were found to be very potent, particularly 8-hydroxyquinazolinones, such as (NU1025) **(31d)** and (NU1057) **(32d)**[116,135]. In general, those with substituted phenyl at the 2-position are also more active. Juxtaposition of the second ring nitrogen of quinazolinones gives rise to another class of PARP-1 inhibitor, the phthalazinones. KuDOS Pharmaceuticals tested various 4-benzyl analogues of phthalazinone **(33a)**. Most of the 52 compounds tested had IC_{50} values between 0.3-2 μM, **(33c)** (IC_{50} 0.04 μM) being the exception[150].

Quinazolinones (31)

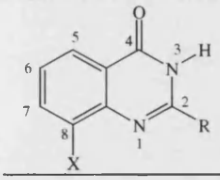

Code	X	R	IC_{50} (μM)
(a)	H	H	9.50
(b)	OMe	Me	0.78
(c)	Me	Me	0.39
(d) [NU1025]	OH	Me	0.40

Phthalazinones (33)

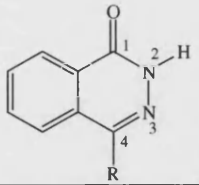

Code	R	IC_{50} (μM)
(a)	H	7.2
(b)	Benzyl groups	2-0.3
(c)	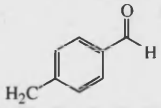	0.04

2-Phenyl substituted quinazolinones (32)

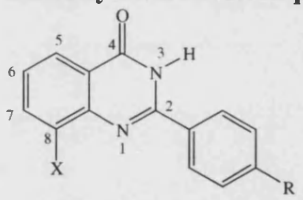

Code	X	R	IC_{50} (μM)
(a)	OH	H	1.06
(b)	OH	NH_2	0.52
(c)	OH	OH	0.29
(d)[NU1057]	OH	NO_2	0.23
(e)	OMe	CF_3	39
(f)	OMe	H	4.2
(g)	OMe	OMe	2.0
(h)	OMe	CN	1.34
(i)	OMe	NO_2	0.85
(j)	Me	H	0.87
(k)	Me	NH_2	0.44
(l)	Me	OH	0.22
(m)	Me	CN	0.27
(n)	Me	OMe	0.19
(o)	Me	NO_2	0.13
(p)	Me	CF_3	> 10

Table 10. *PARP-1 inhibitory activity of quinazolinones and phthalazinones.*

1.10.8 Benzimidazole-related compounds

A natural extension of the benzimidazole class of compounds is to replace the hydrogen-bond that encourages the *anti*-conformation with a covalent bond. This gave rise to hundreds of tricyclic PARP-1 inhibitors based on indole (**dihydrodiazepinoindolinones** and **tetrahydroazapinoindolinones**)[151] and benzimidazole (**imidazobenzodiazepines**)[152,153] structures (Table 11).

Surprisingly, these 7-membered derivatives are no more potent than the benzimidazoles. This may be ascribed to a shift in the orientation of the amido group, which reduces its ability to form productive H-bonding with the active site[154]. As with benzimidazole-4-carboxamides, substituted phenyl groups at C-2 enhances potency over the parent structures, with K_i in the low nM range (1-100 nM)[153]. Potency could be further increased if the 2-phenyl substituents were attached *via* a preferably unsubstituted, ethylene bridge (compare K_i of **(36c)** with that of **(36h)**). However, substituents bulkier than these tends towards higher K_i values **(36h-j)**.

1.10.9 Isoindolinones

Another class of PARP-1 inhibitors, isoindolinones, incorporate the requisite lactam in a 5-membered ring. The simple 5-substituted derivatives **(39)** have only poor potency (IC_{50} > 10 μM) but more elaborate side chains improve activity. Since Guilford's claim on the tetracyclic isoindolinones **(40)**, polycycles incorporating the isoindolinone group have been published, a vast majority of which have IC_{50} values below 100 nM.

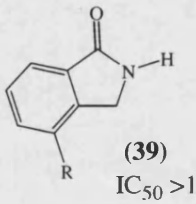

(39)
IC_{50} >10 nM

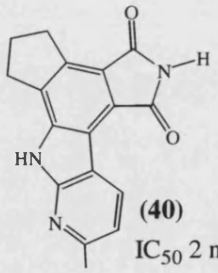

(40)
IC_{50} 2 nM

Dihydrodiazepinoindolinones (34)

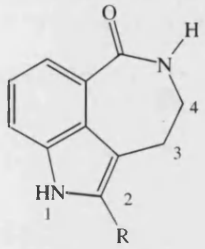

Code	R	K_i (nM)
(a)	H	38 (IC_{50} 366 nM)
(b)	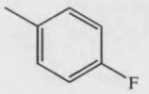	4
(c)	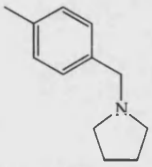	4
(d)	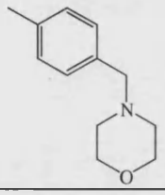	9

Tetrahydroazapinoindolinones (35)

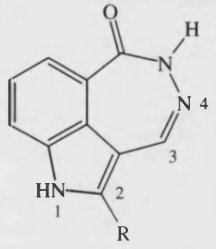

Code	R	K_i (nM)
(a)	H	(IC_{50} 18 nM)
(b)	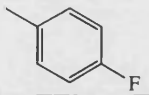	1

Imidazobenzodiazepines (36)

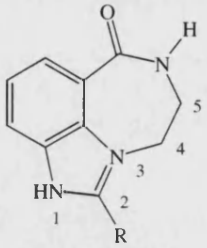

Code	R	IC_{50} (nM)
(a)	H	300
(b)	Me	140
(c)	Ph	90
(d)	2-Me-Ph	330
(e)	3-Me-Ph	97
(f)	4-Me-Ph	110
(g)	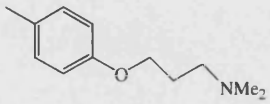	63
(h)	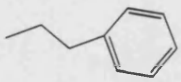	26
(i)		97
(j)	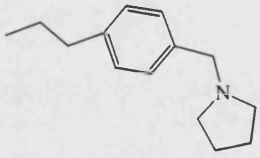	68
(k)	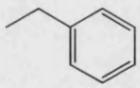	108
(l)	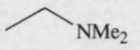	66
(m)	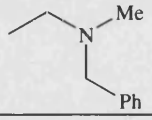	88

Table 11. *PARP-1 inhibitory activity of selected benzimidazole-related compounds.*

1.10.10 Miscellaneous classes of compounds

While much development centred around the lactam or carboxamide pharmacophore, there are several groups of compounds that do not possess this functionality. Most of these are inhibitors of moderate potency compared to those discussed above and they have very different modes of action. For instance, 5-iodo-6-amino-1,2-benzopyrone (INH2BP) **(41)** inhibits PARP-1 by uniquely oxidising one of its two zinc fingers, resulting in zinc ion ejection and a concomitant inactivation of its activity[155]. Other examples include aryl carboxylic acids containing a 4-*t*-butylbenzene-1,2-diol fragment **(42)** and coumalic acid derivatives **(43)**[150].

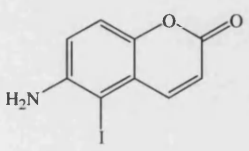

(41) IC_{50} 10 μM

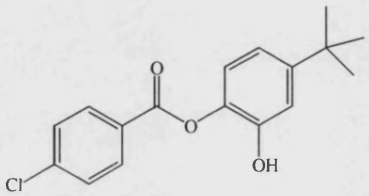

(42) IC_{50} 2.2 μM

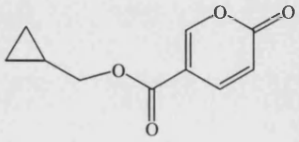

(43) IC_{50} <10 μM

1.10.11 Approaches to irreversible PARP-1 inhibitors

Watson *et al*[158] has recently proposed a design for a mechanism-based irreversible inhibitor of PARP-1. According to the accepted mechanism for PARP-1-catalysed formation of poly(ADP-ribose) from NAD^+ (Figure 4), a benzamide or isoquinolin-1(2*H*)-one with an electrophilic substituents at the 3- or 5-position respectively may trap the attacking glutamate residue (during initiation) or the ribose hydroxyl in ADP-ribosyl moiety (during polymerisation), thus capping the polymer or it may react with other appropriately placed nucleophile within the active site of PARP-1, leading to a blockage of the binding site (Figure 12).

However, subsequent bioassays of a series of 3-substituted benzamide and 5-substituted isoquinolin-1(2*H*)-one showed that these compounds were not acting as time-dependent irreversible inhibitors of PARP-1 as they did not observe any

increase in PARP-1 inhibitory activity when the enzyme was pre-incubated with the inhibitor for different time intervals up to 30 min before the assay was started. Nevertheless, they identified 5-iodoisoquinolin-1(2*H*)-ones and 5-bromoisoquinolin-1(2*H*)-ones as particularly potent PARP-1 inhibitors, with virtually total abolition of enzymatic activity at a concentration of *ca.* 10 μM.

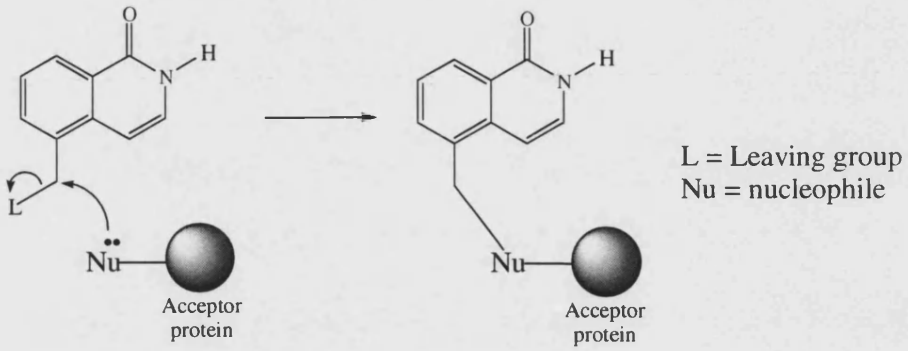

Figure 12. *Proposed mechanism-based irreversible inhibitor of PARP-1*[158].

1.11 Challenges

A better knowledge of the SAR of PARP-1 inhibitors and computer-aided drug design has greatly accelerated drug discovery. The extensive work of the last few years has seen the emergence of several classes of highly potent PARP-1 inhibitors with 10 to 1000-fold increase in potency compared to those compounds described by Banasik ten years ago. Though an increased in potency can be considered a good starting point for the pharmaceutical development of PARP-1 inhibitors, other equally important factors, such as biodistribution and water-solubility should also be considered. However in the passionate quest for greater potency, relatively much less effort has been expended on these areas. To address these challenges, recent works in our laboratory have led to the development of PARP-1 inhibitors with improved biodistribution[159-161] as well as highly water-soluble PARP-1 inhibitors[103].

1.11.1 Bioreductive prodrugs of PARP-1 inhibitors

The inspiration for improvement of the biodistribution of PARP-1 inhibitors came from the observation that many disease states where PARP-1 inhibition is therapeutically beneficial, such as cancers, inflammatory disorders and ischaemia-reperfusion injuries are marked by acute or chronic tissue hypoxia. Such a physiological difference in the concentration of oxygen between normal and hypoxic tissues was being exploited through design of biologically inactive prodrug systems which, upon selective bioreduction in hypoxic tissue, would release PARP-1 inhibitors only in that tissue. This would improve greatly the selectivity of biodistribution and consequently reduce the dosage required for therapy. Four different types of redox-sensitive triggers were designed and the proposed mechanism for bioreductive release of PARP-1 inhibitors (DRUG) from nitroheterocyclylmethyl Trigger[159, 160] and 4,7-dioxoindole-3-methyl Trigger[161] were illustrated in Figure 13 and Figure 14 respectively.

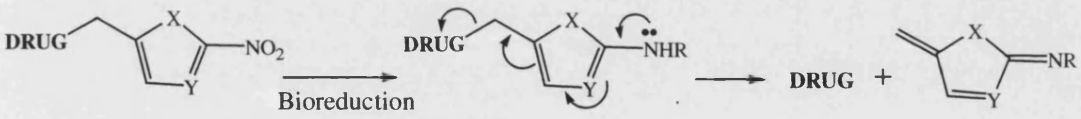

a: X = O, Y = CH
b: X = MeN, Y = N
c: X = S, Y = CH

R = H or OH

Figure 13. *Proposed mechanism of reductively triggered release of drugs from 5-nitrofuran-2-ylmethyl (a), 1-methyl-2-nitroimidazole-5-ylmethyl (b) and 5-nitrothien-2-ylmethoxy (c) prodrugs*[159, 160].

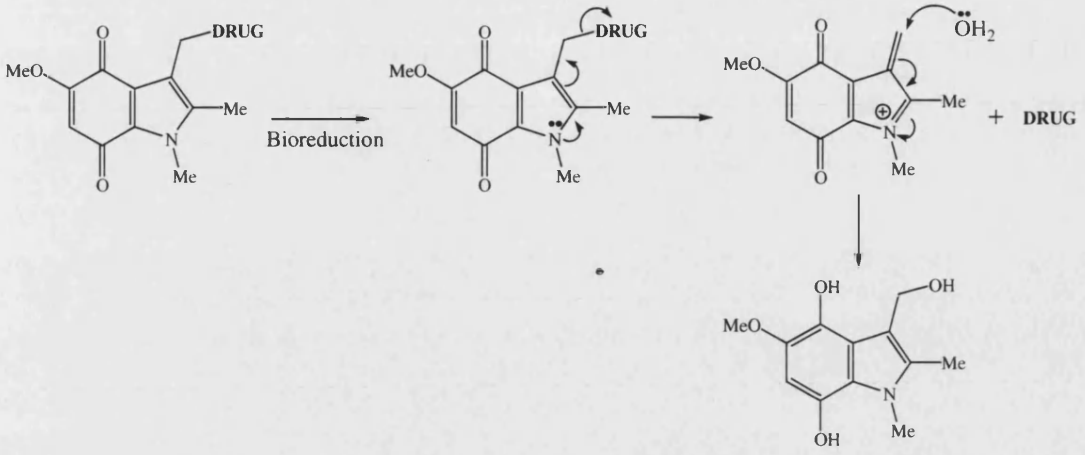

Figure 14. *Proposed mechanism of reductively triggered release of drugs from 4,7-dioxoindole-3-methyl prodrugs*[161].

In view of the high inhibitory potency of 5-iodo- and 5-bromoisoquinolin-1(2*H*)-ones[158], these inhibitors were chosen as the DRUG for linkage to the Triggers. Since the PARP-1 inhibitory activity of isoquinolin-1(2*H*)-ones depends critically on the benzamide group, masking of the pharmacophore was achieved either by attachment of the Trigger at oxygen (giving 1-alkoxyisoquinolinones) or at nitrogen (giving 2-alkylisoquinolin-1-ones) as shown below.

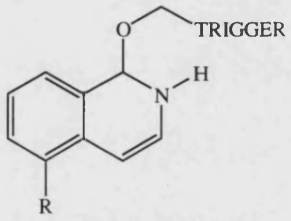

1-alkoxyisoquinolinones

R = H, I or Br

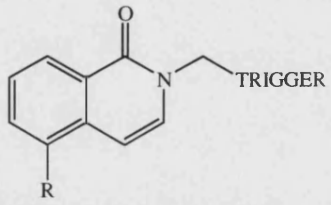

2-alkylisoquinolin-1-ones

Their release studies, performed with reductant systems that were designed to mimic the bioreduction of heterocyclic nitro groups in hypoxic tissues, indicated a successful expulsion of 5-substituted isoquinolin-1-ones from 1-(5-nitrothien-2-ylmethoxy)isoquinolines and 2-(5-nitrofuran-2-ylmethyl)isoquinolines upon reductive triggering with sodium borohydride/ palladium/ aqueous propan-2-ol system. Isoquinolin-1-ones

were also found to be rapidly and quantitatively released from their 2-(1-methyl-2-nitroimidazole-5-ylmethyl)- and 1-(4,7-dioxoindole-3-methoxy) derivatives by treatment with with zinc/ ammonium chloride and tin(II) chloride respectively. Thus, our laboratory has successfully developed highly effective prodrugs for the selective delivery of PARP-1 inhibitors to hypoxic tissues.

1.11.2 Water-soluble PARP-1 inhibitors

It is noteworthy that the planar cyclic systems that appear to be so critical for PARP-1 inhibition, unfortunately, also make the molecule highly water-insoluble. Many of the potent PARP-1 inhibitors, such as 5-hydroxydihydroisoquinolin-1-one **(17d)**, DPQ **(22g)**, PND **(24a),** GPI-6150 **(27)** and INH2BP **(41)** have very poor water-solubility and this gives rise to various inherent practical problems.

As mentioned earlier in section 1.10.2, DMSO is often used in place of water as a biocompatible vehicle for *in vivo* administration. However, it is a potent scavenger of hydroxyl radicals. Thus it is able to reduce the organ injury and dysfunction in situations where the production of hydroxyl radicals is observed, such as haemorrhagic and endotoxic shock. Moreover, DMSO itself also inhibits PARP-1 activity[133]. This causes a great amount of ambiguity in the determination of the actual PARP-1 inhibitory activity of the compound in question. In addition, low water-solubility may also present formulation problems later in the drug development process.

Our laboratory has recently described a new, reliable and efficient synthesis of the known PARP-1 inhibitor 5AIQ **(23d)** (IC_{50} 0.24 μM)[103]. This inhibitor, which was only sparingly soluble in water, was then converted to its highly water-soluble hydrochloride salt, 5AIQ.HCl, and subsequently we, in collaboration with Professor Christoph Thiemermann and other research groups, proceeded to investigate its pharmocological effects in a wide range of diseases *in vivo*, including animal models of myocardiac

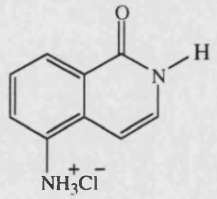

5AIQ.HCl

infarction[86], ischaemia-reperfusion of the liver[98] and kidney[156], heart transplantation[101] and acute lung inflammation[111]. In all these studies, 5AIQ.HCl was found to exhibit tremendous therapeutic benefits. Particularly noteworthy are its protective effects on ischaemia-reperfusion injury caused by severe haemorrhage and resuscitation in anaesthetized rats where it demonstrated exceptional potency in abolishing multiple organ injury and dysfunction[103]. Compared to other PARP-1 inhibitors such as 3-aminobenzamides **(8)** (10 mg Kg^{-1} i.v.) and 5-hydroxyisoquinolin-1(2*H*)-one **(17d)** (1-3 mg Kg^{-1} i.v.), only a remarkably low i.v. dose of 0.03 mg Kg^{-1} is required to confer similar protection. The concentration at which 5AIQ.HCl provides protection against oxidative injury (0.1-0.3 μM) *in vitro* does not appear to be consistent with its unusually high *in vivo* efficacy. It appears that 5AIQ.HCl gains much of its advantage over other PARP-1 inhibitors through its excellent water-solubility, which conferred it with favourable pharmacokinetics, such as good bioavailability and biodistribution.

These pioneering works, with their greatly promising results, set the stage for our present research.

Aims and Objectives

2.1 Aims of the research

The aim of this research is to design and to synthesise potent, selective and water-soluble PARP-1 inhibitors using currently established SAR.

2.2 Research proposal

Armed with highly encouraging potency *in vivo*, enzyme selectivity and the very good water-solubility of 5AIQ.HCl, we decided to build upon this lead by designing and synthesising a series of related inhibitors which are novel. The important design criteria are high selectivity and potency, while retaining the excellent biopharmaceutical properties. As such, the 5-amino group, which enables 5AIQ to be easily converted into the water-soluble hydrochloride salt and consequently giving it excellent *in vivo* potency, will be retained in the design.

Previous studies on the dihydroisoquinolin-1(2*H*)-one and isoquinolin-1(2*H*)-one classes of PARP-1 inhibitors centred around modifications at the 5, 6, 7 or 8-position[138,158] and, to date, very little is known about the effects of substituents on the 3- and 4-positions on their PARP-1 inhibitory activity. However, X-ray crystallographic data from other classes of PARP-1 inhibitors, such as quinazolinones **(31)** and phthalazinones **(33)**, seemed to suggest that substituents may be permitted at these regions and that they probably bind to the hydrophobic pockets[142,149]. Thus an introduction of substituents (alkyl and aryl) at the 3- or 4-position of 5AIQ may further improve its potency through an increased interaction with the active site. This has, therefore, led us to the investigation of a series of 3-substituted **(44)** and 4-substituted isoquinolin-1(2*H*)-one hydrochlorides **(45)**, with

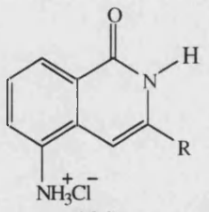

(44)

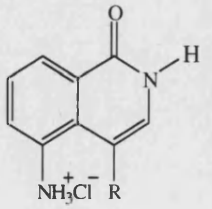

(45)

R = alkyl or aryl

particular emphasis on the former.

The proposed target compounds have many desirable structural properties. It contains the benzamide pharmacophore which is considered an essential pre-requisite for significant PARP-1 inhibitory activity (Figure 10). In addition, the amide function is incorporated into an aromatic, heterocyclic fused ring.

1. This restricts the amide group at an *anti*-conformation which is the orientation required for hydrogen-bonding with the active site.

2. The presence of the electron-rich aromatic ring system will further enhance the ability of the carbonyl group to participate in hydrogen-bonding.

3. A large, planar fused ring will also increase the non-polar interaction between the aromatic ring and the active site and possibly contributing to an increased potency.

Recent X-ray crystallographic data have also demonstrated possible hydrogen-bonding between Glu988 and the amino group of 4-amino-1,8-naphthalimide **(26b)**[142]. Since this corresponds, approximately, to the 5-position of 5AIQ, it is likely that the 5-amino group in 5AIQ may also display similar interactions with the active site, thereby contributing to its exceptional PARP-1 inhibitory potency *in vivo*. It is therefore of interest briefly to examine this interaction through the synthesis of an *N*-substituted 5AIQ **(46)**.

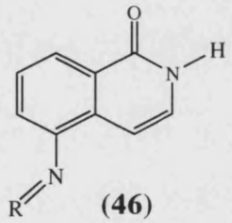

(46)

It was intended that these novel target compounds be initially tested for their water solubility and their *in vitro* PARP-1 inhibitory potency. This would allow a systematic analysis of the SAR on the effects of substituents at the 3-position of this class of compounds, through which further structural refinement for greater potency may be achieved. Selected inhibitors will subsequently be evaluated for their *in vivo* protective ability in various disease models in animals, especially their effects against ischaemia-reperfusion injury and inflammatory disorders.

Results and Discussions

3.1 3-Substituted 5-aminoisoquinolin-1(2*H*)-ones

3.1.1 Retrosynthetic analysis

The first series of target compounds that were investigated were the 3-substituted 5-aminoisoquinolin-1(2*H*)-ones. In designing our synthetic strategies, conscious effort was being made to ensure sufficient versatility to allow for a great variety of substituents (alkyl and aryl substituents of various electronic and steric nature) to be attached at the 3-position *via* a common synthetic route. Ideally, diversification should occur at a late stage of synthesis to avoid inefficient repetition of synthetic steps. Thus, preparative methods that call for a late disconnection of 3-substituents and those that are not generally amenable for the convenient introduction of substituents at the 3-position, such as reduction of phthalides[162], ozonisation of indenes[163] and oxidation of isochromans[164] were not considered.

Retrosynthetic analysis of our 3-substituted target gave the pathway as illustrated in Scheme 1. We approached our retrosynthesis by first performing two functional group interconversions (FGI) on the target molecule and this led us to the corresponding 5-nitroisocoumarin (**47**). These conversions are reasonable, as both the reduction of the nitro group to amine (*e.g. via* hydrogenolysis or acid/metal reduction) and the conversation of isocoumarin to isoquinolin-1(2*H*)-one (*e.g.* by treatment with boiling ammonia-saturated 2-methoxyethanol) are well-established reactions that are highly reliable and efficient. Though the nitro group, being highly electron-withdrawing, is likely to reduce the reactivity of the aromatic ring towards electrophilic attack and should, in most cases, be disconnected first, we reasoned that an incorporation of nitro group during the beginning of synthesis will avoid the need for subsequent regioselective nitration of the 3-substituted isocoumarin or isoquinolin-1(2*H*)-one ring.

The challenge, then, was to devise a synthetic strategy for the construction of the isocoumarin (**47**). Disconnection at the C-O bond of the isocoumarin as shown, *i.e.*, ring opening is rational because the reverse lactonisation process is a very fast reaction, easily accomplished, for instance, through the use of an acid catalyst. This took us to back to synthon (**48**) which may be disguised in the form of an aryl alkyne (**49**) or an alkene with a leaving group attached (**50**).

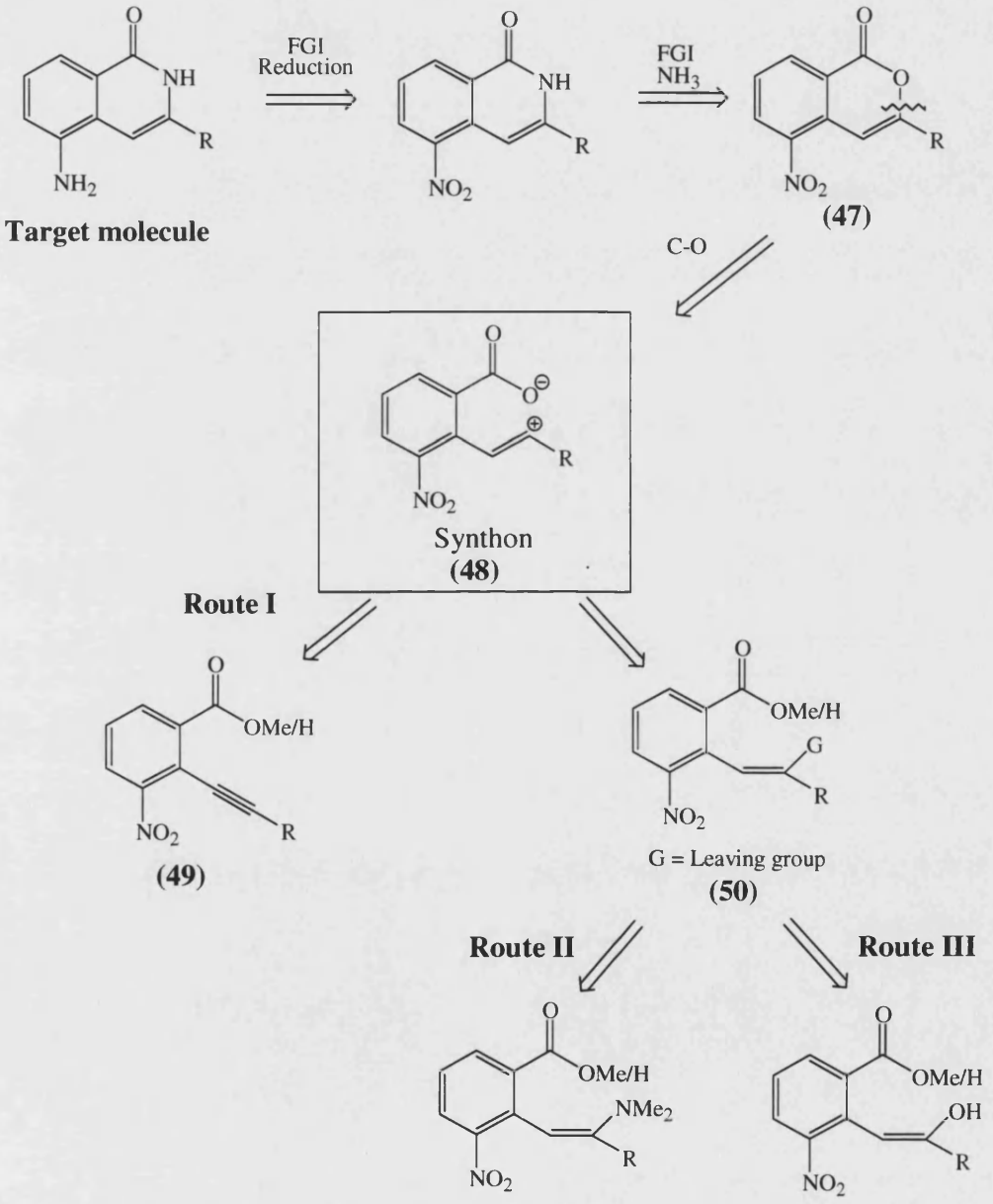

Scheme 1. *Retrosynthetic analysis of the 3-substituted target.*

3.1.2 Route I: aryl alkyne formation

Route I requires the formation of functionalised aryl alkynes **(49)** (Scheme 2) which is most reliably and conveniently achieved using organometallic approaches. A number of aryl-alkyne coupling methodologies have been developed over the past few decades and the most widely exploited methods involved the reaction of aryl halides or triflates with terminal alkynes under palladium or palladium/copper catalysis, such as Sonogashira coupling reaction and alkyne version of Heck coupling reaction[165]. Alternatively, coupling reactions with metallated (tin, zinc) alkynes under palladium catalysis, such as Negishi alkynylation[166] have also been satisfactorily applied in a number of cases.

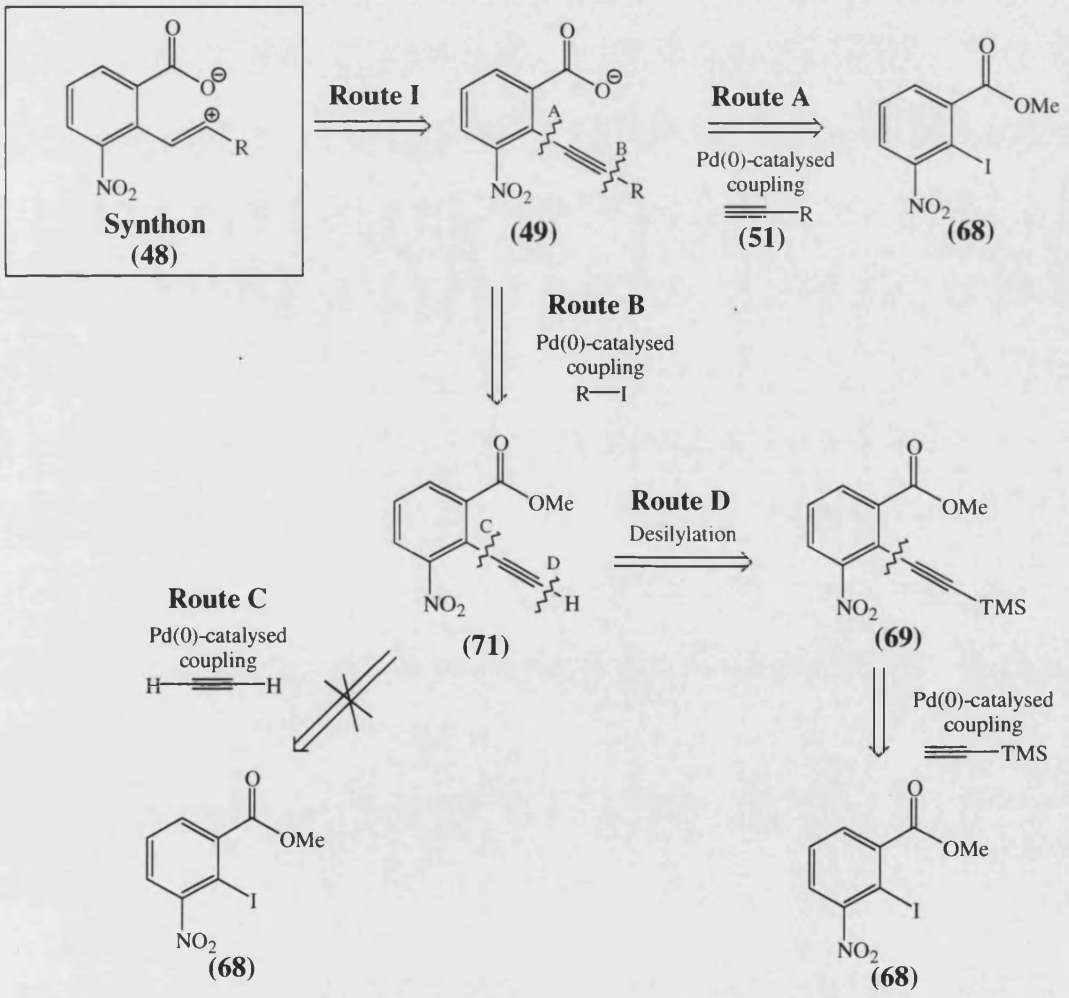

Scheme 2. *Various organometallic approaches to functionalised aryl alkynes (**49**).*

Among this wide array of coupling reactions, it was decided that **Sonogashira coupling reaction**[167] be used for the synthesis of this aromatic alkyne because it has enjoyed tremendous success in the synthesis of a wide range of heterocyclic compounds and is generally considered to be superior over other currently known protocols. It is also highly versatile, has great tolerance for nearly all types of functional groups and may be carried out under extremely mild conditions. This is especially important since two sensitive functional groups (nitro and carbonyl groups) are both present in our initial target **(49)**. Sonogashira reaction cross-couples an aryl or vinyl halide (electrophile) with a terminal alkyne (nucleophile) in the presence of an aliphatic amine (base) and a catalytic amount of palladium-phosphine complex and copper(I) iodide (Scheme 3) (more mechanistic details to be discussed in section 3.1.4).

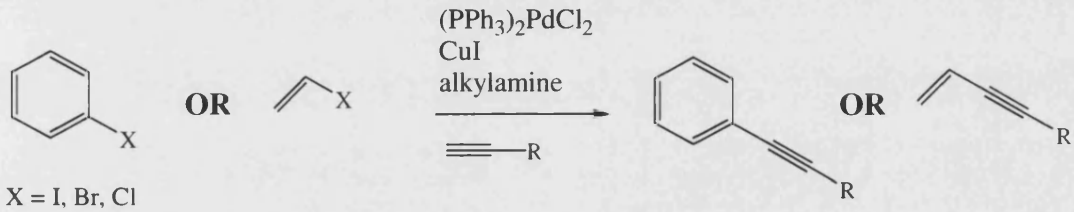

Scheme 3. *Representative reaction conditions for Sonogashira coupling reaction.*

According to Sonogashira[168], the general order of reactivity of the organic halide is in line with the reactivity of the leaving group. Hence an iodo-aryl generally affords shorter reaction times and higher yield compared to its bromo or chloro counterparts. In addition, Sakamoto *et al*[183] recently reported that the cyclisation of ethyl 2-phenylethynylbenzoate, *via* heating with sulphuric acid in the presence of mercury(II) sulphate, gave 3-phenylisocoumarin in much higher yield (97%) compared to its corresponding carboxylic acid, 2-phenylethynylbenzoic acid, which afforded the same product in 18% yield. Thus, to ensure high yield in subsequent annulation process, we decided to use an iodo-ester instead of an iodo-carboxylic acid as the electrophile for the coupling reaction.

Based on these observations, a C-C disconnection of **(49)** (Route A, Scheme 2) led us back to two starting materials: methyl 2-iodo-3-nitrobenzoate **(68)** and the substituted ethyne **(51)**. Accordingly, a direct Sonogashira coupling between the halide **(68)** and the alkyne **(51)** would afford the desired functionalised aryl alkynes **(49)**. However such an approach presents two major potential problems:

1. The use of sterically hindered aryl halides, such as compound **(68)**, is generally known to interfere with the success of the coupling reaction. It has previously been observed that reactions in which one or both *ortho* positions of the halide were substituted were considerably more difficult and they usually suffered from poor yield[168].
2. Most substituted ethynes of the type **(51)** are either very expensive or not commercially available and their synthesis is tedious.

To overcome these difficulties, a conversion of halide **(68)** to a sterically less hindered alkyne **(71)**, *i.e.* a switch of the coupling partners was considered (Route B, Scheme 2). The alkyne **(71)** will then serve as a precursor through which the various desired substituents may be introduced through Sonogashira coupling with appropriate organo-iodides. Unlike substituted ethynes **(51)**, organo-iodides are relatively cheap and widely commercially available. Hence the type of substituents that could be introduced by this route would not be limited.

The most direct route to the synthesis of alkyne **(71)** is to cross-couple the iodo-ester **(68)** with ethyne gas (Route C, Scheme 2). However the alkyne that was initially formed, **(71)**, would be more acidic than ethyne itself, thus competing more favourably for coupling reaction with halide **(68)** and ultimately leading to the formation of 1,2-disubstituted alkyne as shown in Scheme 4.

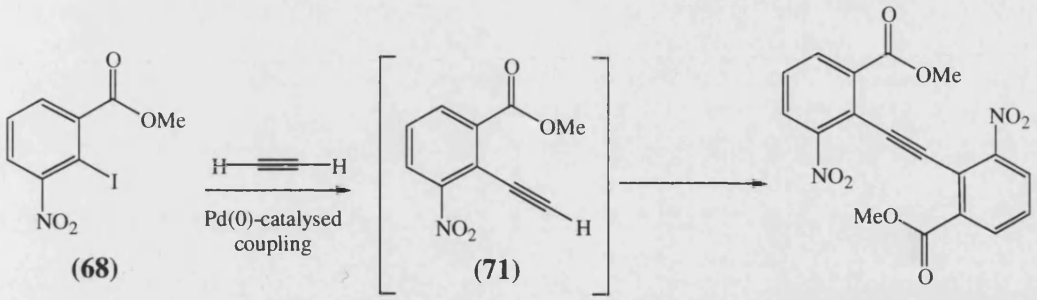

Scheme 4. *Formation of 1,2-disubstituted alkyne from Sonogashira coupling reaction between alkyne (**71**) and iodo-ester (**68**).*

An indirect route involving protection and deprotection of the ethynyl group is, therefore, necessary and the protecting group that is commonly used for this purpose is the trimethylsilyl (TMS) group. Thus, an alternative method for the synthesis of alkyne **(71)** would be to couple halide **(68)** with trimethylsilylacetylene (TMSA), which is commercially available, followed by TMS-deprotection of the resultant alkyne **(69)** as illustrated in Route D (Scheme 2).

Regardless of the actual synthetic route chosen, all the Sonogashira coupling processes outlined above inevitably required the use of methyl 2-iodo-3-nitrobenzoate **(68)** as the halide electrophilic partner. Since this compound was not commercially available, our preliminary aim, was to synthesise this iodo-ester.

3.1.3 Synthesis of methyl 2-iodo-3-nitrobenzoate

Retrosynthetic analysis suggested methyl 2-aminobenzoate as a suitable starting material for the synthesis of **(68)** (Route A, Scheme 5).

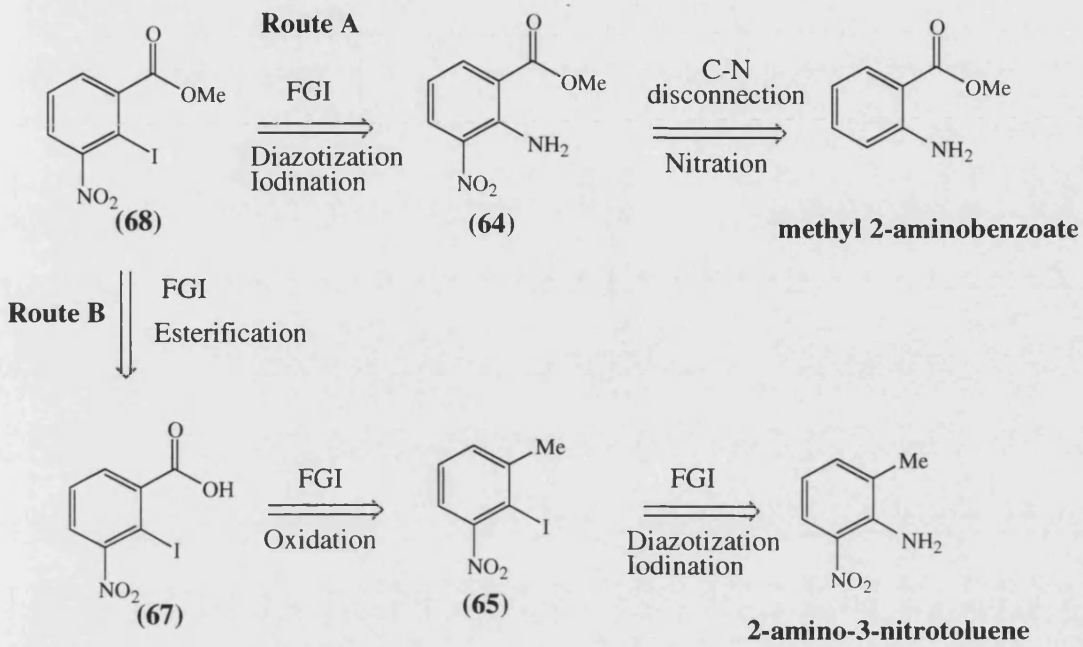

Scheme 5. *Retrosynthetic analysis of methyl 2-iodo-3-nitrobenzoate* ***(68)****.*

A nitro group was first introduced at the 3-position by means of standard nitration procedure utilising a mixture of nitric acid and acetic anhydride in acetic acid at $10 \pm 5^{\circ}C$ (Scheme 6). Relatively mild nitrating conditions were necessary since the employment of more forceful conditions, such as mixed nitric and sulphuric acids, would risk oxidising the amino group. It is likely that the acetic anhydride acetylates the amino group of the starting material, methyl 2-aminobenzoate, thereby protecting it from oxidation. Alternatively, acetylation could also occur after the ring has been nitrated, *i.e.* in compound **(64)**, since the highly electron-donating amino group greatly enhances the rate of electrophilic substitution of NO_2^+ species onto the aromatic ring. This ring-activating property of the amine was taken into consideration in deciding the sequence of synthesis. Reversing the order, *i.e.* to replace the amino group with the iodo function first, would have resulted in a marked

deactivation of the benzene ring, making it much less reactive towards subsequent electrophilic substitution of NO_2^+.

The above reaction yielded a mixture of 5- **(61)** and 3- **(62)** nitro compounds which was in line with the strong *o,p*-directing effect of the amino function. There was no formation of 3,5-dinitro products. This, again, is conceivable since the nitro group is deactivating and the reaction usually stops after one nitro group has entered into the ring. The desired 3-nitro compound **(62)** was then separated from its isomer **(61)** by column chromatography and it was found to be the minor product (20% yield). Given that the electronic environment of the 3- and 5-position are about the same, a preference for the formation of the 5-nitro isomer was probably due to the presence of a bulky acetamido group which made electrophilic attack by the bulky NO_2^+ more difficult at the 3-position compared to the 5-position.

The acetamido function of **(62)** was then hydrolysed back to the amino group with boiling aqueous hydrochloric acid. This gave the carboxylic acid **(63)** which was subsequently converted to the methyl ester **(64)** *via* acid-catalysed esterification process. Finally diazotization ($NaNO_2$, HCl) and iodination (KI, I_2) of this ester gave the desired methyl 2-iodo-3-nitrobenzoate **(68)** but at an unexpectedly low yield of 4%. Since this iodo-ester was required to serve as the starting material for the preparation of the target compounds and a large quantity of it was required, this method of preparation was considered unsatisfactory.

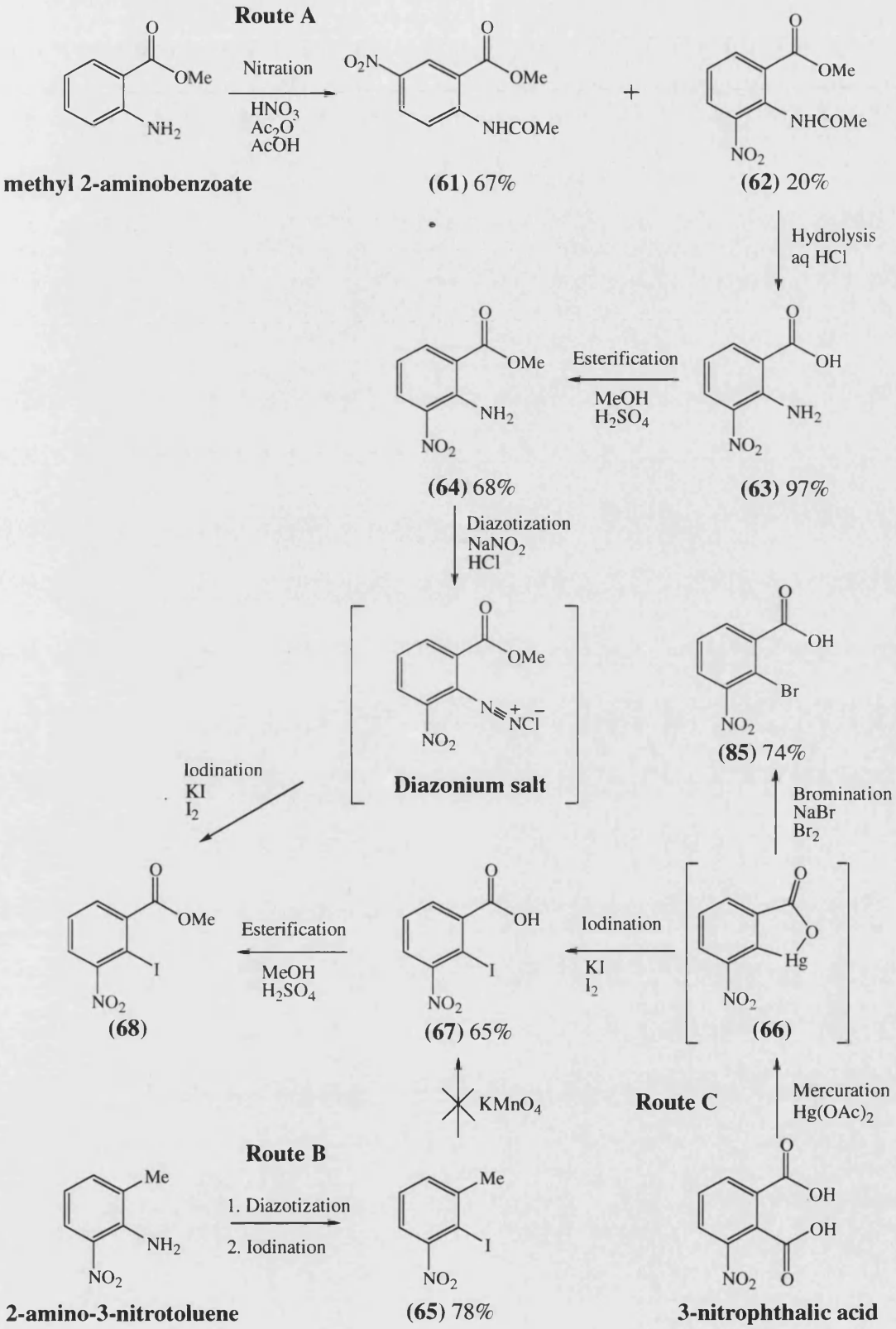

Scheme 6. *Chemical synthesis of methyl 2-iodo-3-nitrobenzoate (68).*

Two possible complications with this reaction were proposed:

1. The amino group of **(64)** is *ortho* to two strongly electron-withdrawing groups, namely the nitro and ester functions and this probably decreases the reactivity of the amine towards diazotization.
2. In addition, highly favourable intramolecular hydrogen-bonding between the amino and the ester groups leads to the formation of a stable six-membered ring which may further decrease its reactivity.

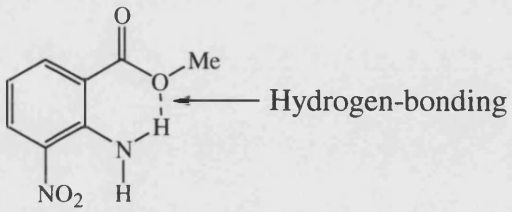

(64)
stable six-membered ring

To circumvent these problems, another method of synthesis employing commercially available 2-amino-3-nitrotoluene as starting material was considered (Route B, Scheme 6). In this starting compound, the nitro group was already correctly placed at the 3-position. This enabled us to avert the highly inefficient nitration process which was previously found to nitrate preferentially at the 5-position. In addition, it was believed that the replacement of the electron-withdrawing ester function with a methyl group would render the amino group more reactive towards diazotization and iodination now that the ring-deactivating effect of the ester function and the highly stabilising intramolecular hydrogen-bonding were removed. Indeed, this was borne out by the relatively much higher yield of iodinated product **(65)** (78%) obtained when 2-amino-3-nitrotoluene was treated with analogous diazotization and iodination conditions. Unfortunately, subsequent oxidation of the methyl group with potassium permanganate was unsuccessful and the reaction gave a black solid that could not be identified, instead of the desired carboxylic acid **(67)**. The presence of the iodo and nitro functions presumably interfered with the oxidation process.

This led us to consider yet another synthetic approach, Route C, which was first described by Culhahe *et al*[169]. Unlike the preceding methods, Route A and B, this route utilises a different mechanism for the introduction of the iodo function, *i.e. via* decarboxylative-iodination of 3-nitrophthalic acid (Scheme 6). The latter was an attractive compound to start with as both the required carboxylic acid (1-position) and nitro functions (3-position) were already in correct relationship (*meta*) to each other. The nitro function also played a crucial role in controlling the regiospecificity of mercuration and decarboxylation as will be discussed later. Finally, 3-nitrophthalic acid was commercially available and was relatively cheap, making large-scale synthesis of the preliminary target **(68)** feasible.

The first stage in the synthesis was to decarboxylate 3-nitrophthalic acid with mercury(II) acetate, followed by electrophilic iodination with a mixture of iodine and potassium iodide (Scheme 6). Interestingly, this afforded only the desired 2-iodo-acid **(67)** (65% yield) without formation of any of the possible side products arising from iodination at the 1-position. Theoretically either one of the two carboxylic acid groups in 3-nitrophthalic acid could undergo mercuration/iodination to give a mixture of 1- and 2-iodinated products. The lack of formation of the former implied that mercuration has occurred regiospecifically at the 2-position. It appeared that the nitro function played an important role in directing electrophilic attack to the carboxylic acid which is *ortho* to itself since such regioselectivity was also observed in the mercuration of nitrobenzene where only the *ortho* position was being substituted[170]. Presumably the reaction proceeded through a free radical mechanism *via* an aryl-mercury intermediate, 2-hydroxymercuri-3-nitrobenzoic acid **(66)** as illustrated in Scheme 7. Incidentally, the nitro function itself is resistant to direct substitution by iodine.

1. Free radical generation

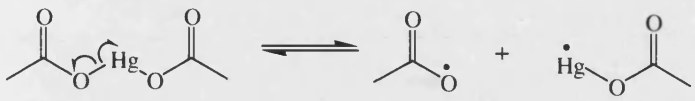

2. Mercuration

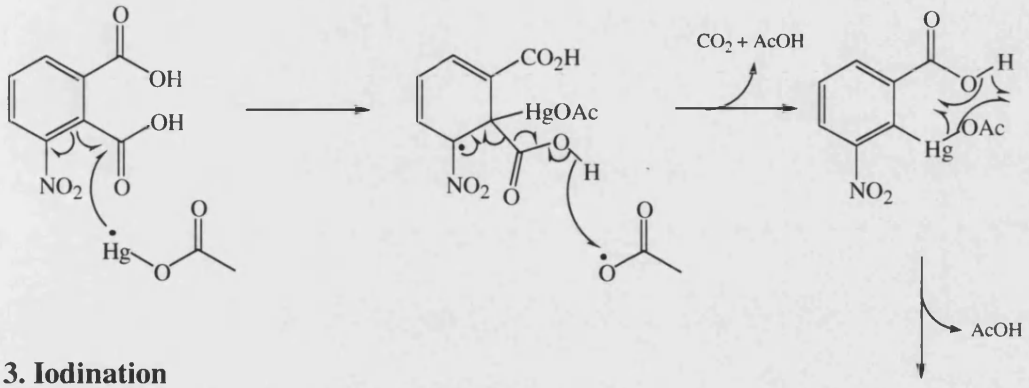

3. Iodination

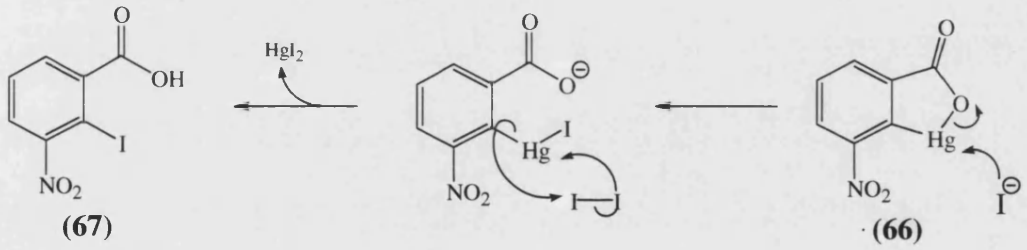

(67) **(66)**

Scheme 7. *Proposed mechanism for the decarboxylative-iodination of 3-nitrophthalic acid.*

The second stage involved an H_2SO_4-catalysed esterification of the iodo-acid **(67)** and this reaction proceeded smoothly affording its corresponding methyl ester **(68)** in excellent yield (95%). Thus, in three simple and reliable steps, we successfully synthesised compound **(68)** which was to serve as an important precursor for the next reaction--- the Sonogashira coupling reaction.

3.1.4 Sonogashira coupling reaction

As discussed earlier in section 3.1.2, it was intended that the synthesis of **(71)** be accomplished *via* a Sonogashira coupling between iodo-ester **(68)** and trimethylsilylacetylene (TMSA), followed by deprotection of the resulting alkyne **(69)** (Route D, Scheme 2). The coupling reaction was performed in the presence of a catalytic amount of bis(triphenylphosphine)palladium(II) chloride [$(PPh_3)_2PdCl_2$] and copper(I) iodide in diisopropylamine (DIPA) and dry THF. The mixture was stirred at 45°C for 72 h under argon.

The catalyst, or pre-catalyst to be exact, used in this reaction, $(PPh_3)_2PdCl_2$, was prepared separately by heating a mixture of palladium(II) chloride and two equivalent of triphenylphosphine in DMF at 80°C for 24 h. Although the coordinatively unsaturated Pd(0) is the catalytically active species, it is often more convenient to use Pd(II) derivatives, such as palladium(II) acetate [$Pd(OAc)_2$] and bis(acetonitrile)palladium(II) chloride [$(MeCN)_2PdCl_2$] because they are usually more stable and less sensitive to air than their Pd(0) counterparts. They are also generally more soluble in organic solvents. The copper(I) salt functions as an important co-catalyst that facilitate the substitution reaction, without which, the reactions invariably fail. Diisopropylamine (DIPA), on the other hand, serves as a base and is sometimes used as a solvent. Other alkyl amine bases that are also commonly used for Sonogashira coupling include triethylamine and diethylamine.

Although the detailed mechanism of the reaction is yet to be established, it seemed likely that the substitution reaction occurs *via* a catalytic cycle which consists of three main steps as proposed by Sonogashira[167,168] (Scheme 8):

1. Oxidative addition
2. Transmetallation
3. Elimination

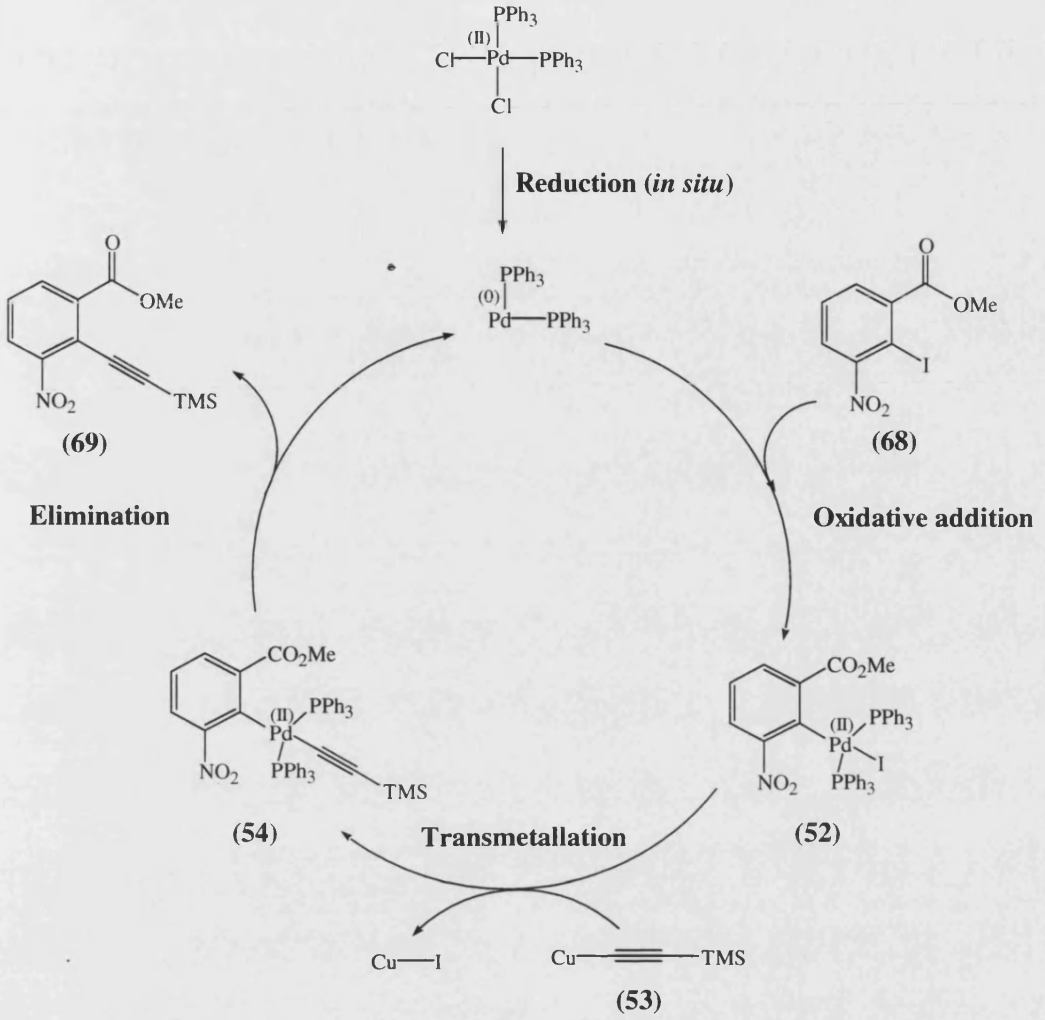

Scheme 8. *Proposed mechanism for Sonogashira coupling between methyl 2-iodo-3-nitrobenzoate (68) and trimethylsilylacetylene.*

Under the reaction conditions, $(PPh_3)_2PdCl_2$ was rapidly reduced *in situ* to give the catalytic species bis(triphenylphosphine)palladium(0). **Oxidative addition** of this Pd(0) complex with the aryl iodide **(68)** gave a Pd(II) intermediate **(52),** which, in turn, underwent **transmetallation** with an alkynyl copper species **(53)** to yield a diorgano-Pd(II) complex **(54)**. The copper species **(53)** was generated *in situ* from a reaction between TMSA and the co-catalyst copper(I) iodide, with the aid of diisopropylamine (DIPA) as shown in Scheme 9. The conversion of TMSA to **(53)**, which underwent transmetallation more readily, greatly accelerated the coupling process since transmetallation is the rate-determining step in the whole cycle. Finally coupling of the two organic ligands and **elimination** gave the desired

methyl 3-nitro-2-(2-trimethylsilylethynyl)benzoate **(69)** in 30% yield with concomitant regeneration of the Pd(0) catalyst, thus closing the catalytic cycle. The reaction also gave methyl 3-nitrobenzoate **(70)** as a side product (39% yield). It was believed that the latter was formed as a result of a replacement of iodine with hydrogen during the coupling process. Presumably steric retardation of the rate of transmetallation provided an opportunity for such iodine-hydrogen exchange to occur.

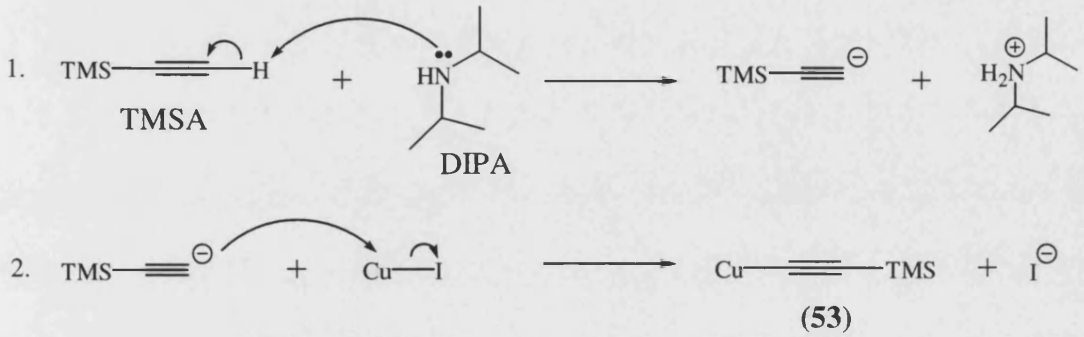

Scheme 9. *Formation of alkynyl copper species (53) from a reaction between TMSA and copper(I) iodide under the presence of diisopropylamine (DIPA).*

In general, the reported yield for most Sonogashira coupling reactions vary from good to excellent (70-95%). The long reaction time (72 h), modest yield of the desired alkyne **(69)** (30%) and relatively high yield of the unwanted side product **(70)** (39%) could be indications of sub-optimal experimental conditions for this particular coupling reaction. Alternatively, it could also signify an inherent problem associated with the use of sterically hindered halides such as compound **(68)** where both its *ortho* positions were substituted with bulky groups. It is noteworthy that virtually all the successful Sonogashira reactions reported, to date, involved relatively unhindered aryl halides. 2-iodonitrobenzene and methyl 2-iodobenzoate were about the closest examples we could find in the literature that were comparable to our experiment. Thus, it was not unexpected that the reaction with halide **(68)** suffered low yield.

If steric factors were indeed the problem, we reasoned that a replacement of the bulky ester function with a "slender" nitrile group might help relieved some of the steric strain on the halide, resulting in better yield. To explore this idea, 2-iodo-3-nitrobenzonitrile **(74)** was synthesised. This was easily achieved in excellent yield from its carboxylic acid **(67)** *via* dehydration of its corresponding amide **(73)** as shown in Scheme 10. Surprisingly, subsequent analogous Sonogashira coupling with TMSA did not afford the desired coupling product or the reduced product **(70)**. Instead it gave the starting material **(74)** in virtually quantitative yield. Hence, factors other than those stemming from steric origin were probably at work.

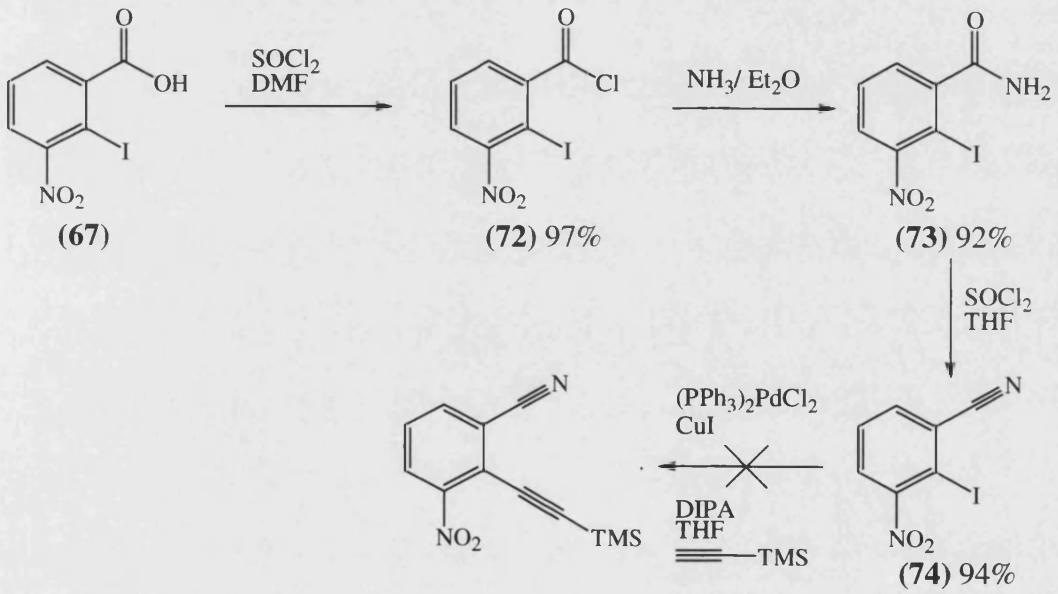

Scheme 10. *Chemical synthesis of 2-iodo-3-nitrobenzonitrile (74) and its Sonogashira coupling with TMSA.*

Simultaneous effort was also directed at re-examining the experimental conditions. Attempts to improve the efficiency of the Sonogashira coupling reaction by varying the following parameters were unsuccessful.

- Reaction temperature
- Palladium catalyst used: tetrakis(triphenylphosphine)palladium(0), palladium(II) acetate
- Alkyl amine base used: diethylamine, triethylamine
- Protecting group for ethyne: triisopropylsilane acetylene (TIPSA)

Despite not being able to improve the yield of the coupling reaction, we moved on to desilylate alkyne **(69)** to methyl 2-ethynyl-3-nitrobenzoate **(71)** (Scheme 11). This was accomplished by stirring compound **(69)** with tetrabutylammonium fluoride (TBAF) in THF at 0°C. However the yield this reaction was disappointingly low (9%). Attempts to improve the yield using other deprotection methods, such as potassium fluoride and methanolic potassium carbonate were unsuccessful. The difficulties encountered and the low yield obtained discouraged further synthetic steps. Nevertheless, it must be said that a successful synthesis of arylalkyne **(69)**, albeit in modest yield, greatly encouraged us to investigate the viability of using direct coupling of the iodo-ester **(68)** with substituted ethyne **(51)** to effect synthesis of functionalised alkynes **(49)** (Route A, Scheme 2).

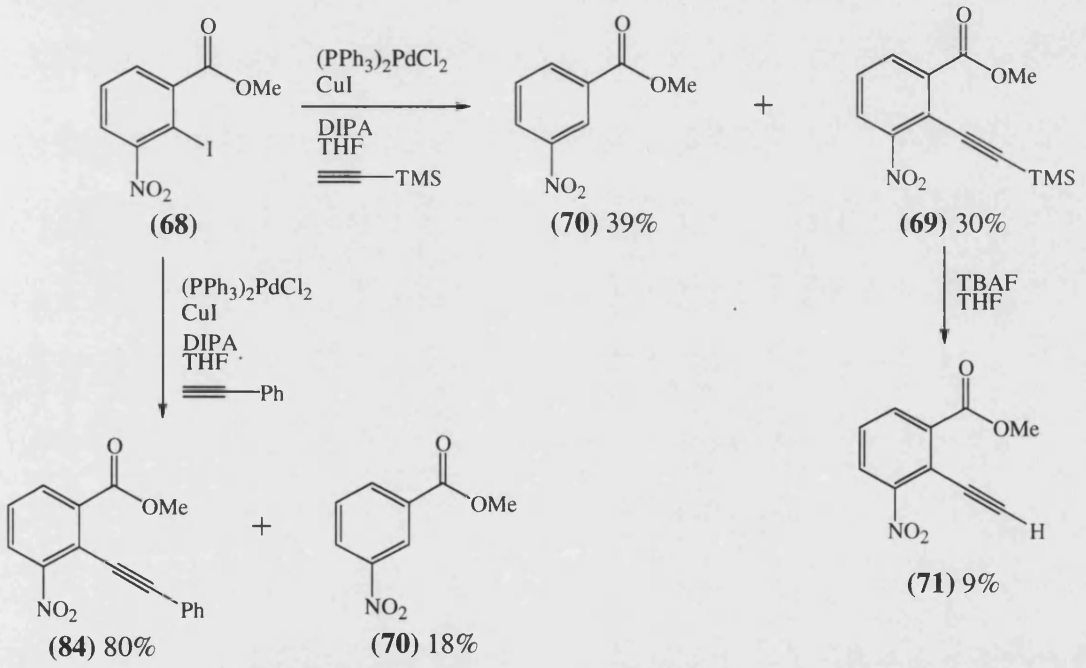

Scheme 11. *Sonogashira coupling of methyl 2-iodo-3-nitrobenzoate (68) with phenylethyne and TMSA and subsequent desilylation of methyl 3-nitro-2-(2-trimethylsilylethynyl)benzoate (69).*

We begin our studies by first performing a Sonogashira coupling reaction between **(68)** and phenylethyne (the least expensive one among the few commercially available aryl ethynes) under the same reaction conditions as with TMSA. Quite unexpectedly, this reaction gave the coupling product,

methyl 3-nitro-2-(2-phenylethynyl)benzoate **(84)**, in very good yield (80%) and the reaction was completed in a much shorter period of time (48 h compared to 72 h with TMSA). Again, as in the previous reaction, the reduced side product **(70)** was isolated, but in relatively lower yield (18%) (Scheme 11).

Having successfully coupled phenylethyne to the iodo-ester **(68)**, we carried on to explore the reaction with other aryl ethynes. This required, first and foremost, the synthesis of a series of ethynes with the desired functionalities since most of them were not commercially available. To achieve this, we cross-coupled the various suitably substituted aryl iodides with TMSA under Sonogashira reaction conditions, followed by desilylation of the coupling products with TBAF. The results of the experiments were summarised in Table 12.

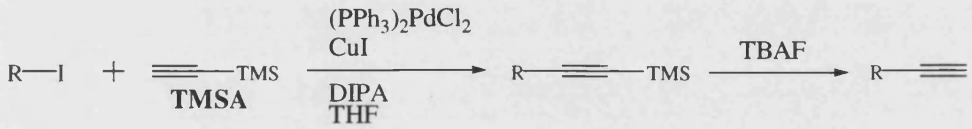

R	Yield of products (%) R—TMS	R—H
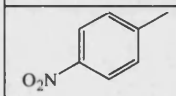	91 **(75)**	83 **(76)**
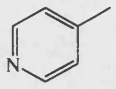	93 **(77)**	64 **(78)**
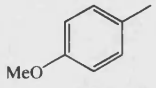	90 **(79)**	-
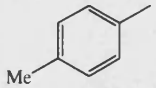	95 **(80)**	-
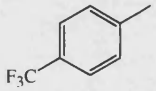	92 **(81)**	-
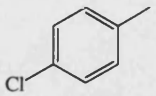	95 **(82)**	-
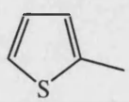	89 **(83)**	-

Table 12. *Synthesis of a series of substituted ethynes via Sonogashira coupling reaction. (-) denotes unsuccessful attempts.*

It is interesting to note that all coupling reactions studied proceeded with excellent yield (*ca* 90%) regardless of the nature of the substituents, demonstrating once again the wide applicability of Sonogashira coupling reaction. Desilylation was again the problematic step in the synthesis. Among the various alkynylated products, only 4-nitro-1-[(trimethylsilyl)ethynyl]benzene **(75)** and 4-[(trimethylsilyl)ethynyl]pyridine **(77)** underwent deprotection smoothly to give 1-ethynyl-4-nitrobenzene **(76)** and 4-ethynylpyridine **(78)**, respectively, while the rest remained largely unchanged under the reaction condition. Unable to account for the repeated lack of success in this seemingly standard deprotection reaction, we decided to switch to another method of synthesis that eliminated the need for desilylation altogether.

Negishi[171] has recently described a novel method for the direct synthesis of terminal alkynes without the need for protection and deprotection of the ethynyl group. It was observed that ethynylmagnesium bromide readily cross-coupled with a variety of aryl iodides in the presence of palladium-phosphine catalyst, such as tetrakis(triphenylphosphine)palladium(0) ($(PPh_3)_4Pd$) to produce directly the corresponding terminal alkynes in high yield. However there is one severe limitation associated with this method of preparation. The high ionicity of C-Mg bond in organo-magnesium reagents renders them extremely reactive towards electrophilic functionalities, such as the carbonyl and the nitro groups. Consequently, this method was not previously considered for the direct synthesis of methyl 2-ethynyl-3-nitrobenzoate **(71)** from methyl 2-iodo-3-nitrobenzoate **(68)**.

Using this **Negishi protocol**, we successfully synthesised 1-ethynyl-4-methoxybenzene **(117)** and 1-ethynyl-4-methylbenzene **(118)** in excellent yields of 90% and 92% respectively. Presumably, functional groups, such as trifluoromethyl, chloro and thiophene were incompatible with the organo-magnesium reagent under the reaction conditions, hence accounting for the failure of these halides to cross-couple with ethynylmagnesium bromide. The results were summarised in Table 13.

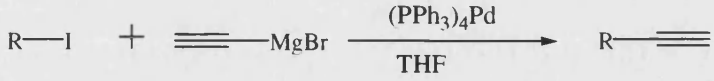

R	Yield of R— (%)
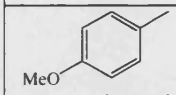	90 **(117)**
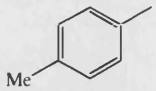	92 **(118)**
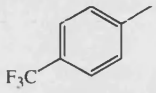	-
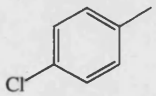	-
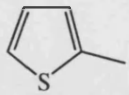	-

Table 13. *Synthesis of a series of substituted ethynes via Negishi coupling reaction. (-) denotes unsuccessful attempts.*

Sonogashira coupling reactions between iodo-ester **(68)** and the following ethynes: 1-ethynyl-4-nitrobenzene **(76)**, 4-ethynylpyridine **(78),** 1-ethynyl-4-methoxybenzene **(117)** and 1-ethynyl-4-methylbenzene **(118)** were then undertaken (Table 14). To our great disappointment, none of the reactions were successful and most of them afforded only the de-iodinated side product **(70)**. This observation is puzzling in view of the success that we had with phenylethyne. We do not consider these substituted aryl ethynes to be sterically very different from phenylethyne, especially 4-ethynylpyridine **(78)**, hence the differences in the fate of these ethynes cannot be explained sterically. The outcome also appeared to be independent of the electronic nature of the ethyne used since both electron-deficient ethynes, 1-ethynyl-4-nitrobenzene **(76),** and electron-rich ethynes, 1-ethynyl-4-methoxybenzene **(117)**, equally failed to participate in the reaction.

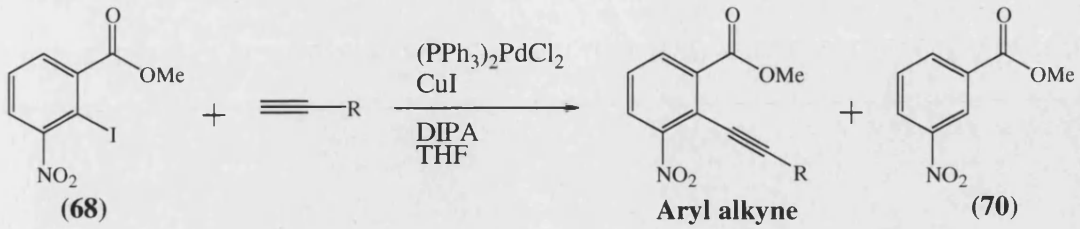

	Yield of products (%)	
R	**Aryl alkyne**	**(70)**
TMS	30 **(69)**	39
TIPS	-	-
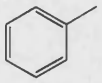	80 **(84)**	18
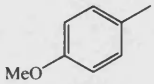	-	26
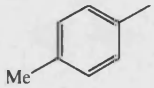	-	6
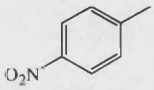	-	12
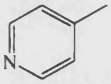	-	-

Table 14. *Sonogashira coupling reaction between halide (**68**) and various substituted ethynes. (-) denotes unsuccessful attempts.*

Thus, we have essentially exhausted all possibilities of synthesising our 3-substituted targets *via* Sonogashira coupling reaction and, regrettably, we were only able to prepare methyl 3-nitro-2-(2-phenylethynyl)benzoate **(84)** in good yield through this protocol.

3.1.5 Cyclisation of methyl 3-nitro-2-(2-phenylethynyl)benzoate

The next step was to cyclise the aryl alkyne **(84)** using mercury(II) sulphate and concentrated sulphuric acid in acetone. It was believed that heteroannulation proceeded *via* the mechanism outlined in Scheme 12. The first step presumably involves the formation of the bridged mercurium complex **(55)** *via* electrophilic addition of Hg^{2+} to the alkyne. This was opened by an intramolecular attack by the carbonyl oxygen of the methyl ester. Theoretically, there are two possible ways in which cyclisation can occur. The carbonyl oxygen may either attack in a 5-exo-dig manner (Path A) to give a 5-membered side product, 3-benzylidene-4-nitro-phthalide **(58)**, *via* cation **(56)** or it may undergo 6-endo-dig ring closure (Path B) to give the desired 5-nitro-3-phenylisocoumarin **(86)** *via* cation **(57)**. According to Baldwin's rules for ring closure[172], both reactions are favourable because both carbon of the acetylene has two π^* orbitals, one of which must always lie in the plane of the new ring, making it very easy for the lone pair on carbonyl oxygen to overlap with. Hence a mixture of phthalide and isocoumarin was expected from the reaction.

This was found to be generally true in the case of transition metal-catalysed cyclisation reactions. In particular, Ogawa *et al*[184] recently reported that 2-(1-alkynyl)benzoic acid gave (Z)-3-(1-alkylidene)-phthalides and 3-alkylisocoumarin as major and minor products, respectively, in the presence of catalytic amounts of silver or silver(I) iodide. Likewise, treatment of the acid with catalytic amount of $(MeCN)_2PdCl_2$[185] or zinc(I) chloride[186] also yielded a mixture of phthalide and isocoumarin, though the latter was now found to be the major product. Sakamoto *et al*[183] also reported similar findings for the mercury-mediated cyclisation of 2-phenylethynylbenzamide. However, they observed that the analogous cyclisation of the corresponding carboxylic acid, 2-phenylethynylbenzoic acid, and ester, ethyl 2-phenylethynylbenzoate, gave 3-phenylisocoumarin exclusively under the same reaction conditions, in contrast to the results obtained by Villemin *et al*[187] where they demonstrated that the sulphuric acid-catalysed heteroannulation of 2-(1-phenylethynyl)benzoic acid led only to phthalide formation.

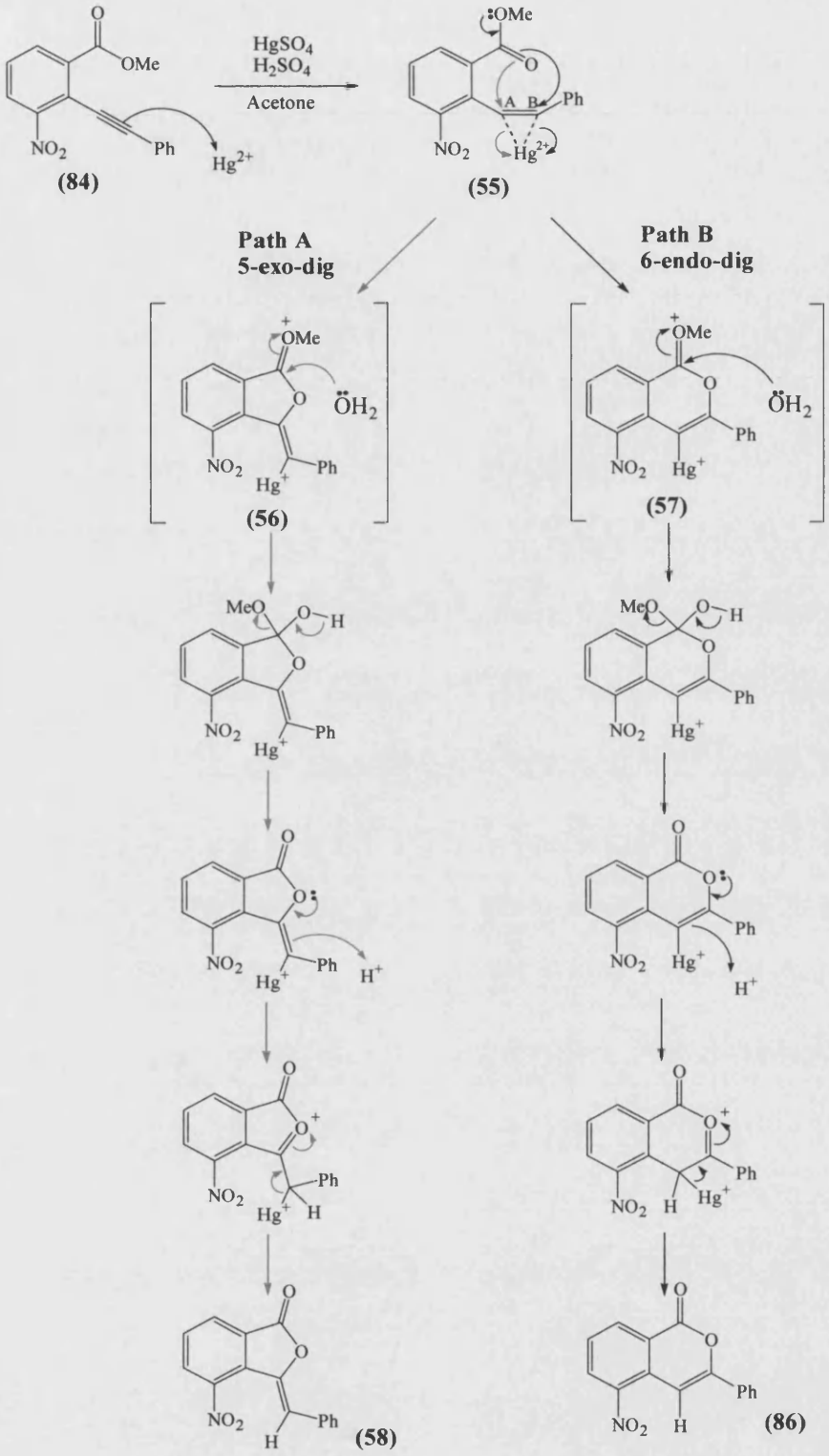

Scheme 12. *Proposed mechanism for the formation of phthalide* ***(58)*** *and isocoumarin* ***(86)***.

It appeared that the outcome of the cyclisation reaction was not only affected by the catalyst used, but also on the functional groups present in the aryl alkyne.

It is interesting to note that the heteroannulation process in our experiment was found to be completely regiospecific in that only one cyclisation product (a yellow solid) was obtained from this reaction and at an excellent yield of 95%. The task, then, was to establish the molecular structure of this yellow solid, or rather, to determine which of the two probable products, phthalide **(58)** or isocoumarin **(86)** was actually formed. It has to be said that both compounds are structural isomers and their differentiation is not straightforward.

1. To begin with, both isomers are novel compounds, hence their identity cannot be easily determined through a comparison of their melting points with authentic samples.
2. Their ^{1}H and ^{13}C NMR spectra are also expected to be very similar. The vinylic protons for both the phthalide and isocoumarin are expected to give a signal at about the same region in the ^{1}H NMR spectrum, *i.e.*, a chemical shift of about 6 to 7 p.p.m.

   NOESY NMR spectra would be invaluable had there not been a nitro group at the 4- and 5-position of the phthalide and isocoumarin respectively.
3. Being isomers, they also share the same molecular mass and their fragmentation pattern from mass spectroscopy (Electron Impact or Chemical Ionisation) would not be very different.
4. Finally, though the yellow solid could be recrystallised easily with hexane-ethyl acetate mixture to form yellow needles, these crystals were considered too small and therefore unsuitable for X-ray crystallography determination.

Fortunately, we were provided with two valuable pieces of information from its IR (KBr disc) and ^{1}H NMR ($CDCl_3$) spectra. The yellow solid has a carbonyl C=O stretch of 1739 cm^{-1}. It is known that the C=O stretch of 5-membered lactone ring normally absorbs in the range between 1780 to 1760 cm^{-1}, whereas that of the

6-membered lactone ring is observed at a lower range of 1750 to 1730 cm^{-1}. Thus, this was our first hint towards a 6-membered isocoumarin structure.

We also observed that the vinylic proton gave a signal at δ_H 7.89 p.p.m. and that this proton is coupled with one of the aromatic protons on the heterocyclic ring (doublet, J = 0.8 Hz). The vinylic proton in phthalide is at least six bond distance apart from the nearest protons on the heterocyclic ring (5-H or 7-H). This is too far away for any significant proton-proton coupling to occur. The vinylic proton in isocoumarin, on the other hand, could interact with the proton at 8-position *via* extended W-type long-range coupling. Indeed, this was found to be the case as 8-H gave a double-double-doublet and one of its coupling constant (^5J) is also 0.8 Hz.

These spectroscopic evidences allowed us to assign tentatively the isocoumarin structure, 5-nitro-3-phenylisocoumarin **(86)**, to the yellow solid. Our result could be rationalised by the proposed mechanism depicted in Scheme 12. The presence of a neighbouring powerfully electron-withdrawing nitro group possibly made carbon B more electron-deficient compared to carbon A, thus greatly favouring 6-endo-dig over 5-exo-dig ring closure, accounting for the lack of formation of any 5-membered phthalide product.

3.1.6 Formation of 5-amino-3-phenyisoquinolin-1(2*H*)-one hydrochloride

Having successfully synthesised isocoumarin (**86**), attempts were then made to reduce selectively the nitro function *via* catalytic hydrogenation with 10% Pd/C and hydrogen. Surprisingly, the compound remained unchanged even after stirring at room temperature for 24 h. It was thought that trace amount of mercury (mercury(II) sulphate was used in cyclisation reaction prior to this), which was not completely removed from the compounds during work-up procedures, could interfere with the reduction process by poisoning the palladium catalyst. This led us to the use of other nitro-selective reducing agents which are not normally affected by the presence of mercury, such as Raney Nickel and tin(II) chloride. However, in both cases, the nitro group remained highly resistant towards reduction. In fact, treatment of the isocoumarin with tin(II) chloride in methanol at 70°C appeared to have resulted in ring opening of the lactone ring. This was evidenced from the ^{1}H NMR ($CDCl_3$) spectrum of the product which gave a singlet for three protons at δ 3.93 p.p.m., indicating the presence of a methyl ester function. Such ring opening could be caused by a nucleophilic attack of the carbonyl carbon of the lactone ring by the methoxy anion. To overcome this problem, a more bulky protic solvent may be used. Alternatively, the isocoumarin could be converted to its corresponding isoquinolin-1(2*H*)-one (**89**) first, in the hope that the lactam ring, which was more resistant to ring-opening than the lactone ring, would be able to survive the conditions used during subsequent tin(II) chloride reduction (Scheme 13).

Many different chemical approaches have been reported in the literature for the conversion of isocoumarins to isoquinolin-1(2*H*)-ones. These include treatment with ethanolic ammonia in a sealed tube[183], reaction with ammonium carbonate in acetic acid[188] and heating with ammonia at high temperature[158,159]. The latter was one of the simplest procedures that have been published without recourse to difficult reagents and elevated pressure. Thus, isocoumarin (**86**) was treated with boiling ammonia-saturated 2-methoxyethanol and this afforded 5-nitro-3-phenylisoquinolin-1(2*H*)-one (**89**) in good yield (73%).

The isoquinolin-1(2*H*)-one was then catalytically reduced with tin(II) chloride by heating at 70°C in ethanol. This time, the reaction went smoothly, albeit in a moderate yield of 57%, affording the target compound 5-amino-3-phenylisoquinolin-1(2*H*)-one **(90)** which was only sparingly soluble in water. The latter was then converted to its hydrochloride salt by stirring with aqueous hydrochloric acid (2 M) for 30 min and the product, 5-amino-3-phenylisoquinolin-1(2*H*)-one hydrochloride **(91),** was found to be readily soluble in water, with an aqueous solubility of more than 10 $mgml^{-1}$. Thus, we have successfully synthesised our first potential water-soluble PARP-1 inhibitor.

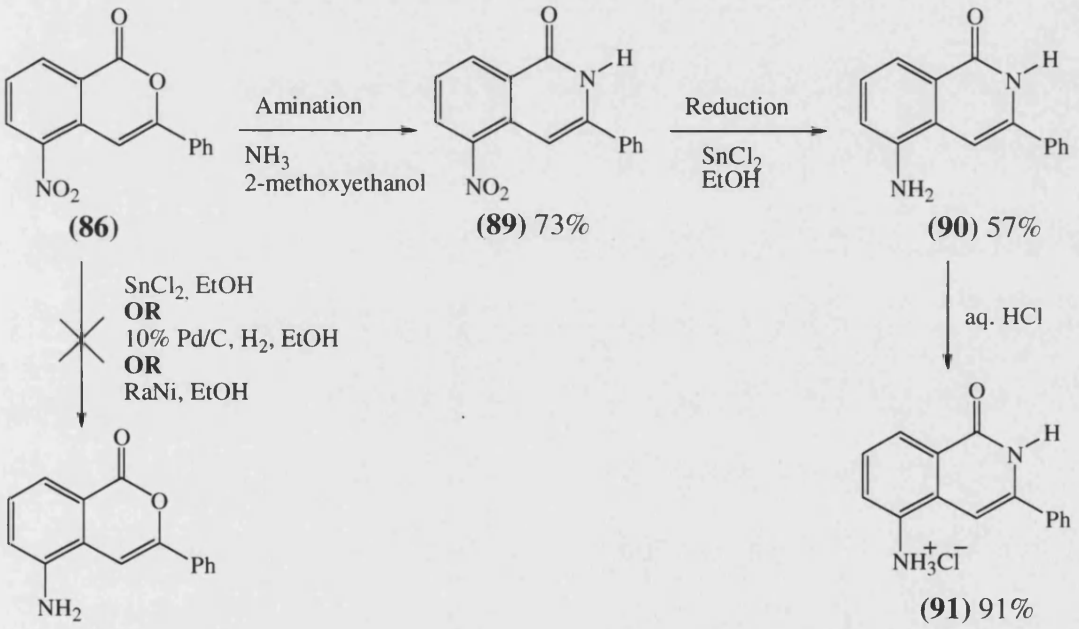

Scheme 13. *Chemical synthesis of 5-amino-3-phenyisoquinolin-1(2H)-one hydrochloride (91).*

3.1.7 Castro-Stephens coupling reaction

Castro and Stephens[173] have previously demonstrated that a variety of aryl alkynes may be obtained by a copper-promoted cross-coupling reaction of aryl halides and copper(I) acetylides. It represents an earlier, "non-palladium" version of Sonogashira coupling reactions now commonly known as the Castro-Stephens coupling reaction. In one of their studies[174] on the scope and utility of the reaction, they reported that the interaction of copper(I) acetylides with aryl halides bearing an *ortho* nucleophilic substituent did not furnish aryl alkynes, but rather underwent rapid cyclisation to the corresponding heterocycles exclusively and they claimed that 2-iodobenzoic acid reacted with copper(I) phenylacetylide to yield 3-phenylisocoumarin. However, regrettably, a few years later, they reported that the product has been erroneously identified and it was, in fact, the isomeric 3-benzylidenephthalide as proven by comparison with an authentic sample. Their work is summarised in Scheme 14 below. Incidentally, Larock *et al*[194] repeated the coupling reaction with copper(I) propylacetylide using the ester equivalent, methyl 2-iodobenzoate and they obtained the alkyne, methyl 2-(1-pentynyl)benzoate in 65% yield without any cyclisation product.

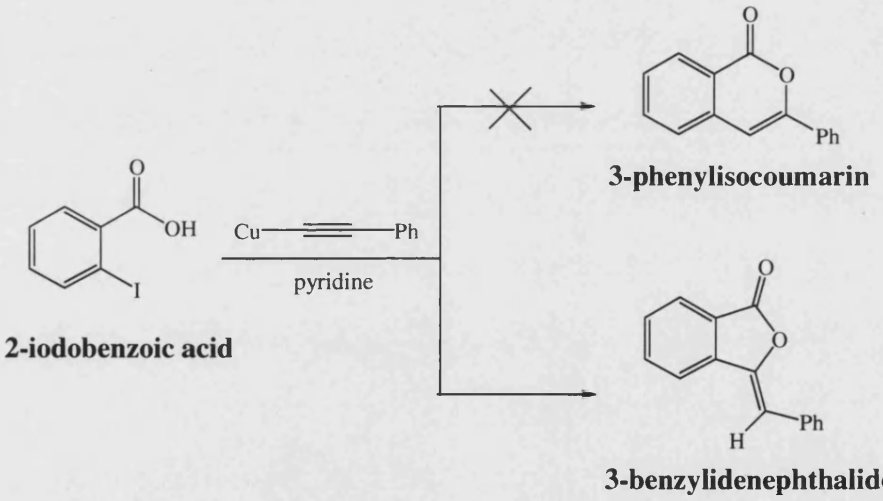

2-iodobenzoic acid

3-phenylisocoumarin

3-benzylidenephthalide

Scheme 14. *2-iodobenzoic acid reacted with copper(I) phenylacetylide to yield 3-benzylidenephthalide instead of the isomeric 3-phenylisocoumarin*[174].

We consider it possibly significant that the presence of a highly electron-withdrawing nitro group in the 2-iodo-3-nitrobenzoic acid **(67)** might favour the formation of isocoumarin rather than phthalide. This assumption was based on our earlier observation on the acid-catalysed, mercury-mediated ring closure of methyl 3-nitro-2-(2-phenylethynyl)benzoate **(84)** (section 3.1.5) where a yellow solid, which was believed to be 5-nitro-3-phenylisocoumarin **(86)**, was the only isomer isolated. Consequently this simple procedure, with appropriate experimental modifications, may provide an acceptable synthetic route to other 3-substituted 5-nitroisocoumarins.

To test this hypothesis, we exposed 2-iodo-3-nitrobenzoic acid **(67)** (synthesised *via* the method described in Route C, Scheme 6) to copper(I) phenylacetylide in boiling pyridine under nitrogen. Copper(I) phenylacetylide is a bright canary yellow solid which was separately prepared by mixing an ethanolic solution of phenylethyne with an equivalent amount of copper(I) iodide in aqueous ammonia. Upon working-up, the coupling reaction gave a product (74% yield) which, to our excitement, has the same melting point and spectroscopic data (IR and ^{1}H NMR) as that of the yellow solid **(86)**. Again, this was the only cyclisation product formed, thus supporting the idea that the *ortho*-nitro group does indeed have a crucial influence on the direction of ring closure. A small amount of the symmetrical diyne **(87)** was also isolated in 5% yield. This was undoubtly the result of oxidative homodimerisation of copper(I) phenylacetylide, *i.e.* **Glaser coupling**, which is a frequent complication in Stephens-Castro coupling reaction if oxygen was not strictly excluded from the reaction mixture[175].

This methodology was then applied to a series of copper(I) acetylides as shown in Table 15. It is interesting to note that, among the five acetylides investigated, only copper(I) 4-methoxyphenylacetylide and copper(I) 4-methylphenylacetylide underwent successful coupling and in both cases they consistently gave just one cyclisation product, **(97)** and **(103)** respectively, along with the Glaser coupling products **(96)** and **(102)** respectively. The novel compounds, **(103)** could be recrystallised with a mixture of hexane and ethyl acetate to form large yellow

needles. Subsequent X-ray crystallography (Appendix) supported the 5-nitro-3-(4-methylphenyl)isocoumarin structure, thus indirectly confirming our previous structural assignment on the yellow solid **(86)**.

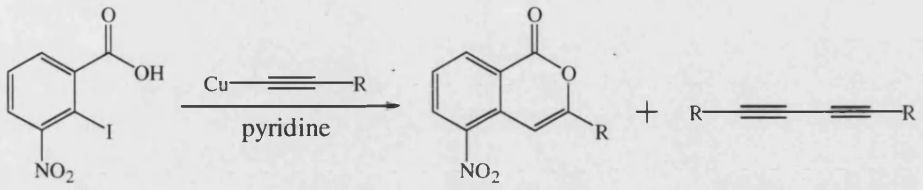

(67) **Isocoumarin** **Glaser product**

	Yield of products (%)	
R	**Isocoumarin**	**Glaser product**
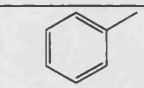	74 **(86)**	5 **(87)**
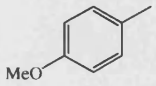	29 **(97)**	1 **(96)**
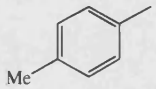	18 **(103)**	0.4 **(102)**
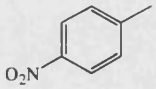	-	-
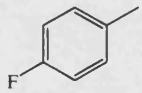	-	-
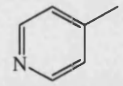	-	-

Table 15: *Castro-Stephens coupling reactions between 2-iodo-3-nitrobenzoic acid (67) and various copper(I) acetylides. (-) denotes unsuccessful attempts.*

It is also noteworthy that though 4-methoxyphenylethyne **(117)** and 4-methylphenylethyne **(118)** failed to cross-couple under the Sonogashira protocol, their copper(I) derivatives underwent Castro-Stephens coupling smoothly. This seemed to suggest that one possible reason for the lack of success previously observed with Sonogashira coupling (Table 14) was that the substituted ethynes were not nucleophilic enough. Presumably they did not react with copper(I) iodide as proposed to give the copper(I) species. Instead they probably served as electrophiles for Michael-type additions with DIPA as shown in Scheme 15.

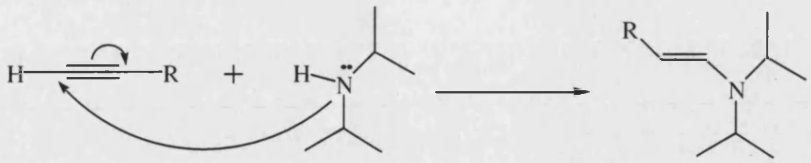

Scheme 15. *Michael-type addition reaction between substituted ethyne and DIPA.*

Such complications have recently been reported by Yoneda *et al*[189] in their attempts to effect Sonogashira coupling of iodobenzene with trifluoromethylethyne under $(PPh_3)_4Pd$ and diethylamine. They found that none of the coupling product was formed, instead the ethyne reacted with the amine to give the disubstituted alkene, *N,N*-diethyl-3,3,3-trifluoro-1-propenylamine.

The poor nucleophilicity of copper(I) 4-nitrophenylacetylide, copper(I) 4-fluorophenylacetylide and copper(I) 4-pyridinylacetylide could also possibly account for their inability to undergo coupling with 2-iodo-3-nitrobenzoic acid **(67)**.

On the basis of these experimental observations, the mechanism for the coupling process, originally proposed by Castro and Stephens[173], may now be adapted as follows (Scheme 16): 2-iodo-3-nitrobenzoic acid **(67)** initially cross-coupled with copper(I) acetylide to give a 4-membered transition state **(58)**. This, upon extrusion of copper(I) iodide, led to the formation of the alkynylated compound which underwent rapid cyclisation to the corresponding isocoumarin. The cyclisation reaction could be catalysed by pyridine (acting as a base) or by copper (acting as a Lewis acid, in a manner similar to mercury-mediated cyclisation).

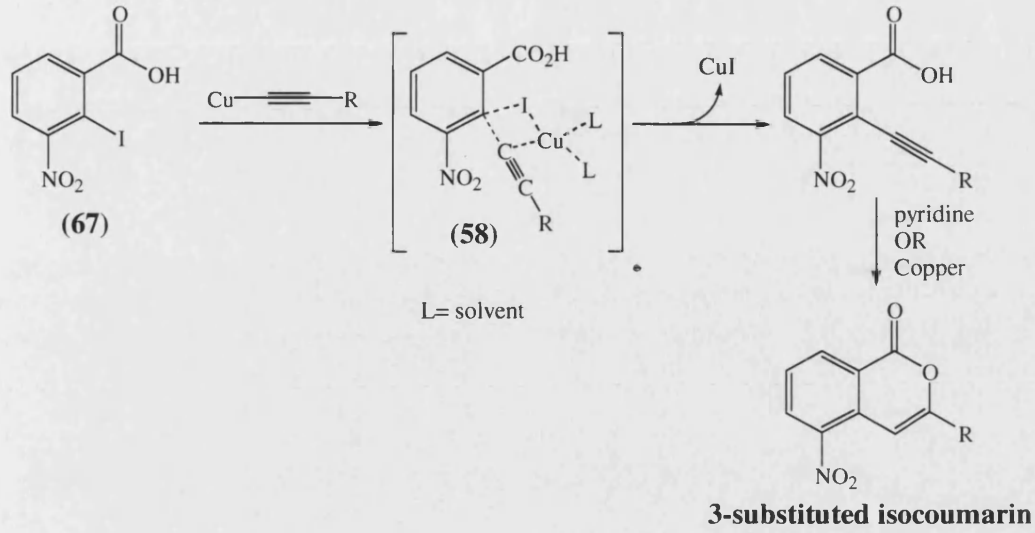

Scheme 16. *Castro-Stephens coupling of 2-iodo-3-nitrobenzoic acid (67) with copper(I) acetylide and subsequent cyclisation to form the 3-substituted isocoumarin.*

Incidentally, it has been reported that the reaction of copper(I) phenylacetylide with 2-iodobenzamide gave a deep red product 3-amino-2-phenylinden-1-one **(59)** instead of 2-(2-phenylethynyl)benzamide **(60)** (Scheme 17)[176]. This discouraged attempt to effect synthesis of 3-substituted 5-nitroisoquinolin-1(2*H*)-ones directly from 2-iodo-3-nitrobenzamide.

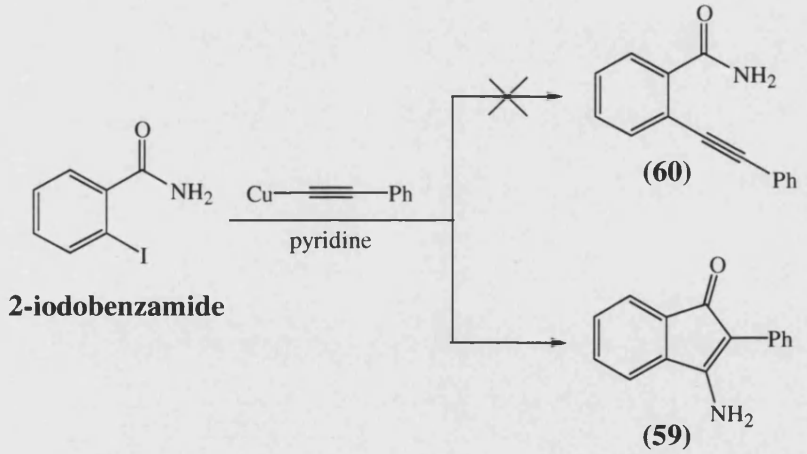

Scheme 17. *Castro-Stephens coupling of 2-iodobenzamide with copper(I) phenylacetylide gave 3-amino-2-phenylinden-1-one (59) instead of 2-(2-phenylethynyl)benzamide (60)*[176].

We have also examined the possibility of using palladium-catalysed **intramolecular Heck coupling reaction**[177], which couple an alkene with the halide to form a new alkene, for the construction of 5-nitro-3-phenylisocoumarin **(86)** as illustrated in Scheme 18. However, attempts to synthesise compound **(166)** *via* nucleophilic substitution of 2-iodo-3-nitrobenzoyl chloride **(72)** with silyl enol ether **(165)** was unsuccessful.

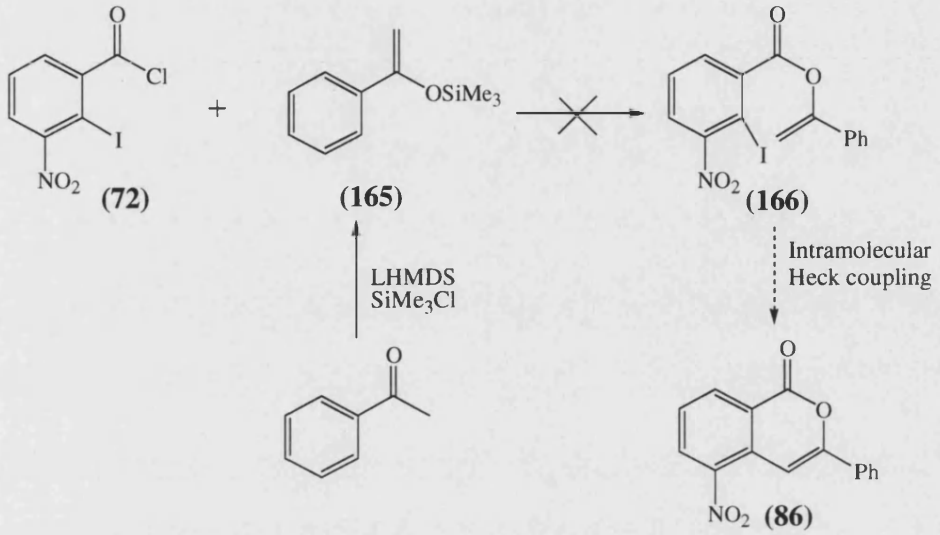

Scheme 18. *Strategy for the synthesis of 5-nitro-3-phenylisocoumarin (86) via intramolecular Heck coupling reaction.*

Thus we have investigated the various organometallic approaches to the synthesis of the 3-substituted isocoumarins and with the exception of 5-nitro-3-phenylisocoumarin **(86)**, 5-nitro-3-(4-methoxyphenyl)isocoumarin **(97)** and 5-nitro-3-(4-methylphenyl)isocoumarin **(103)**, most of them were synthetically inaccessible through these methods.

3.1.8 Route II: enamine formation

While an exploration of Route I was underway, parallel effort was also directed at investigating the alternative synthetic strategy outlined in Scheme 1 which required the use of aryl ethene (**50**) as the equivalent of the synthon (**48**). We were quick to consider the use of the corresponding enamine, where the leaving group is a dimethylamino group (Route II), as our precursor since we have previously described a simple and reliable method of synthesising such enamines[103, 178].

We reported that a condensation of methyl 2-methyl-3-nitrobenzoate with dimethylformamide dimethyl acetal (dimethoxymethyl dimethylamine, DMFDMA) at high temperature (150°C) gave the enamine methyl 2-(2-*E*-dimethylaminoethenyl)-3-nitrobenzoate (**166**) (Scheme 19). Immediate passage of this crude enamine through undried silica gel (column chromatography) not only provides sufficient acid catalysis to hydrolyse the enamine and to cyclise the intermediate enol to 5-nitroisocoumarin, but also purifies the product, all in one elegant step. Greatly encouraged by the success and ease of this synthetic route, we decided to adopt this method for the preparation of our 3-sbustituted targets. We rationalized that similar treatment of methyl 2-methyl-3-nitrobenzoate with dimethylacetamide dimethyl acetal (1,1-dimethoxyethyl dimethylamine, DMADMA) and dimethylbenzamide dimethyl acetal (1,1-dimethoxyphenyl dimethylamine, DMBDMA) may give the desired 3-methyl-5-nitroisocoumarin (**88**) and 5-nitro-3-phenylisocoumarin (**86**), respectively. This would represent a convenient and flexible method for the generation of a whole series of 3-alkyl and 3-aryl substituted targets.

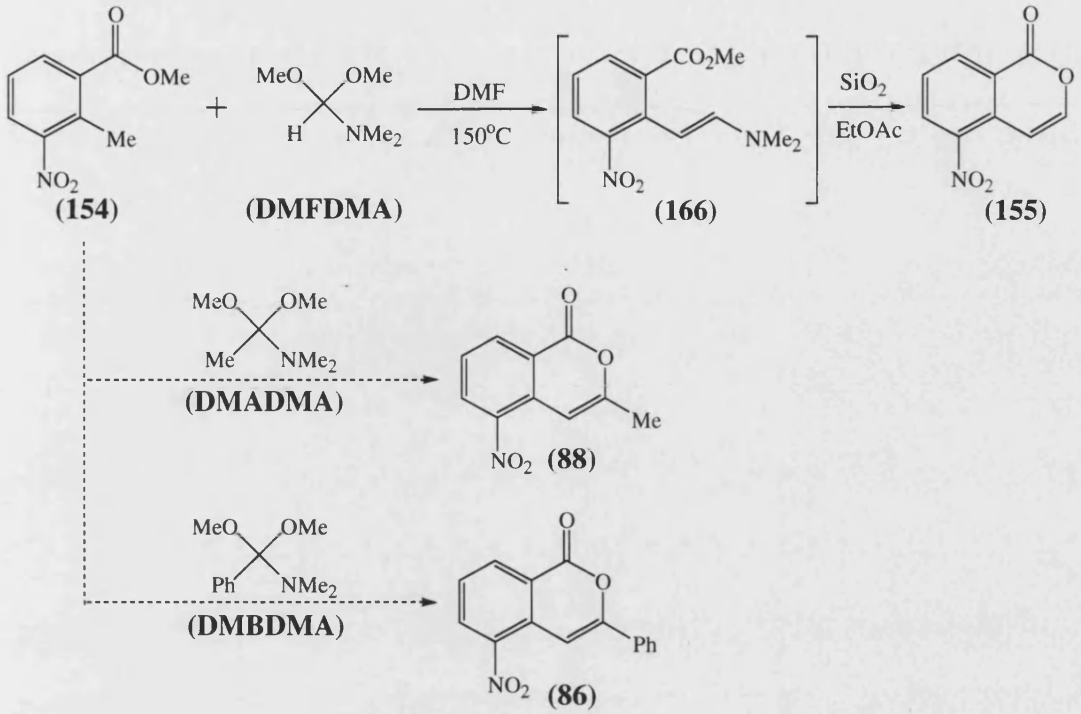

Scheme 19. *Chemical synthesis of 5-nitroisocoumarin (**155**) via condensation of methyl 2-methyl-3-nitrobenzoate (**154**) with DMFDMA and proposed synthesis of 3-methyl-5-nitroisocoumarin (**88**) and 5-nitro-3-phenylisocoumarin (**86**) via similar treatments.*

However, to our surprise, we found that the condensation of compound **(154)** with DMADMA give a deep red solid, the strong colour of which suggested that it was probably not the expected 3-methyl-5-nitroisocoumarin **(88)** as most 5-nitroisocoumarins are yellow. This was supported by the lack of a carbonyl absorption in the IR spectrum. The ^{1}H NMR spectrum showed five aromatic protons together with signals for NMe_2 (a singlet integrating for 6 protons at δ 3.13 p.p.m) and OMe (a singlet integrating for 3 protons at δ 4.00 p.p.m). These data, together with the mass spectrum, allowed the assignment of the naphthalene structure **(167)** to the red solid[178]. This novel compound was possibly formed *via* the following mechanism outlined in Scheme 20. Tautomerism of the enamine **(168)** to the alternative enamine **(169)**, presumably *via* an iminium species, provides a nucleophilic carbon correctly located to attack the ester carbonyl to give **(167)**. It is noteworthy that water is the only leaving group during this condensation reaction as 3-dimethylamino-5-nitronaphth-1-ol **(170)**, which could be formed through the loss of methanol, was not obtained.

Though the above reaction with DMADMA did not give the expected product, we reasoned that the condensation of **(154)** with DMBDMA remains a viable method for the synthesis of 5-nitro-3-phenylisocoumarin **(86)** since the intermediate enamine methyl 2-(2-*Z*-dimethylamino-2-phenylethenyl)-3-nitrobenzoate has no opportunity for tautomerism or further reaction under the conditions used. Unfortunately, we were unable to this examine this hypothesis as DMBDMA was not commercially available and we had difficulties synthesising it. The method described by Hanessian *et al*[179], *i.e.* heating *N,N*-dimethylbenzamide with dimethyl sulphate at 90°C for 4 hours, followed by dropwise addition of the cooled mixture to a dry solution of sodium methoxide in methanol, did not give the desired acetal in our hands.

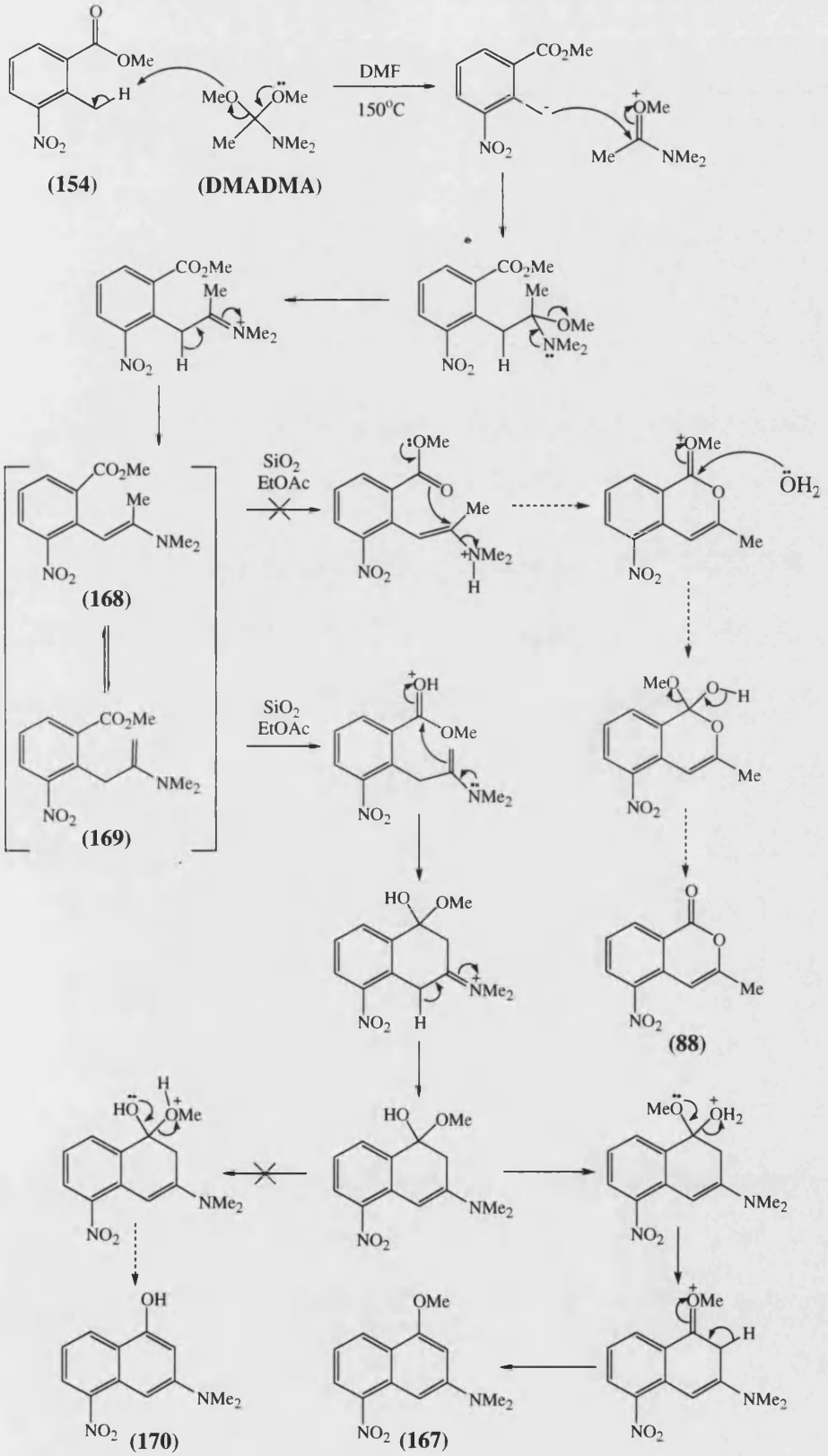

Scheme 20. *Proposed mechanism for the formation of 3-dimethylamino-1-methoxy-5-nitronaphthalene (**167**).*

3.1.9 Route III: enol formation

After several unsuccessful attempts, we decided to consider a different precursor---the enol equivalent (Route III, Scheme 1). This was, by no means, an arbitrary choice. Two major synthetic considerations lie in favour of its use:

1. The enol may be retrosynthetically disconnected to give 2-halo-3-nitrobenzoic acid, a familiar starting material where a reliable method of synthesis for the iodo analogue **(67)** has already been established in the beginning of our study (section 3.1.3).
2. The critical step required for assembling the carbon framework corresponds to a well-known reaction, the **Hurtley reaction**.

Hurtley[180] first observed that 2-bromobenzoic acid condensed smoothly with various β-dicarbonyl compounds in the presence of ethanolic sodium ethoxide and either copper powder or copper(II) acetate as catalyst (Scheme 21). Subsequent systematic investigation of the nature of this reaction by Cirigottis *et al*[181] led to the following conclusions:

1. The reaction succeeds best with 2-bromobenzoic acid although 2-iodobenzoic acid can be expected to give low yields.
2. Replacement of the carboxylic acid by any other functional group such as ester and hydroxyl group prevents the reaction.
3. A copper species is an essential catalyst.

Shinkwin[190] later demonstrated that Hurtley reactions could also be extended to thiophene equivalents. Thus, 4-bromothiophene-3-carboxylic acid condensed with pentane-2,4-dione in the presence of copper, sodium ethoxide and ethanol to afford 4-(1-acetyl-2-oxopropyl)thiophene-3-carboxylic acid. However the reaction failed when the nitro analogue, 4-bromo-5-nitrothiophene-3-carboxylic acid, was used (Scheme 21).

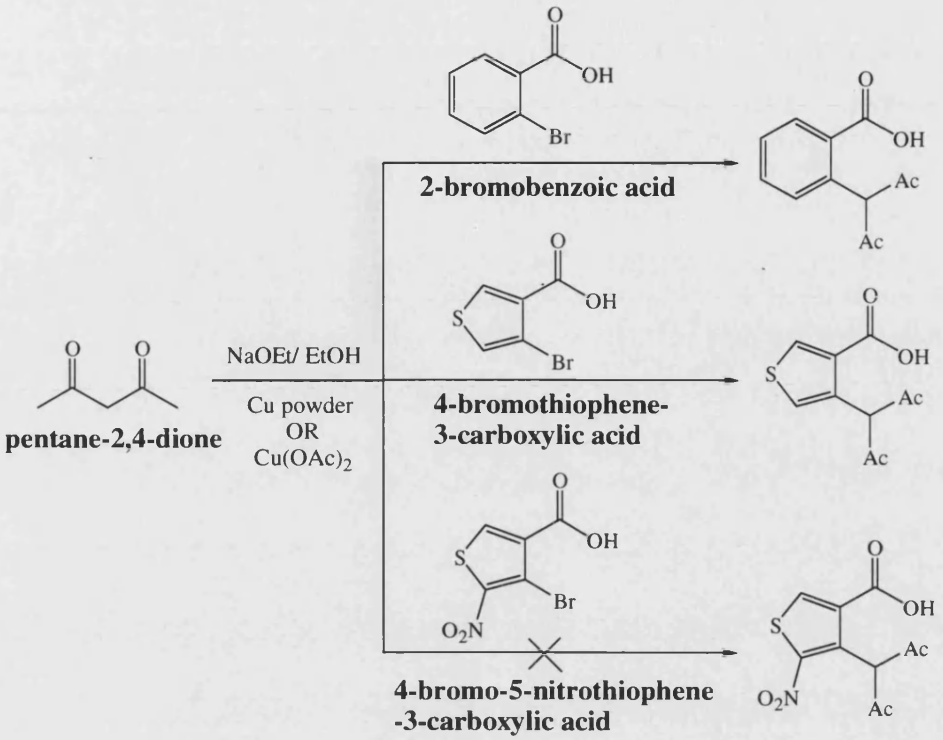

Scheme 21. *Hurtley condensation reaction involving 2-bromobenzoic acid*[180] *and its thiophene analogues*[190].

Accordingly, a possible method of preparing 3-substituted 5-nitroisocoumarin is to condense 2-bromo-3-nitrobenzoic acid **(85)** with the enolate of β-diketones, followed by deacetylation and ring closure as shown in Scheme 22. Deacetylation could be achieved *via* acid hydrolysis while cyclisation may be brought about by treatment with ammonium acetate in boiling acetic acid.

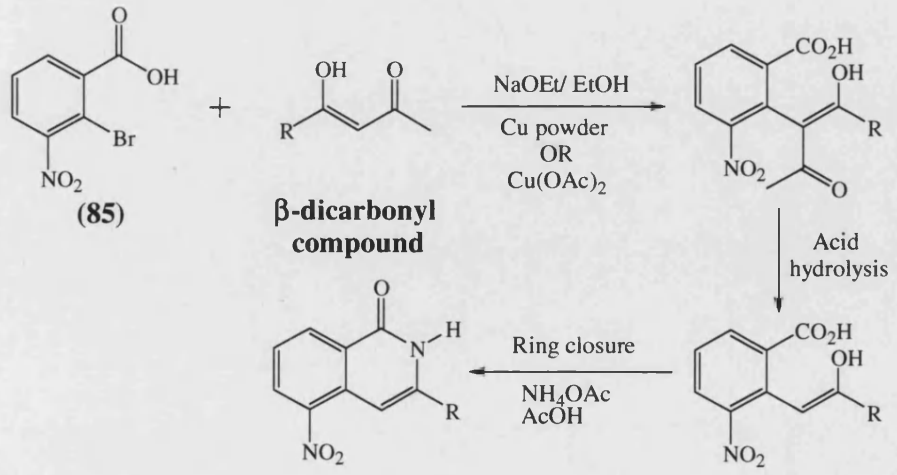

Scheme 22. *Proposed synthesis of 3-substituted 5-nitroisocoumarin.*

Thus, a synthesis of these starting materials was undertaken. The bromo-acid (**85**) was satisfactorily synthesised through mercuration (mercury(II) acetate) and bromination (sodium bromide/bromine) of 3-nitrophthalic acid and this gave a white solid in good yield (74%) (Scheme 6). The β-diketones, on the other hand, were easily prepared in good to excellent yield by Claisen-type condensation reactions between the appropriate ketones and ethyl acetate. The results were summarised in Table 16. We found that most acetophenones could be satisfactorily acylated with acetic anhydride by means of boron trifluoride-acetic acid complex. Heterocyclic counterparts, such as 2-acetylthiophene and 4-acetylpyridine, however, were found to condense poorly under such acidic conditions. Nevertheless their yields were tremendously improved through the use of basic condensing agents, such as sodium amide.

It was found that two equivalents of base (sodium amide), one equivalent of ketone and two equivalents of ester (ethyl acetate) were necessary to ensure optimum yield of the β-diketones. This could be explained by the mechanism proposed in Scheme 23. In the first step of the reaction, the ketone is converted completely to its sodium derivative by one equivalent of sodium amide. In the second step, part of the ketone anion condenses with ethyl acetate to form the β-diketones which reacts rapidly in the third step with unchanged ketone anion to form its anion and the original ketone. However, in the presence of an extra equivalent of sodium amide, the third step will be effected by the strongest base present, which is sodium amide. Hence the use of excess base prevented partial lost of ketone anion, consequently increasing the yield appreciably. An excess of ester was also used as some of them were expected to be lost through side reactions with sodium amide and self-condensation reactions.

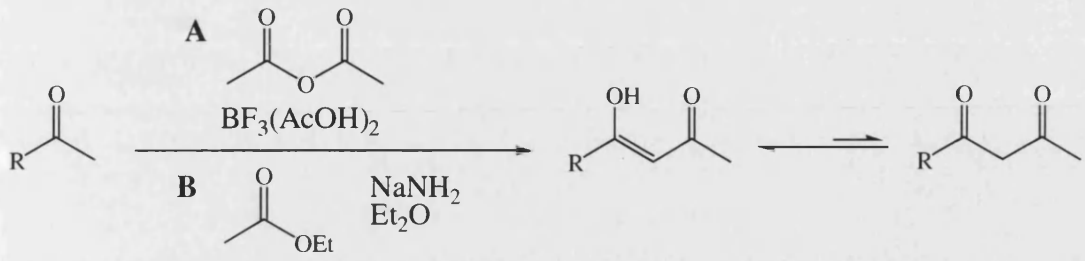

R		Yield of products (%) / (ratio of enol (a): keto (b)) Method A	Method B
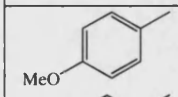	**(95a,b)**	59 (12:1)	*
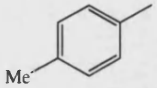	**(101a,b)**	86 (8:1)	*
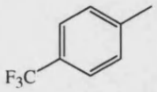	**(108a,b)**	68 (27:1)	*
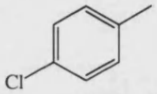	**(115a,b)**	84 (20:1)	*
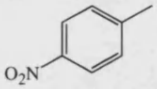	**(127a,b)**	51 (66:1)	*
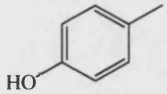	**(129a,b)**	6 (3:1)	*
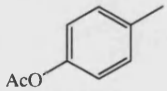	**(130a,b)**	45 (10:1)	*
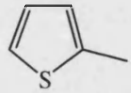	**(122a,b)**	7 (5:1)	55 (10:1)
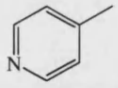	**(128a,b)**	*	39 (11:1)

Table 16. *Synthesis of a series of β-diketones. (*) denotes reaction not attempted.*

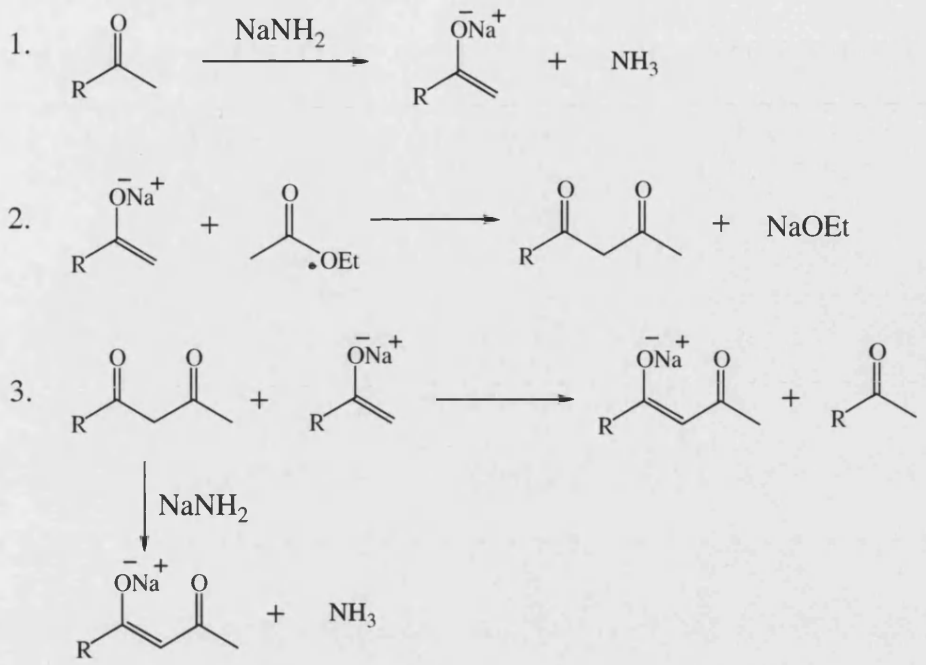

Scheme 23. *Proposed mechanism for the formation of β-diketones under basic conditions ($NaNH_2$).*

In all cases, ^{1}H NMR spectra gave signals that could be ascribed to both the enol and the keto forms, implying the existence of these compounds as a slow equilibrating mixture of both tautomers in deuterated chloroform. The enol tautomers shows characteristic ^{1}H NMR signals at *ca* δ_H16 (OH) and *ca* δ_H 6 (C=CH) whereas their corresponding keto tautomers have CH_2 signals at *ca* δ_H 4. As with most β-diketones, the equilibrium lies well over towards the enol forms (over 90% enol in most cases) due to conjugation and the highly favourable intramolecular hydrogen-bonding (Scheme 24).

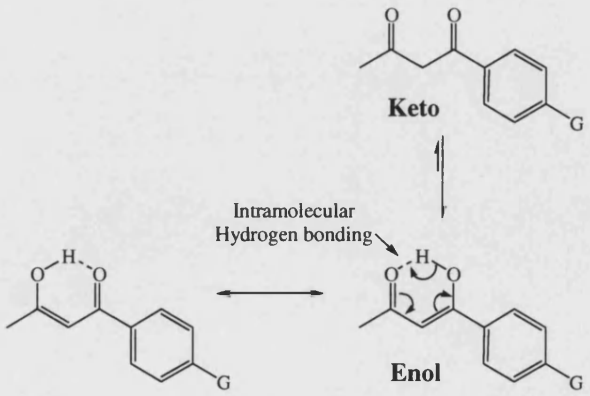

Scheme 24. *Conjugation and intramolecular hydrogen-bonding caused the equilibrium to lie well over towards the enol forms.*

As a preliminary study to establish suitable reaction conditions for the condensation reaction, 2-bromo-3-nitrobenzoic acid **(85)** was boiled under reflux with 4-hydroxy-4-[4-(trifluoromethyl)phenyl]but-3-en-2-one **(108)** using the same reaction conditions prescribed by Hurtley[180], *i.e.*, sodium ethoxide/ethanol/copper powder system (Scheme 25). The result of this reaction is particularly interesting in that none of the expected substitution product **(171)** or de-acetylated compound **(172)** was obtained. Instead the following products were isolated from column chromatography: the desired isocoumarin 5-nitro-3-[4-(trifluoromethyl)phenyl]isocoumarin **(109)** and two side products: 4-(trifluoromethyl)acetophenone **(110)** and ethyl 4-(trifluoromethyl)benzoate **(111)**.

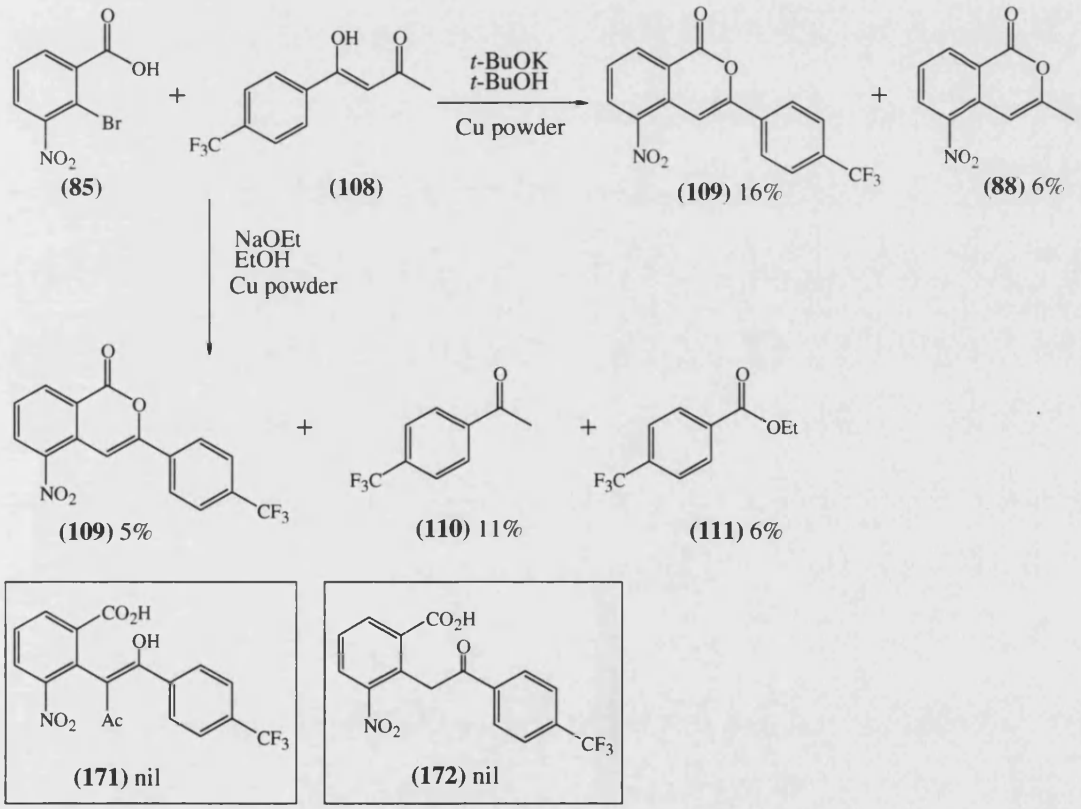

Scheme 25. *Hurtley reaction between 2-bromo-3-nitrobenzoic acid (85) and 4-hydroxy-4-[4-(trifluoromethyl)phenyl]but-3-en-2-one (108).*

It appeared that the initially formed substitution product **(171)** underwent rapid retro-Claisen reaction to give the de-acetylated compound **(172)** which, in turn, cyclised into isocoumarin **(109)** as shown in Scheme 26. Such an effortless

conversion to isocoumarin presumably depends on the unique role of the strongly electron-withdrawing nitroaryl system in stabilising the intermediate carbanion **(173)** which renders compound **(171)** remarkably sensitive to a base, thus promoting the spontaneous loss of acetyl group and cyclisation.

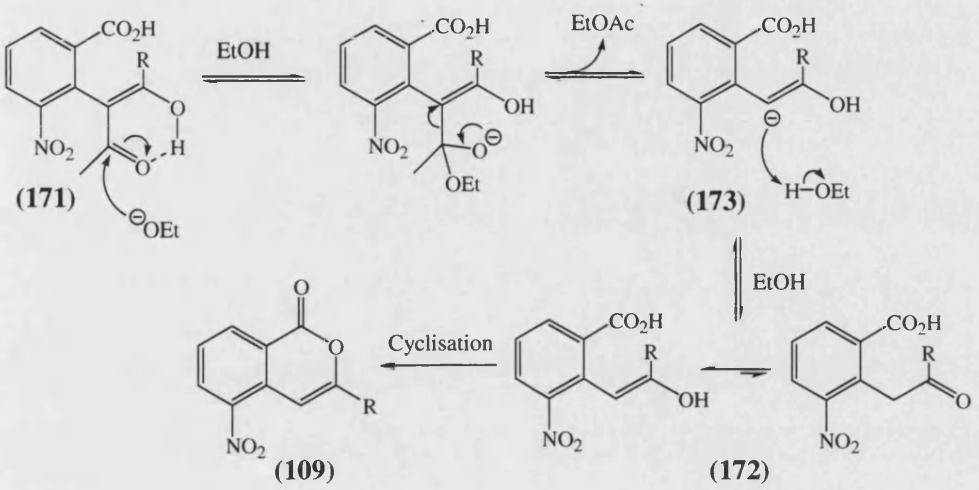

Scheme 26. *Proposed mechanism for the retro-Claisen reaction of substitution product (171) to form the de-acetylated compound (172).*

Under Hurtley's experimental conditions, cleavage of the β-diketones also occurred, affording the side products **(110)** and **(111)**. These were presumably formed *via* nucleophilic attack by ethoxide anion at either of the carbonyl carbon (C-2 or C-4) as illustrated in Scheme 27. It was believed that these side reactions contributed, at least in part, to the low yield of the isocoumarin **(109)** (5%).

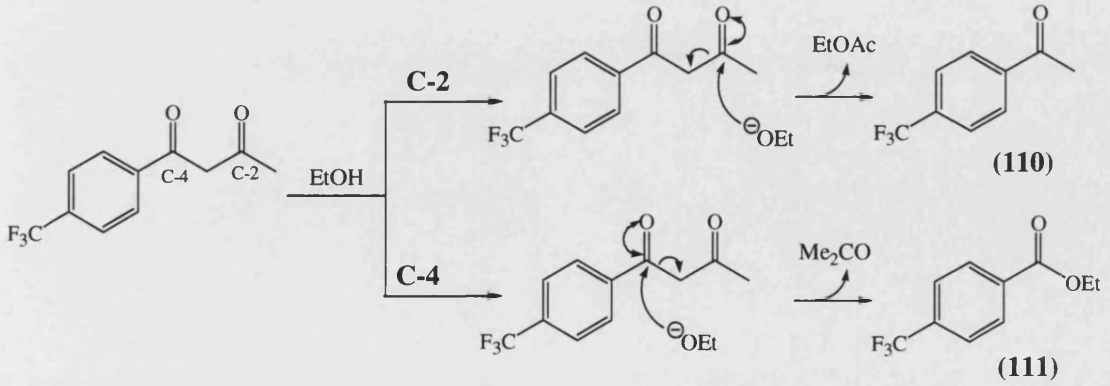

Scheme 27. *Proposed mechanism for the formation of side products (110) and (111).*

In view of these observations, the Hurtley reaction conditions were modified to a potassium *t*-butoxide/*t*-butanol/copper powder system. It was anticipated that the deliberate use of a bulky base/solvent system would discourage nucleophilic attack on the β-diketones, yet without compromising basicity. Although results from Bruggink's studies[182] indicated that copper(I) was the effective catalyst, our decision to keep to the use of copper powder was purely on the ground of operational simplicity. While reaction using copper powder could be conveniently carried out under normal atmospheric condition, the employment of copper(I) salts, such as copper(I) bromide or copper(I) iodide as catalyst would necessitate the total exclusion of oxygen from the reaction to prevent oxidation of copper(I) to copper (II) ions.

Thus, condensations of 2-bromo-3-nitrobenzoic acid **(85)** with the potassium enolate of various β-diketones were undertaken using the above modified reaction conditions. The results were summarised in Method A, Table 17. In general, the reactions went smoothly for most experiments and they were completed within 16 h. A switch to the use of potassium *t*-butoxide as base has successfully prevented the cleavage of β-diketones as demonstrated by the absence of cleavage side products. Consequently, the overall yield of the reaction was improved. For instance, the yield of 5-nitro-3-[4-(trifluoromethyl)phenyl]isocoumarin **(109)** has increased from 5% to 16%. As with the previous system, both the substitution product and the retro-Claisen reaction product were not formed. Instead, the reactions invariably produced a mixture of 3-methyl-5-nitroisocoumarin **(88)** (minor product) and the 3-substituted 5-nitroisocoumarins (major product).

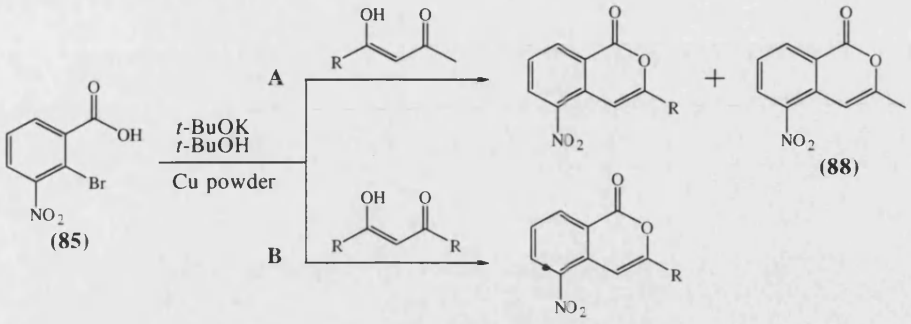

R		Yield of products (%) Method A / (88)	Method B
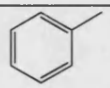	**(86)**	4 / 8	78
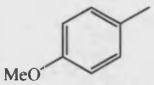	**(97)**	15 / 6	60
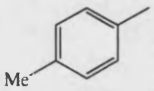	**(103)**	21 / 3	*
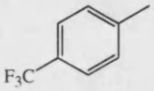	**(109)**	16 / 6	*
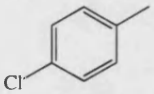	**(116)**	33 / 4	*
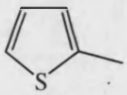	**(123)**	21 / Nil	*
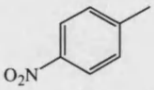		-	*
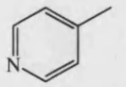		-	*
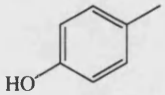		-	*
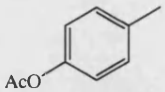		-	*
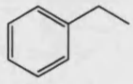		*	
	(147)		32
Methyl	**(88)**	23	23
Ethyl	**(131)**	*	24
Pentyl	**(136)**	4 / 9	36
Isobutyl	**(141)**	*	26
tert-Butyl		-	-

Table 17. *Condensation of compound (85) with various β-diketones. (-) denotes unsuccessful attempts. (*) denotes reaction not attempted.*

It was believed that the 3-aryl substituted 5-nitroisocoumarins and 3-methyl-5-nitroisocoumarin **(88)** were formed *via* de-acetylation and de-benzoylation, respectively, of their arylated intermediate (Scheme 28).

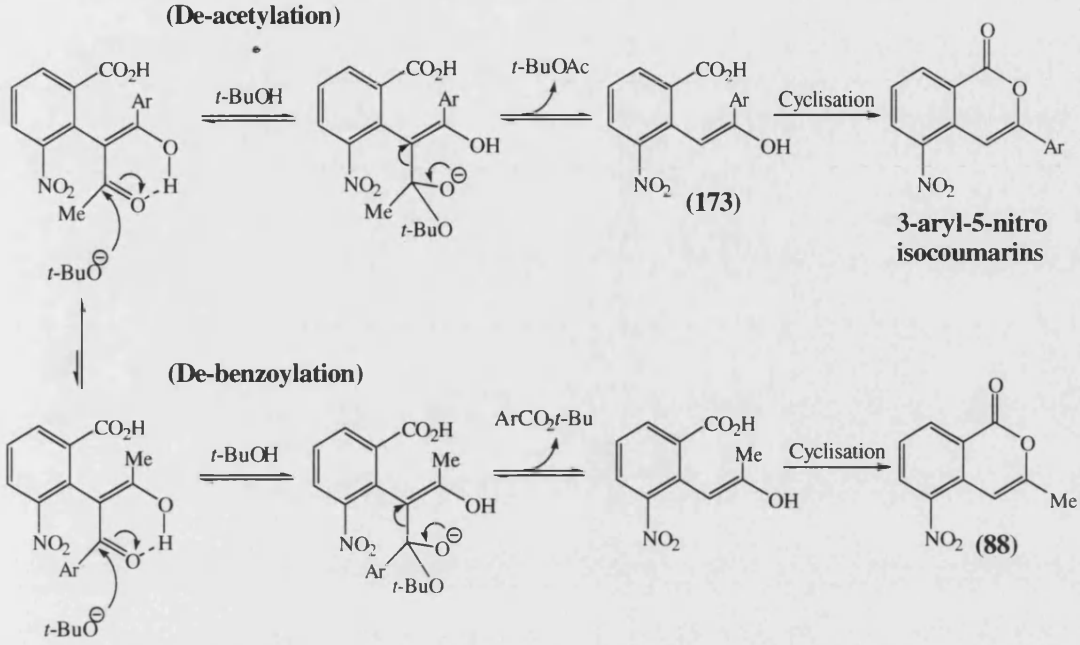

Scheme 28. *Proposed mechanism for the formation of 3-aryl-5-nitroisocoumarins and 3-methyl-5-nitroisocoumarin (88) via de-acetylation and de-benzoylation respectively.*

It seems that a preference for de-acetylation or de-benzoylation depends on a balance of electronic and steric effects. On electronic ground, de-benzoylation is favoured as the benzoyl carbonyl carbon is more electrophilic than the acetyl carbonyl carbon. Sterically, however, de-acetylation is preferred since the methyl group is less bulky compared to the phenyl group. Presumably in the case of isocoumarins **(97)**, **(103)**, **(109)**, **(116)** and **(123)**, steric hindrance of the phenyl ring outweighed its electron-withdrawing effects, thus 3-aryl substituted 5-nitroisocoumarins were obtained in greater yield compared to that of 3-methyl-5-nitroisocoumarin **(88)**.

Accordingly, we postulated that the yield may be increased through the use of 1,3-disubstituted β-diketones, in which case only one isocoumarin product is possible. This was borne out by the comparatively much higher yield obtained when analogous condensations of 2-bromo-3-nitrobenzoic acid **(85)** with 1,3-disubstituted β-diketones were carried out as illustrated in method B, Table 17. (Synthesis of the latter was achieved *via* the use of basic condensation reagents, sodium amide and the results were summarised in Table 18.) Particularly noteworthy were the yields of isocoumarin **(86)** and **(97)** which have escalated from 4% and 15% to 78% and 60% respectively. Improvement in yield for the 3-alkyl substituted isocoumarins, however, was modest, with yields ranging from 20% to 40%.

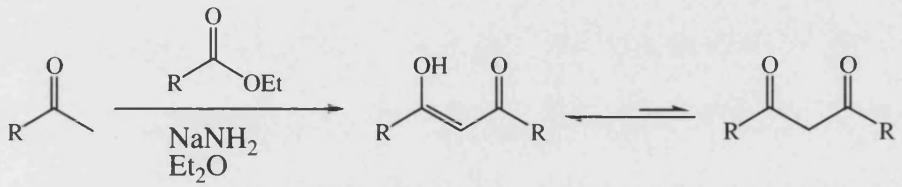

R		Yield of products (%) / (ratio of enol (a): keto (b))
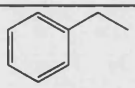	**(135a,b)**	50 (50:1)
Pentyl	**(140a,b)**	75 (4:1)
Isobutyl	**(145a,b)**	26 (10:1)

Table 18. *Synthesis of a series of 1,3-disubstituted β-diketones. Pentane-2,4-dione (R=Me), heptane-3,5-dione (R=Et) and 2,2,6,6-tetramethyl-3,5-heptanedione (R= t-Bu) are commercially available.*

At first thought, the presence of an additional aromatic substituent at the 3-position of the β-diketone was expected to make the latter more bulky and its corresponding carbanion less nucleophilic, hence, less reactive towards 2-bromo-3-nitrobenzoic acid **(85)**. However as postulated by Bruggink and McKillop[182], the mechanism of the Hurtley reaction involved the formation of a copper chelate in which the copper(I) ion is coordinated in a planar manner to the bromo-acid **(85)** and the carbonyl oxygen atom in the β-dicarbonyl anion as illustrated in Scheme 29. Such an interaction brings the nucleophile within bonding distance of the carbon bearing the

bromine, thus enabling it to react efficiently even though it is less nucleophilic. Once the substitution product has formed, retro-Claisen reaction became much easier than before as it now involved a nucleophilic attack by butoxide anion on the more electrophilic benzoyl carbonyl carbon rather than on the acetyl carbonyl carbon. These effects were also operative in the 1,3-dialkylsubstituted β-diketones but presumably less pronounced, thus the less significant improvement in yields.

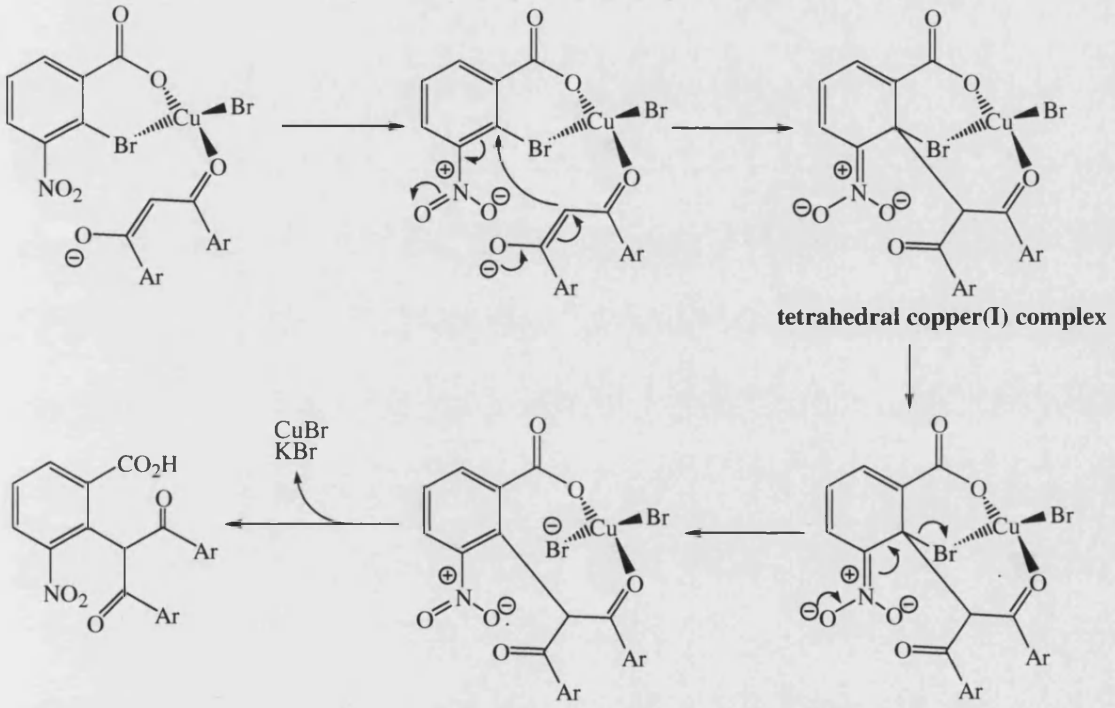

Scheme 29. *Proposed mechanism for Hurtley reaction*[182].

The inability of cyclic or crowded β-diketones, such as 2,2,6,6-tetramethyl-3,5-heptanedione **(174)**, 3-methyl-2,4-pentanedione **(175)** and 1,3-cyclohexanedione **(176)** to react can also be satisfactorily explained by the proposed mechanism. While steric factors prevented the bulky β-diketones **(174)** and **(175)** from coming into close proximity with the electrophilic carbon for reaction, the structural rigidity of the cyclohexane ring in 1,3-cyclohexanedione **(176)** prevented it from assuming the appropriate conformation required for the formation of the tetrahedral copper(I) complex.

Supposedly, β-diketones containing functionalities that are able to coordinate with the copper(I) ion, such as hydroxy and acetoxy groups might also compete with its carbonyl oxygen for binding with copper(I) ion, resulting in a distortion of the tetrahedral intermediate and the failure to react. This may account for the lack of success observed with β-dicarbonyls such as: 4-hydroxy-4-(4-nitrophenyl)but-3-en-2-one (**127**), 4-hydroxy-4-(4-pyridinyl)but-3-en-2-one (**128**), 4-hydroxy-4-(4′-hydroxyphenyl)-but-3-en-2-one (**129**) and 4-hydroxy-4-(4-acetoxyphenyl)but-3-en-2-one (**130**).

What remained to be done was to convert these isocoumarins into their corresponding isoquinolin-1(2*H*)-one hydrochlorides. This was accomplished by repeating the synthetic sequence outlined in Scheme 13, *i.e.*,

1. Conversion of the isocoumarins to isoquinolin-1(2*H*)-ones by treatment with boiling ammonia-saturated 2-methoxyethanol.
2. Catalytic reduction of the nitro function *via* heating at 70°C with tin(II) chloride in ethanol.
3. Formation of its hydrochloride salt by stirring with aqueous hydrochloric acid (2 M).

The yields of the experiments were summarised in Table 19 below.

Hence, we have successfully exploited the high reactivity of halo-organo compounds, under the catalytic influence of copper, for the synthesis of a series of 3-substituted 5-aminoisoquinolin-1(2*H*)-ones. These target compounds will be tested for their water-solubility and their *in vitro* PARP-1 inhibitory potency. This will be followed by systematic studies on their SAR.

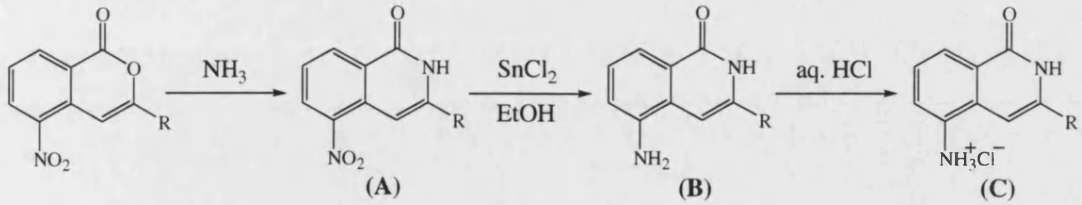

R	Yield of products (%) A	B	C
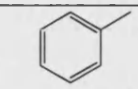	73 **(89)**	57 **(90)**	91 **(91)**
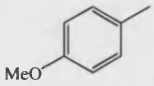	65 **(98)**	83 **(99)**	95 **(100)**
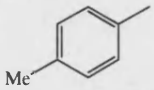	86 **(104)**	92 **(105)**	94 **(106)**
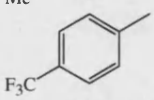	27 **(112)**	40 **(113)**	92 **(114)**	
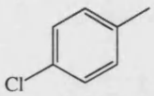	64 **(119)**	41 **(120)**	95 **(121)**
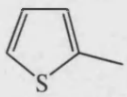	63 **(124)**	66 **(125)**	94 **(126)**
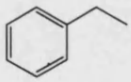	83 **(148)**	64 **(149)**	93 **(150)**
Methyl	68 **(92)**	59 **(93)**	95 **(94)**
Ethyl	38 **(132)**	24 **(133)**	94 **(134)**
Pentyl	29 **(137)**	67 **(138)**	93 **(139)**
Isobutyl	89 **(142)**	83 **(143)**	97 **(144)**

Table 19. *The conversion of a series of 3-substituted isocoumarins into their corresponding isoquinolin-1(2H)-ones hydrochlorides.*

3.2 4-substituted 5-aminoisoquinolin-1(2*H*)-ones

Following the successful synthesis of a series of 3-substituted 5-aminoisoquinolin-1(2*H*)-ones, we directed our attention to the synthesis of the 4-substituted 5-aminoisoquinolin-1(2*H*)-ones. These were also of considerable interest as potential PARP-1 inhibitors, since an examination of the PARP-1 active site indicated that there was a relatively large binding pocket in the region corresponding to the 4-position of the isoquinolin-1(2*H*)-one ring which could potentially be exploited to enhance PARP-1 inhibitory potency. In addition, the SAR studies[150] of a series of 4-substituted phthalazinones **(33)** further suggested that benzyl groups were well tolerated in that region and that they generally improve inhibitory activity. We began by conducting a series of preliminary studies to explore the possibilities of extending some of the synthetic approaches we have previously studied, such as organometallic synthesis, for the preparation of the 4-substituted targets.

3.2.1 Suzuki or Stille coupling reactions

The first approach takes advantage of the electronic differences between the 3- and the 4-position of the isoquinolin-1(2*H*)-one ring. The 4-position is believed to be more nucleophilic, compared to the 3-position, due to mesomeric electron-donating effect of the ring nitrogen. This was borne out by the ^{1}H NMR of 5-nitroisoquinolin-1(2*H*)-one **(160)** in $(CD_3)_2SO$, where the additional shielding effect caused the signal for 4-H to be shifted upfield by 0.48 p.p.m. with respect to 3-H. Such a difference in nucleophilicity, and thus reactivity towards electrophiles, between the 3- and 4-position can be exploited to attach an electrophile selectively, such as iodine or bromine, at the 4-position. The resulting halide **(162)** will be of great value in organometallic synthesis as a scaffold through which a diverse range of substituents may be introduced at the 4-position *via* appropriate organometallic reagents, such as organoboranes (**Suzuki coupling reaction**) or organostannanes (**Stille coupling reaction**). A series of 4-substituted targets would be expected to be easily and conveniently generated (Scheme 30).

Thus, iodination of 5-nitroisoquinolin-1(2*H*)-one **(160)** (synthesised according to the method described by McDonald *et al*[103]) with a solution of iodine in acetic acid was undertaken. However, surprisingly, the reaction mixture remained unchanged even after stirring for 24 h. Employment of more electrophilic conditions, such as a combination of lithium iodide and iodine in acetic acid and a switch to the use of brominating reagents (bromine being more reactive compared to iodine), such as bromine and *N*-bromosuccinimide, also failed to effect halogenation.

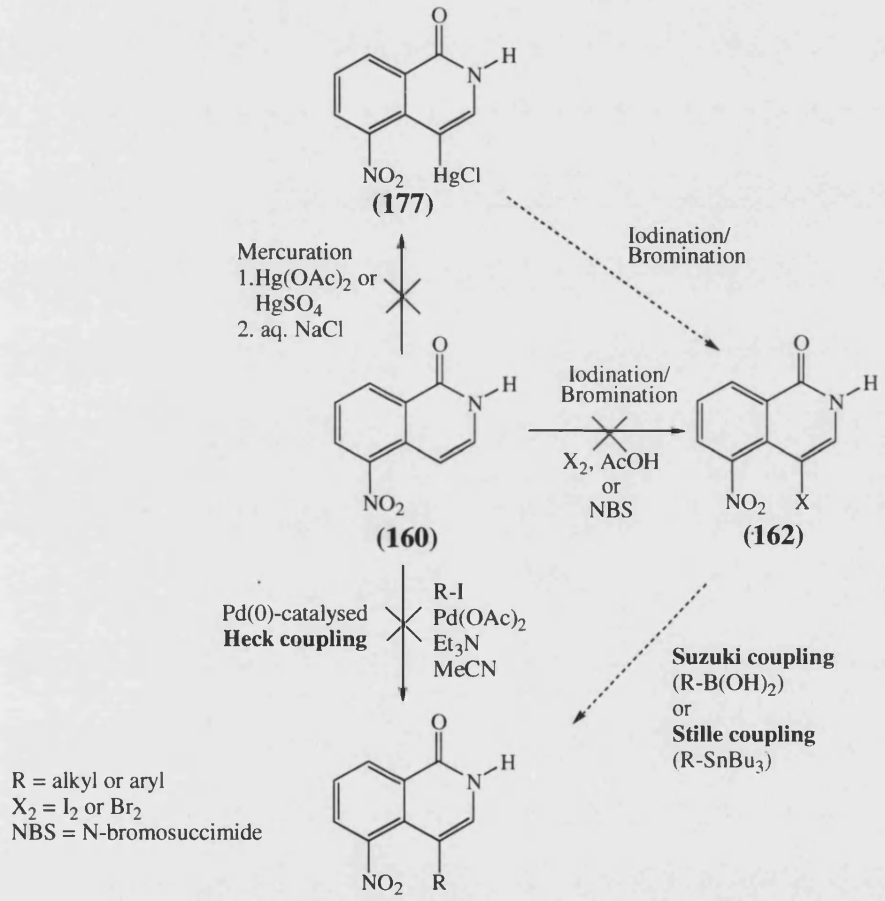

Scheme 30. *Different chemical approaches for the synthesis of 4-substituted isoquinolin-1(2H)-ones.*

An indirect method of iodination was therefore considered. This involved an initial substitution of the 4-position of isoquinolin-1(2*H*)-one **(160)** with mercury(II) chloride to form an aryl mercury salt **(177)** which may subsequently be converted to an iodide or bromide by reaction with iodine or bromine respectively. However,

attempts to mercurate compound **(160)** by treatment with either mercury(II) acetate or mercury(II) sulphate, followed by an exchange of the acetate or the sulphate anion with chloride *via* treatment with aqueous sodium chloride led only to decomposition products.

3.2.2 Heck coupling reaction

The repeated failure of 5-nitroisoquinolin-1(2*H*)-one **(160)** to participate in any variants of iodination or bromination reactions, despite the predicted activation of the 4-position by the carboxamide group was most puzzling and this led us to modify our synthetic strategy. Thus, instead of converting **(160)** into a halide suitable for Suzuki or Stille coupling reactions, it will now serve as the alkene partner in an alternative palladium-mediated coupling reaction--- the **Heck coupling reaction** (Scheme 30).

This is a versatile carbon-carbon bond forming reaction which allows desirable functionalities to be attached across alkenes. Traditionally, the Heck coupling reaction was based on an aryl or vinyl iodide/bromide as the electrophile and a terminal alkene as the nucleophile[177]. However, various aspects of the Heck reaction have been reviewed in recent years, leading to protocols that allowed for the coupling of aryl/vinyl halides onto heteroaryl recipients, such as thiophenes, imidazoles and indoles[218]. Such heteroaryl Heck reaction may be exemplified by the reaction between 2-nitrobromobenzene and benzofuran where addition occurs regioselectively at the more electron-rich position (C-2) of benzofuran to give 2-(2-nitrophenyl)benzofuran[219] (Scheme 31).

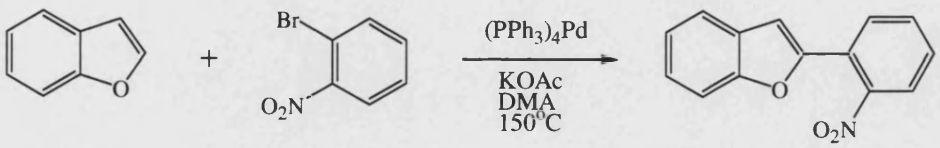

benzofuran 2-bromonitrobenzene 2-(2-nitrophenyl)benzofuran

Scheme 31. *Heteroaryl Heck reaction between 2-nitrobromobenzene and benzofuran*[219].

A Heck coupling reaction between isoquinolin-1(2*H*)-one **(160)** and iodobenzene was therefore attempted. This was carried out in the presence of a catalytic amount of palladium(II) acetate in dry triethylamine and dry acetonitrile and the mixture was allowed to boil for 24 h under argon. However, it gave the starting material **(160)** in virtually quantitative yield, without formation of the 4-substituted product. Repeats of the coupling process employing various combinations of catalysts [e.g. $(PPh_3)_2PdCl_2$, $(PPh_3)_4Pd$] and reaction conditions (base, solvents) and analogous treatments of 5-nitroisocoumarin **(155)** all failed to improve the outcome of the reaction.

Incidentally, the isocoumarin **(155)** also failed to participate in acylation when treated with a mixture of benzoyl chloride and tin(IV) chloride (Lewis acid catalyst) (Scheme 32), even though such reactions were known to proceed with great ease with furans[220]. It appeared that there was an apparent lack of reactivity of the double bond across C-3 and C-4 in both the isocoumarin and the isoquinolin-1(2*H*)-one ring. Presumably, the presence of a highly electron-withdrawing 5-nitro group decreases the nucleophilicity of the double bond and thus causes its lack of reactivity towards iodine, bromine and organometallic reagents. These apparent difficulties resisted further attempts to effect direct synthesis of the 4-substituted targets using organometallic approach.

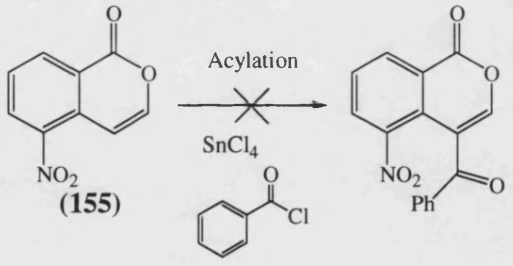

Scheme 32. *Attempted acylation of isocoumarin (155) with a mixture of benzoyl chloride and tin(IV) chloride.*

3.2.3 DMFDMA

In Section 3.1.8, we studied a range of reactions involving condensation between methyl 2-methyl-3-nitrobenzoate **(154)** and various acetals, such as DMFDMA and DMADMA. It occurred to us that this reaction could also be extended for the synthesis of the 4-substituted targets. Analogous condensation of DMFDMA with compounds of the type **(178)** could be employed to introduce the necessary carbon unit for subsequent cyclisation to the corresponding 4-substituted isocoumarins (Scheme 33).

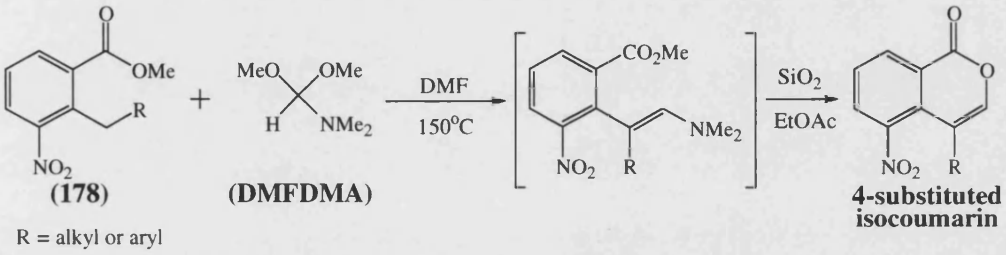

Scheme 33. *Chemical synthesis of 4-substituted isocoumarin via condensation of compound (178) with DMFDMA.*

To investigate this idea, the novel methyl 2-benzyl-3-nitrobenzoate **(161)** was synthesised. This was accomplished in moderate yield (32%) *via* a **Negishi coupling reaction** between methyl 2-iodo-3-nitrobenzoate **(68)** and benzyl zinc bromide under the catalytic influence of palladium. In general, the Negishi reaction enables a cross-coupling between an organozinc reagent and an organohalide or triflate[171]; however, various variations of the protocol, such as those employing organomagnesium and organotin reagents, have also been found to be successful[221]. The use of alkylzinc reagents is advantageous in our experiment in that the carbon-zinc bond is less reactive and thus highly compatible with electrophiles that contain sensitive functionalities such as esters, nitro, amides and nitriles. Many different palladium catalysts, such as those prescribed for Sonogashira protocols, have also been used with much success in Negishi coupling. However, to facilitate the reduction of Pd(II) to Pd(0), thereby ensuring high coupling efficiency, Negishi *et al*[171] used a complex of palladium(II) catalyst, $(PPh_3)_2PdCl_2$, and DIBAL-H (1:2)

as catalyst and this was adopted in our experimental procedure. As with the Sonogashira coupling reaction, the Negishi coupling probably operates by an *oxidative addition-transmetallation-elimination* mechanism as illustrated in Scheme 34 below.

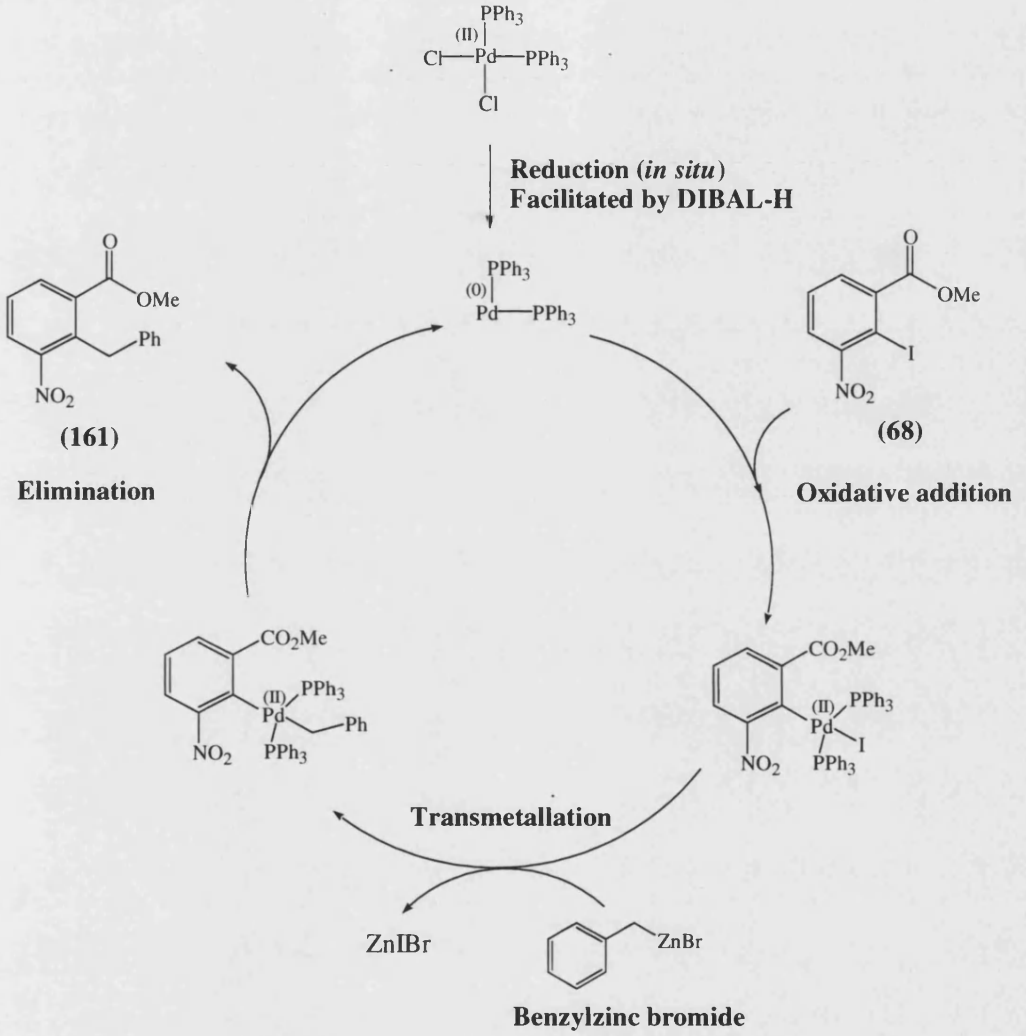

Scheme 34. *Proposed mechanism for Negishi coupling reaction between methyl 2-iodo-3-nitrobenzoate* ***(161)*** *and benzyl zinc bromide.*

It is interesting to note that the use of DIBAL-H in the reaction did not result in a reduction of the ester and nitro functions, as evidenced from the absence of amine and aldehyde/ alcohol absorption peaks in IR spectra.

Unfortunately, subsequent treatment of **(161)** with DMFDMA / silica (column chromatography) did not proceed as anticipated to give the desired 5-nitro-4-phenylisocoumarin **(179)**[178]. A similar reaction with DMADMA also did not afford the expected naphthalene product, 1-methoxy-3-dimethylamino-5-nitro-4-phenylnaphthalene **(180)** (Scheme 35). This was surprising as the arylmethyl in compound **(161)** was expected to be much more reactive due to activation by the phenyl substituent, and thus more susceptible towards condensation reactions with the acetals than its unsubstituted counterpart **(154)**.

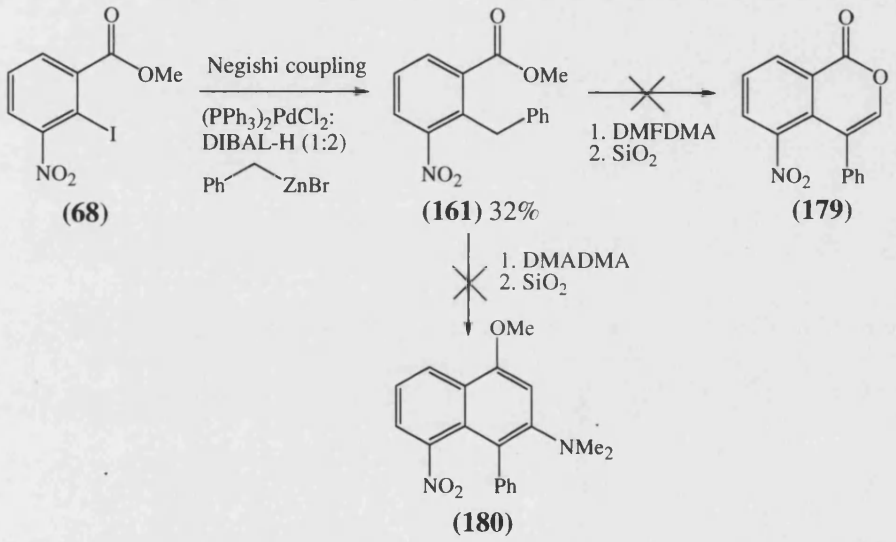

Scheme 35. *Condensation reactions of methyl 2-benzyl-3-nitrobenzoate (161) with DMFDMA and with DMADMA.*

It was thought that the bulky phenyl substituent in **(161)** might have prevented the reaction from occurring. A synthesis of the sterically less hindered nitrile analogue, methyl 2-cyanomethyl-3-nitrobenzoate **(157)** was therefore undertaken and the proposed synthesis was outlined in Scheme 36. The first step involved a radical bromination of the ester **(154)** and this was achieved by subjecting the latter to a boiling mixture of bromine and dibenzoyl peroxide in carbon tetrachloride under irradiation with a 150 W tungsten lamp for 20 h. Additional bromination mixture was then added and the mixture was heated and irradiated for another 29 h. This gave the

mono-brominated product, methyl 2-bromomethyl-3-nitrobenzoate **(156)**, in excellent yield (98%). Subsequent nucleophilic substitution of **(156)** with tetraethylammonium cyanide in acetonitrile at room temperature afforded the nitrile **(157)** in 68% yield.

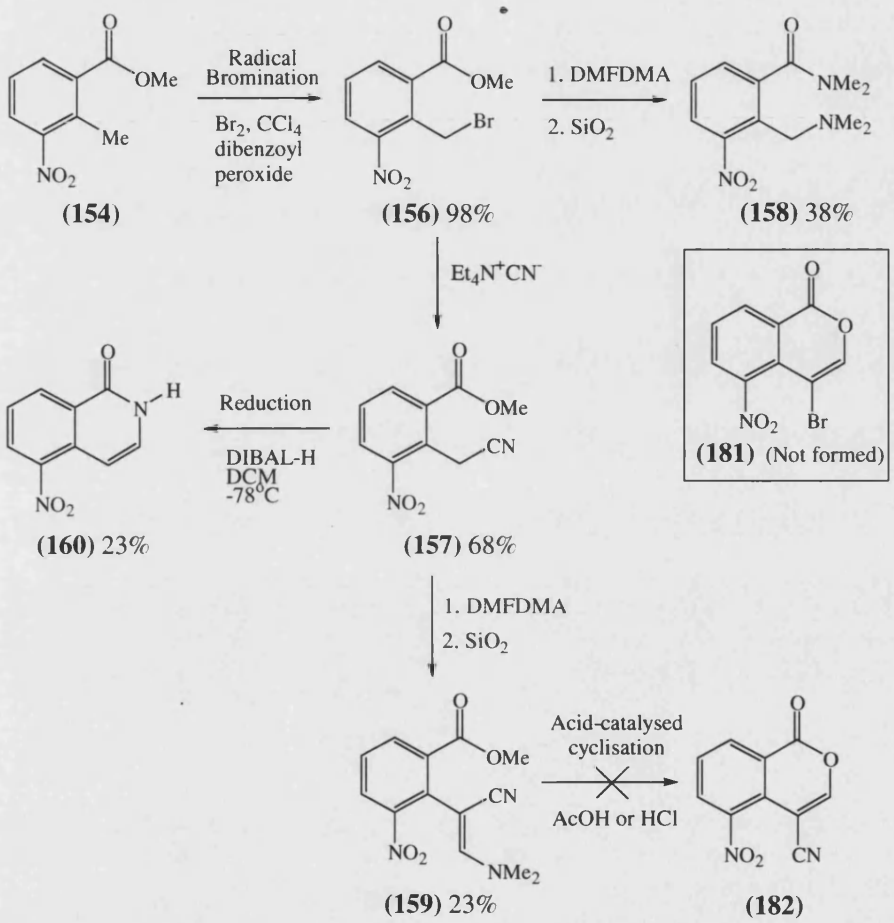

Scheme 36. *Condensation reactions of methyl 2-bromomethyl-3-nitrobenzoate (156) and methyl 2-cyanomethyl-3-nitrobenzoate* **(157)** *with DMFDMA.*

Both compounds **(156)** and **(157)** represents reactive equivalents of the methyl ester **(154)** where the methylene groups are activated by the electron-withdrawing bromo and nitrile groups respectively. Thus, condensation reactions of these two compounds with DMFDMA under similar reaction conditions were expected to give 4-bromo-5-nitroisocoumarin **(181)** and 4-cyano-5-nitroisocoumarin **(182)** respectively. However, it was observed that the bromo-compound **(156)** gave an

orange oil which, upon spectroscopic determination, was found to be compound **(158)** (Scheme 36). This was probably the result of a direct nucleophilic attack of the dimethylamine group on the methylene carbon (mechanism outlined in Scheme 37), which, in this instance, was presumably more favourable than the predicted reaction because bromine is a good leaving group. Accordingly, this side reaction could be avoided by using trimethylorthoformate instead of DMFDMA. The cyano-compound **(157)**, on the other hand, proceeded well to give the intermediate enamine **(159)** (Scheme 36). Unfortunately, attempts to effect cyclisation of this enamine with acetic acid and aqueous hydrochloric acid (2 M) were unsuccessful.

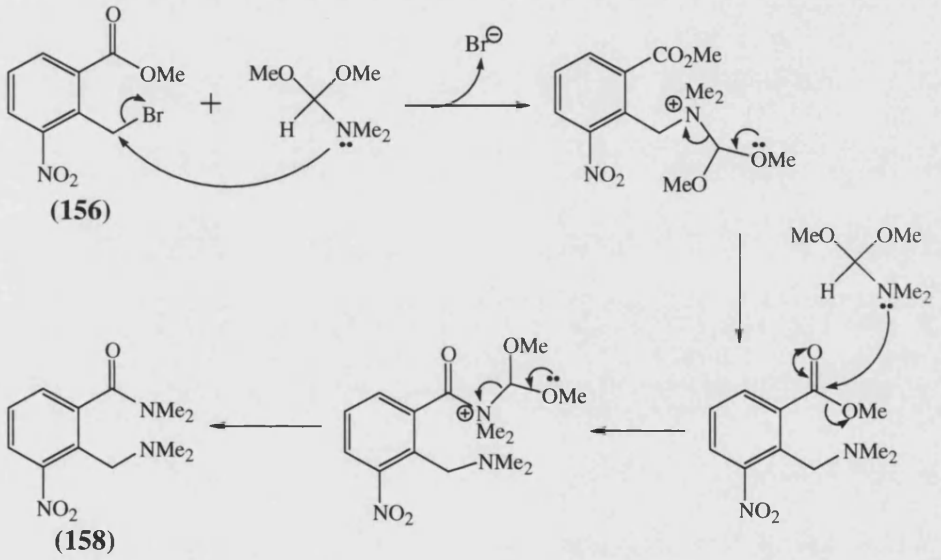

Scheme 37. *Proposed mechanism for the condensation reactions between methyl 2-bromomethyl-3-nitrobenzoate (**156**) and DMFDMA.*

Nevertheless, reduction of the nitrile function in compound **(157)** with DIBAL-H at -78°C successfully afforded 5-nitroisoquinolin-1(2*H*)-one **(160)** in 23% yield (Scheme 36). Presumably, during aqueous acid work-up, the transitional imine underwent rapid intramolecular nucleophilic substitution with the neighbouring methyl ester, resulting in the formation of a lactam ring. The proposed mechanism for this reaction is given in Scheme 38.

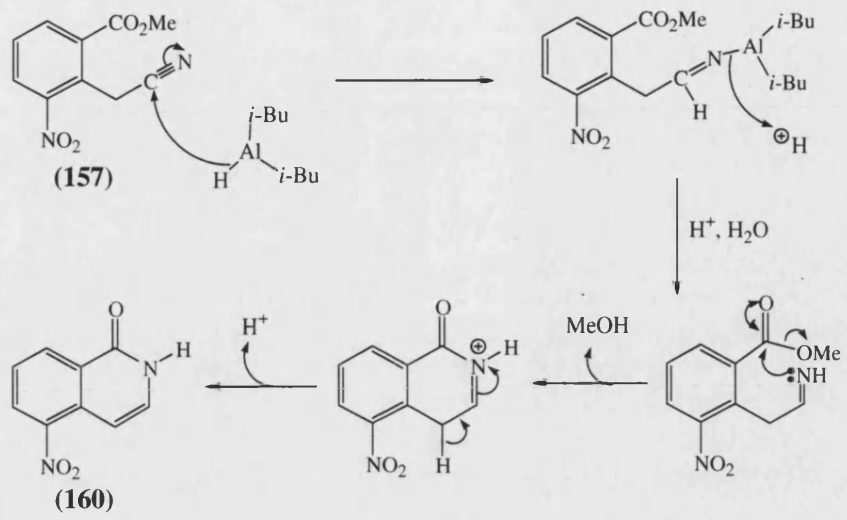

Scheme 38. *Proposed mechanism for the reductive cyclisation of methyl 2-cyanomethyl-3-nitrobenzoate (157).*

The successful synthesis of compound **(160)** is very encouraging. It not only provides a novel, reliable and simple route for the preparation of 5AIQ, but also represents a promising synthetic strategy for the synthesis of the 4-substituted targets (results to be published).

Accordingly, the desired substituents could first be introduced *via* alkylation of the methylene carbon of compound **(157)**. This could be achieved quite simply, for instance *via* initial deprotonation with a hindered base such as lithium hexamethyldisilazide (LHMDS), followed by reaction with an appropriate alkylating agent such as methyl iodide. Subsequent ring closure of the alkylated species **(184)** with DIBAL-H could lead to the formation of 4-substituted 5-nitroisoquinolin-1(2*H*)-ones (Route I, Scheme 39).

Alternatively, substituents could also be introduced, *via* similar alkylation procedures, onto the methyl group in compound **(154)**. Subsequent bromination, conversion to nitrile and reduction with DIBAL-H could also lead to the formation of the desired isoquinolin-1(2*H*)-ones (Route II, Scheme 39).

Regrettably, we were not able to carry out the actual synthesis of the 4-substituted targets due to a shortage of time. However, since the alkylation process is a reliable and standard process and that we have already overcome the potentially most difficult step in the proposed routes, *i.e.* reductive cyclisation of nitrile, we believe that the 4-substituted targets are synthetically accessible through these pathways (Scheme 39).

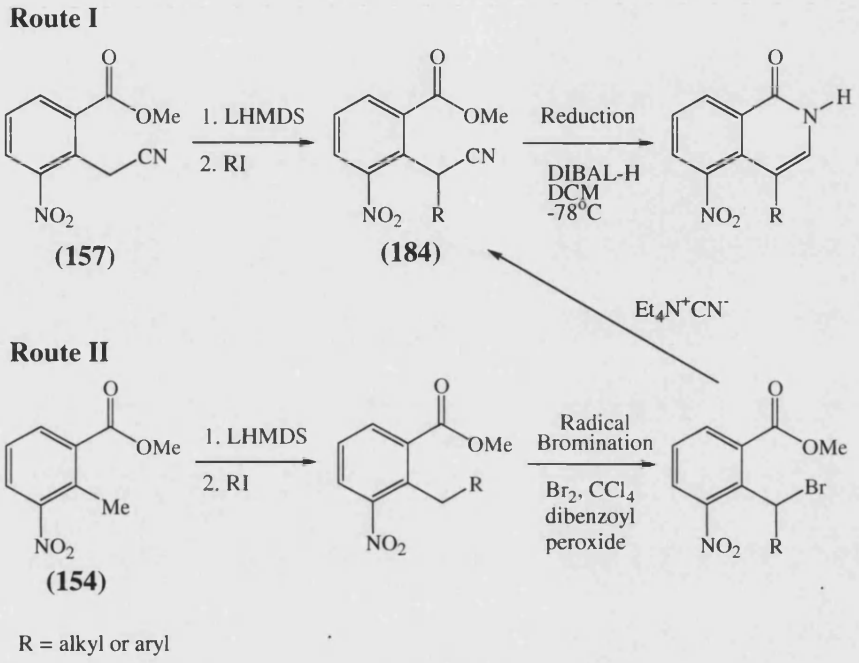

Scheme 39. *Proposed synthetic pathway for the formation of 4-substituted 5-nitroisoquinolin-1(2H)-ones.*

3.3 5-[(*N,N*-Dimethylamino)methyleneamino]isoquinolin-1(2*H*)-one

The exceptional *in vivo* PARP-1 inhibitory potency demonstrated by 5AIQ.HCl was previously accredited to its good water-solubility and its excellent biopharmaceutical properties. However, recent X-ray crystallographic data has demonstrated possible hydrogen-bonding between Glu988 and the amino group of 4-amino-1,8-naphthalimide (**26b**)[142]. Since this corresponds, approximately, to the 5-position of 5AIQ, it is likely that the 5-amino group in 5AIQ may also form (water-mediated) hydrogen-bonds with the active site, thus contributing, at least in part, to the enhanced potency. It is therefore of interest to examine the nature of this interaction through the synthesis of amidine analogues of 5AIQ as exemplified by 5-[(*N,N*-dimethylamino)methyleneamino]isoquinolin-1(2*H*)-one (**163**). Whilst the 5-amino substituent in 5AIQ can function both as hydrogen-bond donor and acceptor, compound (**163**), in the absence of any hydrogen atom attached to the amino group, can only serve as hydrogen-bond acceptor. This would allow an investigation of the manner in which the 5-amino group participated in hydrogen-bonding and the effects of *N*-substitution on PARP-1 inhibitory activity.

Compound (**163**) was readily synthesised in high yield (83%) by stirring with DMFDMA in dry dimethylformamide under nitrogen at 45°C as shown in Scheme 40.

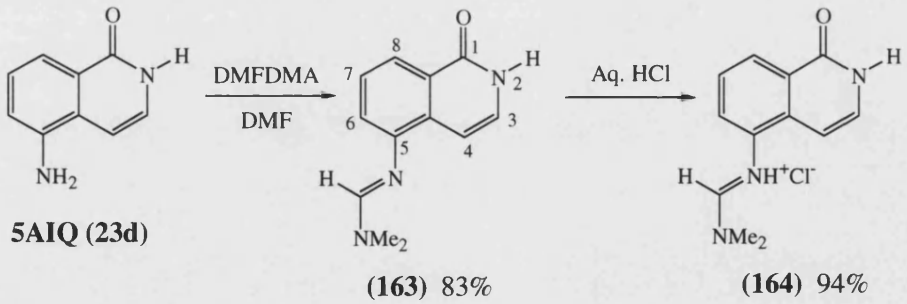

Scheme 40. *Chemical synthesis of 5-[(N,N-dimethylamino)methyleneamino] isoquinolin-1(2H)-one hydrochloride* (***164***).

Its ^{1}H NMR spectrum is particularly interesting:

1. The spectrum of the starting material, 5AIQ (**23d**), in $(CD_3)_2SO$ showed separate doublet signals for isoquinolin-1(2*H*)-one 3-H and 4-H, the former being 0.35 p.p.m. downfield with respect with the latter. Whereas in the spectrum of the product (**163**) in $CDCl_3$, the signal for 3-H was moved upfield due to electron-donating effect of the amidine group and this coincided with the chemical shift for 4-H, resulting in a singlet signal for 2 protons at δ 7.14. The location of these two protons was confirmed by a ^{1}H-^{13}C COSY (HMQC) spectrum (Figure 15) which showed that they were directly attached to C-3 (δ 126.50) and C-4 (δ 103.74).

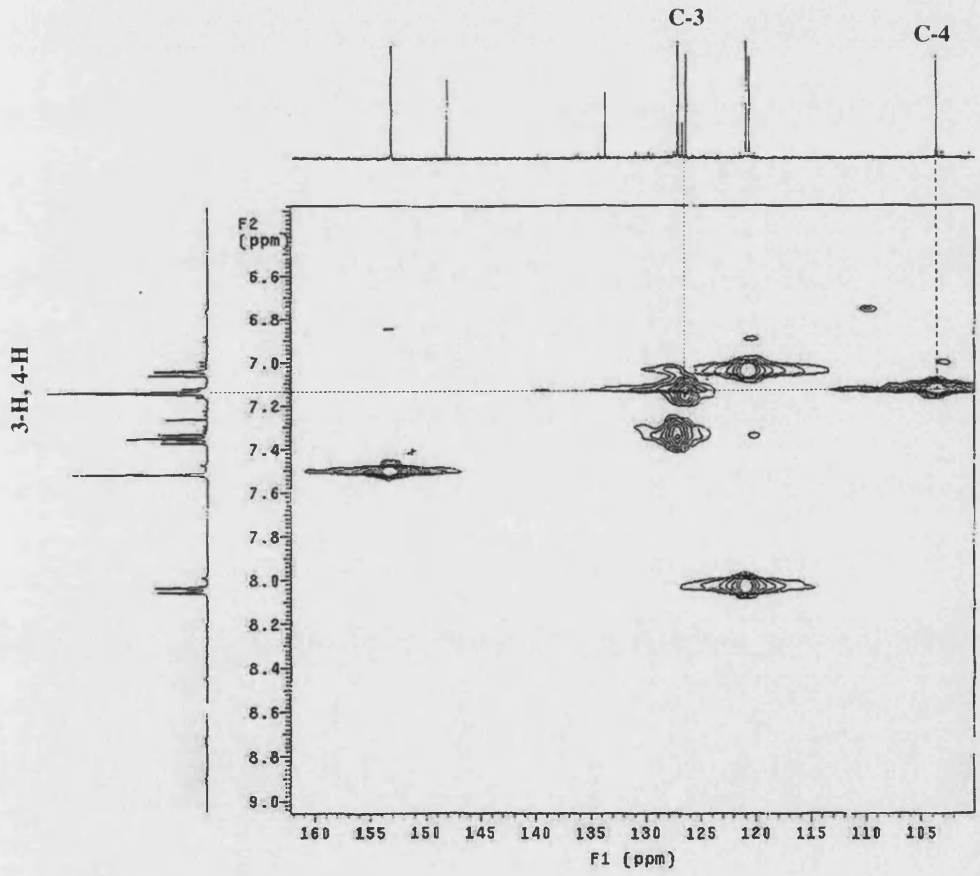

Figure 15. *^{1}H-^{13}C COSY (HMQC) spectrum of 5-[(N,N-dimethylamino)methyleneamino] isoquinolin-1(2H)-one* (***163***).

2. Usually vinylic protons resonate at between 5 to 6 p.p.m.; however, the signal observed for the N=CH proton was shifted markedly downfield at δ 7.52. This was presumably due to the anisotropic effect produced by the π-system. Incidentally the chemical shift of 6-H (usually observed at *ca* δ 6.5) was also moved downfield to δ 7.05, implying that the (*N,N*-dimethylamino)methyleneamino- substituent is in plane with the isoquinolin-1(2*H*)-one ring. The assignment of these protons was again supported by the ^{1}H-^{13}C COSY spectrum (Figure 15).

3. The appearance of two broad singlets for NMe_2 at δ 3.05 and 3.08 indicates the presence of partial π-bonding between this nitrogen atom and the amidine carbon atom which slows down rotation of the two methyl groups about this bond.

4. The establishment of the conformation **(163a)** from its alternative rotamers **(163b)**, **(163c)** and **(163d)** was made through the NOESY spectrum (Figure 16), which showed NOE connectivity between N=CH proton (δ 7.52) and 6-H (δ 7.05). Apparently, this is the least sterically demanding conformation.

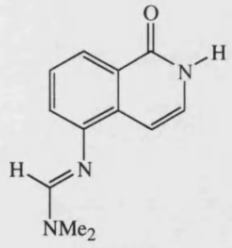

(163a)

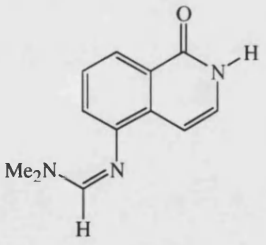

(163b)

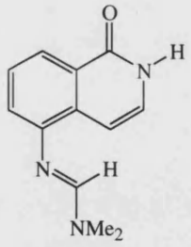

(163c)

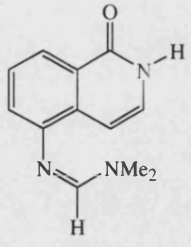

(163d)

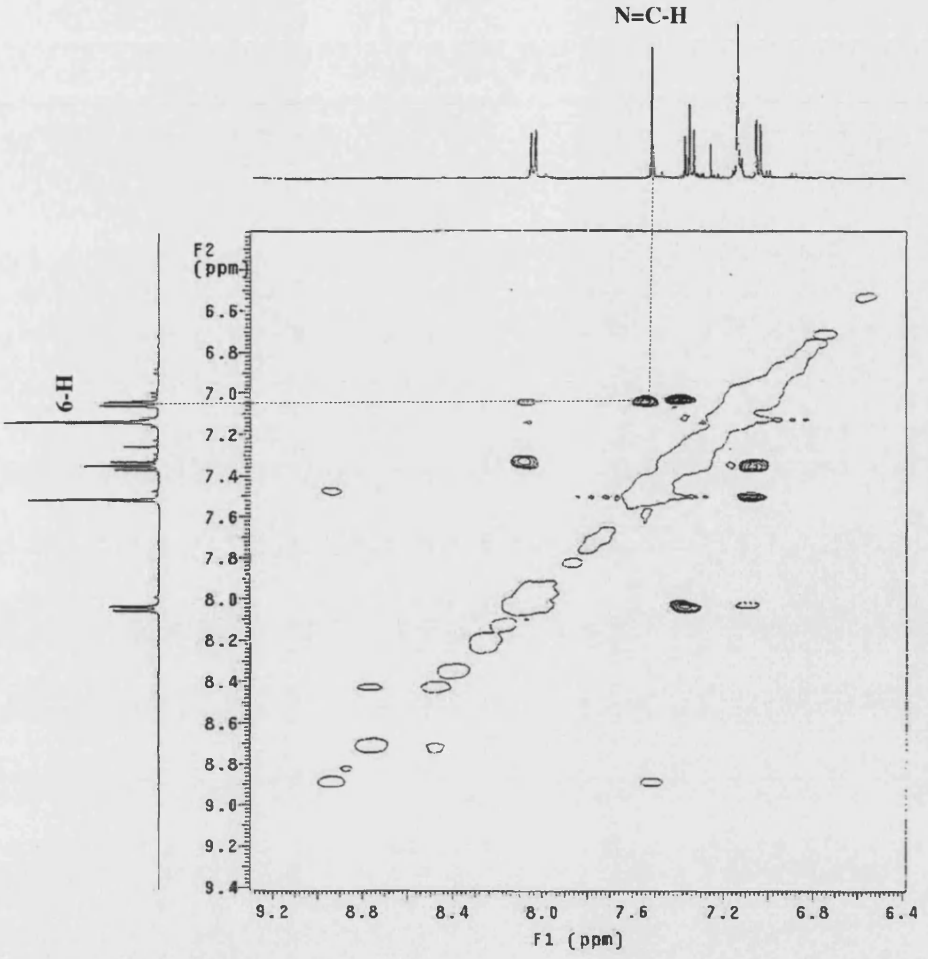

Figure 16. *^{1}H-^{1}H NOESY spectrum of 5-[(N,N-dimethylamino)methyleneamino] isoquinolin-1(2H)-one* ***(163)***.

Such a preference for conformation may possibly explain why **(163)** did not undergo further intramolecular cyclisation to give a 3-ring product **(183)** as shown in Scheme 41 below. Alternatively, the lack of formation of this side-product may also be further indication of the unusual low reactivity of the double bond across C-3 and C-4 of the isoquinolin-1(2*H*)-one ring.

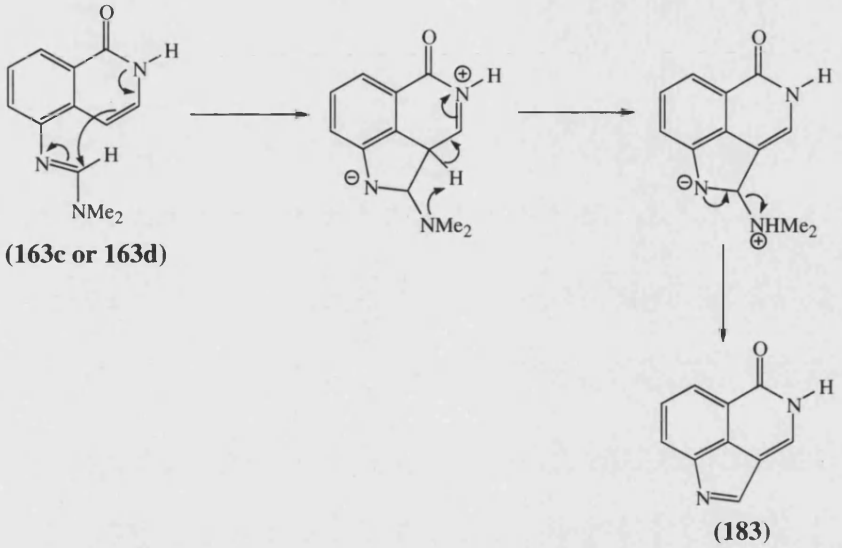

Scheme 41. *Proposed mechanism for the intramolecular cyclisation of 5-[(N,N-dimethylamino)methyleneamino]isoquinolin-1(2H)-one* ***(163)****.*

Subsequent conversion of the compound **(163)** to its hydrochloride salt **(164)** was achieved in 94% yield by stirring with aqueous hydrochloric acid (2 M) at room temperature for 5 min (Scheme 40). Thus, we have successfully synthesised a novel amidine analogue of 5AIQ which is highly water-soluble. Subsequent molecular modelling experiments on this potential PARP-1 inhibitor would allow an examination of any possible interaction between the 5-amino group and the active site and its effect on PARP-1 inhibitory activity.

Biological Evaluation and Molecular Modelling

4.1 Enzyme-inhibition assays

As a preliminary screen, the various 3-substituted 5-aminoisoquinolin-1(2*H*)-one hydrochlorides prepared in this study were evaluated for *in vitro* activity against purified PARP-1 enzyme isolated from HeLa nuclear extract. The above enzyme-inhibition assays were kindly conducted by KuDOS Pharmaceuticals Ltd. using the novel FlashPlate scintillation proximity assay method[222], which is an isotopic assay that measure the activity of the inhibitor based on its ability to prevent PARP-1 from synthesising [^{3}H]ADP-ribose polymers from [^{3}H]NAD$^+$. Any tritiated signal that was bound to the FlashPlate was then counted using a scintillation plate reader, from which the percentage inhibition was determined.

In the evaluation, five different concentrations of the inhibitor, in a range surrounding the IC_{50} value, were used. The IC_{50} value of the inhibitor was then estimated graphically from a plot of the percentage inhibition against the concentration of the inhibitor. For each inhibitor, three independent determinations were performed and their mean IC_{50} values were reported in Table 20. These assays were highly sensitive and reproducible, with standard error of mean (SEM) of less than 20% for most compounds tested. 5AIQ and the benchmark PARP-1 inhibitor, 3-aminobenzamide (3AB), were also tested for comparison purposes.

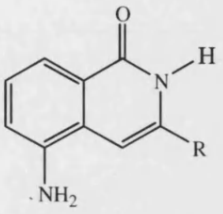

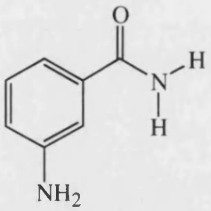

3AB (IC_{50} 33μM)

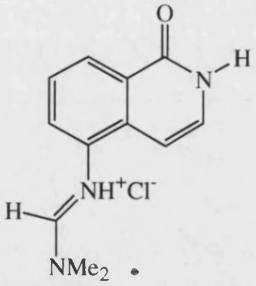

(164) (IC_{50} 4.04 ± 0.89μM)

Compound	R	IC_{50} (μM) ± SEM
5AIQ	H	1.60
(91)		1.07 ± 0.24
(100)	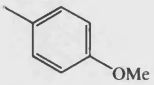	0.90 ± 0.48
(106)	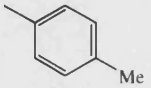	0.88 ± 0.14
(114)	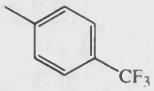	0.33 ± 0.07
(121)	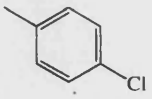	0.57 ± 0.03
(126)	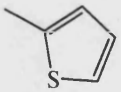	5.61 ± 2.20
(94)	Methyl	0.23 ± 0.02
(134)	Ethyl	0.49 ± 0.04
(139)	Pentyl	0.32 ± 0.17
(144)	Isobutyl	1.17 ± 0.56
(150)	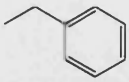	5.14 ± 1.60

Table 20. *The IC_{50} values of the various 3-substituted 5-aminoisoquinolin-1(2H)-one hydrochlorides.*

It must be noted in advance that a direct comparison of IC_{50} values from different laboratories must be exercised with caution since different assay conditions have been employed by different investigators and this may cause considerable variations in the inhibition constants. Suto *et al*[138], for instance, measured the incorporation of [^{3}H]ADP-ribose polymers onto histones by PARP purified from calf thymus and they found that 3AB has an IC_{50} of 9.0 μM. On the other hand, Banasik *et al*[136], using a similar assay but a different radioactive label for the substrate, [^{14}C]NAD^+, reported a much higher IC_{50} value of 33 μM while Griffin *et al*[148], in quantifying the incorporation of [^{32}P]ADP-ribose into acid-insoluble materials by permeabilised L1210 murine cells, obtained an IC_{50} value of 19.1 μM.

In addition to the assay methods, the varying concentrations of NAD^+ and PARP used in the evaluation further hinder direct comparison of results. Nevertheless, these published values remained valuable in providing information with regards to the general trends in inhibitory activity. It is noteworthy that the IC_{50} values obtained for known PARP-1 inhibitors using the FlashPlate method were largely comparable to those reported in the literatures[222], however those obtained for 5AIQ (1.6 μM) and 3AB (33 μM) were a few fold higher than the values reported by Suto *et al*[138], *i.e.* 0.24 μM and 9.0 μM respectively. Such differences should be taken into consideration during subsequent discussion on the SARs of our target compounds.

4.2 Structure-activity relationship

In general, besides having very good water-solubility profile, most of the 3-substituted isoquinolin-1(2*H*)-ones exhibited excellent PARP-1 inhibitory potency with IC_{50} values in low micromolar range (Table 20). These compounds are also considerably more active than the classical 3AB (*ca* 30-fold) and, with the exception of **(126)** (R = thiophene) and **(150)** (R = benzyl), all 3-substituents led to an improvement of potency with respect to the parent compound, 5AIQ, though no clear SARs have been observed (Figure 17).

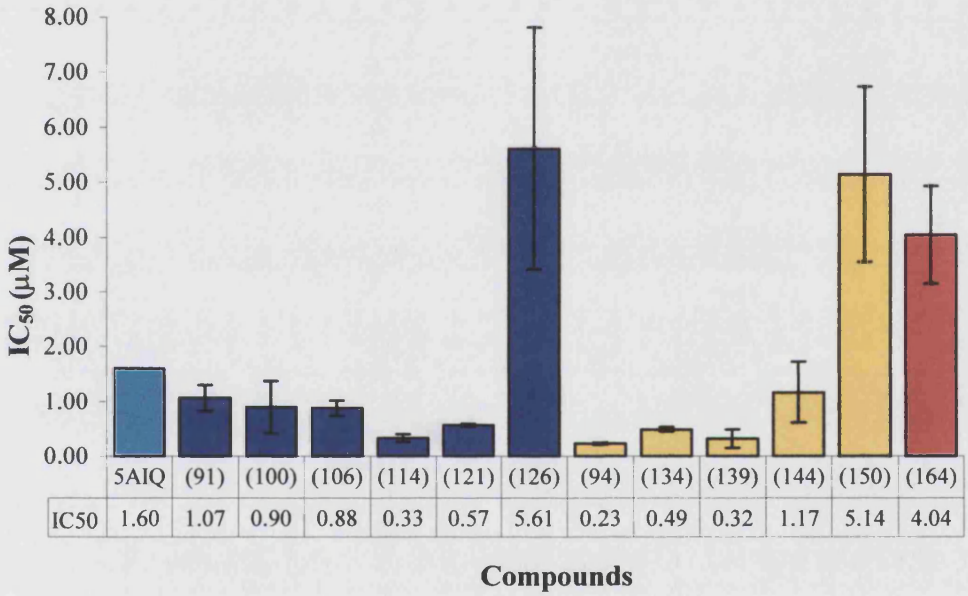

Figure 17. *The IC_{50} values of the 3-aryl substituted 5AIQ (blue bars) and 3-alkyl substituted 5AIQ (yellow bars). The red bar represents the 5-amidine analogue of 5AIQ.*

Apart from this generalisation, however, more subtle effects cooperate in determining the potency of the individual inhibitors. It appeared that the presence of an alkyl substituent (Figure 17, yellow bars) confers a slightly greater enhancement in PARP-1 inhibitory activities than an aryl moiety (Figure 17, blue bars), possibly suggesting a slightly more favourable interaction between these alkyl groups and the active site at the 3-position. This is especially evident with compounds

(94) (R = methyl, IC_{50} 0.23 μM) and **(139)** (R = pentyl, IC_{50} 0.32 μM), which are about 5- and 3-fold, respectively, more potent than the 3-phenyl substituted compound **(91)** (IC_{50} 1.07 μM), making them among the most potent members in this series. These observations are in line with those reported by Griffin *et al*[148] where they found that the 2-methylquinazolin-4-ones, **(31b)** (IC_{50} 0.78 μM) and **(31c)** (IC_{50} 0.39 μM), were 5- and 2-fold more potent than their 2-phenyl counterparts, **(32f)** (IC_{50} 4.2 μM) and **(32j)** (IC_{50} 0.87 μM) respectively (Table 21). Also notable is the significant loss of activity with **(150)** (R = benzyl, IC_{50} 5.14 μM) and, to a lesser extend, **(144)** (R = isobutyl, IC_{50} 1.17 μM), indicating a possible discrimination against rigid substituents at this end of the binding site.

Quinazolinones (31)

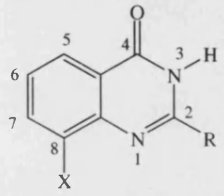

Code	X	R	IC_{50} (μM)
(a)	H	H	9.50
(b)	OMe	Me	0.78
(c)	Me	Me	0.39

2-Phenyl substituted quinazolinones (32)

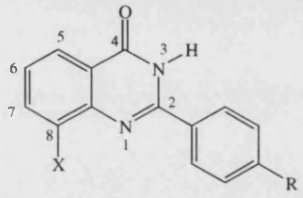

Code	X	R	IC_{50} (μM)
(f)	OMe	H	4.20
(j)	Me	H	0.87
(l)	Me	OH	0.22
(m)	Me	CN	0.27
(n)	Me	OMe	0.19
(o)	Me	NO_2	0.13
(p)	Me	CF_3	> 10

Table 21. *IC_{50} values of a series of 3-alkyl and 3-phenyl substituted quinazolinones against PARP-1.*

The inhibition data further suggest that a phenyl group (compound **(91)**) is well accepted at the 3-position and that the presence of a *para*-substituent in the phenyl ring seemed to increase the activity slightly, though there is no clear relationship between the nature of the substituent and inhibitory potency since the active site is able to tolerate a variety of electronically and sterically differing substituents. Nevertheless, inductive electron-withdrawing functionalities, such as trifluoromethyl

and chloro, appear to confer slightly greater improvement in activity as compound **(114)** (IC_{50} 0.33 μM) and **(121)** (IC_{50} 0.57 μM) are both slightly (*ca* 2 to 3-fold) more potent than the rest.

Such beneficial effects of a *para*-substituent on the phenyl group have also been noted with the 2-phenylquinazolin-4-ones, such as **(32j)**, where the presence of electron-donating groups, such as hydroxy and methoxy (compounds **(32l)** and **(32n)**) and electron-withdrawing groups, such as nitro and cyano (compounds **(32o)** and **(32m)**) markedly increased inhibitory potencies[148]. However, contrary to our findings, a trifluoromethyl group caused deleterious effect on activity as demonstrated by **(32p)** (Table 21).

It is also interesting to note that the introduction of a thiophene ring at the 3-position resulted in a drastic loss of potency, as demonstrated by **(126)** (IC_{50} 5.61 μM), which is 5-fold less potent with respect to **(91)** (IC_{50} 1.07 μM). Such a peculiar behaviour is most unexpected since the thiophene ring is isosteric with the phenyl ring and is electronically very similar.

4.3 Molecular Modelling

To better understand the above observations, molecular modelling of 5AIQ and the novel PARP-1 inhibitors, **(94)**, **(114)**, **(126)** and **(164)**, was undertaken and this was effected using Hyperchem® 7.5. The molecular structure of these compounds were constructed from previously solved co-crystal X-ray structure of 2-methyl-8-hydroxyquinazolin-4-one **(31d)** bound to the catalytic domain of chicken PARP-1, the atomic coordinates of which were being retrieved from the Protein Data Bank (PDB) database (PDB code: 4PAX). The use of the active site of chicken PARP-1 is reasonable since it bears a close homology to human PARP-1. The inhibitor-enzyme complex thus formed was then minimised, requiring the crucial interaction between the nicotinamide moiety and the active site to be fixed.

All the inhibitors examined displayed **conserved** and **non-conserved interactions**. Conserved interactions are those involving the benzamide pharmacophore and are exhibited across all classes of competitive PARP-1 inhibitors (Figure 18-23). These include:

1. Three critical hydrogen bond interactions between the carboxamide moiety and two amino acid residues, Ser904 and Gly863, where the inhibitor carbonyl oxygen accepts two hydrogen bonds, one from the side chain of Ser904 (2.25 Å) and the other from Gly863 polypeptide amide NH (1.59 Å). The third hydrogen-bond is formed between the carboxamide NH and Gly863 carbonyl oxygen (2.08 Å). Presumably, steric repulsion between the large sulphur atom in the thiophene ring of **(126)** and the carboxamide group disrupts its favourable binding conformation to the active site, thereby leading to a decrease in potency (Figure 21).
2. A parallel tyrosine residue, Tyr907, within the active site also forms a "π-electron sandwich" which is beneficial for binding planar aromatic compounds, especially extended planar structure, such as the isoquinolin-1(2*H*)-one ring.

Non-conserved interactions are strictly dependent on the structural diversity of the inhibitors. The alkyl and aryl side chains of the 3-substituted 5AIQ were able to form additional interactions with the deep hydrophobic pocket extending from that region, as exemplified by **(94)** and **(114)** (Figure 24 and 25), thus possibly accounting for their increased potencies with respect to 5AIQ. Further studies also established another large hydrophobic pocket in the region corresponding to the 4-position and this could potentially be exploited for further enhancement of inhibitory activity through substitution at that position.

It was also observed that the 5-amino group in these inhibitors were well accommodated within a relatively smaller binding pocket and were in close proximity with the important catalytic Glu988 in the active site. X-ray crystal structure of the catalytic fragment of chicken PARP-1 further revealed the presence of an ordered water molecule between the amino group and the carboxylate side chain of Glu988. Both observations are consistent with our postulate that a putative water-mediated hydrogen bond exists between the 5-amino group and Glu988 within the active site.

To explore the nature of this hydrogen bond, 5AIQ was substituted, at the *N*5-position, with an amidine group and this resulted in a 2.5-fold reduction in activity ((**164**), IC_{50} 4.04 μM). Such a loss of potency could suggest the requirement for a hydrogen bond donor, rather than an acceptor, at this position. Alternatively, it could also be the result of steric interference between the rigid and bulky amidine group and the active site as illustrated in Figure 26. Further work with less bulky substituents at the 5-position is required to elucidate the exact influence such hydrogen-bonding on PARP-1 activities.

Incidentally, an energy minimisation experiment on **(163)** (Figure 27) provided further evidence in support of our previous assignment of **(163a)** as the lower energy conformation and, hence, the preferred rotamer (Section 3.3). The alternative rotamer **(163c)**, formed *via* rotation about the C_5-N bond, revealed steric clash between 4-H and amidine-CH, making it energetically unfavourable.

Thus, we have described, herein, a series of novel, water-soluble and potent PARP-1 inhibitors. A combination of favourable physical properties and highly promising *in vitro* profiles renders them excellent candidates for pre-clinical development. Patent application is currently underway and publications will soon follow.

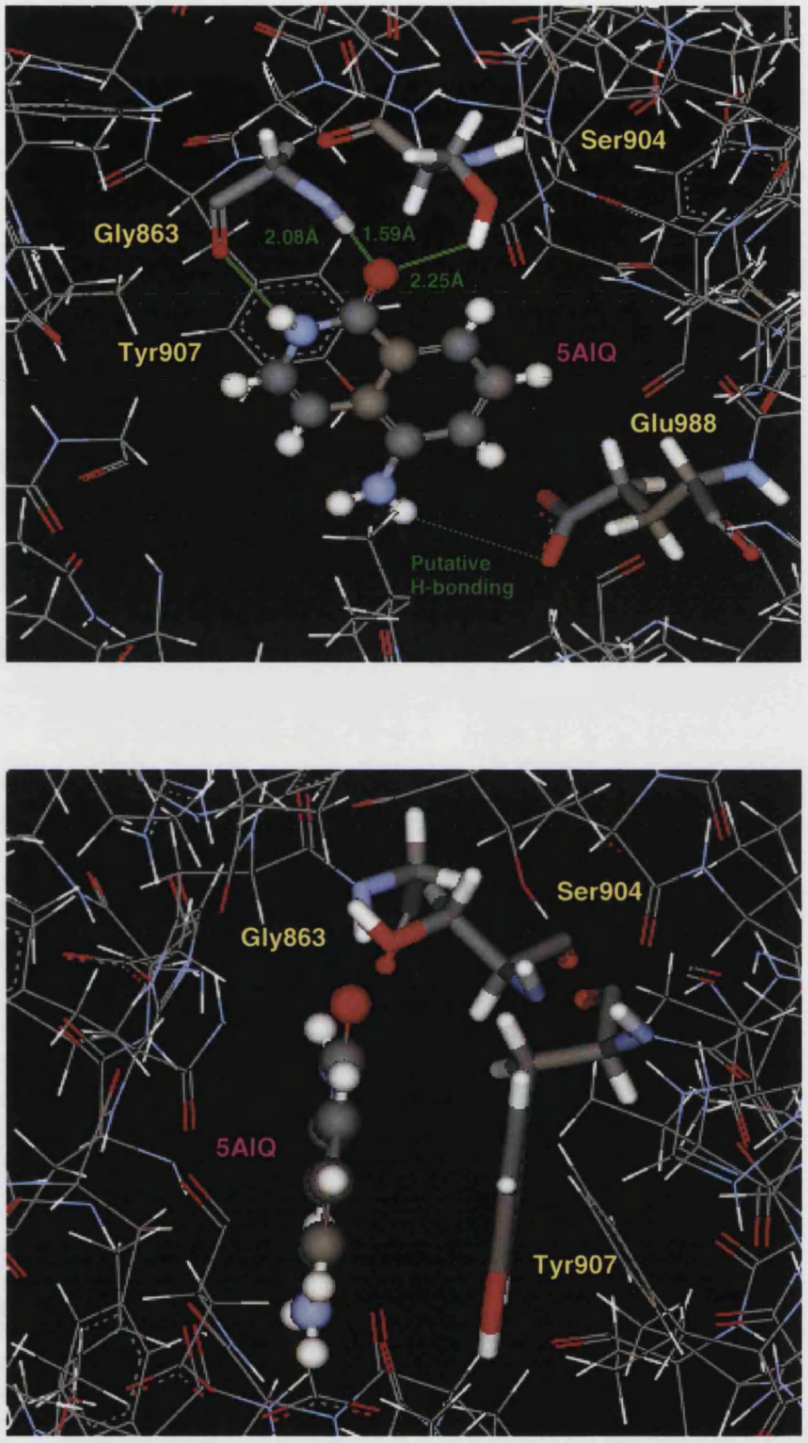

Figure 18. *Molecular modelling of 5AIQ, showing three critical hydrogen bond interactions between the carboxamide moiety and two amino acid residues, Ser904 and Gly863 (top) and "π-electron sandwich" with the parallel Tyr907 (bottom).*

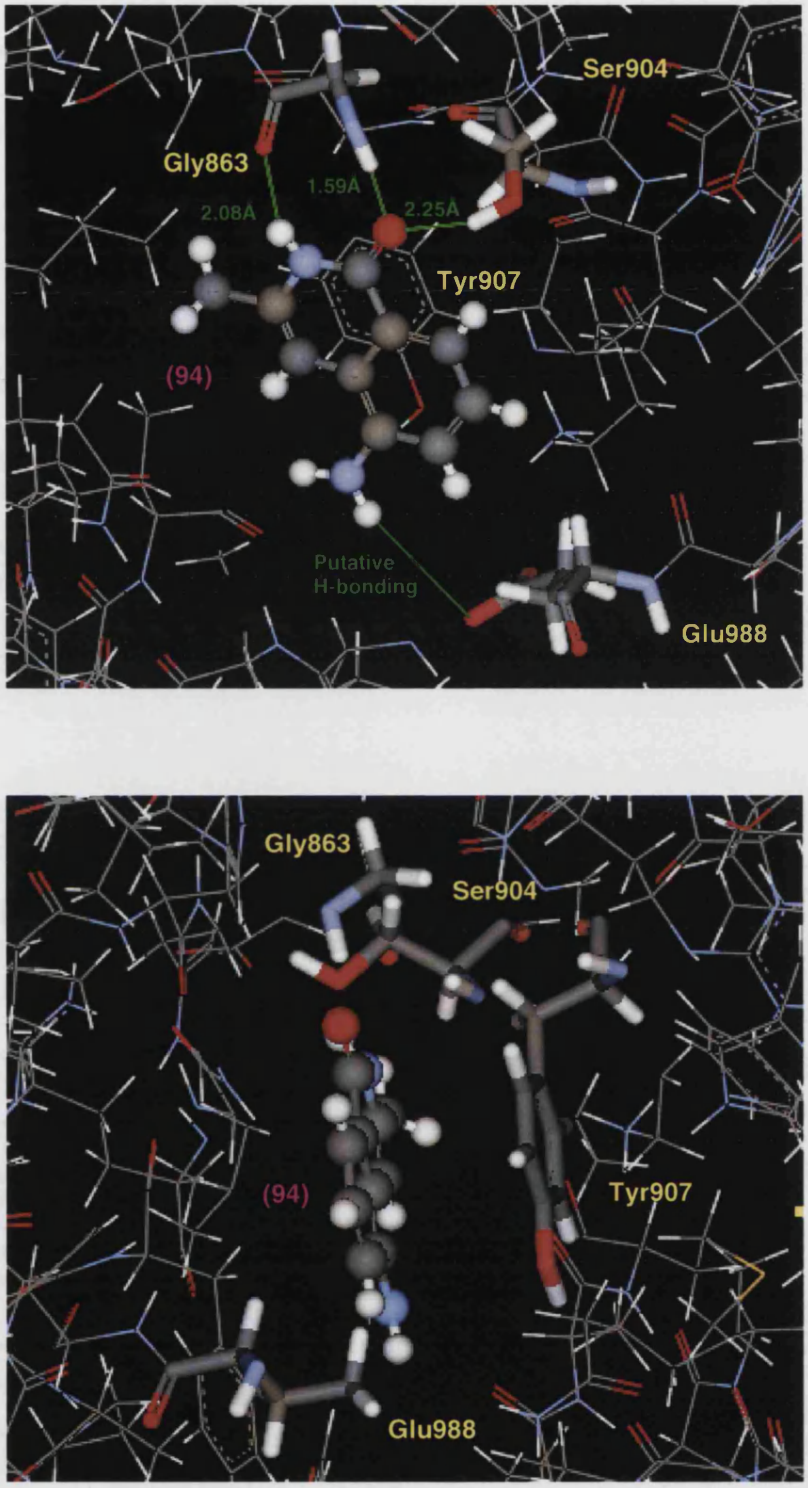

Figure 19. *Molecular modelling of* ***(94)****, showing three critical hydrogen bond interactions between the carboxamide moiety and two amino acid residues, Ser904 and Gly863 (top) and "π-electron sandwich" with the parallel Tyr907 (bottom).*

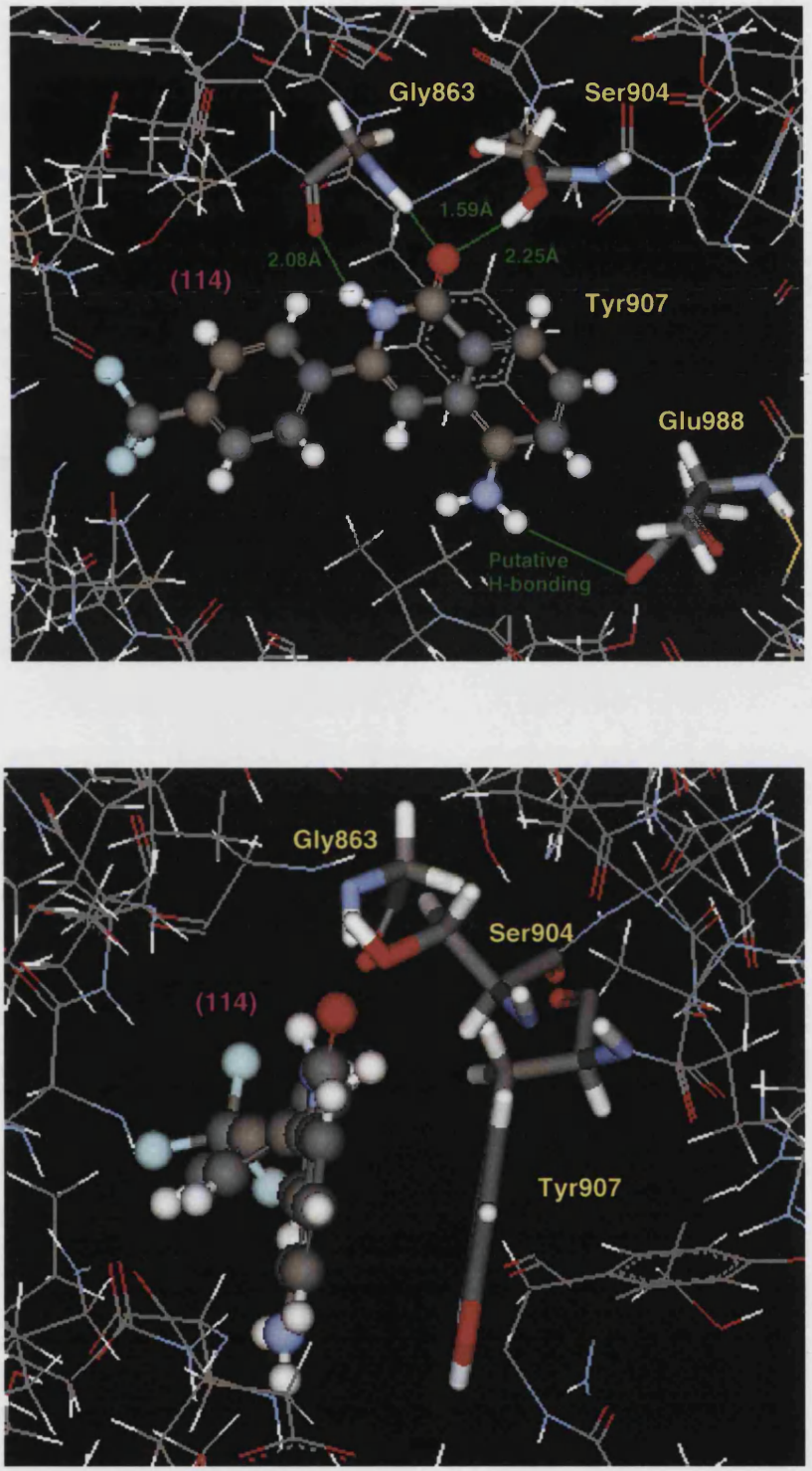

Figure 20. *Molecular modelling of* ***(114)****, showing three critical hydrogen bond interactions between the carboxamide moiety and two amino acid residues, Ser904 and Gly863 (top) and "π-electron sandwich" with the parallel Tyr907 (bottom).*

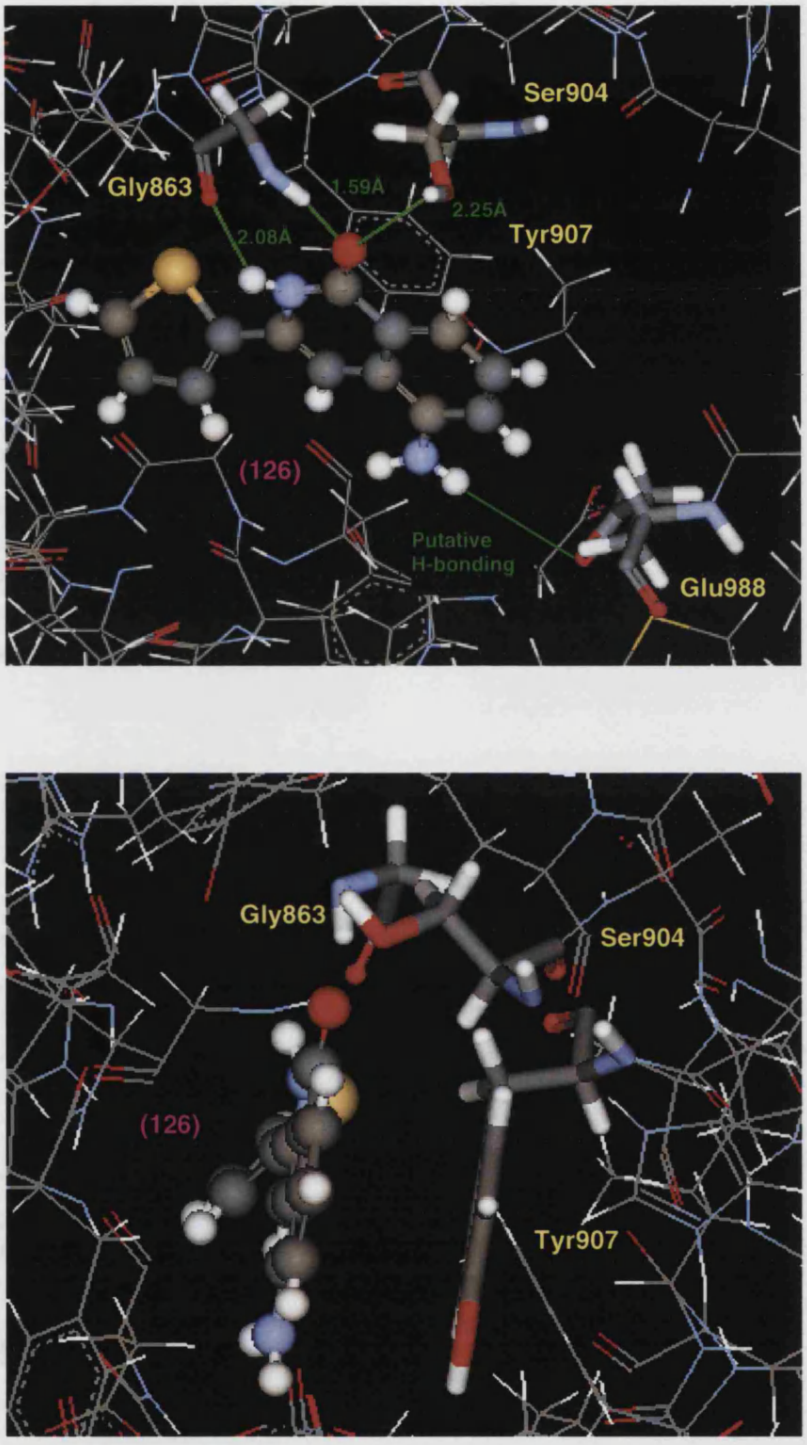

Figure 21. *Molecular modelling of one rotamer of* ***(126)****, showing three critical hydrogen bond interactions between the carboxamide moiety and two amino acid residues, Ser904 and Gly863 (top) and "π-electron sandwich" with the parallel Tyr907 (bottom).*

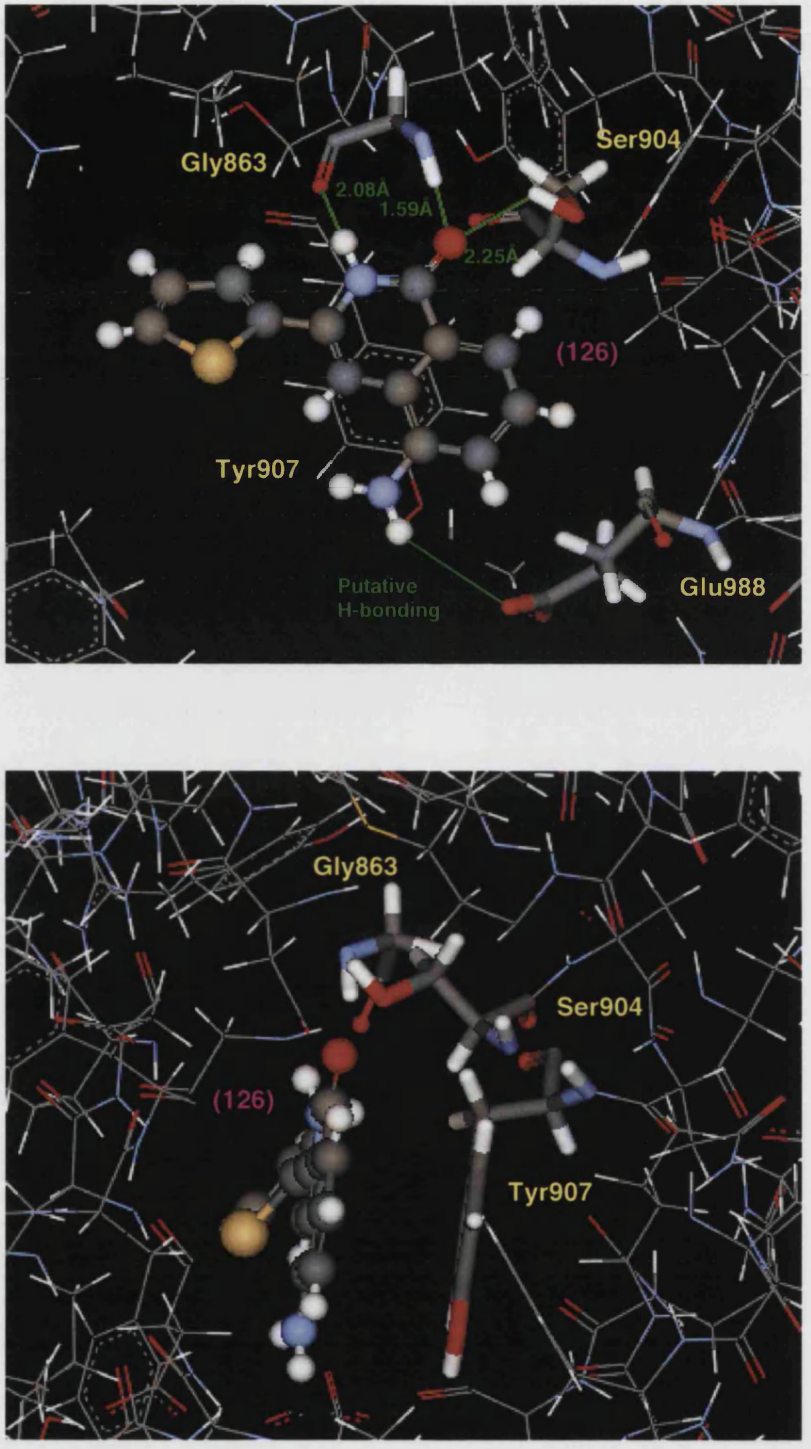

Figure 22. *Molecular modelling of another rotamer of* ***(126)***.

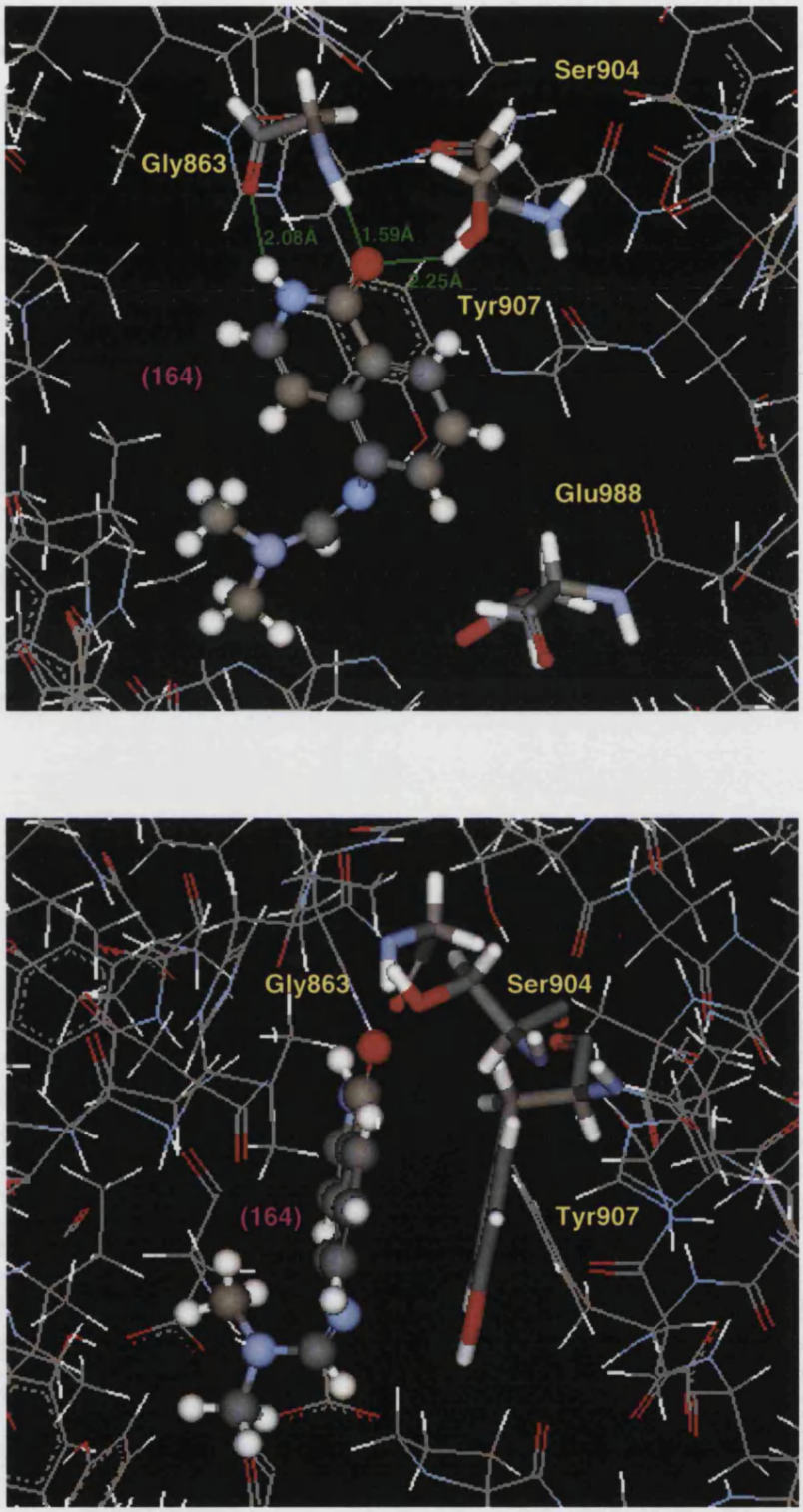

Figure 23. *Molecular modelling of* ***(164)****, showing three critical hydrogen bond interactions between the carboxamide moiety and two amino acid residues, Ser904 and Gly863 (top) and "π-electron sandwich" with the parallel Tyr907 (bottom).*

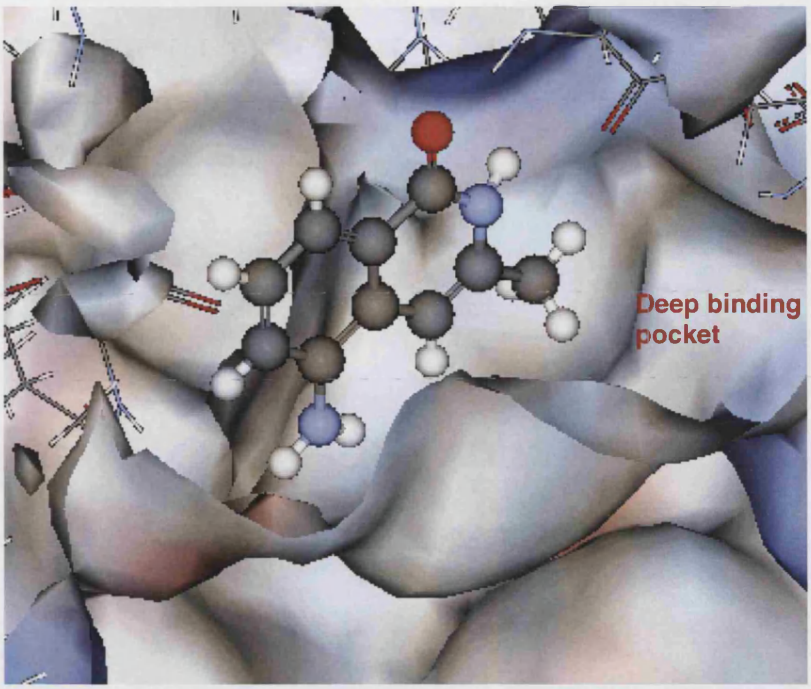

Figure 24. *Molecular modelling of* ***(94)*** *revealed the presence of a large binding pocket extending from the region corresponding to the 3-position of 5AIQ and a relatively smaller pocket beneath the 5-amino group.*

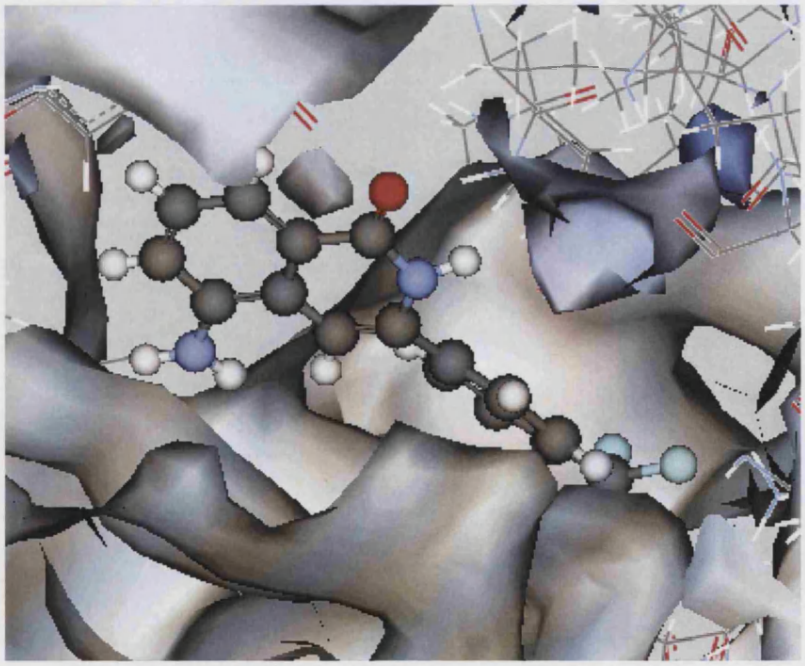

Figure 25. *Insertion of the phenyl ring of* ***(114)*** *into the large binding pocket.*

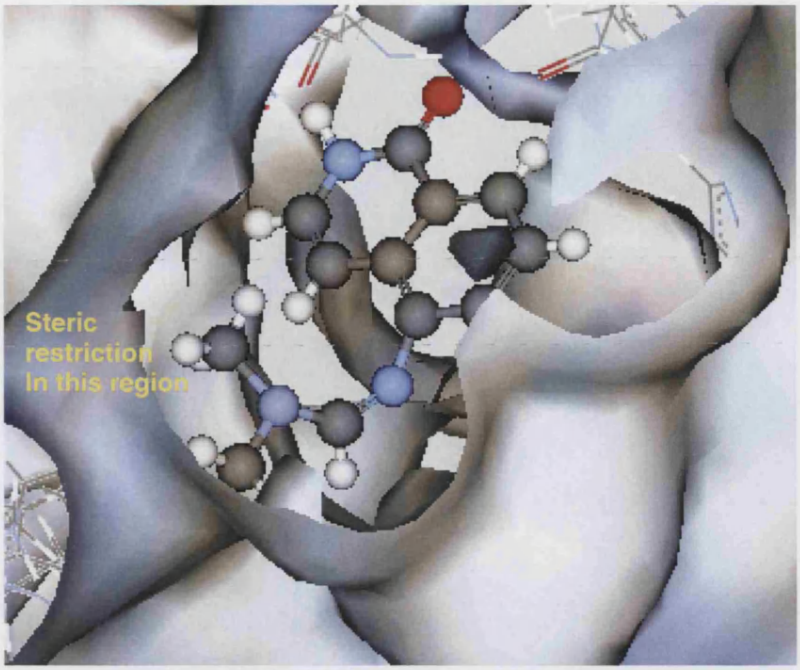

Figure 26. *Steric restriction between the bulky 5-amidine substituent of* ***(164)*** *and the active site.*

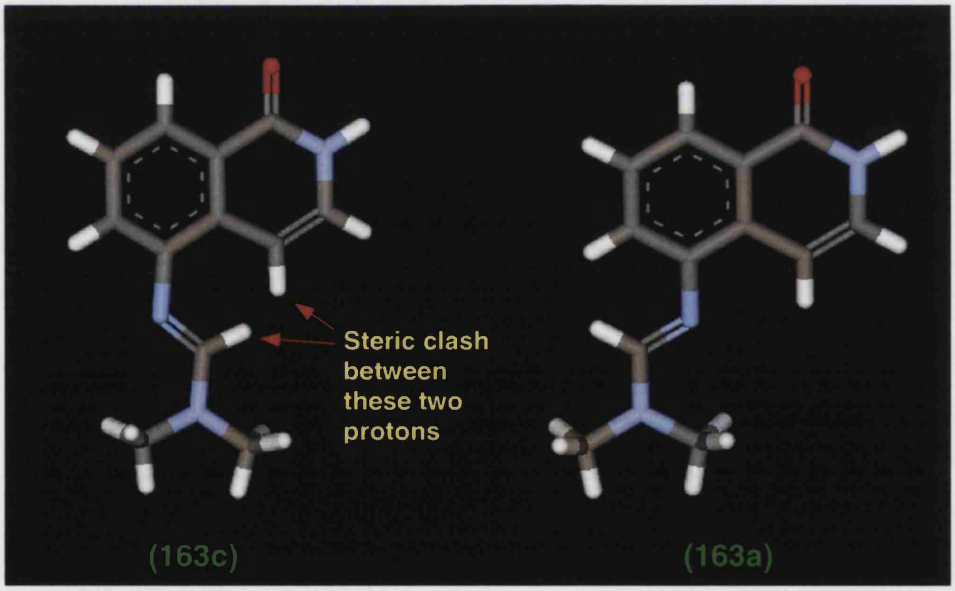

Figure 27. *Energy minimisation experiment revealed* ***(163a)*** *as having the preferred conformation.*

Conclusions

In conclusion, various approaches to the synthesis of the novel class of PARP-1 inhibitor, 3-substituted 5-aminoisoquinolin-1(2*H*)-one hydrochlorides, have been investigated and we have successfully developed a reliable, efficient and versatile synthetic route, through which a series of highly water-soluble target compounds, bearing varying substituents at the 3-position, was generated.

In addition, a novel synthesis of the lead compound, 5AIQ, *via* the reductive cyclisation of methyl 2-cyanomethyl-3-nitrobenzoate (**157**) has also been realised. This strategy could potentially be extended to the synthesis of another class of potential PARP-1 inhibitors, the 4-substituted isoquinolin-1(2*H*)-ones.

Effort to synthesise the 3-substituted targets *via* organometallic approaches, such as Sonogashira coupling, Castro-Stephens coupling and Negishi coupling were largely frustrated by the use of sterically demanding, trisubstituted halide partners. The presence of a highly electron-withdrawing nitro function, which is conjugated with the double bond across C-3 and C-4 in both the isocoumarin and the isoquinolin-1(2*H*)-one ring, also interfered with the Heck synthesis of the 4-substituted targets. Thus, these experiments revealed some of the limitations and difficulties associated with the use of these organometallic protocols as synthetic tools.

Many interesting chemistry has also been observed, presumably owing to the presence of a 3-nitro function. In particular, decarboxylation/mercuration and iodination of 3-nitrophthalic acid was found to occur regiospecifically at the 2-position, giving 2-iodo-3-nitrobenzoic acid (**67**) as the only substitution product. Such regioselectivity was also consistently observed in our mercury and copper-catalysed cyclisation of arylalkyne where only the desired isocoumarin was formed (*via* a 6-endo-dig route), as opposed to the non-nitrated analogue, which gave the 5-membered phthalide as the major product. Finally, the strongly

electron-withdrawing nitroaryl system played a unique role in promoting spontaneous retro-Claisen reaction on the Hurtley condensation product and its subsequent cyclisation into the desired isocoumarin.

Preliminary biological evaluation of this series of compounds showed excellent *in vitro* inhibitory activity against PARP-1, with IC_{50} values in low micromolar range. Most of the 3-substituents were well received by the active site and they resulted in a significant enhancement of PARP-1 inhibitory potency with respect to 5AIQ. This was particularly evident for 5-amino-3-methylisoquinolin-1(2*H*)-one **(94)** (IC_{50} 0.23 μM), 5-amino-3-pentylisoquinolin-1(2*H*)-one **(139)** (IC_{50} 0.32 μM) and 5-amino-3-[4-(trifluoromethyl)phenyl]isoquinolin-1(2*H*)-one **(114)** (IC_{50} 0.33 μM), which were among the most potent members of this series. Besides the usual conserved interactions, molecular modelling experiments further identified additional favourable interactions between the 3-substituents and a deep hydrophobic pocket within the active site, as well as a putative, water-mediated hydrogen bond between the 5-amino group and Glu988, all of which unquestionably contributed towards their outstanding potencies.

Greatly encouraged by these highly promising data, our immediate interest would be to evaluate the *in vivo* protective ability of selected inhibitors in various disease models in animals, especially their effects against ischaemia-reperfusion injury and inflammatory disorders. Future work would involve effecting the synthesis of the 4-substituted targets *via* the proposed synthetic routes and, possibly, a synthesis of the 3,4-disubstituted 5AIQ as well as the development of these PARP-1 inhibitors into selectively-activated prodrugs.

Experimental

General Procedures

All melting points were determined using a Reichert-Jung Thermo Galen Kofler block and are uncorrected. IR spectra were recorded on a Perkim-Elmer RXI FT-IR spectrometer, either as a liquid (film) or as a KBr disc (KBr). υ_{max} values are given in cm^{-1}. NMR spectra were recorded on either a JOEL GX 270 (270.05 MHz ^{1}H; 67.8 MHz ^{13}C) or EX 400 (399.65 MHz ^{1}H; 100.4 MHz ^{13}C; 376.05 MHz ^{19}F) spectrometer. Tetramethylsilane was used as an internal standard for samples dissolved in $CDCl_3$ and $(CD_3)_2SO$. For samples dissolved in D_2O, 3-(Trimethylsilyl)propanoic-2,2,3,3-d_4 acid sodium salt was used instead. Multiplicities are indicated by s (singlet), d (doublet), t (triplet), q (quartet), m (multiplet) and br (broad). Mass spectra were obtained by either Electron Impact (EI) or Fast Atom Bombardment (FAB) (with *m*-nitrobenzyl alcohol as the matrix) at the University of Bath Mass Spectrometry Service using a VG 7070 Mass Spectrometer. Microanalysis was carried out at the University of Bath Microanalysis Service. Thin layer chromatography (TLC) was performed on silica gel 60 F_{254}-coated aluminium sheets (Merck) and visualisation was accomplished by UV light or $FeCl_3$. Flash column chromatography was performed using silica gel 60 (0.040-0.063 mm, Merck) as the stationary phase.

All reagents for chemical synthesis were purchased from Aldrich and Lancaster Chemical Company and were used without further purification. Experiments were conducted at ambient temperature, unless otherwise stated. Where experiments were repeated, only one description was provided. Solutions in organic solvents were dried using anhydrous $MgSO_4$ and solvents were evaporated under reduced pressure. THF and diisoproplyamine were freshly distilled under nitrogen from sodium/benzophenone and calcium hydride respectively.

Methyl 2-acetamido-5-nitrobenzoate (61)

Methyl 2-acetamido-3-nitrobenzoate (62)

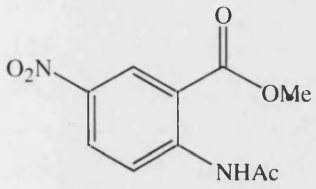

(61)

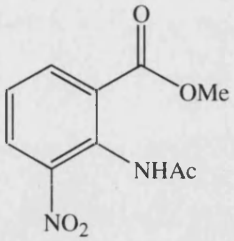

(62)

A solution of Ac_2O (35.0 g, 343 mmol) and HNO_3 (70%, 50 ml, 556 mmol) in AcOH (30 ml) was added dropwise to a solution of methyl 2-aminobenzoate (24.5 g, 162 mmol) in Ac_2O (170 g, 1.7 mol) during 2 h at 10 ± 5°C and stirred (at that temperature) for 2.5 h. The solution was then poured into ice-H_2O (100 ml) and the precipitate was filtered, washed (H_2O) and recrystallised ($CHCl_3$, MeOH) to give **(61)** (25.9 g, 67%) as yellow crystals; R_f = 0.48 (hexane / EtOAc 3:2); mp 122-123°C (lit.[191] mp 121-123°C); ^{1}H NMR ($CDCl_3$) δ 2.31 (3 H, s, $COCH_3$), 4.01 (3 H, s, CO_2CH_3), 8.37 (1 H, dd, *J* = 9.8, 2.7 Hz, 4-H), 8.93 (1 H, d, *J* = 2.7 Hz, 6-H), 8.94 (1 H, d, *J* = 9.8 Hz, 3-H), 11.39 (1 H, br s, NH).

The filtrate was extracted with $CHCl_3$, dried and evaporated. This gave an oily residue which was recrystallised from Et_2O to give **(62)** (7.6 g, 20%) as pale yellow crystals; R_f = 0.28 (hexane / EtOAc 3:2); mp 115-116°C (lit.[192] mp 115-117°C); IR υ_{max} (KBr) 1326 & 1535 (NO_2), 1682 (amide I), 1723 (ester C=O), 3320 (NH); ^{1}H NMR ($CDCl_3$) δ 2.09 (3 H, s, $COCH_3$), 3.97 (3 H, s, CO_2CH_3), 7.31 (1 H, t, *J* = 7.8 Hz, 5-H), 8.08 (1 H, dd, *J* = 7.8, 1.6 Hz, 4-H), 8.21 (1 H, dd, *J* = 7.8, 1.6 Hz, 6-H), 10.35 (1 H, br s, NH); MS (FAB +ve ion) *m/z* 239.0658 (M + H) ($^{12}C_{10}H_{11}N_2O_5$ requires 239.0668), 180 (M + H – CO_2Me).

2-Amino-3-nitrobenzoic acid (63).

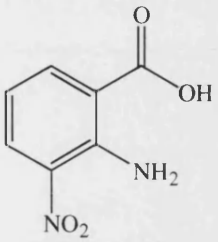

Compound **(62)** (2.3 g, 9.7 mmol) was boiled under reflux with aqueous HCl (9 M, 100 ml) for 48 h. Filtration and drying of the precipitate yielded **(63)** (1.7 g, 97%) as orange crystals; R_f = 0.63 ($CHCl_3$ / MeOH / AcOH 10:1:0.1); mp 207-208°C (lit.[193] mp 202-204°C); IR υ_{max} (KBr) 1351 & 1538 (NO_2), 1680 (C=O), 2800-3100 (OH), 3340 & 3460 (NH_2); ^{1}H NMR ($(CD_3)_2SO$) δ 6.73 (1 H, t, *J* = 7.8 Hz, 5-H), 8.24 (1 H, dd, *J* = 7.8, 1.7 Hz, 4-H), 8.31 (1 H, dd, *J* = 7.8, 1.7 Hz, 6-H), 8.55 (2 H, br s, NH_2), 13.45 (1 H, br s, OH); MS (EI +) *m/z* 182.0322 (M) ($^{12}C_7H_6N_2O_4$ requires 182.0328).

Methyl 2-amino-3-nitrobenzoate (64).

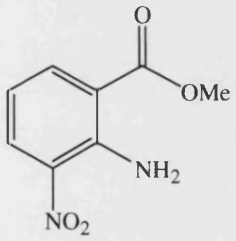

A solution of **(63)** (1.5 g, 8.2 mmol) in MeOH (100 ml) and H_2SO_4 (1 ml) was boiled under reflux for 48 h. The solution was poured into ice-H_2O (300 ml) and the precipitate was filtered, dried and recrystallised (MeOH). This gave **(64)** (1.1 g, 68%) as bright yellow crystals; R_f = 0.61 (hexane / EtOAc 2:3); mp 94°C (hexane, EtOAc) (lit.[148] mp 96°C); IR υ_{max} (KBr) 1343 & 1526 (NO_2), 1702 (C=O), 3317 & 3452 (NH_2); ^{1}H NMR ($CDCl_3$) δ 3.92 (3 H, s, CO_2CH_3), 6.66 (1 H, t, *J* = 7.8 Hz, 5-H), 8.24 (1 H, dd, *J* = 7.8, 1.7 Hz, 4-H), 8.38 (1 H, dd, *J* = 7.8, 1.7 Hz, 6-H), 8.50 (2 H, br s, NH_2); MS (EI +) *m/z* 196.0486 (M) ($^{12}C_8H_8N_2O_4$ requires 196.0484).

2-Iodo-3-nitromethylbenzene (65).

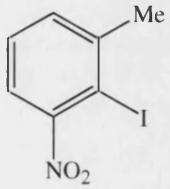

A solution of $NaNO_2$ (1.0 g, 15 mmol) in H_2O (10 ml) was added dropwise to a solution of 2-methyl-6-nitroaniline (2.0 g, 13 mmol) in aqueous HCl (2 M, 30 ml) at 0°C. After stirring for 15 min, KI (6.0 g, 36 mmol) in H_2O (10 ml) was added and the mixture was allowed to stand at room temperature for 1 h. The mixture was then carefully heated until evolution of N_2 and I_2 ceased. Evaporation and recrystallisation (EtOH) gave **(65)** (2.7 g, 78%) as orange crystals; R_f = 0.52 (hexane / EtOAc 4:1); mp 69°C (EtOH) (lit.[195] mp 68-69°C); ^{1}H NMR ($CDCl_3$) δ 2.58 (3 H, s, CH_3), 7.34 (1 H, t, *J* = 7.8 Hz, 5-H), 7.43 (2 H, d, *J* = 7.8 Hz, 4,6-H_2); MS (EI +) *m/z* 262.9437 (M) ($^{12}C_7H_6INO_2$ requires 262.9443), 217 (M – NO_2).

2-Iodo-3-nitrobenzoic acid (67).

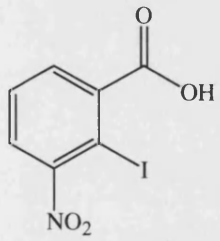

3-Nitrophthalic acid (21.1 g, 100 mmol) in hot aqueous NaOH (10%, 80 ml) was added to $Hg(OAc)_2$ (35.0 g, 110 mmol) in hot AcOH (5 ml) and H_2O (70 ml). The mixture was heated at 170°C (oil bath temperature) for 70 h and was then filtered. The precipitate was washed (H_2O, then EtOH), dried and boiled under reflux in aqueous NaOH (3.5%, 500 ml). Aqueous HCl (2 M, 12 ml) was then slowly added, with vigorous stirring, and the solution was allowed to cool to room temperature. AcOH (3 ml) was then added and this gave a curdy cream precipitate, which dissolved upon addition of a mixture of KI (19.0 g, 114 mmol) and I_2 (29.0 g, 114 mmol) in H_2O (30 ml). The solution was boiled under reflux for 24 h, cooled and

neutralised with aqueous NaOH. It was then filtered and acidified with concentrated HCl. The precipitate formed was filtered, dried and recrystallised (EtOH) to give **(67)** (19.1 g, 65%) as yellow crystals; R_f = 0.61 (CH_2Cl_2 / MeOH / AcOH 9:1:0.1); mp 204-205°C (lit.[196] mp 205-206°C); IR υ_{max} (KBr) 1375 & 1542 (NO_2), 1712 (C=O), 2543–3063 (OH); ^{1}H NMR ($(CD_3)_2SO$) δ 7.66 (1 H, t, *J* = 7.8 Hz, 5-H), 7.79 (1 H, dd, *J* = 7.8, 1.7 Hz, 4-H), 7.92 (1 H, dd, *J* = 7.8, 1.7 Hz, 6-H); ^{13}C NMR ($CDCl_3$) δ 86.87 (C-2), 125.48 (C-5), 130.32 (C-4), 131.64 (C-6), 142.54 (C-1), 156.40 (C-3), 168.70 (C=O); MS (FAB +ve ion) *m/z* 293.9250 (M + H) ($^{12}C_7H_5INO_4$ requires 293.9263).

Methyl 2-iodo-3-nitrobenzoate (68).

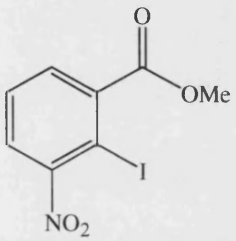

Method A:

$NaNO_2$ (1.30 g, 18.8 mmol) in H_2O (5 ml) was added to a suspension of **(64)** (300 mg, 1.5 mmol) in aqueous HCl (2 M, 20 ml) at 2 ± 2°C during 30 min. The diazonium solution was then added dropwise to a solution of KI (2.5 g, 15 mmol) and I_2 (1.8 g, 7.1 mmol) in DMSO (35 ml) at 5°C and the mixture was stirred at 50°C for 20 min. Extraction (EtOAc), washing (H_2O), drying ($MgSO_4$) and evaporation to give **(68)** (20 mg, 4%) as yellow crystals; R_f = 0.33 (hexane / EtOAc 4:1); mp 66-67°C (lit.[196] mp 64-66°C); IR υ_{max} (KBr) 1351 & 1533 (NO_2), 1705 (C=O); ^{1}H NMR ($CDCl_3$) δ 3.99 (3 H, s, CH_3), 7.54 (1 H, t, *J* = 7.8 Hz, 5-H), 7.70 (1 H, dd, *J* = 7.8, 1.7 Hz, 4-H), 7.77 (1 H, dd, *J* = 7.8, 1.7 Hz, 6-H); MS (EI +) *m/z* 306.9347 (M) ($^{12}C_8H_6INO_4$ requires 306.9342), 276 (M – OMe).

Method B:

Compound **(67)** (4.0 g, 14 mmol) in MeOH (120 ml) and H_2SO_4 (3 ml) was boiled under reflux for 48 h, then poured into ice-H2O (300 ml). The precipitate formed

was filtered, dried and recrystallised (MeOH) gave **(68)** (4.0 g, 95%) as yellow crystals. The data were identical to those above.

Methyl 3-nitro-2-(2-trimethylsilylethynyl)benzoate (69).

Methyl 3-nitrobenzoate (70).

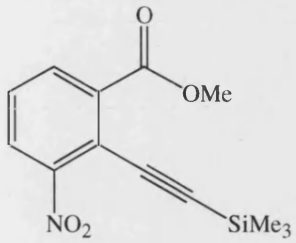

(69)

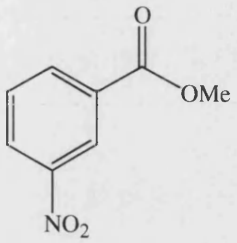

(70)

The Pd catalyst, $(PPh_3)_2PdCl_2$, used in this reaction was prepared as follows:
A mixture of PPh_3 (375 mg, 1.4 mmol) and $PdCl_2$ (130 mg, 0.7 mmol) in DMF (20 ml) was heated at 80°C for 24 h. Filtration and drying yielded $(PPh_3)_2PdCl_2$ as a yellow powder (470 mg, 94%).

A solution of **(68)** (3.0 g, 9.8 mmol) in dry THF (120 ml) was added to a suspension of $(PPh_3)_2PdCl_2$ (300 mg, 0.4 mmol) and CuI (400 mg, 2.1 mmol) in dry diisopropylamine (40 ml) and the mixture was stirred at 45°C for 30 min under Ar. Trimethylsilylethyne (1.1 g, 11 mmol) was then added during 30 min and the mixture was stirred for another 72 h at 45°C. Filtration (through Celite®), evaporation and chromatography (hexane / CH_2Cl_2 3:2) gave **(69)** (810 mg, 30%) as a reddish-brown oil; R_f = 0.38 (hexane / EtOAc 4:1); IR υ_{max} (KBr) 1351 & 1532 (NO_2), 1738 (C=O), 2219 (C≡C); ^{1}H NMR ($CDCl_3$) δ 0.28 (9 H, s, $Si(CH_3)_3$), 3.96 (3 H, s, CH_3), 7.49 (1 H, t, *J* = 7.8 Hz, 5-H), 7.96 (1 H, dd, *J* = 7.8, 1.6 Hz, 4-H), 8.01 (1 H, dd, *J* = 7.8, 1.6 Hz, 6-H); MS (FAB +ve ion) *m/z* 278.0843 (M + H) ($^{12}C_{13}H_{16}NO_4Si$ requires 278.0849).

Also isolated by chromatography was **(70)** (690 mg, 39%) as yellow crystals; R_f = 0.50 (hexane / EtOAc 4:1); mp 75-76°C (lit.[197] mp 78-80°C); ^{1}H NMR ($CDCl_3$) δ 3.99 (3 H, s, CH_3), 7.66 (1 H, t, *J* = 7.8 Hz, 5-H), 8.37 (1 H, ddd, *J* = 7.8, 2.4,

1.2 Hz, 4-H), 8.42 (1 H, ddd, J = 7.8, 2.4, 1.2, Hz, 6-H), 8.87 (1 H, t, J = 2.4 Hz, 2-H); MS (EI +) m/z 181.0373 (M) ($^{12}C_8H_7NO_4$ requires 181.0375).

Methyl 2-ethynyl-3-nitrobenzoate (71).

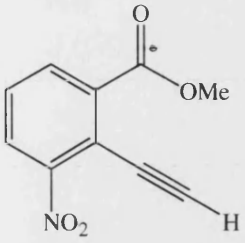

To a solution of **(69)** (400 mg, 1.4 mmol) in THF (50 ml) and H_2O (2.5 ml) was added tetrabutylammonium fluoride (1.0 M in THF, 5.0 ml, 5.0 mmol) at 0°C and the mixture was stirred at room temperature for 16 h. The mixture was then diluted with Et_2O and washed successively with saturated aqueous NH_4Cl solution and H_2O. Evaporation and chromatography (hexane / EtOAc 7:3) gave **(71)** (28 mg, 9%) as a yellow oil; R_f = 0.53 (hexane / EtOAc 7:3); IR υ_{max} (KBr) 1351 & 1532 (NO_2), 1738 (C=O), 2219 (C≡C); ^{1}H NMR ($CDCl_3$) δ 3.67 (1 H, s C≡CH), 3.90 (3 H, s, CH_3), 7.48 (1 H, t, J = 7.8 Hz, 5-H), 7.91 (1 H, dd, J = 7.8, 1.2 Hz, 4-H), 8.00 (1 H, dd, J = 7.8, 1.2 Hz, 6-H); MS (EI +) m/z 205.0381 (M) ($^{12}C_{10}H_7NO_4$ requires 205.0375).

2-iodo-3-nitrobenzoyl chloride (72).

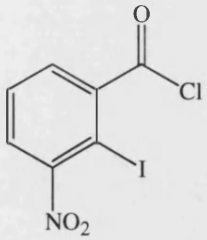

To a solution of **(67)** (3.0 g, 10 mmol) in DMF (5 ml) was carefully added $SOCl_2$ (30 ml) and the mixture was boiled under reflux for 24 h. Evaporation and recrystallisation (petroleum ether) yielded **(72)** (3.1 g, 97%) as yellow crystals; R_f = 0.88 (hexane / EtOAc 1:4); mp 70-71°C (petroleum ether) (lit.[198] mp 71-73°C); IR υ_{max} (KBr) 1348 & 1530 (NO_2), 1758 (C=O); ^{1}H NMR ($CDCl_3$) δ 7.64 (1 H, t,

J = 7.8 Hz, 5-H), 7.78 (1 H, dd, J = 7.8, 1.6 Hz, 4-H), 7.95 (1 H, dd, J = 7.8, 1.6 Hz, 6-H); MS (EI +) *m/z* 312.8821 (M) ($^{12}C_7H_3{}^{37}ClINO_3$ requires 312.8817), 310.8848 (M) ($^{12}C_7H_3{}^{35}ClINO_3$ requires 310.8846), 276 (M – Cl).

2-Iodo-3-nitrobenzamide (73).

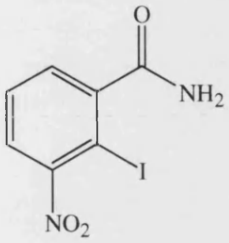

A solution of ethereal NH_3 was produced by slow addition of K_2CO_3 to an immiscible mixture of Et_2O (200 ml) and concentrated aqueous NH_3 (20 ml). The top ethereal layer was then carefully transferred to **(72)** (3.0 g, 9.6 mmol) in Et_2O (10 ml) *via* a glass pipette. The mixture was stirred at room temperature for 1 h, then evaporated to yield **(73)** (2.6 g, 92%) as yellow crystals; R_f = 0.53 (hexane / EtOAc 1:4); 220-221°C (lit.[199] mp 223-225°C); IR υ_{max} (KBr) 1365 & 1525 (NO_2), 1627 (Amide II), 1654 (Amide I), 3177 & 3358 (NH_2); ^{1}H NMR ($(CD_3)_2SO$) δ 7.51 (1 H, dd, J = 7.8, 1.2 Hz, 6-H), 7.61 (1 H, t, J = 7.8 Hz, 5-H), 7.75 (1 H, br s, NH), 7.82 (1 H, dd, J = 7.8, 1.2 Hz, 4-H), 8.02 (1 H, br s, NH); MS (FAB +ve ion) *m/z* 292.9423 (M + H) ($^{12}C_7H_5IN_2O_3$ requires 292.9423).

2-Iodo-3-nitrobenzonitrile (74).

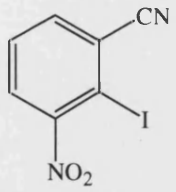

To **(73)** (2.6 g, 8.9 mmol) in THF (50 ml) was carefully added $SOCl_2$ (15 ml) and the suspension was boiled under reflux for 24 h. Ice-H_2O (100 ml) was then added and the mixture made alkaline with cold aqueous NaOH (10%, 100 ml). Extraction ($CHCl_3$), washing (saturated $NaHCO_3$, then H_2O) and evaporation gave **(74)** (2.3 g,

94%) as yellow crystals; R_f = 0.70 (hexane / EtOAc 1:4); mp 147-148°C; IR υ_{max} (KBr) 1357 & 1532 (NO_2), 2233 (CN); ^{1}H NMR ($(CD_3)_2SO$) δ 7.80 (1 H, t, *J* = 8.2 Hz, 5-H), 8.12 (1 H, dd, *J* = 8.2, 1.6 Hz, 6-H), 8.18 (1 H, dd, *J* = 8.2, 1.6 Hz, 4-H); MS (EI +) *m/z* 273.9245 (M) ($^{12}C_7H_3IN_2O_2$ requires 273.9239), 228 (M $-NO_2$).

4-Nitro-1-[(trimethylsilyl)ethynyl]benzene (75).

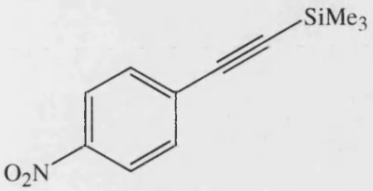

Trimethylsilylethyne (1.2 g, 12 mmol) was slowly added to a suspension of 4-nitroiodobenzene (2.5 g, 10 mmol), $(PPh_3)_2PdCl_2$ (200 mg, 0.3 mmol) and CuI (100 mg, 0.5 mmol) in dry Et_3N (25 ml). The mixture was stirred at 45°C for 1 h under Ar, then quenched with H_2O (200 ml) and filtered through Celite®. The filtrate was extracted with Et_2O, dried and evaporated to give **(75)** (2.0 g, 91%) as yellow crystals; R_f = 0.69 (hexane); mp 93-94°C (lit.[200] mp 97-98°C); IR υ_{max} (KBr) 1345 & 1520 (NO_2), 2160 (C≡C); ^{1}H NMR ($CDCl_3$) δ 0.09 (9 H, s, $Si(CH_3)_3$), 7.41 (2 H, d, *J* = 9.0 Hz, 2,6-H_2), 7.98 (2 H, d, *J* = 9.0 Hz, 3,5-H_2).

1-Ethynyl-4-nitrobenzene (76).

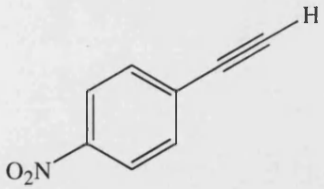

Tetrabutylammonium fluoride (1.0 M in THF, 2.5 ml, 2.5 mmol) was added dropwise to a solution of **(75)** (500 mg, 2.3 mmol) in THF (20 ml) and H_2O (3 ml) at -78°C. The mixture was stirred for 1 h, then quenched with H_2O (200 ml) and extracted with Et_2O. Evaporation and chromatography (hexane / EtOAc 7:3) gave **(76)** (280 mg, 83%) as orange-brown crystals; R_f = 0.40 (hexane); mp 145-146°C (lit.[201] mp 147-149°C); IR υ_{max} (KBr) 1343 & 1512 (NO_2), 2012 (C≡C), 3260

(C≡CH); ^{1}H NMR ($CDCl_3$) δ 3.36 (1 H, s, C≡CH), 7.64 (2 H, d, *J* = 9.0 Hz, 2,6-H_2), 8.20 (2 H, d, *J* = 9.0 Hz, 3,5-H_2); MS (EI +) *m/z* 147.0322 (M) ($^{12}C_8H_5NO_2$ requires 147.0320), 101 (M – NO_2).

4-[(Trimethylsilyl)ethynyl]pyridine (77).

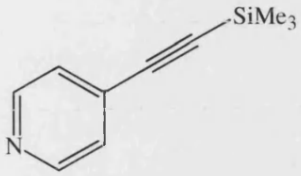

Trimethylsilylethyne (460 mg, 4.7 mmol) was slowly added to a suspension of 4-iodopyridine (1.0 g, 4.9 mmol), $(PPh_3)_2PdCl_2$ (100 mg, 0.1 mmol) and CuI (300 mg, 1.6 mmol) in dry diisopropylamine (25 ml). The mixture was stirred at 45°C for 1 h under Ar, then quenched with H_2O (200 ml) and filtered through Celite®. The filtrate was extracted with Et_2O, dried and evaporated to give **(77)** (790 mg, 93%) as a yellow oil; R_f = 0.72 (hexane); IR υ_{max} (KBr) 2165 (C≡C); ^{1}H NMR ($CDCl_3$) δ 0.26 (9 H, s, $Si(CH_3)_3$), 7.31 (2 H, d, *J* = 4.3 Hz, 3,5-H_2), 8.55 (2 H, d, *J* = 4.3 Hz, 2,6-H_2).

4-Ethynylpyridine (78).

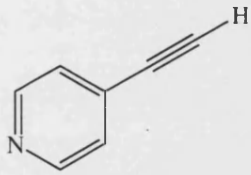

TBAF (1.0 M in THF, 2.5 ml, 2.5 mmol) was added dropwise to a solution of **(77)** (400 mg, 2.3 mmol) in THF (20 ml) and H_2O (3 ml) at -78°C. The mixture was stirred for 1 h, then quenched with H_2O (200 ml), extracted with Et_2O and evaporated to give **(78)** (150 mg, 64%) as a yellow, light-sensitive oil; R_f = 0.23 (CH_2Cl_2 / MeOH 50:1); IR υ_{max} (film) 2120 (C≡C), 3300 (C≡CH); ^{1}H NMR ($CDCl_3$) δ 3.29 (1 H, s, C≡CH), 7.32 (2 H, d, *J* = 5.6 Hz, 3,5-H_2), 8.57 (2 H, d, *J* = 5.6 Hz, 2,6-H_2); MS (EI +) *m/z* 103.0426 (M) ($^{12}C_7H_5N$ requires 103.0422).

4-Methoxy-1-[(trimethylsilyl)ethynyl]benzene (79).

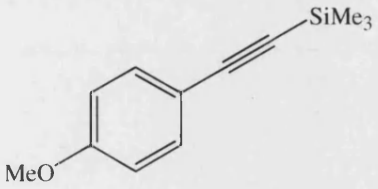

Trimethylsilylethyne (1.2 g, 12 mmol) was slowly added to a suspension of 4-methoxyiodobenzene (2.3 g, 9.8 mmol), $(PPh_3)_2PdCl_2$ (200 mg, 0.3 mmol) and CuI (100 mg, 0.5 mmol) in dry Et_3N (25 ml). The mixture was stirred at 45°C for 1 h under Ar, then quenched with H_2O (200 ml) and filtered through Celite®. The filtrate was extracted with Et_2O, dried and evaporated to give **(79)** (1.8 g, 90%) as a colourless oil; R_f = 0.33 (hexane); lit.[202] bp 96 (1.5 torr); IR υ_{max} (KBr) 2160 (C≡C); ^{1}H NMR ($CDCl_3$) δ 0.24 (9 H, s, $Si(CH_3)_3$), 3.81 (3 H, s, OCH_3), 6.81 (2 H, d, J = 9.0 Hz, 3,5-H_2), 7.40 (2 H, d, J = 9.0 Hz, 2,6-H_2); MS (EI +) *m/z* 204.0973 (M) ($^{12}C_{12}H_{16}OSi$ requires 204.0970), 189 (M – Me).

4-Methyl-1-[(trimethylsilyl)ethynyl]benzene (80).

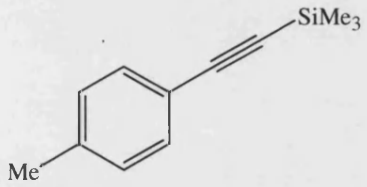

Trimethylsilylethyne (1.2 g, 12 mmol) was slowly added to a suspension of 4-methyliodobenzene (2.2 g, 10 mmol), $(PPh_3)_2PdCl_2$ (200 mg, 0.3 mmol) and CuI (100 mg, 0.5 mmol) in dry Et_3N (25 ml). The mixture was stirred at 45°C for 1 h under Ar, then quenched with H_2O (200 ml) and filtered through Celite®. The filtrate was extracted with Et_2O, dried and evaporated to give **(80)** (1.7 g, 95%) as a colourless oil; R_f = 0.72 (hexane); lit.[223] bp 116 (16 torr); IR υ_{max} (KBr) 2120 (C≡C); ^{1}H NMR ($CDCl_3$) δ 0.24 (9 H, s, $Si(CH_3)_3$), 2.31 (3 H, s, CH_3), 7.07 (2 H, d, J = 8.2 Hz, 3,5-H_2), 7.34 (2 H, d, J = 8.2 Hz, 2,6-H_2); MS (EI +) *m/z* 188.1027 (M) ($^{12}C_{12}H_{16}Si$ requires 188.1021).

4-Trifluoromethyl-1-[(trimethylsilyl)ethynyl]benzene (81).

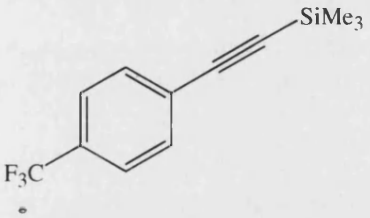

Trimethylsilylethyne (1.2 g, 12 mmol) was slowly added to a suspension of 4-(trifluoromethyl)iodobenzene (2.7 g, 9.9 mmol), $(PPh_3)_2PdCl_2$ (200 mg, 0.3 mmol) and CuI (100 mg, 0.5 mmol) in dry Et_3N (25 ml). The mixture was stirred at 45°C for 1 h under Ar, then quenched with H_2O (200 ml) and filtered through Celite®. The filtrate was extracted with Et_2O, dried and evaporated to give **(81)** (2.2 g, 92%) as a yellow oil; R_f = 0.69 (hexane); IR υ_{max} (KBr) 2155 (C≡C); ^{1}H NMR ($CDCl_3$) δ 0.26 (9 H, s, $Si(CH_3)_3$), 7.45 (2 H, d, *J* = 8.2 Hz, 3,5-H_2), 7.67 (2 H, d, *J* = 8.2 Hz, 2,6-H_2); MS (EI +) *m/z* 242.0737 (M) ($^{12}C_{12}H_{13}F_3Si$ requires 242.0739).

4-Chloro-1-[(trimethylsilyl)ethynyl]benzene (82).

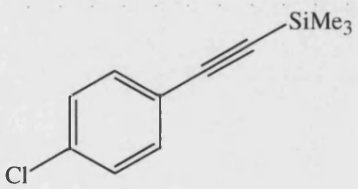

Trimethylsilylethyne (1.2 g, 12 mmol) was slowly added to a suspension of 4-chloroiodobenzene (2.4 g, 10 mmol), $(PPh_3)_2PdCl_2$ (200 mg, 0.3 mmol) and CuI (100 mg, 0.5 mmol) in dry diisopropylamine (30 ml). The mixture was stirred at 45°C for 1 h under Ar, then quenched with H_2O (200 ml) and filtered through Celite®. The filtrate was extracted with Et_2O, dried and evaporated to give **(82)** (2.0 g, 95%) as yellow crystals; R_f = 0.79 (hexane); mp 56-57°C (lit.[204] mp 55°C); IR υ_{max} (KBr) 2098 (C≡C); ^{1}H NMR ($CDCl_3$) δ 0.25 (9 H, s, $Si(CH_3)_3$), 7.27 (2 H, d, *J* = 8.6 Hz, 3,5-H_2), 7.38 (2 H, d, *J* = 8.6 Hz, 2,6-H_2), MS (EI +) *m/z* 210.0448 (M) ($^{12}C_{11}H_{13}{}^{37}ClSi$ requires 210.0445), 208.0477 (M) ($^{12}C_{11}H_{13}{}^{35}ClSi$ requires 208.0475).

2-[(Trimethylsilyl)ethynyl]thiophene (83).

Trimethylsilylethyne (1.2 g, 12.2 mmol) was slowly added to a suspension of 2-iodothiophene (2.1 g, 10.0 mmol), $(PPh_3)_2PdCl_2$ (200 mg, 0.3 mmol) and CuI (100 mg, 0.5 mmol) in dry diisopropylamine (30 ml). The mixture was stirred at 45°C for 1 h under Ar, then quenched with H_2O (200 ml) and filtered through Celite®. The filtrate was extracted with Et_2O, dried and evaporated to give **(83)** (1.6 g, 89%) as a colourless oil; R_f = 0.64 (hexane); lit.[205] bp 104 (15 torr); IR υ_{max} (KBr) 2144 (C≡C); ^{1}H NMR ($CDCl_3$) δ 0.25 (9 H, s, $Si(CH_3)_3$), 6.95 (1 H, dd, *J* = 4.9, 3.9 Hz, 4-H), 7.24 (2 H, m, 3,5-H_2), MS (EI +) *m/z* 180.0433 (M) ($^{12}C_9H_{12}SSi$ requires 180.0429).

Methyl 3-nitro-2-(2-phenylethynyl)benzoate (84) & methyl 3-nitrobenzoate (70).

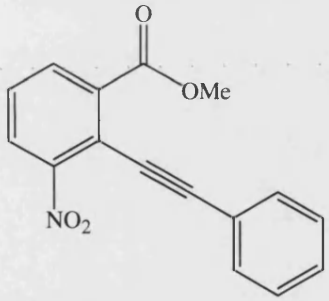

(84)

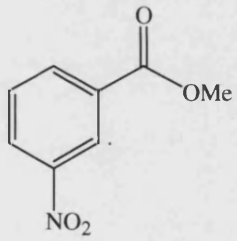

(70)

The Pd catalyst, $(PPh_3)_2PdCl_2$, used in this reaction was prepared as follows:
A mixture of PPh_3 (375 mg, 1.4 mmol) and $PdCl_2$ (130 mg, 0.7 mmol) in DMF (20 ml) was heated at 80°C for 24 h. Filtration and drying yielded $(PPh_3)_2PdCl_2$ as a yellow powder (470 mg, 94%).

A solution of **(68)** (3.0 g, 9.8 mmol) in dry THF (120 ml) was added to a suspension of $(PPh_3)_2PdCl_2$ (300 mg, 0.4 mmol) and CuI (400 mg, 2.1 mmol) in dry diisopropylamine (40 ml) and the mixture was stirred at 45°C for 30 min under Ar. Phenylethyne (1.5 g, 15 mmol) was then added during 30 min and the mixture was

stirred for another 48 h. Filtration (through Celite®), evaporation and chromatography (hexane / CH_2Cl_2 1:1) gave **(84)** (2.2 g, 80%) as reddish-brown crystals; R_f = 0.78 (hexane / EtOAc 4:1); mp 59-60°C; IR υ_{max} (KBr) 1343 & 1527 (NO_2), 1737 (C=O), 2219 (C≡C); ^{1}H NMR ($CDCl_3$) δ 4.01 (3 H, s, CH_3), 7.36-7.41 (3 H, m, 3′,4′,5′-H_3), 7.49 (1 H, t, *J* = 7.8 Hz, 5-H), 7.57-7.62 (2 H, m, 2′,6′-H_2), 8.04 (1 H, dd, *J* = 7.8, 1.2 Hz, 4-H), 8.10 (1 H, dd, *J* = 7.8, 1.2 Hz, 6-H); MS (FAB +ve ion) *m/z* 282.0757 (M + H) ($^{12}C_{16}H_{12}NO_4$ requires 282.0766), 266 (M – Me), 250 (M – OMe), 222 (M – CO_2Me).

Also isolated by chromatography was **(70)** (320 mg, 18%) as yellow crystals. Data as above.

2-Bromo-3-nitrobenzoic acid (85).

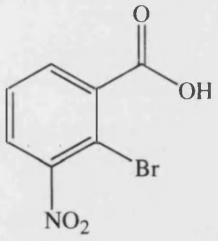

3-Nitrophthalic acid (21.1 g, 100 mmol) in hot aqueous NaOH (10%, 80 ml) was added to $Hg(OAc)_2$ (35.0 g, 110 mmol) in hot AcOH (5 ml) and H_2O (70 ml). The mixture was heated at 170°C (oil bath temperature) for 70 h and was then filtered. The precipitate was washed (H_2O, then EtOH), dried and boiled under reflux in aqueous NaOH (3.5%, 500 ml). Aqueous HCl (2 M, 12 ml) was then slowly added, with vigorous stirring, and the solution was allowed to cool to room temperature. AcOH (3 ml) was then added and this gave a curdy cream precipitate, which dissolved upon addition of a mixture of NaBr (12.0 g, 117 mmol) and Br_2 (19.0 g, 119 mmol) in H_2O (20 ml). The solution was boiled under reflux for 24 h, cooled and neutralised with aqueous NaOH. It was then filtered and acidified with concentrated HCl. The precipitate formed was filtered, dried and recrystallised (EtOH) to give **(85)** (18.2 g, 74%) as a white solid; R_f = 0.24 (hexane / EtOAc 1:4); mp 187-188°C (EtOAc) (lit.[206] mp 187-188°C (EtOAc)); IR υ_{max} (KBr) 1372 & 1545 (NO_2),

1713 (C=O), 2514-3068 (OH); ^{1}H NMR ($(CD_3)_2SO$) δ 7.70 (1 H, t, *J* = 7.9 Hz, 5-H), 7.93 (1 H, dd, *J* = 7.9, 1.5 Hz, 4-H), 8.08 (1 H, dd, *J* = 7.9, 1.5 Hz, 6-H); MS (EI +) *m/z* 246.9308 (M) ($^{12}C_7H_4{}^{81}BrNO_4$ requires 246.9303), 244.9326 (M) ($^{12}C_7H_4{}^{79}BrNO_4$ requires 244.9324).

5-Nitro-3-phenylisocoumarin (86).

1,4-Diphenyl-1,3-butadiyne (87).

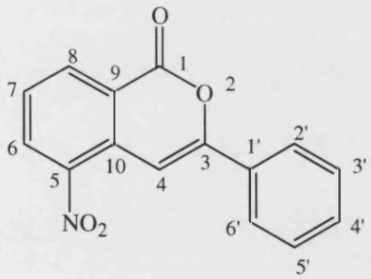

(86)

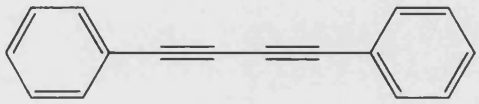

(87)

Method A:

A mixture of **(84)** (2.5 g, 8.9 mmol) and $HgSO_4$ (3.0 g, 10 mmol) in acetone (80 ml) and concentrated H_2SO_4 (4 ml) was boiled under reflux for 48 h, then evaporated to yield a brown residue. Extraction ($CHCl_3$), evaporation and chromatography (hexane / Et_2O 9:1) gave **(86)** (2.3 g, 95%) as yellow crystals; R_f = 0.55 (hexane / EtOAc 4:1); mp 142-143°C; IR υ_{max} (KBr) 1341 & 1525 (NO_2), 1626 (C=C), 1739 (C=O); ^{1}H NMR ($CDCl_3$) δ 7.50-7.53 (3 H, m, 3′,4′,5′-H_3), 7.62 (1 H, t, *J* = 7.8 Hz, 7-H), 7.89 (1 H, d, *J* = 0.8 Hz, 4-H), 7.93-7.97 (2 H, m, 2′,6′-H_2), 8.51 (1 H, dd, *J* = 8.2, 1.2 Hz, 6-H), 8.65 (1 H, ddd, *J* = 8.2, 1.2, 0.8 Hz, 8-H); ^{13}C NMR ($CDCl_3$) δ 117.18 (C-4), 121.01 (C-3), 125.61 (C-1′), 127.59 (C-7), 127.90 (C-4′), 128.28 (C-3′,5′), 128.77 (C-2′,6′), 129.83 (C-10), 131.18 (C-6), 135.44 (C-8), 148.42 (C-9), 157.06 (C-5), 165.07 (C=O); MS (EI +) *m/z* 267.0532 (M) ($^{12}C_{15}H_9NO_4$ requires 267.0532).

Method B:

A solution of CuI (7.5 g, 39 mmol) in aqueous NH_3 (35%, 100 ml) was slowly added to a solution of phenylethyne (4.0 g, 39 mmol) in EtOH (200 ml). The mixture was stirred at room temperature for 15 min, then filtered. The precipitate was washed 5 times each with H_2O, EtOH, then Et_2O until the filtrate became colourless. It was then dried in a vacuum oven at 50°C (20 mmHg) for 2 h. This afforded copper(I) phenylacetylide (4.7 g, 73%) as a bright canary-yellow solid. A solution of **(67)** (3.0 g, 10.2 mmol) and copper(I) phenylacetylide (1.7 g, 10 mmol) in dry pyridine (100 ml) was boiled under reflux for 6 h under N_2. The solution was then poured into H_2O (300 ml), extracted (Et_2O) and washed (2 M aqueous HCl, 5% aqueous $NaHCO_3$, then H_2O). Evaporation of the organic layer and chromatography (hexane / EtOAc 12:1) yielded **(87)** (105 mg, 5%) as a white solid; R_f = 0.95 (hexane / EtOAc 9:1); mp 83-84°C (lit.[207] mp 86-88°C); IR υ_{max} (KBr) 2158 (C≡C); ^{1}H NMR ($CDCl_3$) δ 7.26–7.35 (6 H, m, 2 × 3′,4′,5′-H_3), 7.45–7.50 (4 H, m, 2 × 2′,6′-H_2); MS (EI +) *m/z* 202.0784 (M) ($^{12}C_{16}H_{10}$ requires 202.0783).

Further elution yielded **(86)** (2.0 g, 74%) as yellow crystals; data as above.

Method C:

To a stirred solution of 1-phenyl-1,3-butanedione (8.3 g, 51 mmol) and potassium *t*-butoxide (2.3 g, 20 mmol) in 2-methyl-2-propanol (50 ml) was added **(85)** (2.5 g, 10 mmol) and Cu powder (65 mg, 1.0 mmol). The mixture was boiled under reflux for 16 h, then poured into H_2O (350 ml) and acidified with aqueous HCl (2 M). Extraction (Et_2O), evaporation and chromatography (hexane / EtOAc 10:1) gave **(86)** (120 mg, 4%) as yellow crystals; data as above. Further elution yielded **(88)** (170 mg, 8%) as yellow crystals; data as below.

Method D:

To a stirred solution of dibenzoylmethane (22.9 g, 102 mmol) and potassium *t*-butoxide (4.6 g, 41 mmol) in 2-methyl-2-propanol (100 ml) was added **(85)** (5.0 g, 20 mmol) and Cu powder (150 mg, 2.4 mmol). The mixture was boiled under reflux for 16 h, then poured into H_2O (350 ml) and acidified with aqueous HCl (2 M).

Extraction (Et_2O), evaporation and chromatography (hexane / EtOAc 10:1) gave **(86)** (4.2 g, 78%) as yellow crystals; data as above.

3-Methyl-5-nitroisocoumarin (88).

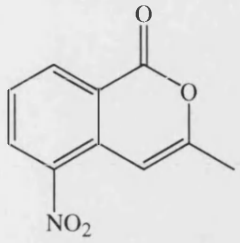

To a stirred solution of 2,4-pentanedione (5.3 g, 53 mmol) and potassium *t*-butoxide (2.3 g, 20 mmol) in 2-methyl-2-propanol (50 ml) was added **(85)** (2.5 g, 10 mmol) and Cu powder (67 mg, 1.1 mmol). The mixture was boiled under reflux for 16 h, then poured into H_2O (350 ml) and acidified with aqueous HCl (2 M). Extraction (Et_2O), evaporation and chromatography (hexane / EtOAc 3:2) gave **(88)** (470 mg, 23%) as yellow crystals; R_f = 0.59 (hexane / EtOAc 4:1); mp 199-200°C; IR υ_{max} (KBr) 1331 & 1520 (NO_2), 1648 (C=C), 1746 (C=O); ^{1}H NMR ($CDCl_3$) δ 2.37 (3 H, s, CH_3), 7.13 (1 H, d, *J* = 0.8 Hz, 4-H), 7.55 (1 H, t, *J* = 8.2 Hz, 7-H), 8.41 (1 H, dd, *J* = 8.2, 1.2 Hz, 6-H), 8.56 (1 H, ddd, *J* = 8.2, 1.2, 0.8 Hz, 8-H); ^{13}C NMR ($CDCl_3$) δ 20.46 (CH_3), 98.36 (C-4), 121.92 (C-3), 126.88 (C-7), 131.36 (C-6), 131.84 (C-10), 135.74 (C-8), 143.85 (C-9), 158.63 (C-5), 160.83 (C=O); MS (EI +) *m/z* 205.0384 (M) ($^{12}C_{10}H_7NO_4$ requires 205.0375), 159 (M – NO_2); Anal. Calcd. for $C_{10}H_7NO_4$: C, 58.54; H, 3.44; N, 6.83. Found: C, 58.3; H, 3.47; N, 6.78.

5-Nitro-3-phenylisoquinolin-1(2*H*)-one (89).

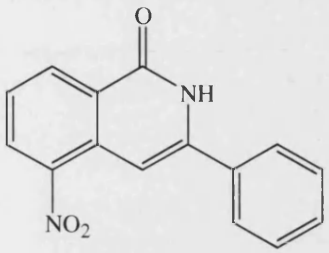

A solution of **(86)** (1.0 g, 3.7 mmol) in 2-methoxyethanol (100 ml) was saturated with NH_3, boiled under reflux for 4 h, then evaporated until 10 ml remained. The concentrate was stored at 4°C for 16 h and the precipitated crystals were filtered, washed (H_2O, then EtOH) and recrystallised (MeOH) to give **(89)** (730 mg, 73%) as bright yellow crystals; R_f = 0.33 (hexane / EtOAc 4:1); mp 127-128°C (MeOH); IR υ_{max} (KBr) 1348 & 1536 (NO_2), 1655 (C=O), 3482 (NH); ^{1}H NMR ($(CD_3)_2SO$) δ 7.25 (1 H, s, 4-H), 7.53-7.55 (3 H, m, 3′,4′,5′-H_3), 7.66 (1 H, t, *J* = 7.8 Hz, 7-H), 7.78-7.80 (2 H, m, 2′,6′-H_2), 8.49 (1 H, d, *J* = 7.8 Hz, 6-H), 8.60 (1 H, d, *J* = 7.8 Hz, 8-H), 12.11 (1 H, br s, NH); MS (EI +) *m/z* 266.0694 (M) ($^{12}C_{15}H_{10}N_2O_3$ requires 266.0691).

5-Amino-3-phenylisoquinolin-1(2*H*)-one (90).

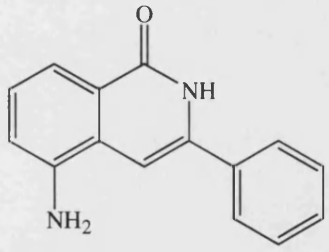

A mixture of **(89)** (100 mg, 376 μmol) and $SnCl_2$ (220 mg, 1.2 mmol) in EtOH (20 ml) was heated at 70°C for 4 h, then carefully poured into ice-H_2O (200 ml). The resulting suspension was made alkaline with aqueous NaOH and the precipitate was filtered. Extraction of the filtrate (EtOAc), evaporation and recrystallisation (hexane, EtOAc) gave **(90)** (51 mg, 57%) as yellow crystals; R_f = 0.91 (hexane / EtOAc 1:4); mp 215-217°C; IR υ_{max} (KBr) 1655 (C=O), 3230 & 3329 (NH_2), 3569 (NH);

^{1}H NMR ($CDCl_3$) δ 4.00 (2 H, br s, NH_2), 6.64 (1 H, s, 4-H), 6.93 (1 H, dd, *J* = 7.8, 1.2 Hz, 6-H), 7.22 (1 H, t, *J* = 7.8 Hz, 7-H), 7.36-7.45 (3 H, m, 3′,4′,5′-H_3), 7.64-7.66 (2 H, m, 2′,6′-H_2), 7.80 (1 H, dd, *J* = 7.8, 1.2 Hz, 8-H), 10.08 (1 H, br s, NH); MS (FAB +ve ion) *m/z* 237.1019 (M + H) ($^{12}C_{15}H_{13}N_2O$ requires 237.1028).

5-Amino-3-phenylisoquinolin-1(2*H*)-one hydrochloride (91).

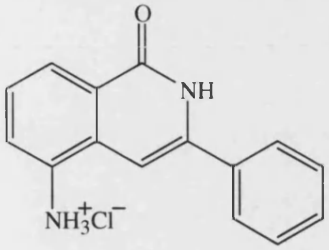

A mixture of **(90)** (50 mg, 0.2 mmol) and aqueous HCl (2 M, 20 ml) were stirred at room temperature for 30 min. Evaporation and recrystallisation (MeOH) yielded **(91)** (53 mg, 91%) as a yellow-brown solid; R_f = 0.59 (MeOH); mp 192-193°C; ^{1}H NMR (D_2O) δ 6.98 (1 H, s, 4-H), 7.52-7.59 (3 H, m, 3′,4′,5′-H_3), 7.59 (1 H, t, *J* = 8.1 Hz, 7-H), 7.68-7.75 (2 H, m, 2′,6′-H_2), 7.84 (1 H, d, *J* = 8.1 Hz, 6-H), 8.31 (1 H, d, *J* = 8.1 Hz, 8-H).

3-Methyl-5-nitroisoquinolin-1(2*H*)-one (92).

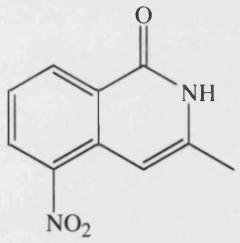

A solution of **(88)** (470 mg, 2.3 mmol) in 2-methoxyethanol (100 ml) was saturated with NH_3, boiled under reflux for 4 h, then evaporated until 10 ml remained. The concentrate was stored at 4°C for 16 h and the precipitated crystals were filtered, washed (H_2O, then EtOH) and recrystallised (MeOH) to give **(92)** (320 mg, 68%) as bright yellow crystals; R_f = 0.33 (hexane / EtOAc 4:1); mp (decomp.) 231-232°C; IR υ_{max} (KBr) 1346 & 1523 (NO_2), 1668 (C=O), 3435 (NH); ^{1}H NMR ($(CD_3)_2SO$)

δ 2.29 (3 H, s, CH_3), 6.78 (1 H, s, 4-H), 7.55 (1 H, t, *J* = 7.8 Hz, 7-H), 8.38 (1 H, dd, *J* = 7.8, 1.2 Hz, 6-H), 8.49 (1 H, dd, *J* = 7.8, 1.2 Hz, 8-H), 11.79 (1 H, br s, NH); MS (FAB +ve ion) *m/z* 205.0617 (M + H) ($^{12}C_{10}H_9N_2O_3$ requires 205.0613), 189 (M – Me); Anal. Calcd. for $C_{10}H_8N_2O_3$: C, 58.82; H, 3.95; N, 13.72. Found: C, 58.4; H, 3.99; N, 13.5.

5-Amino-3-methylisoquinolin-1(2*H*)-one (93).

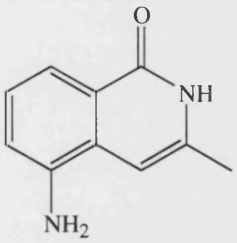

A mixture of **(92)** (320 mg, 1.6 mmol) and $SnCl_2$ (900 mg, 4.7 mmol) in EtOH (20 ml) was heated at 70°C for 4 h, then carefully poured into ice-H_2O (200 ml). The resulting suspension was made alkaline with aqueous NaOH and the precipitate was filtered. Extraction of the filtrate (EtOAc), evaporation and recrystallisation (hexane, EtOAc) gave **(93)** (160 mg, 59%) as yellow crystals; R_f = 0.27 (hexane / EtOAc 1:9); mp 183-184°C; IR υ_{max} (KBr) 1655 (C=O), 3298 & 3375 (NH_2), 3467 (NH); ^{1}H NMR ($(CD_3)_2SO$) δ 2.18 (3 H, s, CH_3), 5.47 (2 H, br s, NH_2), 6.44 (1 H, s, 4-H), 6.80 (1 H, dd, *J* = 7.8, 1.2 Hz, 6-H), 7.05 (1 H, t, *J* = 7.8 Hz, 7-H), 7.32 (1 H, dd, *J* = 7.8, 1.2 Hz, 8-H), 11.06 (1 H, br s, NH); MS (FAB +ve ion) *m/z* 175.0874 (M + H) ($^{12}C_{10}H_{11}N_2O$ requires 175.0871), 159 (M – Me).

5-Amino-3-methylisoquinolin-1(2*H*)-one hydrochloride (94).

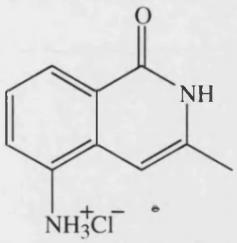

A mixture of **(93)** (160 mg, 0.9 mmol) and aqueous HCl (2 M, 20 ml) were stirred at room temperature for 30 min. Evaporation and recrystallisation (MeOH) yielded **(94)** (180 mg, 95%) as a pale brown solid; R_f = 0.24 (MeOH); mp >350°C; ^{1}H NMR ($(CD_3)_2SO$) δ 2.23 (3 H, s, CH_3), 6.48 (1 H, s, 4-H), 7.37 (1 H, t, *J* = 7.8 Hz, 7-H), 7.69 (1 H, d, *J* = 7.8 Hz, 6-H), 7.99 (1 H, d, *J* = 7.8 Hz, 8-H), 11.50 (1 H, br s, NH).

4-Hydroxy-4-(4-methoxyphenyl)but-3-en-2-one (95a).

1-(4-Methoxyphenyl)butane-1,3-dione (95b).

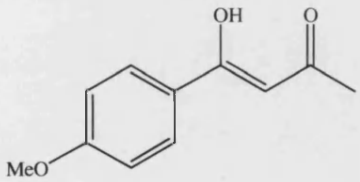

(95a)

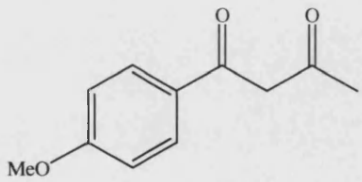

(95b)

A solution of 4-methoxyacetophenone (2.3 g, 15 mmol) in Ac_2O (6.2 g, 60 mmol) was added to $BF_3(AcOH)_2$ (8.5 g, 45 mmol) at 0°C. The mixture was stirred for 30 min and allowed to stand at room temperature for 24 h. The mixture was then poured into an aqueous solution of NaOAc (13%, 100 ml) and boiled under reflux for 1 h. Extraction (Et_2O), evaporation and chromatography (hexane / EtOAc 15:1) afforded **(95a,b)** (12:1)(1.7 g, 59%) as colourless crystals; R_f = 0.64 (hexane / EtOAc 15:1); mp 59-60°C (lit.[208] mp 55-56°C); **(95a):** ^{1}H NMR ($CDCl_3$) δ 2.15 (3 H, s, $COCH_3$), 3.85 (3 H, s, OCH_3), 6.10 (1 H, s, CH), 6.92 (2 H, d, *J* = 9.2 Hz, 3′,5′-H_2), 7.85 (2 H, d, *J* = 9.2 Hz, 2′,6′-H_2), 16.30 (1 H, br s, OH); **(95b):** ^{1}H NMR ($CDCl_3$) δ 2.27 (3 H, s, $COCH_3$), 3.86 (3 H, s, OCH_3), 4.03 (1 H, s, CH_2), 6.92 (2 H, d, *J* = 9.2 Hz, 3′,5′-H_2), 7.85 (2 H, d, *J* = 9.2 Hz, 2′,6′-H_2); MS (EI +) *m/z* 192.0778 (M)

($^{12}C_{11}H_{12}O_3$ requires 192.0786), 177 (M – Me), 161 (M – OMe), 135 (M – CH_2COMe).

1,4-Di(4-methoxyphenyl)-1,3-butadiyne (96).

3-(4-Methoxyphenyl)-5-nitroisocoumarin (97).

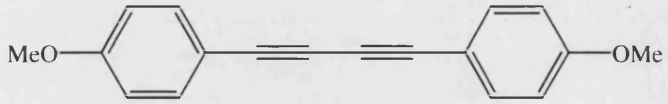

(96)

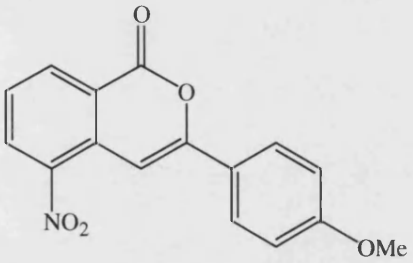

(97)

Method A:

A solution of CuI (7.3 g, 38 mmol) in aqueous NH_3 (100 ml) was slowly added to a solution of **(117)** (5.0 g, 38 mmol) in EtOH (200 ml). The mixture was stirred at room temperature for 15 min, then filtered. The precipitate was washed 5 times each with H_2O, EtOH, then Et_2O until the filtrate became colourless. It was then dried in a vacuum oven at 50°C (20 mmHg) for 2 h. This afforded copper(I) 4-methoxyphenylacetylide (5.6 g, 76%) as a bright canary-yellow solid. A solution of **(67)** (1.7 g, 5.8 mmol) and copper(I) 4-methoxyphenylacetylide (1.2 g, 6.2 mmol) in dry pyridine (100 ml) was boiled under reflux for 6 h under N_2. The solution was then poured into H_2O (300 ml), extracted (Et_2O) and washed (2 M aqueous HCl, 5% aqueous $NaHCO_3$, then H_2O). Evaporation of the organic layer and chromatography (hexane / EtOAc 10:1) yielded **(96)** (20 mg, 1%) as pale yellow crystals; R_f = 0.71 (hexane / EtOAc 4:1); mp 144-145°C (lit.[209] mp 149°C); IR υ_{max} (KBr) 2145 (C≡C); ^{1}H NMR ($CDCl_3$) δ 3.82 (6 H, s, 2 × OCH_3), 6.85 (4 H, d, J = 8.9 Hz, 2 × 3′,5′-H_2), 7.46 (4 H, d, J = 8.9 Hz, 2 × 2′,6′-H_2); MS (EI +) *m/z* 262.0995 (M) ($^{12}C_{18}H_{14}O_2$ requires 262.0994), 247 (M – Me).

Further elution gave **(97)** (500 mg, 29%) as yellow crystals; R_f = 0.61 (hexane / EtOAc 4:1); mp 241-242°C; IR υ_{max} (KBr) 1346 & 1511 (NO_2), 1620 (C=C), 1738 (C=O); ^1H NMR ($CDCl_3$) δ 3.88 (3 H, s, OCH_3), 6.99 (2 H, d, *J* = 9.0 Hz, 3′,5′-H_2), 7.54 (1 H, t, *J* = 8.2 Hz, 7-H), 7.76 (1 H, s, 4-H), 7.88 (2 H, d, *J* = 9.0 Hz, 2′,6′-H_2), 8.46 (1 H, dd, *J* = 8.2, 1.2 Hz, 6-H), 8.59 (1 H, dd, *J* = 8.2, 1.2 Hz, 8-H); ^{13}C NMR ($CDCl_3$) δ 55.56 (OCH_3), 94.74 (C-4), 114.52 (C-3′,5′), 126.56 (C-7), 127.73 (C-2′,6′), 131.71 (C-6), 135.92 (C-8); MS (EI +) *m/z* 297.0639 (M) ($^{12}C_{16}H_{11}NO_5$ requires 297.0637), 266 (M – OMe).

Method B:

To a stirred solution of **(95a)** and **(95b)** (16.9 g, 88.1 mmol) and potassium *t*-butoxide (4.0 g, 36 mmol) in 2-methyl-2-propanol (50 ml) was added **(85)** (4.3 g, 17 mmol) and Cu powder (120 mg, 1.9 mmol). The mixture was boiled under reflux for 16 h, then poured into H_2O (350 ml) and acidified with aqueous HCl (2 M). Extraction (Et_2O), evaporation and chromatography (hexane / EtOAc 4:1) gave **(97)** (790 mg, 15%) as yellow crystals; data as above.

Further elution yielded **(88)** (200 mg, 6%) as yellow crystals; data as above.

Method C:

To a stirred solution of 1,3-di(4-methoxyphenyl)-1,3-propanedione (10.0 g, 35 mmol) and potassium *t*-butoxide (2.3 g, 20 mmol) in 2-methyl-2-propanol (50 ml) was added **(85)** (2.5 g, 10 mmol) and Cu powder (63 mg, 1.0 mmol). The mixture was boiled under reflux for 16 h, then poured into H_2O (350 ml) and acidified with aqueous HCl (2 M). Extraction (Et_2O), evaporation and chromatography (hexane / EtOAc 4:1) gave **(97)** (180 mg, 60%) as yellow crystals; data as above.

3-(4-Methoxyphenyl)-5-nitroisoquinolin-1(2*H*)-one (98).

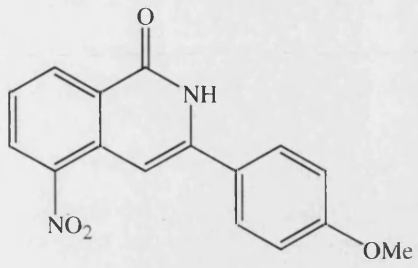

A solution of **(97)** (230 mg, 0.8 mmol) in 2-methoxyethanol (50 ml) was saturated with NH_3, boiled under reflux for 4 h, then evaporated until 10 ml remained. The concentrate was stored at 4°C for 16 h and the precipitated crystals were filtered, washed (H_2O, then EtOH) and recrystallised (MeOH) to give **(98)** (150 mg, 65%) as bright yellow crystals; R_f = 0.45 (hexane / EtOAc 9:1); mp (decomp.) 236-237°C; IR υ_{max} (KBr) 1323 & 1515 (NO_2), 1615 (C=C), 1677 (C=O), 3468 (NH); ^{1}H NMR ($(CD_3)_2SO$) δ 3.82 (3 H, s, OCH_3), 7.07 (2 H, d, *J* = 9.0 Hz, 3′,5′-H_2), 7.18 (1 H, d, *J* = 0.8 Hz, 4-H), 7.60 (1 H, t, *J* = 8.2 Hz, 7-H), 7.73 (2 H, d, *J* = 9.0 Hz, 2′,6′-H_2), 8.45 (1 H, dd, *J* = 8.2, 1.2 Hz, 6-H), 8.55 (1 H, ddd, *J* = 8.2, 1.2, 0.8 Hz, 8-H), 12.00 (1 H, br s, NH); MS (EI +) *m/z* 296.0802 (M) ($^{12}C_{16}H_{12}N_2O_4$ requires 296.0797), 250 (M – NO_2); Anal. Calcd. for $C_{16}H_{12}N_2O_4 \cdot 0.5H_2O$: C, 62.95; H, 4.26; N, 9.18. Found: C, 63.2; H, 4.12; N, 9.49.

5-Amino-3-(4-methoxyphenyl)isoquinolin-1(2*H*)-one (99).

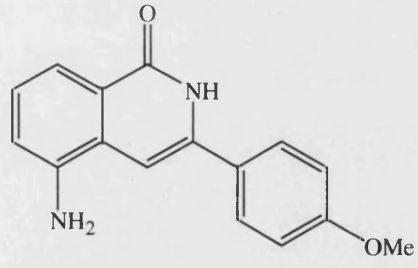

A mixture of **(98)** (80 mg, 0.3 mmol) and $SnCl_2$ (160 mg, 0.8 mmol) in EtOH (30 ml) was heated at 70°C for 4 h, then carefully poured into ice-H2O (200 ml). The resulting suspension was made alkaline with aqueous NaOH and the precipitate was filtered. Extraction of the filtrate (EtOAc), evaporation and recrystallisation

(hexane / EtOAc) gave **(99)** (60 mg, 83%) as yellow crystals; R_f = 0.60 (hexane / EtOAc 1:4); mp 189-190°C; IR υ_{max} (KBr) 1660 (C=O), 3233 (NH_2), 3438 (NH); ^{1}H NMR ($CDCl_3$) δ 3.86 (3 H, s, OCH_3), 4.11 (2 H, br s, NH_2), 6.64 (1 H, s, 4-H), 6.97 (1 H, dd, *J* = 7.8, 1.2 Hz, 6-H), 6.99 (2 H, d, *J* = 8.8 Hz, 3′,5′-H_2), 7.25 (1 H, t, *J* = 7.8 Hz, 7-H), 7.66 (2 H, d, *J* = 8.8 Hz, 2′,6′-H_2), 7.85 (1 H, dd, *J* = 7.8, 1.2 Hz, 8-H), 10.45 (1 H, br s, NH); MS (FAB +ve ion) *m/z* 267.1132 (M + H) ($^{12}C_{16}H_{15}N_2O_2$ requires 267.1134), 251 (M + H – NH_2).

5-Amino-3-(4-methoxyphenyl)isoquinolin-1(2*H*)-one hydrochloride (100).

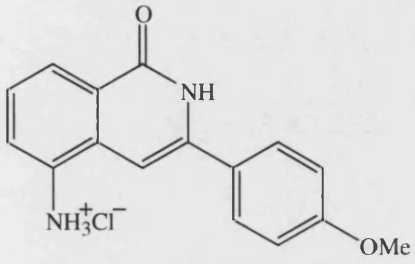

A mixture of **(99)** (60 mg, 0.2 mmol) and aqueous HCl (2 M, 20 ml) were stirred at room temperature for 30 min. Evaporation and recrystallisation (MeOH) yielded **(100)** (65 mg, 95%) as a dark brown solid; R_f = 0.83 (MeOH); mp >350°C; ^{1}H NMR (D_2O) δ 3.86 (3 H, s, OCH_3), 6.84 (2 H, d, *J* = 8.1 Hz, 3′,5′-H_2), 6.92 (1 H, s, 4-H), 7.11 (1 H, t, *J* = 8.1 Hz, 7-H), 7.55 (1 H, d, *J* = 8.1 Hz, 6-H), 7.70 (1 H, d, *J* = 8.1 Hz, 8-H), 7.94 (2 H, *J* = 8.1 Hz, 2′,6′-H_2).

4-Hydroxy-4-(4-methylphenyl)but-3-en-2-one (101a).

1-(4-Methylphenyl)butane-1,3-dione (101b).

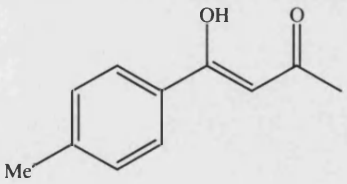

(101a)

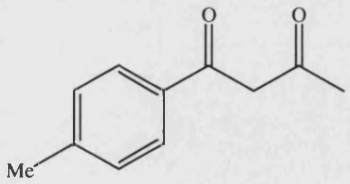

(101b)

A solution of 4-methylacetophenone (2.0 g, 14.9 mmol) in Ac_2O (6.2 g, 60.8 mmol) was added to $BF_3(AcOH)_2$ (8.5 g, 45.2 mmol) at 0°C. The mixture was stirred for 30

min and allowed to stand at room temperature for 24 h. The mixture was then poured into an aqueous solution of NaOAc (13%, 100 ml) and boiled under reflux for 1 h. Extraction (Et_2O), evaporation and chromatography (hexane / EtOAc 20:1) afforded **(101a,b)** (8:1) (2.3 g, 86%) as a colourless oil; R_f = 0.40 (hexane / EtOAc 20:1); **(101a):** ^{1}H NMR ($CDCl_3$) δ 2.20 (3 H, s, $COCH_3$), 2.41 (3 H, s, $ArCH_3$), 6.16 (1 H, s, CH), 7.24 (2 H, d, *J* = 8.2 Hz, 3′,5′-H_2), 7.78 (2 H, d, *J* = 8.2 Hz, 2′,6′-H_2), 16.22 (1 H, br s, OH); **(101b):** ^{1}H NMR ($CDCl_3$) δ 2.30 (3 H, s, $COCH_3$), 2.59 (3 H, s, $ArCH_3$), 4.08 (1 H, s, CH_2), 7.24 (2 H, d, *J* = 8.2 Hz, 3′,5′-H_2), 7.78 (2 H, d, *J* = 8.2 Hz, 2′,6′-H_2); MS (EI +) *m/z* 176.0838 (M) ($^{12}C_{11}H_{12}O_2$ requires 176.0837), 161 (M – Me), 119 (M – CH_2COMe).

1,4-Di(4-methylphenyl)-1,3-butadiyne (102).

3-(4-Methylphenyl)-5-nitroisocoumarin(103).

(102)

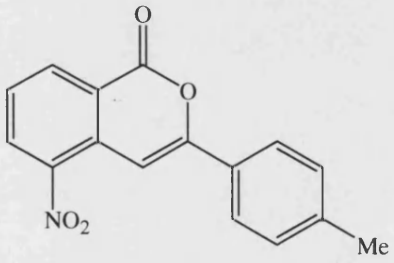

(103)

Method A:

A solution of CuI (6.6 g, 35 mmol) in aqueous NH_3 (35%, 100 ml) was slowly added to a solution of 1-ethynyl-4-methylbenzene (4.0 g, 35 mmol) in EtOH (200 ml). The mixture was stirred at room temperature for 15 min, then filtered. The precipitate was washed 5 times each with H_2O, EtOH, then Et_2O until the filtrate became colourless. It was then dried in a vacuum oven at 50°C (20 torr) for 2 h. This afforded copper(I) 4-methylphenylacetylide (4.4 g, 71%) as a bright canary-yellow solid. A solution of **(67)** (6.0 g, 20 mmol) and copper(I) 4-methylphenylacetylide

(3.7 g, 21 mmol) in dry pyridine (100 ml) was boiled under reflux for 6 h under N_2. The solution was then poured into H_2O (300 ml), extracted (Et_2O) and washed (2 M aqueous HCl, 5% aqueous $NaHCO_3$, then H_2O). Evaporation of the organic layer and chromatography (hexane / EtOAc 10:1) yielded **(102)** (20 mg, 0.4%) as pale yellow crystals; R_f = 0.98 (hexane / EtOAc 4:1); mp 180-181°C (lit.[210] mp 183°C (Et_2O)); IR υ_{max} (KBr) 2130 (C≡C); ^{1}H NMR ($CDCl_3$) δ 2.36 (6 H, s, 2 × CH_3), 7.14 (4 H, d, *J* = 8.1 Hz, 2 × 3′,5′-H_2), 7.41 (4 H, d, *J* = 8.1 Hz, 2 × 2′,6′-H_2); MS (FAB +ve ion) *m/z* 231.1141 (M + H) ($^{12}C_{18}H_{15}$ requires 231.1174).

Further elution gave **(103)** (1.0 g, 18%) as yellow crystals; R_f = 0.48 (hexane / EtOAc 4:1); mp 161-162°C; IR υ_{max} (KBr) 1321 & 1511 (NO_2), 1618 (C=C), 1737 (C=O); ^{1}H NMR ($CDCl_3$) δ 2.42 (3 H, s, CH_3), 7.29 (2 H, d, *J* = 8.2 Hz, 3′,5′-H_2), 7.56 (1 H, t, *J* = 8.2 Hz, 7-H), 7.80 (1 H, s, 4-H), 7.81 (2 H, d, *J* = 8.2 Hz, 2′,6′-H_2), 8.46 (1 H, dd, *J* = 8.2, 1.2 Hz, 6-H), 8.60 (1 H, td, *J* = 8.2, 1.2 Hz, 8-H); MS (FAB +ve ion) *m/z* 282.0762 (M + H) ($^{12}C_{16}H_{11}NO_4$ requires 282.0766).

Method B:

To a stirred solution of **(101a)** and **(101b)** (22.7 g, 0.1 mol) and potassium *t*-butoxide (5.8 g, 52 mmol) in 2-methyl-2-propanol (50 ml) was added **(85)** (6.3 g, 26 mmol) and Cu powder (170 mg, 2.7 mmol). The mixture was boiled under reflux for 16 h, then poured into H_2O (350 ml) and acidified with aqueous HCl (2 M). Extraction (Et_2O), evaporation and chromatography (hexane / EtOAc 10:1) gave **(103)** (1.5 g, 21%) as yellow crystals; data as above.

Further elution yielded **(88)** (140 mg, 3%) as yellow crystals; data as above.

3-(4-Methylphenyl)-5-nitroisoquinolin-1(2*H*)-one (104).

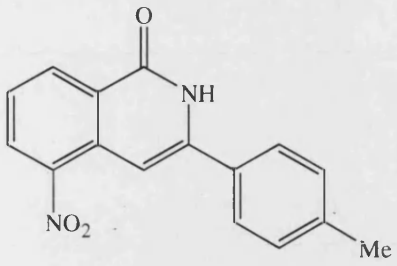

A solution of **(103)** (1.0 g, 3.6 mmol) in 2-methoxyethanol (50 ml) was saturated with NH_3, boiled under reflux for 4 h, then evaporated until 10 ml remained. The concentrate was stored at 4°C for 16 h and the precipitated crystals were filtered, washed (H_2O, then EtOH) and recrystallised (MeOH) to give **(104)** (860 mg, 86%) as bright yellow crystals; R_f = 0.23 (hexane / EtOAc 3:2); mp 175°C; IR υ_{max} (KBr) 1324 & 1516 (NO_2), 1620 (C=C), 1673 (C=O), 3457 (NH); ^{1}H NMR ($(CD_3)_2SO$) δ 2.37 (3 H, s, CH_3), 7.20 (1 H, d, *J* = 0.8 Hz, 4-H), 7.32 (2 H, d, *J* = 8.2 Hz, 3′,5′-H_2), 7.62 (1 H, t, *J* = 8.2 Hz, 7-H), 7.66 (2 H, d, *J* = 8.2 Hz, 2′,6′-H_2), 8.45 (1 H, dd, *J* = 8.2, 1.2 Hz, 6-H), 8.56 (1 H, ddd, *J* = 8.2, 1.2, 0.8 Hz, 8-H), 12.03 (1 H, br s, NH); MS (EI +) *m/z* 280.0856 (M) ($^{12}C_{16}H_{12}N_2O_3$ requires 280.0848); Anal. Calcd. for $C_{16}H_{12}N_2O_3$: C, 68.56; H, 4.32; N, 9.99. Found: C, 68.2; H, 4.28; N, 10.0.

5-Amino-3-(4-methylphenyl)isoquinolin-1(2*H*)-one (105).

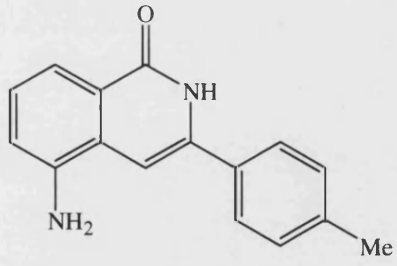

A mixture of **(104)** (280 mg, 1.0 mmol) and $SnCl_2$ (550 mg, 2.9 mmol) in EtOH (30 ml) was heated at 70°C for 4 h, then carefully poured into ice-H_2O (200 ml). The resulting suspension was made alkaline with aqueous NaOH and the precipitate was filtered. Extraction of the filtrate (EtOAc), evaporation and recrystallisation (hexane,

EtOAc) gave **(105)** (230 mg, 92%) as yellow crystals; R_f = 0.24 (hexane / EtOAc 3:2); mp 213-214°C; IR υ_{max} (KBr) 1669 (C=O), 3253 (NH_2), 3476 (NH); ^{1}H NMR ($CDCl_3$) δ 2.41 (3 H, s, CH_3), 4.06 (2 H, br s, NH_2), 6.68 (1 H, s, 4-H), 6.99 (1 H, d, *J* = 7.8 Hz, 6-H), 7.28 (1 H, t, *J* = 7.8 Hz, 7-H), 7.29 (2 H, d, *J* = 7.8 Hz, 3′,5′-H_2), 7.59 (2 H, d, *J* = 7.8 Hz, 2′,6′-H_2), 7.86 (1 H, d, *J* = 7.8 Hz, 8-H), 9.92 (1 H, br s, NH); MS (FAB +ve ion) *m/z* 251.1181 (M + H) ($^{12}C_{16}H_{15}N_2O$ requires 251.1184).

5-Amino-3-(4-methylphenyl)isoquinolin-1(2*H*)-one hydrochloride (106).

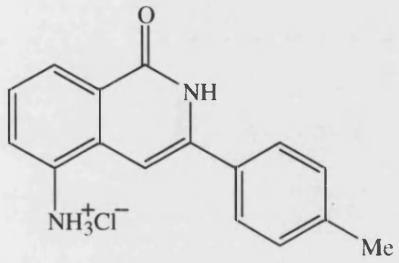

A mixture of **(105)** (25 mg, 0.1 mmol) and aqueous HCl (2 M, 20 ml) were stirred at room temperature for 30 min. Evaporation and recrystallisation (MeOH) yielded **(106)** (27 mg, 94%) as a brown solid; R_f = 0.74 (MeOH); mp >350°C; ^{1}H NMR ($(CD_3)_2SO$) δ 2.23 (3 H, s, CH_3), 6.48 (1 H, s, 4-H), 7.31 (2 H, d, *J* = 7.8 Hz, 3′,5′-H_2), 7.36 (1 H, t, *J* = 7.8 Hz, 7-H), 7.61 (1 H, d, *J* = 7.8 Hz, 6-H), 7.75 (1 H, d, *J* = 7.8 Hz, 8-H), 7.96 (2 H, d, *J* = 7.8 Hz, 2′,6′-H_2), 11.47 (1 H, br s, NH).

4-Hydroxy-4-[4-(trifluoromethyl)phenyl]but-3-en-2-one (108a).

1-[4-(Trifluoromethyl)phenyl]butane-1,3-dione (108b).

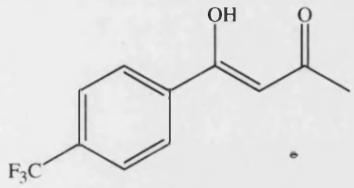

(108a)

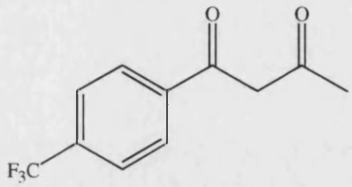

(108b)

A solution of 4-(trifluoromethyl)acetophenone (2.5 g, 13 mmol) in Ac_2O (5.5 g, 54 mmol) was added to $BF_3(AcOH)_2$ (7.6 g, 40 mmol) at 0°C. The mixture was stirred for 30 min and allowed to stand at room temperature for 24 h. The mixture was then poured into an aqueous solution of NaOAc (13%, 100 ml) and boiled under reflux for 1 h. Extraction (Et_2O), evaporation and chromatography (hexane / EtOAc 7:3) afforded **(108a,b)** (27:1) (2.1 g, 68%) as pale orange crystals; R_f = 0.57 (hexane / EtOAc 4:1); mp 48-49°C; **(108a):** ^{1}H NMR ($CDCl_3$) δ 2.23 (3 H, s, CH_3), 6.19 (1 H, s, CH), 7.68 (2 H, d, *J* = 8.2 Hz, 3′,5′-H_2), 7.95 (2 H, d, *J* = 8.2 Hz, 2′,6′-H_2), 15.98 (1 H, br s, OH); ^{19}F NMR ($CDCl_3$) δ –63.62 (3 F, s, CF_3); **(108b):** ^{1}H NMR ($CDCl_3$) δ 2.32 (3 H, s, CH_3), 4.13 (2 H, s, CH_2), 7.71 (2 H, d, *J* = 8.2 Hz, 3′,5′-H_2), 8.04 (2 H, d, *J* = 8.2 Hz, 2′,6′-H_2); ^{19}F NMR ($CDCl_3$) δ -63.62 (3 F, s, CF_3); MS (EI +) *m/z* 230.0551 (M) ($^{12}C_{11}H_9F_3O_2$ requires 230.0555), 173 (M – CH_2COMe), 161 (M – CF_3).

5-Nitro-3-[4-(trifluoromethyl)phenyl]isocoumarin (109).

4-(Trifluoromethyl)acetophenone (110).

Ethyl 4-(trifluoromethyl)benzoate (111).

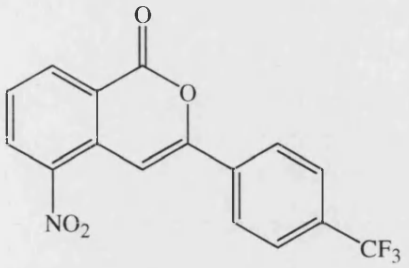

(109)

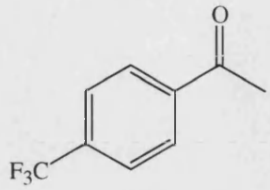

(110)

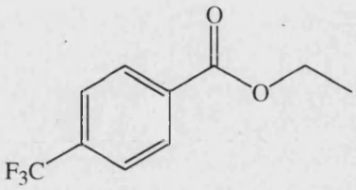

(111)

Method A:

To a stirred solution of **(108a)** and **(108b)** (3.5 g, 15 mol) and NaOEt (1.6 g, 23 mmol) in EtOH (35 ml) was added **(85)** (2.5 g, 10 mmol) and Cu powder (220 mg, 3.5 mmol). The mixture was boiled under reflux for 16 h, then poured into H_2O (350 ml) and acidified with aqueous HCl (2 M). Extraction (Et_2O), evaporation and chromatography (hexane / EtOAc 4:1) gave **(109)** (160 mg, 5%) as yellow crystals; R_f = 0.50 (hexane / EtOAc 4:1); mp 163-164°C; IR υ_{max} (KBr) 1324 & 1531 (NO_2), 1615 (C=C), 1732 (C=O); ^{1}H NMR ($CDCl_3$) δ 7.67 (1 H, t, *J* = 8.2 Hz, 7-H), 7.77 (2 H, d, *J* = 8.2 Hz, 3′,5′-H_2), 7.96 (1 H, d, *J* = 0.8 Hz, 4-H), 8.06 (2 H, d, *J* = 8.2 Hz, 2′,6′-H_2), 8.53 (1 H, dd, *J* = 8.2, 1.6 Hz, 6-H), 8.57 (1 H, ddd, *J* = 8.2, 1.6, 0.8 Hz, 8-H); ^{19}F NMR ($CDCl_3$) δ -63.54 (3 F, s, CF_3); MS (EI +) *m/z* 335.0404 (M) ($^{12}C_{16}H_8F_3NO_4$ requires 335.0405).

Also isolated were the following side products:

(110) (210 mg, 11%) as a colourless oil; ^{1}H NMR ($CDCl_3$) δ 2.56 (3 H, s, CH_3), 7.55 (2 H, d, *J* = 8.2 Hz, 3′,5′-H_2), 8.14 (2 H, d, *J* = 8.2 Hz, 2′,6′-H_2); MS (EI +) *m/z* 188.0457 (M) ($^{12}C_9H_7F_3O$ requires 188.0450).

(111) (130 mg, 6%) as a colourless oil; ^{1}H NMR ($CDCl_3$) δ 1.41 (3 H, t, *J* = 7.2 Hz, CH_2CH_3), 4.41 (2 H, q, *J* = 7.2 Hz, CH_2CH_3), 7.75 (2 H, d, *J* = 8.2 Hz, 3′,5′-H_2),

8.16 (2 H, d, J = 8.2 Hz, 2′,6′-H_2); MS (EI +) *m/z* 218.0553 (M) ($^{12}C_{10}H_9F_3O_2$ requires 218.0555).

Method B:

To a stirred solution of **(108a)** and **(108b)** (3.6 g, 16 mol) and potassium *t*-butoxide (700 mg, 6.3 mmol) in 2-methyl-2-propanol (50 ml) was added **(85)** (760 mg, 3.1 mmol) and Cu powder (20 mg, 0.3 mmol). The mixture was boiled under reflux for 16 h, then poured into H_2O (350 ml) and acidified with aqueous HCl (2 M). Extraction (Et_2O), evaporation and chromatography (hexane / EtOAc 9:1) gave **(109)** (160 mg, 16%) as yellow crystals; data as above.

Further elution yielded **(88)** (40 mg, 6%) as yellow crystals; data as above.

5-Nitro-3-[4-(trifluoromethyl)phenyl]isoquinolin-1(2*H*)-one (112).

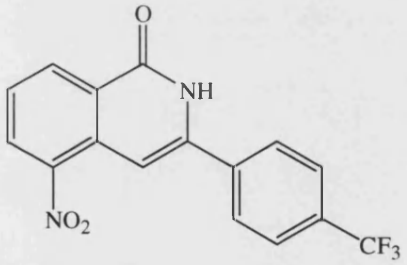

A solution of **(109)** (560 mg, 1.7 mmol) in 2-methoxyethanol (50 ml) was saturated with NH_3, boiled under reflux for 4 h, then evaporated until 10 ml remained. The concentrate was stored at 4°C for 16 h and the precipitated crystals were filtered, washed (H_2O, then EtOH) and recrystallised (MeOH) to give **(112)** (150 mg, 27%) as bright yellow crystals; R_f = 0.43 (hexane / EtOAc 1:4); mp 230-231°C; IR υ_{max} (KBr) 1323 & 1526 (NO_2), 1663 (C=O), 3437 (NH); ^{1}H NMR ($(CD_3)_2SO$) δ 7.28 (1 H, s, 4-H), 7.68 (1 H, t, J = 7.8 Hz, 7-H), 7.88 (2 H, d, J = 8.2 Hz, 3′,5′-H_2), 7.97 (2 H, d, J = 8.2 Hz, 2′,6′-H_2), 8.47 (1 H, dd, J = 7.8, 1.2 Hz, 6-H), 8.58 (1 H, d, J = 7.8, 1.2 Hz, 8-H), 12.21 (1 H, br s, NH); ^{19}F NMR ($(CD_3)_2SO$) δ -61.84 (3 F, s, CF_3); MS (EI +) *m/z* 334.0560 (M) ($^{12}C_{16}H_9F_3N_2O_3$ requires 334.0565).

5-Amino-3-[4-(trifluoromethyl)phenyl]isoquinolin-1(2*H*)-one (113).

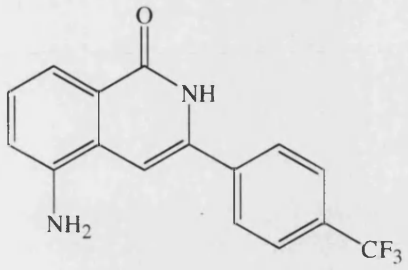

A mixture of **(112)** (1.0 g, 3.0 mmol) and $SnCl_2$ (1.8 g, 9.5 mmol) in EtOH (50 ml) was heated at 70°C for 4 h, then carefully poured into ice-H_2O (200 ml). The resulting suspension was made alkaline with aqueous NaOH and the precipitate was filtered. Extraction of the filtrate (EtOAc), evaporation and recrystallisation (hexane, EtOAc) gave **(113)** (360 mg, 40%) as yellow crystals; R_f = 0.35 (hexane / EtOAc 1:4); mp 214-215°C; IR υ_{max} (KBr) 1651 (C=O), 3218 (NH_2), 3419 (NH); ^{1}H NMR ($(CD_3)_2SO$) δ 5.86 (2 H, br s, NH_2), 6.88 (1 H, dd, *J* = 7.8, 1.2 Hz, 6-H), 7.18 (1 H, t, *J* = 7.8 Hz, 7-H), 7.22 (1 H, s, 4-H), 7.40 (1 H, d, *J* = 7.8, 1.2 Hz, 8-H), 7.82 (2 H, d, *J* = 8.2 Hz, 3′,5′-H_2), 8.02 (2 H, d, *J* = 8.2 Hz, 2′,6′-H_2), 11.45 (1 H, br s, NH); ^{19}F NMR ($(CD_3)_2SO$) δ -61.60 (3 F, s CF_3); MS (FAB +ve ion) *m/z* 305.0898 (M + H) ($^{12}C_{16}H_{12}F_3N_2O$ requires 305.0902).

5-Amino-3-[4-(trifluoromethyl)phenyl]isoquinolin-1(2*H*)-one hydrochloride (114).

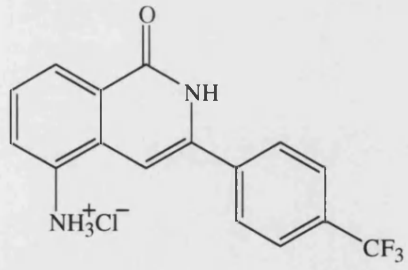

A mixture of **(113)** (360 mg, 1.2 mmol) and aqueous HCl (2 M, 20 ml) were stirred at room temperature for 30 min. Evaporation and recrystallisation (MeOH) yielded **(114)** (370 mg, 92%) as a pale brown solid; R_f = 0.81 (MeOH); mp >350°C; ^{1}H NMR ($(CD_3)_2SO$) δ 7.14 (1 H, dd, *J* = 7.8, 1.2 Hz, 6-H), 7.18 (1 H, s, 4-H),

7.31 (1 H, t, J = 7.8 Hz, 7-H), 7.63 (1 H, dd, J = 7.8, 1.2 Hz, 8-H), 7.85 (2 H, d, J = 8.2 Hz, 3′,5′-H_2), 8.01 (2 H, d, J = 8.2 Hz, 2′,6′-H_2), 11.60 (1 H, br s, NH); ^{19}F NMR ($(CD_3)_2SO$) δ -59.50 (3 F, s, CF_3).

4-Hydroxy-4-(4-chlorophenyl)but-3-en-2-one (115a).

1-(4-Chlorophenyl)butane-1,3-dione (115b).

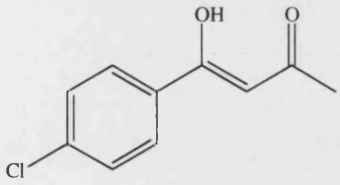

(115a)

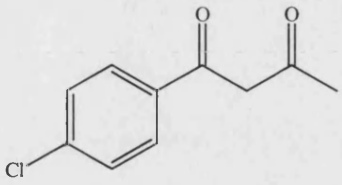

(115b)

A solution of 4-chloroacetophenone (4.6 g, 30 mmol) in Ac_2O (12.3 g, 121 mmol) was added to $BF_3(AcOH)_2$ (17.1 g, 91 mmol) at 0°C. The mixture was stirred for 30 min and allowed to stand at room temperature for 24 h. The mixture was then poured into an aqueous solution of NaOAc (13%, 100 ml) and boiled under reflux for 1 h. Extraction (Et_2O), evaporation and chromatography (hexane / EtOAc 4:1) afforded **(115a,b)** (20:1) (4.9 g, 84%) as pale orange crystals; R_f = 0.54 (hexane / EtOAc 4:1); mp 58-59°C; **(115a):** ^{1}H NMR ($CDCl_3$) δ 2.20 (3 H, s, CH_3), 6.13 (1 H, s, CH), 7.40 (2 H, d, J = 8.6 Hz, 3′,5′-H_2), 7.79 (2 H, d, J = 8.6 Hz, 2′,6′-H_2), 16.09 (1 H, br s, OH); **(115b):** ^{1}H NMR ($CDCl_3$) δ 2.30 (3 H, s, CH_3), 4.07 (2 H, s, CH_2), 7.43 (2 H, d, J = 8.6 Hz, 3′,5′-H_2), 7.87 (2 H, d, J = 8.2 Hz, 2′,6′-H_2); MS (EI +) *m/z* 198.0261 (M) ($^{12}C_{10}H_9{}^{37}ClO_2$ requires 198.0262), 196.0290 (M) ($^{12}C_{10}H_9{}^{35}ClO_2$ requires 196.0291), 161 (M – Cl), 139 (M – CH_2COMe), 111 (M – $COCH_2COMe$).

3-(4-Chlorophenyl)-5-nitroisocoumarin (116).

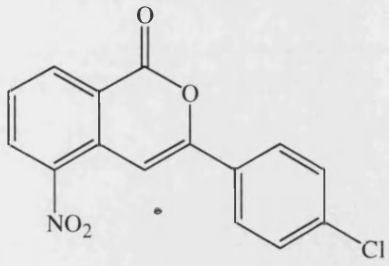

To a stirred solution of **(115a)** and **(115b)** (7.1 g, 36 mmol) and potassium *t*-butoxide (1.7 g, 15 mmol) in 2-methyl-2-propanol (50 ml) was added **(85)** (1.8 g, 7.3 mmol) and Cu powder (47 mg, 0.7 mmol). The mixture was boiled under reflux for 16 h, then poured into H_2O (350 ml) and acidified with aqueous HCl (2 M). Extraction (Et_2O), evaporation and chromatography (hexane / EtOAc 9:1) gave **(116)** (720 mg, 33%) as yellow crystals; R_f = 0.71 (hexane / EtOAc 9:1); mp 204-205°C; IR υ_{max} (KBr) 1340 & 1522 (NO_2), 1626 (C=C), 1745 (C=O); ^{1}H NMR ($CDCl_3$) δ 7.47 (2 H, d, *J* = 9.0 Hz, 3′,5′-H_2), 7.61 (1 H, t, *J* = 8.2 Hz, 7-H), 7.85 (1 H, d, *J* = 0.8 Hz, 4-H), 7.87 (2 H, d, *J* = 9.0 Hz, 2′,6′-H_2), 8.49 (1 H, dd, *J* = 8.2, 1.2 Hz, 6-H), 8.62 (1 H, ddd, *J* = 8.2, 1.2, 0.8 Hz, 8-H); ^{13}C NMR ($CDCl_3$) δ 96.62 (C-4), 127.23 (C-3′,5′), 127.50 (C-7), 129.44 (C-2′,6′), 131.74 (C-6), 135.92 (C-8); MS (EI +) *m/z* 303.0111 (M) ($^{12}C_{15}H_8{}^{37}ClNO_4$ requires 303.0112), 301.0137 (M) ($^{12}C_{15}H_8{}^{35}ClNO_4$ requires 301.0142).

Further elution yielded **(88)** (60 mg, 4%) as yellow crystals; data as above.

1-Ethynyl-4-methoxybenzene (117).

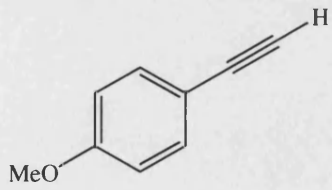

To ethynylmagnesium bromide (0.5 M in THF, 44 ml, 22 mmol) were sequentially added 4-methoxyiodobenzene (4.0 g, 17 mmol) in dry THF (10 ml) and $(PPh_3)_4Pd$ (1.0 g, 0.9 mmol) in dry THF (10 ml). The mixture was stirred at room temperature

for 1 h under Ar, then quenched with aqueous NaCl solution. Extraction (Et_2O), evaporation and chromatography (hexane / EtOAc 20:1) yielded **(117)** (2.0 g, 90%) as a colourless oil; R_f = 0.65 (hexane / EtOAc 15:1); lit.[203] bp 118 (20 torr); IR υ_{max} (KBr) 2122 (C≡C), 3303 (C≡CH); ^{1}H NMR ($CDCl_3$) δ 3.00 (1 H, s, C≡CH), 3.80 (3 H, s, OCH_3), 6.83 (2 H, d, *J* = 9.0 Hz, 3,5-H_2), 7.42 (2 H, d, *J* = 9.0 Hz, 2,6-H_2); MS (EI +) *m/z* 132.0571 (M) ($^{12}C_9H_8O$ requires 132.0575), 117 (M – Me).

1-Ethynyl-4-methylbenzene (118).

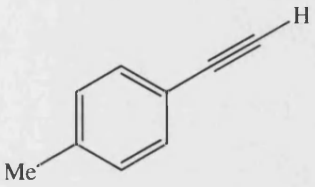

To ethynylmagnesium bromide (0.5 M in THF, 44 ml, 22 mmol) were sequentially added 4-methyliodobenzene (3.7 g, 17 mmol) in dry THF (10 ml) and $(PPh_3)_4Pd$ (1.0 g, 0.9 mmol) in dry THF (10 ml). The mixture was stirred at room temperature for 1 h under Ar, then quenched with aqueous NaCl solution. Extraction (Et_2O), evaporation and chromatography (hexane / EtOAc 15:1) yielded **(118)** (1.8 g, 92%) as a colourless oil; R_f = 0.74 (hexane / EtOAc 15:1); lit.[224] bp 54 (10 torr); IR υ_{max} (KBr) 2125 (C≡C), 3303 (C≡CH); ^{1}H NMR ($CDCl_3$) δ 2.36 (3 H, s, CH_3), 3.04 (1 H, s, C≡CH), 7.13 (2 H, d, *J* = 8.2 Hz, 3,5-H_2), 7.40 (2 H, d, *J* = 8.2 Hz, 2,6-H_2); MS (EI +) *m/z* 116.0628 (M) ($^{12}C_9H_8$ requires 116.0626).

3-(4-Chlorophenyl)-5-nitroisoquinolin-1(2*H*)-one (119).

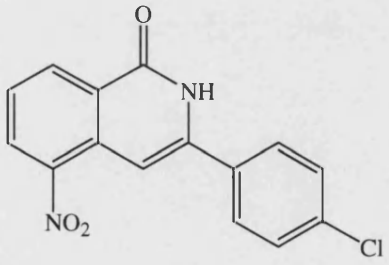

A solution of **(116)** (720 mg, 2.4 mmol) in 2-methoxyethanol (50 ml) was saturated with NH_3, boiled under reflux for 4 h, then evaporated until 10 ml remained. The

concentrate was stored at 4°C for 16 h and the precipitated crystals were filtered, washed (H_2O, then EtOH) and recrystallised (MeOH) to give **(119)** (460 mg, 64%) as bright yellow crystals; R_f = 0.33 (hexane / EtOAc 1:4); mp (decomp.) 271-273°C; IR υ_{max} (KBr) 1325 & 1525 (NO_2), 1625 (C=C), 1674 (C=O), 3465 (NH); ^{1}H NMR ($(CD_3)_2SO$) δ 7.22 (1 H, d, *J* = 0.8 Hz, 4-H), 7.59 (2 H, d, *J* = 8.6 Hz, 3′,5′-H_2), 7.65 (1 H, t, *J* = 8.2 Hz, 7-H), 7.79 (2 H, d, *J* = 8.6 Hz, 2′,6′-H_2), 8.47 (1 H, dd, *J* = 8.2, 1.2 Hz, 6-H), 8.58 (1 H, ddd, *J* = 8.2, 1.2, 0.8 Hz, 8-H), 12.13 (1 H, br s, NH); MS (FAB +ve ion) *m/z* 303.0360 (M + H) ($^{12}C_{15}H_{10}{}^{37}ClN_2O_3$ requires 303.0350), 301.0377 (M + H) ($^{12}C_{15}H_{10}{}^{35}ClN_2O_3$ requires 301.0380); Anal. Calcd. for $C_{15}H_9ClN_2O_3 \cdot 0.25H_2O$: C, 59.02; H, 3.11; N, 9.18. Found: C, 58.8; H, 3.11; N, 9.11.

5-Amino-3-(4-chlorophenyl)isoquinolin-1(2*H*)-one (120).

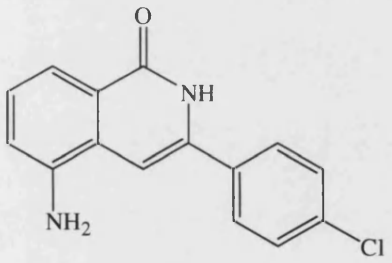

A mixture of **(119)** (460 mg, 1.5 mmol) and $SnCl_2$ (870 mg, 4.6 mmol) in EtOH (30 ml) was heated at 70°C for 4 h, then carefully poured into ice-H_2O (200 ml). The resulting suspension was made alkaline with aqueous NaOH and the precipitate was filtered. Extraction of the filtrate (EtOAc), evaporation and recrystallisation (hexane, EtOAc) gave **(120)** (170 mg, 41%) as yellow crystals; R_f = 0.72 (hexane / EtOAc 1:4); mp 231-232°C; IR υ_{max} (KBr) 1654 (C=O), 3236 & 3338 (NH_2), 3548 (NH); ^{1}H NMR ($(CD_3)_2SO$) δ 5.81 (2 H, br s, NH_2), 6.86 (1 H, dd, *J* = 7.8, 1.2 Hz, 6-H), 7.11 (1 H, s, 4-H), 7.15 (1 H, t, *J* = 7.8 Hz, 7-H), 7.38 (1 H, dd, *J* = 7.8, 1.2 Hz, 8-H), 7.53 (2 H, d, *J* = 9.0 Hz, 3′,5′-H_2), 7.83 (2 H, d, *J* = 9.0 Hz, 2′,6′-H_2), 11.34 (1 H, br s, NH); MS (FAB +ve ion) *m/z* 273.0618 (M + H) ($^{12}C_{15}H_{12}{}^{37}ClN_2O$ requires 273.0609); 271.0629 (M + H) ($^{12}C_{15}H_{12}{}^{35}ClN_2O$ requires 271.0638).

5-Amino-3-(4-chlorophenyl)isoquinolin-1(2*H*)-one hydrochloride (121).

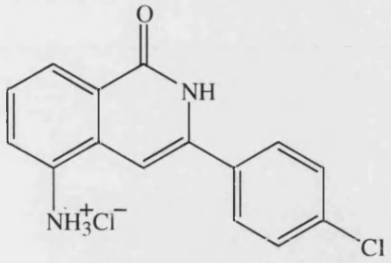

A mixture of **(120)** (170 mg, 0.6 mmol) and aqueous HCl (2 M, 20 ml) were stirred at room temperature for 30 min. Evaporation and recrystallisation (MeOH) yielded **(121)** (180 mg, 95%) as a brown solid; R_f = 0.74 (MeOH); mp >350°C; ^{1}H NMR ($(CD_3)_2SO$) δ 7.08 (1 H, s, 4-H), 7.14 (1 H, dd, *J* = 7.8, 1.2 Hz, 6-H), 7.28 (1 H, t, *J* = 7.8 Hz, 7-H), 7.56 (2 H, d, *J* = 9.0 Hz, 3′,5′-H_2), 7.64 (1 H, dd, *J* = 7.8, 1.2 Hz, 8-H), 7.83 (2 H, d, *J* = 9.0 Hz, 2′,6′-H_2), 11.50 (1 H, br s, NH).

4-Hydroxy-4-(2-thienyl)but-3-en-2-one (122a).

1-(2-Thienyl)butane-1,3-dione (122b).

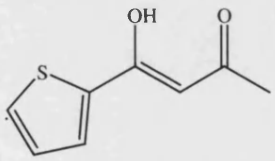

(122a)

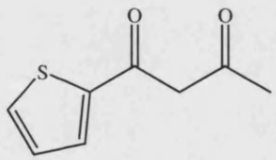

(122b)

Method A:

A solution of 2-acetylthiophene (13.2 g, 105 mmol) in Ac_2O (42.8 g, 420 mmol) was added to $BF_3(AcOH)_2$ (59.5 g, 316 mmol) at 0°C. The mixture was stirred for 30 min and allowed to stand at room temperature for 24 h. The mixture was then poured into an aqueous solution of NaOAc (13%, 100 ml) and boiled under reflux for 1 h. Extraction (Et_2O), evaporation and chromatography (hexane / EtOAc 9:1) afforded **(122a,b)** (5:1) (1.2 g, 7%) as reddish-brown solid; R_f = 0.40 (hexane / EtOAc 9:1); mp 30-31°C; **(122a):** ^{1}H NMR ($CDCl_3$) δ 2.12 (3 H, s, CH_3), 6.01 (1 H, s, CH), 7.10 (1 H, dd, *J* = 4.9, 3.6 Hz, 4′-H), 7.57 (1 H, dd, *J* = 4.9, 1.1 Hz, 5′-H), 7.66 (1 H, dd, *J* = 3.6, 1.1 Hz, 3′-H), 15.64 (1 H, br s, OH); **(122b):** ^{1}H NMR ($CDCl_3$)

δ 2.30 (3 H, s, CH_3), 4.01 (2 H, s, CH_2), 7.12 (1 H, dd, *J* = 4.9, 3.6 Hz, 4′-H), 7.68 (1 H, dd, *J* = 4.9, 1.1 Hz, 5′-H), 7.70 (1 H, dd, *J* = 3.6, 1.1 Hz, 3′-H); MS (EI +) *m/z* 168.0241 (M) ($^{12}C_8H_8O_2S$ requires 168.0245), 111 (M – CH_2COMe).

Method B:

To a solution of $NaNH_2$ (50% in toluene, 31.2 ml, 0.4 mol) in dry Et_2O (100 ml) was added, during 10 min, a solution of 2-acetylthiophene (25.2 g, 0.2 mol) in dry Et_2O (50 ml). After stirring for 30 min, dry EtOAc (35.2 g, 0.4 mol) in dry Et_2O (50 ml) was slowly added. The mixture was boiled under reflux for 2 h, poured into H_2O (300 ml), then neutralised with aqueous HCl (2 M). Extraction (Et_2O) and evaporation (Et_2O) yielded a residue which was dissolved in an equal volume of MeOH. To this methanolic solution was added a hot, filtered solution of $Cu(OAc)_2$ (40.0 g) in H_2O (350 ml) and the mixture was allowed to stand until it cooled to room temperature. The precipitated copper salt was filtered, washed with cold petroleum ether and shaken with a mixture of H_2SO_4 (10%, 300 ml) and Et_2O (100 ml) until the Et_2O layer was colourless. Evaporation of the organic layer yielded **(122a,b)** (18.6 g, 55%) as reddish-brown crystals. Data identical to above.

5-Nitro-3-(2-thienyl)isocoumarin (123).

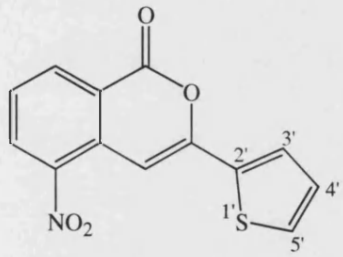

To a stirred solution of **(122a)** and **(122b)** (18.6 g, 111 mmol) and potassium *t*-butoxide (5.1 g, 45 mmol) in 2-methyl-2-propanol (100 ml) was added **(85)** (5.5 g, 22 mmol) and Cu powder (145 mg, 2.3 mmol). The mixture was boiled under reflux for 16 h, then poured into H_2O (350 ml) and acidified with aqueous HCl (2 M). Extraction (Et_2O), evaporation and chromatography (hexane / EtOAc 10:1) gave **(123)** (1.3 g, 21%) as yellow crystals; R_f = 0.68 (hexane / EtOAc 10:1); mp 189-190°C; IR υ_{max} (KBr) 1338 & 1530 (NO_2), 1619 (C=C), 1744 (C=O);

^{1}H NMR ($CDCl_3$) δ 7.15 (1 H, dd, *J* = 5.1, 3.9 Hz, 4′-H), 7.50 (1 H, dd, *J* = 5.1, 1.2 Hz, 5′-H), 7.55 (1 H, t, *J* = 8.2 Hz, 7-H), 7.71 (1 H, dd, *J* = 3.9, 1.2 Hz, 3′-H), 7.71 (1 H, d, *J* = 0.8 Hz, 4-H), 8.47 (1 H, dd, *J* = 8.2, 1.2 Hz, 6-H), 8.59 (1 H, ddd, *J* = 8.2, 1.2, 0.8 Hz, 8-H); MS (EI +) *m/z* 273.0088 (M) ($^{12}C_{13}H_7NO_4S$ requires 273.0096).

5-Nitro-3-(2-thienyl)isoquinolin-1(2*H*)-one (124).

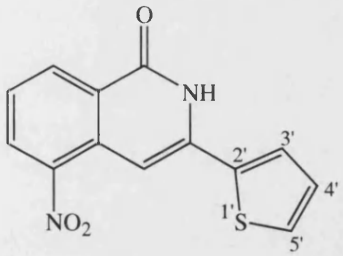

A solution of **(123)** (810 mg, 3.0 mmol) in 2-methoxyethanol (50 ml) was saturated with NH_3, boiled under reflux for 4 h, then evaporated until 10 ml remained. The concentrate was stored at 4°C for 16 h and the precipitated crystals were filtered, washed (H_2O, then EtOH) and recrystallised (MeOH) to give **(124)** (510 mg, 63%) as orange crystals; R_f = 0.44 (hexane / EtOAc 1:4); mp (decomp.) 225°C; IR υ_{max} (KBr) 1319 & 1514 (NO_2), 1616 (C=C), 1670 (C=O), 3458 (NH); ^{1}H NMR ($(CD_3)_2SO$) δ 7.21 (1 H, dd, *J* = 5.1, 3.9 Hz, 4′-H), 7.33 (1 H, d, *J* = 0.8 Hz, 4-H), 7.60 (1 H, t, *J* = 8.2 Hz, 7-H), 7.77 (1 H, dd, *J* = 5.1, 1.2 Hz, 5′-H), 7.93 (1 H, dd, *J* = 3.9, 1.2 Hz, 3′-H), 8.47 (1 H, dd, *J* = 8.2, 1.2 Hz, 6-H), 8.54 (1 H, ddd, *J* = 8.2, 1.2, 0.8 Hz, 8-H), 12.13 (1 H, br s, NH); MS (EI +) *m/z* 272.0257 (M) ($^{12}C_{13}H_8N_2O_3S$ requires 272.0256), 226 (M – NO_2); Anal. Calcd. for $C_{13}H_8N_2O_3S{\cdot}0.25H_2O$: C, 56.42; H, 3.07; N, 10.13. Found: C, 56.7; H, 3.15; N, 10.0.

5-Amino-3-(2-thienyl)isoquinolin-1(2*H*)-one (125).

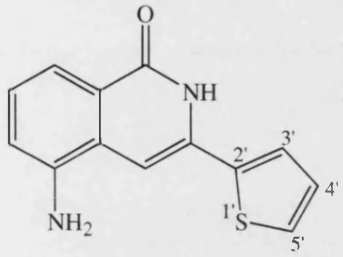

A mixture of **(124)** (510 mg, 1.9 mmol) and $SnCl_2$ (1.1 g, 5.8 mmol) in EtOH (30 ml) was heated at 70°C for 4 h, then carefully poured into ice-H_2O (200 ml). The resulting suspension was made alkaline with aqueous NaOH and the precipitate was filtered. Extraction of the filtrate (EtOAc), evaporation and recrystallisation (hexane, EtOAc) gave **(125)** (300 mg, 66%) as yellow crystals; R_f = 0.74 (hexane / EtOAc 3:7); mp 229-230°C; IR υ_{max} (KBr) 1659 (C=O), 3365 (NH_2), 3470 (NH); ^{1}H NMR ($CDCl_3$) δ 4.03 (2 H, br s, NH_2), 6.70 (1 H, s, 4-H), 6.99 (1 H, dd, *J* = 7.8, 1.1 Hz, 6 H), 7.14 (1 H, dd, *J* = 4.9, 3.8 Hz, 4′-H), 7.28 (1 H, t, *J* = 7.8 Hz, 7-H), 7.37 (1 H, dd, *J* = 4.9, 1.1 Hz, 5′-H), 7.49 (1 H, dd, *J* = 3.8, 1.1 Hz, 3′-H), 7.86 (1 H, dd, *J* = 7.8, 1.1 Hz, 8-H), 9.50 (1 H, br s, NH); MS (EI +) *m/z* 242.0517 (M) ($^{12}C_{13}H_{10}N_2OS$ requires 242.0514).

5-Amino-3-(2-thienyl)isoquinolin-1(2*H*)-one hydrochloride (126).

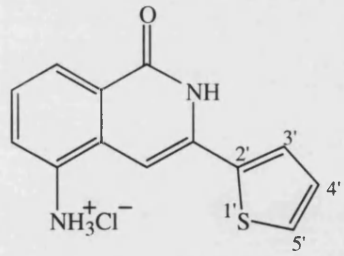

A mixture of **(120)** (24 mg, 0.1 mmol) and aqueous HCl (2 M, 20 ml) were stirred at room temperature for 30 min. Evaporation and recrystallisation (MeOH) yielded **(121)** (26 mg, 94%) as a dark brown solid; R_f = 0.64 (MeOH); mp >350°C; ^{1}H NMR (D_2O) δ 6.87 (1 H, s, 4-H), 7.07 (1 H, dd, *J* = 4.9, 3.8 Hz, 4′-H), 7.26 (1 H,

d, J = 4.9 Hz, 5′-H), 7.53 (1 H, d, J = 3.8 Hz, 3′-H), 7.58 (1 H, t, J = 7.8 Hz, 7-H), 7.77 (1 H, d, J = 7.8 Hz, 6-H), 8.22 (1 H, d, J = 7.8 Hz, 8-H).

4-Hydroxy-4-(4-nitrophenyl)but-3-en-2-one (127a).

1-(4-Nitrophenyl)butane-1,3-dione (127b).

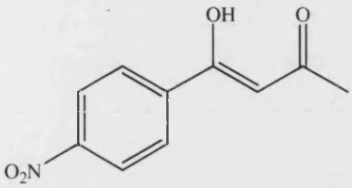

(127a)

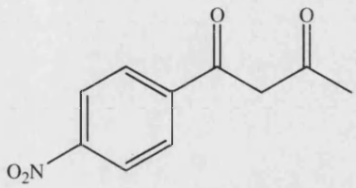

(127b)

A solution of 4-nitroacetophenone (5.0 g, 30 mmol) in Ac_2O (12.3 g, 121 mmol) was added to $BF_3(AcOH)_2$ (17.1 g, 91.0 mmol) at 0°C. The mixture was stirred for 30 min and allowed to stand at room temperature for 24 h. The mixture was then poured into an aqueous solution of NaOAc (13%, 100 ml) and boiled under reflux for 1 h. Extraction (Et_2O), evaporation and chromatography (hexane / EtOAc 4:1) afforded **(127a,b)** (66:1) (3.2 g, 51%) as yellow crystals; R_f = 0.63 (hexane / EtOAc 7:3); mp 115-116°C (lit.[208] mp 112-113°C (EtOH)); **(127a):** ^{1}H NMR ($CDCl_3$) δ 2.26 (3 H, s, CH_3), 6.22 (1 H, s, CH), 8.00 (2 H, d, J = 9.0 Hz, 2′,6′-H_2), 8.27 (2 H, d, J = 9.0 Hz, 3′,5′-H_2), 15.89 (1 H, br s, OH); **(127b):** ^{1}H NMR ($CDCl_3$) δ 2.35 (3 H, s, CH_3), 4.16 (2 H, s, CH_2), 8.10 (2 H, d, J = 9.0 Hz, 2′,6′-H_2), 8.31 (2 H, d, J = 9.0 Hz, 3′,5′-H_2); MS (EI +) *m/z* 207.0536 (M) ($^{12}C_{10}H_9NO_4$ requires 207.0532), 150 (M – CH_2COMe).

4-Hydroxy-4-(4-pyridinyl)but-3-en-2-one (128a).

1-(4-Pyridinyl)butane-1,3-dione (128b).

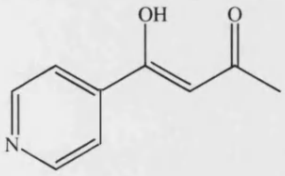

(128a)

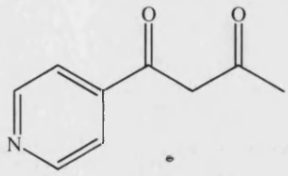

(128b)

To a solution of $NaNH_2$ (50% in toluene, 31.2 ml, 0.4 mol) in dry Et_2O (100 ml) was added, during 10 min, a solution of 2-acetylpyridine (24.2 g, 0.2 mol) in dry Et_2O (50 ml). After stirring for 30 min, dry EtOAc (35.2 g, 0.4 mol) in dry Et_2O (50 ml) was slowly added. The mixture was boiled under reflux for 2 h, poured into H_2O (300 ml), then neutralised with aqueous HCl (2 M). Extraction (Et_2O) and evaporation (Et_2O) yielded a residue which was dissolved in an equal volume of MeOH. To this methanolic solution was added a hot, filtered solution of $Cu(OAc)_2$ (40 g) in H_2O (350 ml) and the mixture was allowed to stand until it cooled to room temperature. The precipitated copper salt was filtered, washed with cold petroleum ether and shaken with a mixture of H_2SO_4 (10%, 300 ml) and Et_2O (100 ml) until the Et_2O layer was colourless. Evaporation of the organic layer yielded **(128a,b)** (11:1) (11.9 g, 37%) as a yellow oil; R_f = 0.60 (hexane / EtOAc 9:1); lit.[211] bp 118-120 (5 torr); **(128a):** ^{1}H NMR ($CDCl_3$) δ 2.24 (3 H, s, CH_3), 6.20 (1 H, s, CH), 7.68 (2 H, d, *J* = 5.2 Hz, 3′,5′-H_2), 8.73 (2 H, d, *J* = 5.2 Hz, 2′,6′-H_2), 15.73 (1 H, br s, OH); **(128b):** ^{1}H NMR ($CDCl_3$) δ 2.39 (3 H, s, CH_3), 3.97 (2 H, s, CH_2), 7.62 (2 H, d, *J* = 5.2 Hz, 3′,5′-H_2), 8.69 (2 H, d, *J* = 5.2 Hz, 2′,6′-H_2); MS (EI +) *m/z* 163.0629 (M) ($^{12}C_9H_9NO_2$ requires 163.0633), 106 (M – CH_2COMe).

4-Hydroxy-4-(4′-hydroxyphenyl)-but-3-en-2-one (129a).

1-(4-Hydroxyphenyl)butane-1,3-dione (129b).

4-Hydroxy-4-(4-acetoxyphenyl)but-3-en-2-one (130a).

1-(4-Acetoxyphenyl)butane-1,3-dione (130b).

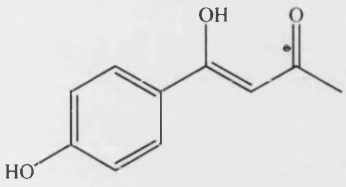

(129a)

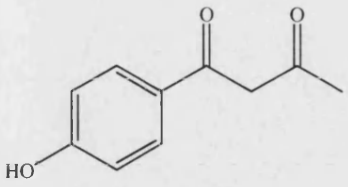

(129b)

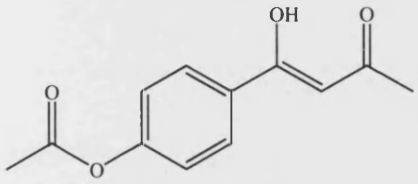

(130a)

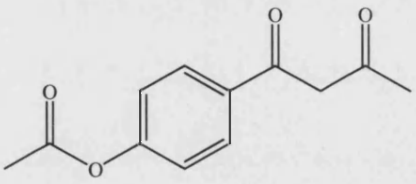

(130b)

A solution of 4-hydroxyacetophenone (12.2 g, 90 mmol) in Ac_2O (37.3 g, 366 mmol) was added to $BF_3(AcOH)_2$ (51.4 g, 273 mmol) at 0°C. The mixture was stirred for 30 min and allowed to stand at room temperature for 24 h. The mixture was then poured into an aqueous solution of NaOAc (13%, 100 ml) and boiled under reflux for 1 h. Extraction (Et_2O), evaporation and chromatography (hexane / EtOAc 4:1) afforded **(129a,b)** (3:1) (1.0 g, 6%) as a cream solid; R_f = 0.20 (hexane / EtOAc 4:1); mp 112-113°C; **(129a):** ^{1}H NMR ($CDCl_3$) δ 2.13 (3 H, s, CH_3), 6.40 (1 H, s, CH), 6.85 (2 H, d, *J* = 9.0 Hz, 3′,5′-H_2), 7.83 (2 H, d, *J* = 9.0 Hz, 2′,6′-H_2), 10.37 (1 H, br s, phenolic OH), 16.05 (1 H, br s, enolic OH); **(129b):** ^{1}H NMR ($CDCl_3$) δ 2.20 (3 H, s, CH_3), 4.14 (1 H, s, CH_2), 6.84 (2 H, d, *J* = 9.0 Hz, 3′,5′-H_2), 7.79 (2 H, d, *J* = 9.0 Hz, 2′,6′-H_2), 10.37 (1 H, br s, phenolic OH); MS (EI +) *m/z* 178.0625 (M) ($^{12}C_{10}H_{10}O_3$ requires 178.0630), 121 (M – CH_2COMe).

Also isolated from the column was **(130a,b)** (10:1) (8.9 g, 45%) as a white solid; R_f = 0.33 (hexane / EtOAc 4:1); mp 65-66°C; **(130a):** ^{1}H NMR ($CDCl_3$) δ 2.19 (3 H, s, $COCH_3$), 2.32 (3 H, s, $OCOCH_3$), 6.13 (1 H, s, CH), 7.16 (2 H, d, *J* = 8.8 Hz, 2′,6′-H_2), 7.88 (2 H, d, *J* = 8.8 Hz, 3′,5′-H_2), 16.10 (1 H, br s, OH);

(130b): ^{1}H NMR ($CDCl_3$) δ 2.29 (3 H, s, $COCH_3$), 2.32 (3 H, s, $OCOCH_3$), 4.07 (2 H, s, CH_2), 7.20 (2 H, d, *J* = 8.8 Hz, 2′,6′-H_2), 7.96 (2 H, d, *J* = 8.8 Hz, 3′,5′-H_2); MS (EI +) *m/z* 220.0736 (M) ($^{12}C_{12}H_{12}O_4$ requires 220.0736), 163 (M – CH_2COMe).

3-Ethyl-5-nitroisocoumarin (131).

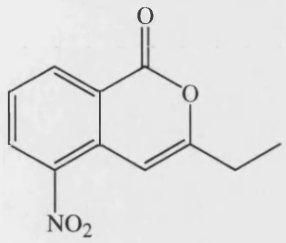

To a stirred solution of heptane-3,5-dione (6.4 g, 50 mmol) and potassium *t*-butoxide (2.3 g, 20 mmol) in 2-methyl-2-propanol (50 ml) was added **(85)** (2.5 g, 10.2 mmol) and Cu powder (65 mg, 1.0 mmol). The mixture was boiled under reflux for 16 h, then poured into H_2O (350 ml) and acidified with aqueous HCl (2 M). Extraction (Et_2O), evaporation and chromatography (hexane / EtOAc 9:1) gave **(131)** (520 mg, 24%) as yellow crystals; R_f = 0.52 (hexane / EtOAc 4:1); mp 77-78°C; IR υ_{max} (KBr) 1347 & 1524 (NO_2), 1645 (C=C), 1747 (C=O); ^{1}H NMR ($CDCl_3$) δ 1.17 (3 H, t, *J* = 7.6 Hz, CH_3), 2.55 (2 H, q, *J* = 7.6 Hz, CH_2), 7.01 (1 H, d, *J* = 0.9 Hz, 4-H), 7.48 (1 H, t, *J* = 8.1 Hz, 7-H), 8.32 (1 H, dd, *J* = 8.1, 2.6 Hz, 6-H), 8.44 (1 H, ddd, *J* = 8.1, 2.6, 0.9 Hz, 8-H); ^{13}C NMR ($CDCl_3$) δ 11.73 (CH_3), 27.99 (CH_2), 97.41 (C-4), 122.65 (C-3), 127.41 (C-7), 131.84 (C-6), 132.38 (C-10), 136.22 (C-8), 144.43 (C-9), 161.43 (C-5), 163.92 (C=O); MS (EI +) *m/z* 219.0533 (M) ($^{12}C_{11}H_9NO_4$ requires 219.0532).

3-Ethyl-5-nitroisoquinolin-1(2*H*)-one (132).

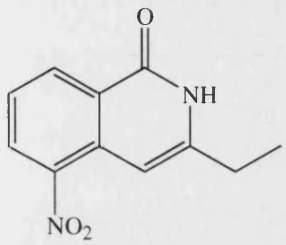

A solution of **(131)** (520 mg, 2.4 mmol) in 2-methoxyethanol (50 ml) was saturated with NH_3, boiled under reflux for 4 h, then evaporated until 10 ml remained. The concentrate was stored at 4°C for 16 h and the precipitated crystals were filtered, washed (H_2O, then EtOH) and recrystallised (MeOH) to give **(132)** (200 mg, 38%) as bright yellow crystals; R_f = 0.13 (hexane / EtOAc 4:1); mp (decomp.) 196-197°C; IR υ_{max} (KBr) 1372 & 1524 (NO_2), 1666 (C=O), 3432 (NH); ^{1}H NMR ($(CD_3)_2SO$) δ 1.22 (3 H, t, *J* = 7.5 Hz, CH_3), 2.59 (2 H, q, *J* = 7.5 Hz, CH_2), 6.80 (1 H, s, 4-H), 7.56 (1 H, t, *J* = 8.1 Hz, 7-H), 8.40 (1 H, dd, *J* = 8.1, 1.5 Hz, 6-H), 8.51 (1 H, dd, *J* = 8.1, 1.5 Hz, 8-H), 11.79 (1 H, br s, NH); MS (FAB +ve ion) *m/z* 219.0779 (M + H) ($^{12}C_{11}H_{11}N_2O_3$ requires 219.0770), 173 (M – NO_2).

5-Amino-3-ethylisoquinolin-1(2*H*)-one (133).

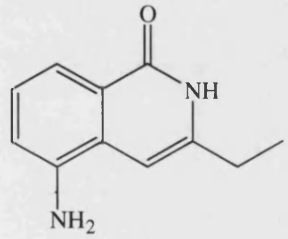

A mixture of **(132)** (200 mg, 0.9 mmol) and $SnCl_2$ (520 mg, 2.7 mmol) in EtOH (20 ml) was heated at 70°C for 4 h, then carefully poured into ice-H_2O (200 ml). The resulting suspension was made alkaline with aqueous NaOH and the precipitate was filtered. Extraction of the filtrate (EtOAc), evaporation and recrystallisation (hexane, EtOAc) gave **(133)** (40 mg, 24%) as yellow crystals; R_f = 0.50 (hexane / EtOAc 1:9); mp 162-163°C; IR υ_{max} (KBr) 1646 (C=O), 3164 & 3395 (NH_2), 3447 (NH); ^{1}H NMR ($(CD_3)_2SO$) δ 1.21 (3 H, t, *J* = 7.5 Hz, CH_3), 2.47 (2 H, q, *J* = 7.4 Hz, CH_2),

5.51 (2 H, br s, NH_2), 6.44 (1 H, d, *J* = 0.8 Hz, 4-H), 6.80 (1 H, dd, *J* = 7.8, 1.2 Hz, 6-H), 7.05 (1 H, t, *J* = 7.8 Hz, 7-H), 7.33 (1 H, ddd, *J* = 7.8, 1.2, 0.8 Hz, 8-H), 11.04 (1 H, br s, NH); MS (FAB +ve ion) *m/z* 189.1026 (M + H) ($^{12}C_{11}H_{13}N_2O$ requires 189.1028).

5-Amino-3-ethylisoquinolin-1(2*H*)-one hydrochloride (134).

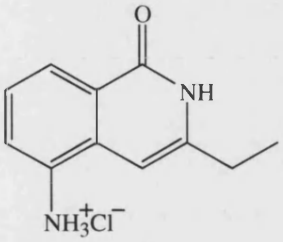

A mixture of **(133)** (40 mg, 0.2 mmol) and aqueous HCl (2 M, 20 ml) were stirred at room temperature for 30 min. Evaporation and recrystallisation (MeOH) yielded **(134)** (45 mg, 94%) as a brown solid; R_f = 0.74 (MeOH); mp 133-134°C; ^{1}H NMR ($(CD_3)_2SO$) δ 1.22 (3 H, t, *J* = 7.4 Hz, CH_3), 2.53 (2 H, q, *J* = 7.4 Hz, CH_2), 6.44 (1 H, s, 4-H), 7.34 (1 H, t, *J* = 7.8 Hz, 7-H), 7.47 (1 H, dd, *J* = 7.8, 1.2 Hz, 6-H), 7.91 (1 H, dd, *J* = 7.8, 1.2 Hz, 8-H), 11.41 (1 H, br s, NH).

8-Hydroxytridec-7-en-6-one (135a).

Tridecane-6,8-dione (135b).

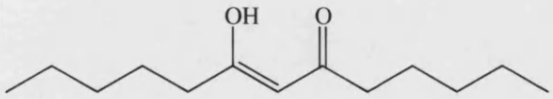

(135a)

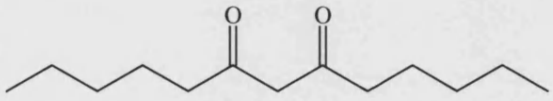

(135b)

To a solution of $NaNH_2$ (50% in toluene, 46.8 ml, 0.6 mol) in dry Et_2O (100 ml) was added, during 10 min, a solution of 2-heptanone (34.2 g, 0.3 mol) in dry Et_2O (50 ml). After stirring for 30 min, ethyl hexanoate (86.4 g, 0.6 mol) in dry Et_2O (50 ml) was slowly added. The mixture was boiled under reflux for 2 h, poured into H_2O

(300 ml), then neutralised with aqueous HCl (2 M). Extraction (Et_2O) and evaporation (Et_2O) yielded a residue which was dissolved in an equal volume of MeOH. To this methanolic solution was added a hot, filtered solution of $Cu(OAc)_2$ (40.0 g) in H_2O (350 ml) and the mixture was allowed to stand until it cooled to room temperature. The precipitated copper salt was filtered, washed with cold petroleum ether and shaken with a mixture of H_2SO_4 (10%, 300 ml) and Et_2O (100 ml) until the Et_2O layer was colourless. Evaporation of the organic layer yielded **(135a,b)** (4:1) (32.0 g, 50%) as a colourless oil; R_f = 0.44 (hexane / EtOAc 20:1); **(135a):** ^1H NMR ($CDCl_3$) δ 0.82-0.87 (6 H, m, 1,13-H_6), 1.19-1.33 (8 H, m, 2,3,11,12-H_8), 1.49-1.60 (4 H, m, 4,10-H_4), 2.22 (4 H, t, *J* = 7.6 Hz, 5,9-H_4), 5.43 (1 H, s, 7-H), 15.49 (1 H, br s, OH); **(135b):** ^1H NMR ($CDCl_3$) δ 0.82-0.87 (6 H, m, 1,13-H_6), 1.19-1.33 (8 H, m, 2,3,11,12-H_8), 1.49-1.60 (4 H, m, 4,10-H_4), 2.45 (4 H, t, *J* = 7.6 Hz, 5,9-H_4), 3.50 (2 H, s, 7-H); MS (EI +) *m/z* 212.1775 (M) ($^{12}C_{13}H_{24}O_2$ requires 212.1776), 141 (M – $(CH_2)_4CH_3$), 99 (M – $CH_2CO(CH_2)_4CH_3$).

5-Nitro-3-pentylisocoumarin (136).

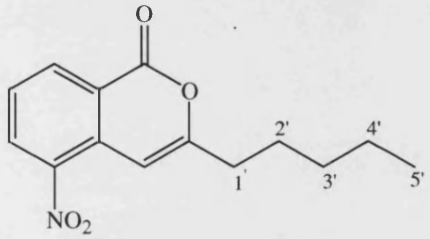

Method A:

To a stirred solution of nonane-2,4-dione (5.0 g, 32 mmol) and potassium *t*-butoxide (1.5 g, 13 mmol) in 2-methyl-2-propanol (50 ml) was added **(85)** (1.6 g, 6.5 mmol) and Cu powder (42 mg, 0.7 mmol). The mixture was boiled under reflux for 16 h, then poured into H_2O (350 ml) and acidified with aqueous HCl (2 M). Extraction (Et_2O), evaporation and chromatography (hexane / EtOAc 10:1) gave **(136)** (70 mg, 4%) as a yellow oil; R_f = 0.65 (hexane / EtOAc 15:1); IR υ_{max} (film) 1344 & 1530 (NO_2), 1646 (C=C), 1736 (C=O); ^1H NMR ($CDCl_3$) δ 0.90-0.94 (3 H, m, 5′-H_3), 1.35-1.40 (4 H, m, 3′,4′-H_4), 1.70-1.78 (2 H, m, 2′-H_2), 2.59 (2 H, t,

J = 7.8 Hz, 1′-H_2), 7.12 (1 H, d, J = 0.8 Hz, 4-H), 7.55 (1 H, t, J = 7.8 Hz, 7-H), 8.41 (1 H, dd, J = 7.8, 1.6 Hz, 6-H), 8.56 (1 H, ddd, J = 7.8, 1.6, 0.8 Hz, 8-H); ^{13}C NMR ($CDCl_3$) δ 13.96 (C-5′), 22.37 (C-4′), 26.61 (C-3′), 31.18 (C-2′), 34.20 (C-1′), 97.69 (C-4), 122.08 (C-3), 126.83 (C-7), 131.34 (C-6), 131.85 (C-10), 135.71 (C-8), 143.82 (C-9), 160.99 (C-5), 162.36 (C=O); MS (EI +) *m/z* 261.1002 (M) ($^{12}C_{14}H_{15}NO_4$ requires 261.1001).

Further elution yielded **(88)** (120 mg, 9%) as yellow crystals; data as above.

Method B:

To a stirred solution of **(135a)** and **(135b)** (31.8 g, 150 mmol) and potassium *t*-butoxide (6.8 g, 61 mmol) in 2-methyl-2-propanol (100 ml) was added **(85)** (7.4 g, 30 mmol) and Cu powder (190 mg, 3.0 mmol). The mixture was boiled under reflux for 16 h, then poured into H_2O (350 ml) and acidified with aqueous HCl (2 M). Extraction (Et_2O), evaporation and chromatography (hexane / EtOAc 4:1) gave **(136)** (2.8 g, 36%) as a yellow oil; data as above.

5-Nitro-3-pentylisoquinolin-1(2*H*)-one (137).

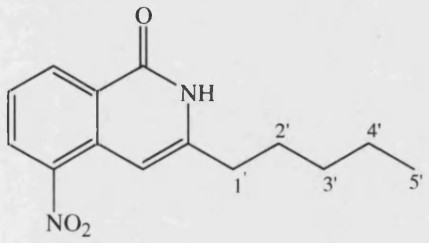

A solution of **(136)** (70 mg, 0.3 mmol) in 2-methoxyethanol (50 ml) was saturated with NH_3, boiled under reflux for 4 h, then evaporated until 10 ml remained. The concentrate was stored at 4°C for 16 h and the precipitated crystals were filtered, washed (H_2O, then EtOH) and recrystallised (MeOH) to give **(137)** (20 mg, 29%) as bright yellow crystals; R_f = 0.13 (hexane / EtOAc 4:1); mp (decomp.) 158-159°C; IR υ_{max} (KBr) 1375 & 1524 (NO_2), 1666 (C=O), 3467 (NH); ^{1}H NMR ($(CD_3)_2SO$) δ 0.86-0.89 (3 H, m, 5′-H_3), 1.28-1.34 (4 H, m, 3′,4′-H_4), 1.60-1.67 (2 H, m, 2′-H_2), 2.55 (2 H, t, J = 7.6 Hz, 1′-H_2), 6.79 (1 H, s, 4-H), 7.56 (1 H, t, J = 7.8 Hz, 7-H),

8.39 (1 H, dd, J = 7.8, 1.2 Hz, 6-H), 8.50 (1 H, dd, J = 7.8, 1.2 Hz, 8-H), 11.77 (1 H, br s, NH); MS (EI +) *m/z* 260.1162 (M) ($^{12}C_{14}H_{16}N_2O_3$ requires 260.1161).

5-Amino-3-pentylisoquinolin-1(2*H*)-one (138).

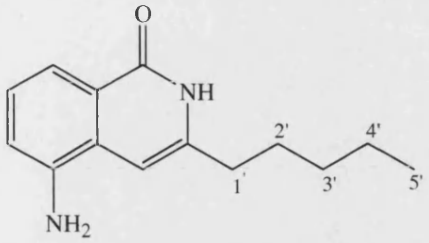

A mixture of **(137)** (240 mg, 0.9 mmol) and $SnCl_2$ (550 mg, 2.9 mmol) in EtOH (20 ml) was heated at 70°C for 4 h, then carefully poured into ice-H_2O (200 ml). The resulting suspension was made alkaline with aqueous NaOH and the precipitate was filtered. Extraction of the filtrate (EtOAc), evaporation and recrystallisation (hexane, EtOAc) gave **(138)** (140 mg, 67%) as yellow crystals; R_f = 0.30 (hexane / EtOAc 1:4); mp 75-76°C; IR υ_{max} (KBr) 1651 (C=O), 3166 & 3395 (NH_2), 3448 (NH); ^{1}H NMR ($CDCl_3$) δ 0.76-0.88 (3 H, m, 5′-H_3), 1.21-1.34 (4 H, m, 3′,4′-H_4), 1.66-1.78 (2 H, m, 2′-H_2), 2.57 (2 H, t, J = 7.6 Hz, 1′-H_2), 3.94 (2 H, br s, NH_2), 6.21 (1 H, s, 4-H), 6.92 (1 H, dd, J = 7.7, 1.2 Hz, 6-H), 7.20 (1 H, t, J = 7.7 Hz, 7-H), 7.84 (1 H, dd, J = 7.7, 1.2 Hz, 8-H), 11.75 (1 H, br s, NH); MS (EI +) *m/z* 230.1418 (M) ($^{12}C_{14}H_{18}N_2O$ requires 230.1419).

5-Amino-3-pentylisoquinolin-1(2*H*)-one hydrochloride (139).

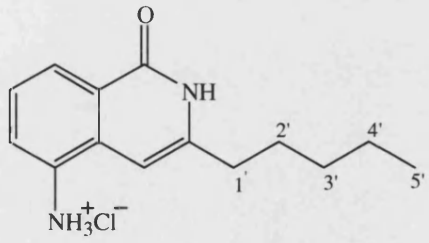

A mixture of **(138)** (130 mg, 0.6 mmol) and aqueous HCl (2 M, 20 ml) were stirred at room temperature for 30 min. Evaporation and recrystallisation (MeOH) yielded **(139)** (140 mg, 93%) as a brown solid; R_f = 0.83 (MeOH); mp 129-130°C;

^{1}H NMR (D_2O) δ 0.74-0.82 (3 H, m, 5′-H_3), 1.19-1.29 (4 H, m, 3′,4′-H_4), 1.55-1.66 (2 H, m, 2′-H_2), 2.55 (2 H, t, *J* = 7.6 Hz, 1′-H_2), 6.53 (1 H, s, 4-H), 7.49 (1 H, t, *J* = 7.8 Hz, 7-H), 7.74 (1 H, d, *J* = 7.8 Hz, 6-H), 8.20 (1 H, d, *J* = 7.8 Hz, 8-H).

6-Hydroxy-2,8-dimethylnon-5-en-4-one (140a).

2,8-Dimethylnonane-4,6-dione (140b).

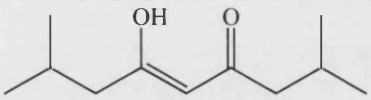

(140a)

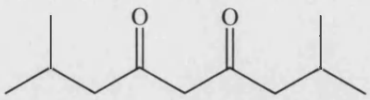

(140b)

To a solution of $NaNH_2$ (50% in toluene, 31.2 ml, 0.4 mol) in dry Et_2O (100 ml) was added, during 10 min, a solution of 4-methyl-2-pentanone (20.0 g, 0.2 mol) in dry Et_2O (50 ml). After stirring for 30 min, ethyl 2-methylbutanoate (52.0 g, 0.4 mol) in dry Et_2O (50 ml) was slowly added. The mixture was boiled under reflux for 2 h, poured into H_2O (300 ml), then neutralised with aqueous HCl (2 M). Extraction (Et_2O) and evaporation (Et_2O) yielded a residue which was dissolved in an equal volume of MeOH. To this methanolic solution was added a hot, filtered solution of $Cu(OAc)_2$ (40.0 g) in H_2O (350 ml) and the mixture was allowed to stand until it cooled to room temperature. The precipitated copper salt was filtered, washed with cold petroleum ether and shaken with a mixture of H_2SO_4 (10%, 300 ml) and Et_2O (100 ml) until the Et_2O layer was colourless. Evaporation of the organic layer yielded **(140a,b)** (10:1) (27.5 g, 75%) as a colourless oil; R_f = 0.53 (hexane / EtOAc 25:1); **(140a):** ^{1}H NMR ($CDCl_3$) δ 0.92 (12 H, d, *J* = 6.6 Hz, 1,9-H_6, 2 × CH_3), 2.01-2.08 (2 H, m, 2,8-H_2), 2.12 (4 H, d, *J* = 6.6 Hz, 3,7-H_4), 5.41 (1 H, s, 5-H), 15.58 (1 H, br s, OH); **(140b):** ^{1}H NMR ($CDCl_3$) δ 0.90 (12 H, d, *J* = 6.6 Hz, 1,9-H_6, 2 × CH_3), 2.01-2.08 (2 H, m, 2,8-H_2), 2.36 (4 H, d, *J* = 6.6 Hz, 3,7-H_4), 3.49 (2 H, s, 5-H); MS (EI +) *m/z* 184.1459 (M) ($^{12}C_{11}H_{20}O_2$ requires 184.1463), 127 (M – $CH_2CH(CH_3)_2$), 85 (M – $CH_2COCH_2CH(CH_3)_2$).

3-(2-Methylpropyl)-5-nitroisocoumarin (141).

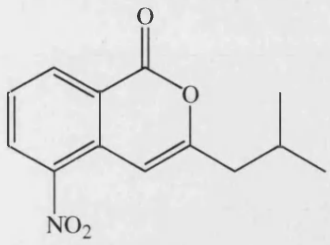

To a stirred solution of **(140a)** and **(140b)** (17.4 g, 94.6 mmol) and potassium *t*-butoxide (4.4 g, 39 mmol) in 2-methyl-2-propanol (100 ml) was added **(85)** (4.7 g, 19 mmol) and Cu powder (123 mg, 1.9 mmol). The mixture was boiled under reflux for 16 h, then poured into H_2O (350 ml) and acidified with aqueous HCl (2 M). Extraction (Et_2O), evaporation and chromatography (hexane / EtOAc 4:1) gave **(141)** (1.2 g, 26%) as yellow crystals; R_f = 0.61 (hexane / EtOAc 1:4); mp 71-72°C; IR υ_{max} (KBr) 1346 & 1531 (NO_2), 1645 (C=C), 1737 (C=O); ^{1}H NMR ($CDCl_3$) δ 0.99 (6 H, d, *J* = 6.6 Hz, 2 × CH_3), 2.12-2.19 (1 H, m, CH_2CH), 2.45 (2 H, d, *J* = 7.4 Hz, CH_2CH), 7.09 (1 H, s, 4-H), 7.55 (1 H, t, *J* = 8.2 Hz, 7-H), 8.40 (1 H, dd, *J* = 8.2, 1.2 Hz, 6-H), 8.54 (1 H, dd, *J* = 8.2, 1.2 Hz, 8-H); MS (EI +) *m/z* 247.0848 (M) ($^{12}C_{13}H_{13}NO_4$ requires 247.0845).

5-Nitro-3-(2-methylpropyl)isoquinolin-1(2*H*)-one (142).

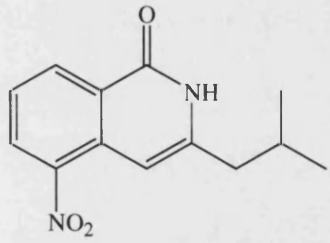

A solution of **(141)** (620 mg, 2.5 mmol) in 2-methoxyethanol (50 ml) was saturated with NH_3, boiled under reflux for 4 h, then evaporated until 10 ml remained. The concentrate was stored at 4°C for 16 h and the precipitated crystals were filtered, washed (H_2O, then EtOH) and recrystallised (MeOH) to give **(142)** (550 mg, 89%) as bright yellow crystals; R_f = 0.74 (hexane / EtOAc 1:4); mp 184-185°C; IR υ_{max} (KBr) 1376 & 1523 (NO_2), 1655 (C=O), 3436 (NH); ^{1}H NMR ($(CD_3)_2SO$) δ 0.91 (6 H, d,

J = 6.6 Hz, 2 × CH_3), 1.97-2.04 (1 H, m, CH_2CH), 2.43 (2 H, d, J = 7.0 Hz, CH_2CH), 6.77 (1 H, s, 4-H), 7.56 (1 H, t, J = 7.8 Hz, 7-H), 8.40 (1 H, dd, J = 7.8, 1.2 Hz, 6-H), 8.50 (1 H, dd, J = 7.8, 1.2 Hz, 8-H), 11.76 (1 H, br s, NH); MS (EI +) *m/z* 246.1003 (M) ($^{12}C_{13}H_{14}N_2O_3$ requires 246.1004).

5-Amino-3-(2-methylpropyl)isoquinolin-1(2*H*)-one (143).

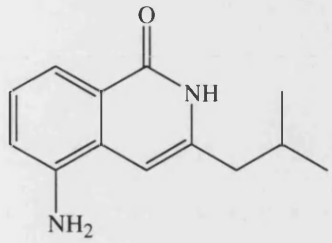

A mixture of **(142)** (370 mg, 1.5 mmol) and $SnCl_2$ (900 mg, 4.7 mmol) in EtOH (20 ml) was heated at 70°C for 4 h, then carefully poured into ice-H_2O (200 ml). The resulting suspension was made alkaline with aqueous NaOH and the precipitate was filtered. Extraction of the filtrate (EtOAc), evaporation and recrystallisation (hexane, EtOAc) gave **(143)** (270 mg, 83%) as yellow crystals; R_f = 0.58 (hexane / EtOAc 1:4); mp 113-114°C; IR υ_{max} (KBr) 1645 (C=O), 3165 & 3396 (NH_2), 3468 (NH); ^{1}H NMR ($CDCl_3$) δ 0.82 (6 H, d, J = 6.4 Hz, 2 × CH_3), 1.90-2.02 (1 H, m, CH_2CH), 2.32 (2 H, d, J = 7.4 Hz, CH_2CH), 3.99 (2 H, br s, NH_2), 6.14 (1 H, s, 4-H), 6.84 (1 H, dd, J = 7.9, 1.2 Hz, 6-H), 7.10 (1 H, t, J = 7.9 Hz, 7-H), 7.71 (1 H, dd, J = 7.9, 1.2 Hz, 8-H), 11.52 (1 H, br s, NH); MS (EI +) *m/z* 216.1263 (M) ($^{12}C_{13}H_{16}N_2O$ requires 216.1263).

5-Amino-3-(2-methylpropyl)isoquinolin-1(2*H*)-one hydrochloride (144).

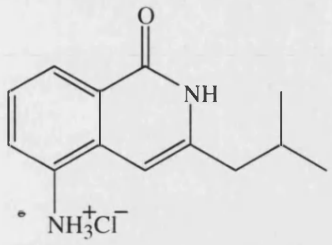

A mixture of **(143)** (220 mg, 1.0 mmol) and aqueous HCl (2 M, 20 ml) were stirred at room temperature for 30 min. Evaporation and recrystallisation (MeOH) yielded **(144)** (250 mg, 97%) as a brown solid; R_f = 0.76 (MeOH); mp 151-152°C; ^{1}H NMR (D_2O) δ 0.88 (6 H, d, *J* = 6.6 Hz, 2 × CH_3), 1.89-1.93 (1 H, m, CH_2CH), 2.47 (2 H, d, *J* = 7.4 Hz, CH_2CH), 6.52 (1 H, s, 4-H), 7.50 (1 H, t, *J* = 7.9 Hz, 7-H), 7.76 (1 H, d, *J* = 7.9 Hz, 6-H), 8.22 (1 H, d, *J* = 7.9 Hz, 8-H).

4-Hydroxy-1,5-diphenylpent-3-en-2-one (145a).

1,5-Diphenyl-2,4-pentanedione (145b).

Ethyl 2,4-diphenylacetoacetate (146).

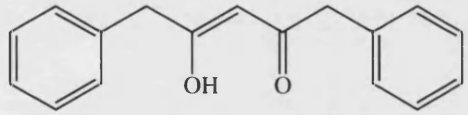

(145a)

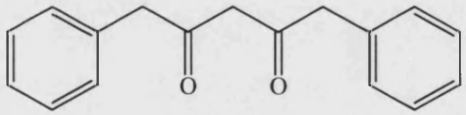

(145b)

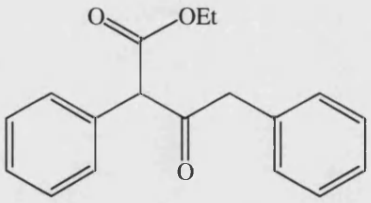

(146)

To a solution of $NaNH_2$ (50% in toluene, 31.2 ml, 0.4 mol) in dry Et_2O (100 ml) was added, during 10 min, a solution of 3-phenyl-2-propanone (26.8 g, 0.2 mol) in dry Et_2O (50 ml). After stirring for 30 min, ethyl phenylacetate (65.6 g, 0.4 mol) in dry Et_2O (50 ml) was slowly added. The mixture was boiled under reflux for 2 h, poured into H_2O (300 ml), then neutralised with aqueous HCl (2 M). Extraction (Et_2O) and

evaporation (Et_2O) yielded a residue which was dissolved in an equal volume of MeOH. To this methanolic solution was added a hot, filtered solution of $Cu(OAc)_2$ (40.0 g) in H_2O (350 ml) and the mixture was allowed to stand until it cooled to room temperature. The precipitated copper salt was filtered, washed with cold petroleum ether and shaken with a mixture of H_2SO_4 (10%, 300 ml) and Et_2O (100 ml) until the Et_2O layer was colourless. Evaporation and recrystallisation (hexane, EtOAc) yielded **(145a,b)** (50:1) (12.9 g, 26%) as orange crystals; R_f = 0.50 (hexane / CH_2Cl_2 1:1); mp 68-69°C (lit.[212] mp 65.2-66.5°C); **(145a):** ^{1}H NMR ($CDCl_3$) δ 3.56 (4 H, s, 1,5-H_4), 5.43 (1 H, s, 3-H), 7.18-7.32 (10 H, m, 2 × Ph-H_5), 15.27 (1 H, br s, OH); **(145b):** ^{1}H NMR ($CDCl_3$) δ 3.55 (2 H, s, 3-H_2), 3.68 (4 H, s, 1,5-H_4), 7.11-7.27 (10 H, m, 2 × Ph-H_5); MS (EI +) *m/z* 252.1144 (M) ($^{12}C_{17}H_{16}O_2$ requires 252.1150), 161 (M – CH_2Ph), 133 (M – $COCH_2Ph$).

Also isolated was the Claisen condensation product **(146)** (23.4 g, 41%) as colourless crystals; R_f = 0.43 (hexane / CH_2Cl_2 1:1); mp 76-78°C (lit.[213] mp 75°C); IR υ_{max} (KBr) 1715 (ketone C=O), 1734 (ester C=O); ^{1}H NMR ($CDCl_3$) δ 1.22 (3 H, t, *J* = 7.1 Hz, CH_2CH_3), 3.74 (2 H, s, 4-H_2), 4.17 (2 H, q, *J* = 7.1 Hz, CH_2CH_3), 4.81 (1 H, s, 2-H), 7.05-7.39 (10 H, m, 2 × Ph-H_5); MS (EI +) *m/z* 282.1255 (M) ($^{12}C_{18}H_{18}O_3$ requires 282.1256).

3-Benzyl-5-nitroisocoumarin (147).

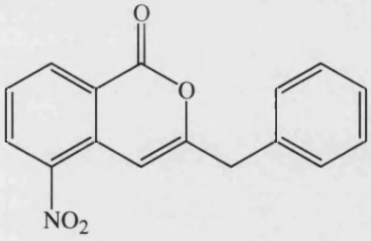

To a stirred solution of **(145a)** and **(145b)** (7.5 g, 33 mmol) and potassium *t*-butoxide (1.3 g, 12 mmol) in 2-methyl-2-propanol (100 ml) was added **(85)** (1.5 g, 6.1 mmol) and Cu powder (40 mg, 0.6 mmol). The mixture was boiled under reflux for 16 h, then poured into H_2O (350 ml) and acidified with aqueous HCl (2 M). Extraction (Et_2O), evaporation and chromatography (hexane / EtOAc 9:1) gave

(147) (540 mg, 32%) as yellow crystals; R_f = 0.44 (hexane / EtOAc 4:1); mp 137-138°C; IR υ_{max} (KBr) 1346 & 1564 (NO_2), 1647 (C=C), 1740 (C=O); ^{1}H NMR ($CDCl_3$) δ 3.88 (2 H, s CH_2), 7.13 (1 H, d, *J* = 0.5 Hz, 4-H), 7.24-7.36 (5 H, m, 2′,3′,4′,5′,6′-H_5), 7.54 (1 H, t, *J* = 8.0 Hz, 7-H), 8.39 (1 H, dd, *J* = 8.0, 1.4 Hz, 6-H), 8.53 (1 H, ddd, *J* = 8.0, 1.4, 0.5 Hz, 8-H); MS (EI +) *m/z* 281.0690 (M) ($^{12}C_{16}H_{11}NO_4$ requires 281.0688), 190 (M – CH_2Ph).

3-Benzyl-5-nitroisoquinolin-1(2*H*)-one (148).

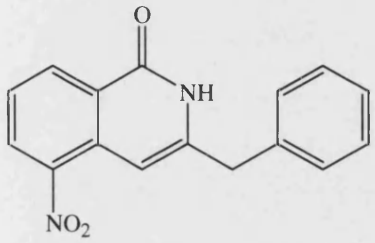

A solution of **(147)** (340 mg, 1.2 mmol) in 2-methoxyethanol (50 ml) was saturated with NH_3, boiled under reflux for 4 h, then evaporated until 10 ml remained. The concentrate was stored at 4°C for 16 h and the precipitated crystals were filtered, washed (H_2O, then EtOH) and recrystallised (MeOH) to give **(148)** (280 mg, 83%) as bright yellow crystals; R_f = 0.73 (hexane / EtOAc 1:4); mp (decomp.) 203-204°C; IR υ_{max} (KBr) 1323 & 1524 (NO_2), 1645 (C=C), 1688 (C=O), 3186 (NH); ^{1}H NMR ($(CD_3)_2SO$) δ 3.92 (2 H, s CH_2), 6.80 (1 H, s, 4-H), 7.24–7.34 (5 H, m, 2′,3′,4′,5′,6′-H_5), 7.57 (1 H, t, *J* = 7.8 Hz, 7-H), 8.39 (1 H, d, *J* = 7.8 Hz, 6-H), 8.49 (1 H, d, *J* = 7.8 Hz, 8-H), 11.93 (1 H, br s, NH); MS (EI +) *m/z* 280.0848 (M) ($^{12}C_{16}H_{12}N_2O_3$ requires 280.0848).

5-Amino-3-benzylisoquinolin-1(2*H*)-one (149).

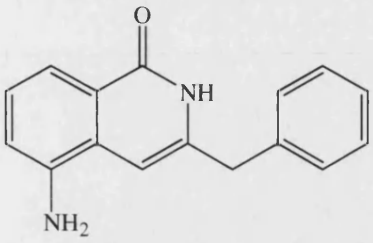

A mixture of **(148)** (280 mg, 1.0 mmol) and $SnCl_2$ (530 mg, 2.8 mmol) in EtOH (20 ml) was heated at 70°C for 4 h, then carefully poured into ice-H_2O (200 ml). The resulting suspension was made alkaline with aqueous NaOH and the precipitate was filtered. Extraction of the filtrate (EtOAc), evaporation and recrystallisation (hexane, EtOAc) gave **(149)** (160 mg, 64%) as yellow crystals; R_f = 0.53 (hexane / EtOAc 1:4); mp 85-86°C; IR υ_{max} (KBr) 1661 (C=O), 3162 & 3394 (NH_2), 3469 (NH); ^{1}H NMR ($CDCl_3$) δ 3.91 (2 H, s CH_2), 4.00 (2 H, br s, NH_2), 6.72 (1 H, d, *J* = 8.1 Hz, 6-H), 6.86 (1 H, s, 4-H), 6.91 (1 H, t, *J* = 8.1 Hz, 7-H), 7.17–7.43 (5 H, m, 2′,3′,4′,5′,6′-H_5), 7.83 (1 H, d, *J* = 8.1 Hz, 8-H), 10.94 (1 H, br s, NH); MS (EI +) *m/z* 250.1100 (M) ($^{12}C_{16}H_{14}N_2O$ requires 250.1106).

Amino-3-benzylisoquinolin-1(2*H*)-one hydrochloride (150).

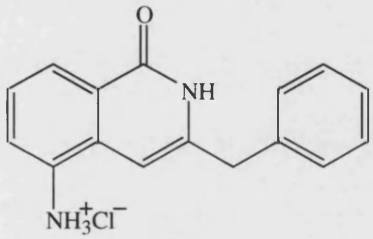

A mixture of **(149)** (150 mg, 0.6 mmol) and aqueous HCl (2 M, 20 ml) were stirred at room temperature for 30 min. Evaporation and recrystallisation (MeOH) yielded **(150)** (160 mg, 93%) as a dark brown solid; R_f = 0.60 (MeOH); mp >350°C; ^{1}H NMR (D_2O) δ 3.94 (2 H, s CH_2), 6.49 (1 H, s, 4-H), 7.25–7.37 (5 H, m, 2′,3′,4′,5′,6′-H_5), 7.51 (1 H, t, *J* = 7.8 Hz, 7-H), 7.73 (1 H, d, *J* = 7.8 Hz, 6-H), 8.23 (1 H, d, *J* = 7.8 Hz, 8-H).

Methyl 2-methyl-3-nitrobenzoate (154).

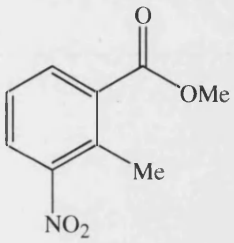

A solution of 2-methyl-3-nitrobenzoic acid (10.0 g, 55.2 mmol) in MeOH (200 ml) and concentrated H_2SO_4 (1 ml) was boiled under reflux for 48 h, then poured into ice-H2O (300 ml). The precipitated ester was filtered, washed (H_2O) and recrystallised (MeOH) to give **(154)** (9.7 g, 90%) as yellow crystals; R_f = 0.55 (hexane / EtOAc 4:1); mp 65-66°C (lit.[215] mp 64.2-65.5°C); IR υ_{max} (KBr) 1352 & 1548 (NO_2), 1724 (C=O); ^{1}H NMR ($CDCl_3$) δ 2.53 (3 H, s, $ArCH_3$), 3.87 (3 H, s, CO_2CH_3), 7.30 (1 H, t, *J* = 8.2 Hz, 5-H), 7.74 (1 H, dd, *J* = 8.2, 1.2 Hz, 4-H), 7.89 (1 H, dd, *J* = 8.2, 1.2 Hz, 6-H); MS (EI +) *m/z* 195.0535 (M) ($^{12}C_9H_9NO_4$ requires 195.0532).

5-Nitroisocoumarin (155).

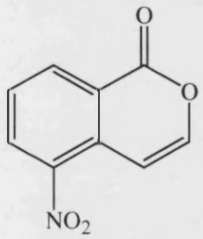

The ester **(154)** (5.0 g, 25.6 mmol) was heated with dimethylformamide dimethyl acetal (2.5 g, 21 mmol) in DMF (30 ml) at 150°C for 16 h. Evaporation, chromatography (hexane / EtOAc 10:1) and recrystallisation (EtOH) gave **(155)** (2.6 g, 53%) as yellow crystals; R_f = 0.34 (hexane / EtOAc 10:1); mp 171-172°C; ^{1}H NMR ($CDCl_3$) δ 7.39 (1 H, dd, *J* = 6.0, 0.5 Hz, 4-H), 7.44 (1 H, dd, *J* = 6.0 Hz, 3-H), 7.68 (1 H, t, *J* = 8.0 Hz, 7-H), 8.50 (1 H, dd, *J* = 8.0, 1.3 Hz, 6-H), 8.64 (1 H, ddd, *J* = 8.0, 1.3, 0.5 Hz, 8-H); MS (EI +) *m/z* 191.1220 (M) ($^{12}C_9H_5NO_4$ requires 191.0219).

Methyl 2-bromomethyl-3-nitrobenzoate (156)

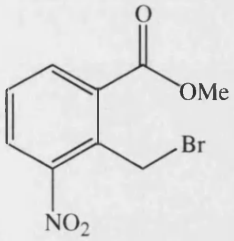

A solution of Br_2 (11.8 g, 73.7 mmol) in CCl_4 (30 ml) was added over 30 min to a boiling solution of **(154)** (11.5 g, 59.0 mmol) and dibenzoyl peroxide (1.1 g, 4.5 mmol) in CCl_4 (100 ml) under irradiation using a 150 W tungsten lamp. After 20 h, additional Br_2 (0.9 ml, 17 mmol) and dibenzoyl peroxide (240 mg, 1.0 mmol) in CCl_4 (10 ml) was added. Heating and irradiation were continued for another 29 h. Evaporation and recrystallisation (MeOH) gave **(156)** (15.9 g, 98%) as pale brown crystals; R_f = 0.40 (hexane / EtOAc 4:1); mp 68-69°C (lit.[216] mp 68-69°C); IR υ_{max} (KBr) 1271 & 1530 (NO_2), 1722 (C=O); ^{1}H NMR ($CDCl_3$) δ 3.98 (3 H, s, CH_3), 5.14 (2 H, s, CH_2), 7.52 (1 H, t, *J* = 7.9 Hz, 5-H), 7.94 (1 H, d, *J* = 7.9 Hz, 4-H), 8.09 (1 H, d, *J* = 7.9 Hz, 6-H); MS (EI +) *m/z* 274.9612 (M) ($^{12}C_9H_8{}^{81}BrNO_4$ requires 274.9607); 272.9641 (M) ($^{12}C_9H_8{}^{79}BrNO_4$ requires 272.9637).

Methyl 2-cyanomethyl-3-nitrobenzoate (157).

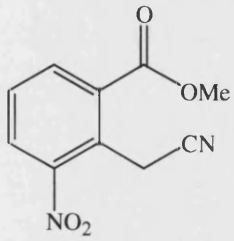

To a solution of **(156)** (7.0 g, 25 mmol) in acetonitrile (100 ml) was added tetraethylammonium cyanide (4.8 g, 31 mmol) and the mixture was stirred at room temperature for 4 h. Evaporation and chromatography (Et_2O / heptane 1:1) yielded **(157)** (3.8 g, 68%) as pale yellow crystals; R_f = 0.17 (Et_2O / heptane 1:1); mp 93-94°C (lit.[217] mp 95.5-96°C); IR υ_{max} (KBr) 1353 & 1538 (NO_2), 1728 (C=O), 2265 (CN); ^{1}H NMR ($CDCl_3$) δ 4.01 (3 H, s, CO_2CH_3), 4.35 (2 H, s, CH_2),

7.62 (1 H, t, J = 8.2 Hz, 5-H), 8.12 (1 H, dd, J = 8.2, 1.2 Hz, 4-H), 8.27 (1 H, dd, J = 8.2, 1.2 Hz, 6-H); MS (EI +) *m/z* 220.0489 (M) ($^{12}C_{10}H_8N_2O_4$ requires 220.0484).

2-(Dimethylaminomethyl)-3-nitro-*N,N*-dimethylbenzamide (158).

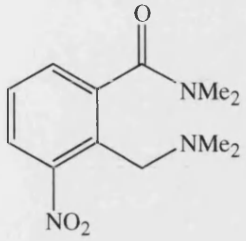

A solution of **(156)** (2.7 g, 9.9 mmol) and dimethylformamide dimethyl acetal (4.2 g, 35 mmol) in DMF (20 ml) was heated at 150°C for 16 h. Evaporation and chromatography (hexane / EtOAc 9:1) gave **(158)** (940 mg, 38%) as orange oil; R_f = 0.40 (hexane / EtOAc 9:1); IR υ_{max} (film) 1364 & 1537 (NO_2), 1629 (C=O); ^{1}H NMR ($CDCl_3$) δ 2.15 (6 H, s, $CH_2N(CH_3)_2$), 2.82 (3 H, s, NCH_3), 3.11 (3 H, s, NCH_3), 3.40 (1 H, d, J = 13.4 Hz) and 3.80 (1 H, d, J = 13.4 Hz) (CH_2), 7.34 (1 H, dd, J = 7.7, 1.5 Hz, 6-H), 7.39 (1 H, t, J = 7.7 Hz, 5-H), 7.62 (1 H, dd, J = 7.7, 1.5 Hz, 4-H); MS (EI +) *m/z* 251.1271 (M) ($^{12}C_{12}H_{17}N_3O_3$ requires 251.1270).

Methyl 2-[1-cyano-(*N,N*-Dimethyl)ethenamine]-3-nitrobenzoate (159).

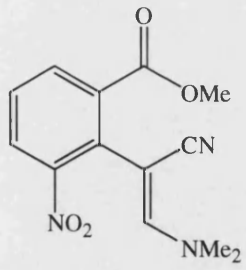

Compound **(157)** (550 mg, 2.5 mmol) was heated with dimethylformamide dimethyl acetal (1.1 g, 9.2 mmol) in DMF (10 ml) at 150°C for 16 h. Evaporation and chromatography (hexane / EtOAc 2:3) gave **(159)** (160 mg, 23%) as orange crystals; R_f = 0.47 (hexane / EtOAc 2:3); mp 87-88°C; IR υ_{max} (KBr) 1362 & 1537 (NO_2), 1631 (C=C), 1728 (C=O), 2195 (CN); ^{1}H NMR ($CDCl_3$) δ 3.17 (6 H, s, 2 × NCH_3),

3.95 (3 H, s, CO_2CH_3), 6.34 (1 H, s, CH), 7.45 (1 H, t, *J* = 7.8 Hz, 5-H), 7.76 (1 H, dd, *J* = 7.8, 1.6 Hz, 4-H), 7.91 (1 H, dd, *J* = 7.8, 1.6 Hz, 6-H); MS (EI +) *m/z* 275.0902 (M) ($^{12}C_{13}H_{13}N_3O_4$ requires 275.0906).

5-Nitroisoquinolin-1(*2H*)-one (160).

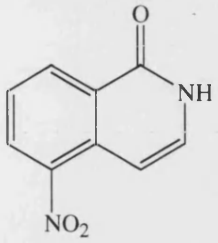

Method A:

A solution of **(155)** (1.5 g, 7.9 mmol) in 2-methoxyethanol (100 ml) was saturated with NH_3 and boiled under reflux for 4 h, then evaporated until 10 ml remained. The concentrate was stored at 4°C for 16 h and the precipitated crystals were filtered, washed (H_2O, then EtOH) and recrystallised (MeOH) to give **(160)** (1.1 g, 73%) as yellow crystals; R_f = 0.49 (hexane / EtOAc 2:3); mp (decomp.) 247-249°C; ^{1}H NMR ($(CD_3)_2SO$) δ 6.97 (1 H, dd, *J* = 7.7, 0.7 Hz, 4-H), 7.45 (1 H, dd, *J* = 7.7, 1.8 Hz, 3-H), 7.66 (1 H, t, *J* = 7.7 Hz, 7-H), 8.46 (1 H, dd, *J* = 7.7, 1.5 Hz, 6-H), 8.58 (1 H, ddd, *J* = 7.7, 1.5, 0.7 Hz, 8-H), 11.80 (1 H, br s, NH); MS (EI +) *m/z* 190.0383 (M) ($^{12}C_9H_6N_2O_3$ requires 190.0378).

Method B:

DIBAL-H (1.0 M in hexane, 7.5 ml, 7.5 mmol) was added dropwise to a solution of **(157)** (1.1 g, 5.0 mmol) in dry CH_2Cl_2 (50 ml) at -78°C and the solution was stirred for 1 h. Aqueous HCl (2 M, 35 ml) was then added the solution was extracted with CH_2Cl_2. Evaporation and chromatography (hexane / EtOAc 2:3) afforded **(160)** (220 mg, 23%) as yellow crystals; data as above.

Methyl 2-benzyl-3-nitrobenzoate (161).

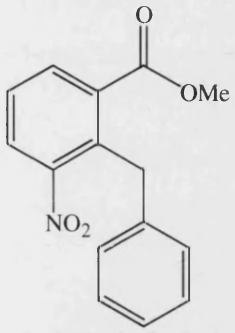

A mixture of **(68)** (2.5 g, 8.1 mmol) and benzyl zinc bromide (0.5 M in THF, 24.5 ml, 12.2 mmol) in dry THF (30 ml) was added to $(PPh_3)_2PdCl_2$ (330 mg, 500 μmol) and DIBAL-H (1.0 M in hexane, 1.0 ml, 1.0 mmol) in dry THF (15 ml) under Ar and the mixture was stirred at 45°C for 72 h. Extraction ($CHCl_3$), evaporation and chromatography (hexane / EtOAc 9:1) afforded **(161)** (700 mg, 32%) as a yellow oil; R_f = 0.53 (hexane / EtOAc 9:1); IR υ_{max} (film) 1362 & 1532 (NO_2), 1731 (C=O); ^{1}H NMR ($CDCl_3$) δ 3.77 (3 H, s, CH_3), 4.52 (2 H, s, CH_2), 7.01-7.04 (2 H, m, 2′,6′-H_2), 7.12-7.23 (3 H, m, 3′,4′,5′-H_3), 7.42 (1 H, t, *J* = 7.8 Hz, 5-H), 7.81 (1 H, dd, *J* = 7.8, 1.6 Hz, 4-H), 7.95 (1 H, dd, *J* = 7.8, 1.6 Hz, 6-H); MS (FAB +ve ion) *m/z* 272.0921 (M + H) ($^{12}C_{15}H_{14}NO_4$ requires 272.0923), 240 (M – OMe), 195 (M – Ph).

5-Aminoisoquinolin-1 (*2H*)-one (23d).

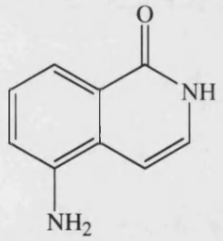

A mixture of **(160)** (190 mg, 1.0 mmol) and $SnCl_2$ (600 mg, 3.2 mmol) in EtOH (30 ml) was heated at 70°C for 4 h, then carefully poured into ice-H_2O (200 ml). The resulting suspension was made alkaline with aqueous NaOH and the precipitate was filtered. Extraction of the filtrate (EtOAc), evaporation and recrystallisation (hexane, EtOAc) gave **(23d)** (98 mg, 61%) as yellow crystals; R_f = 0.79 (hexane / EtOAc 1:4); mp 249-250°C; ^{1}H NMR ($(CD_3)_2SO$) δ 5.59 (2 H, br s, NH_2), 6.65 (1 H, d,

J = 7.0 Hz, 4-H), 6.83 (1 H, d, J = 7.8 Hz, 6-H), 7.00 (1 H, d, J = 7.0 Hz, 3-H), 7.12 (1 H, t, J = 7.8 Hz, 7-H), 7.36 (1 H, d, J = 7.8 Hz, 8-H), 11.04 (1 H, br s, NH); MS (EI +) *m/z* 160.0639 (M) ($^{12}C_9H_8N_2O$ requires 160.0637).

5-[(*N,N*-Dimethylamino)methyleneamino]isoquinolin-1(2*H*)-one (163).

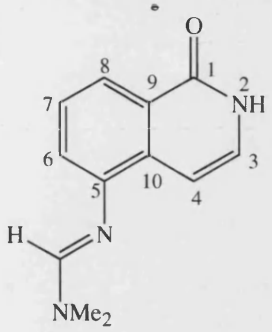

A solution of **(23d)** (900 mg, 5.6 mmol) in dry DMF (15 ml) was stirred with dimethylformamide dimethyl acetal (3.7 g, 31 mmol) under N_2 at 45°C for 3 h. Evaporation and chromatography (CH_2Cl_2 / MeOH / NMe_3 95:5:0.5) gave **(163)** (1.0 g, 83%) as yellow crystals; R_f = 0.47 (hexane / EtOAc 4:1); mp 195-196°C; IR υ_{max} (KBr) 1634 (C=O), 3410 (NH); ^{1}H NMR ($CDCl_3$) δ 3.05 (3 H, s, NCH_3), 3.08 (3 H, s, NCH_3), 7.05 (1 H, dd, J = 7.8, 0.8 Hz, 6-H), 7.14 (2 H, s, 3-H, 4-H), 7.35 (1 H, t, J = 7.8 Hz, 7-H), 7.52 (1 H, s, N=CH), 8.05 (1 H, dd, J = 7.8, 0.8 Hz, 8-H), 12.00 (1 H, br s, NH); ^{13}C NMR ($CDCl_3$) δ 34.95 (NCH_3), 40.63 (NCH_3), 103.74 (C-4), 120.76 (C-6), 121.00 (C-8), 126.50 (C-3), 126.81 (C-10), 127.24 (C-7), 133.79 (C-9), 148.18 (C-5), 153.23 (C=N), 164.88 (C=O); MS (EI +) *m/z* 215.1057 (M) ($^{12}C_{12}H_{13}N_3O$ requires 215.1059), 158 (M – $CHNMe_2$).

5-[(*N*,*N*-Dimethylamino)methyleneamino]isoquinolin-1(2*H*)-one hydrochloride (164).

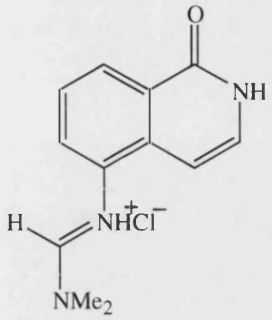

A mixture of **(163)** (1.0 g, 4.7 mmol) and aqueous HCl (2 M, 15 ml) was stirred at room temperature for 5 min. Evaporation and recrystallisation (MeOH) yielded **(164)** (1.1 g, 94%) as orange crystals; R_f = 0.50 (hexane / EtOAc 1:4); mp 154-155°C; ^{1}H NMR (D_2O) δ 3.27 (3 H, s, NCH_3), 3.36 (3 H, s, NCH_3), 6.62 (1 H, d, *J* = 7.4 Hz, 4-H), 7.06 (1 H, d, *J* = 7.4 Hz, 3-H), 7.30 (1 H, t, *J* = 7.8 Hz, 7-H), 7.49 (1 H, dd, *J* = 7.8, 1.2 Hz, 6-H), 7.79 (1 H, dd, *J* = 7.8, 1.2 Hz, 8-H), 8.14 (1 H, s, N=CH).

1-Phenyl-1-(trimethylsilyloxy)ethylene (165).

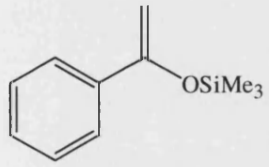

Acetophenone (5.0 ml, 43 mmol) was added dropwise to a mixture of DIPA (6.5 ml, 46 mmol) and n-butyllithium (18.5 ml, 46 mmol, 2.5 M in hexane) in THF (80 ml) at –78°C and the mixture was allowed to stir at that temperature for 2 h. Chlorotrimethylsilane (6 ml, 47 mmol) was then added and the mixture was allowed to stir at room temperature for 6 h. Evaporation and chromatography (hexane / EtOAc 10:1) gave **(165)** (7.6 g, 92%) as a colourless oil; R_f = 0.90 (hexane / EtOAc 4:1); lit.[225] bp 53-54 (0.3 torr); ^{1}H NMR ($CDCl_3$) δ 0.38 (9 H, s, $Si(CH_3)_3$), 4.54 (1 H, d, *J* = 1.7 Hz, 2-H), 5.02 (1 H, d, *J* = 1.7 Hz, 2-H), 7.35-7.45

(3 H, m, 3′,4′,5′-H_3), 7.67-7.74 (2 H, m, 2′,6′-H_2); MS (EI +) *m/z* 192.0963 (M) ($^{12}C_{11}H_{16}OSi$ requires 192.0970), 103 (M – $OSiMe_3$).

1-methoxy-3-(*N,N*-dimethylamino)-5-nitronaphthalene (167).

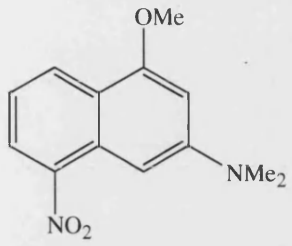

Ester **(154)** (1.01 g, 5.2 mmol) was heated at 150°C with $MeC(OMe)_2NMe_2$ (2.5 g, 19 mmol) in $MeCONMe_2$ (6 ml) for 16 h. Evaporation and chromatography (hexane / EtOAc 10:1) gave **(167)** (990 mg, 77%) as dark red needles; R_f = 0.50 (hexane / EtOAc 1:4); mp 123-124°C; IR υ_{max} (KBr) 1343 and 1522 (NO_2); ^{1}H NMR ($CDCl_3$) δ 3.13 (6 H, s, NMe_2), 4.00 (3 H, s, OMe), 6.48 (1 H, d, *J* = 2.3 Hz, 2-H), 7.11 (1 H, dd, *J* = 8.2, 7.8 Hz, 7-H), 7.37 (1 H, d, *J* = 2.3 Hz, 4-H), 8.24 (1 H, dd, *J* = 7.8, 1.2 Hz, 8-H), 8.37 (1 H, dd, *J* = 8.2, 1.2 Hz, 6-H); MS (EI +) *m/z* 246.1006 (M) ($^{12}C_{13}H_{14}N_2O_3$ requires 246.1004); Anal. Calcd. for $C_{13}H_{14}N_2O_3$: C, 63.41; H, 5.69; N, 11.38. Found: C, 63.4; H, 5.72; N, 11.4.

References

1. S. Shall, *Adv. Radiat. Biol.* 1984, **11**, 1.

2. K. Ueda, M. Kawaichi and O. Hayaishi, In *ADP-Ribosylation Reactions*, eds. O. Hayaishi and K. Ueda, Academic Press, New York, 1982.

3. S. Shall and G. de Murcia, *Mutat. Res.*, 2002, **460**, 1.

4. J. E. Cleaver and W. E. Morgan, *Mutat. Res.*, 1991, **257**, 1.

5. T. Eki, *FEBS Lett.*, 1994, **356**, 261.

6. A. Nishio, S. Nakanishi, J. Doull and E. M. Uyeki, *Biochem. Biophys. Res. Commun.*, 1983, **111**, 750.

7. S. Yamagoe, T. Kohda and M. Oishi, *Mol. Cell Biol.*, 1991, **11**, 3522.

8. C. Szabo, In *Cell Death: the Role of PARP*, ed. C. Szabo, CRC Press, Boca Raton, 2002.

9. C. Szabo, L. Virag, S. Cuzzocrea, G. S. Scott, P. Hake, M. P. O'Connor, B. Zingarelli, A. Salzman and E. Kun, *Proc. Natl. Acad. Sci. USA*, 1998, **95**, 3867.

10. C. Cosi and M. Marien, *Ann. NY. Acad. Sci.*, 1999, **890**, 227.

11. M. Kameoka, Y. Tanaka, K. Ota, A. Itaya and K. Yoshihara, *Biochem. Biophys. Res. Commun.*, 1999, **262**, 285.

12. Z. Yang, B. Zingarelli and C. Szabo, *Shock*, 2000, **13**, 60.

13. B. W. Cherney, O. W. McBride, D. Chen, H. Alkhatib, K. Bhatia, P. Hensley and M. E. Smulson, *Proc. Natl. Acad. Sci. USA*, 1987, **84**, 8370.

14. B. Auer, U. Nagl, H. Herzog, R. Schneider and M. Schweiger, *DNA*, 1989, **8**, 575.

15. I. Kameshita, Z. Matsuda, T. Taniguchi and Y. Shizuta, *J Biol. Chem.*, 1984, **259**, 4770.

16. A. Mazen, J. Ménissier-de Murcia, M. Molinete, F. Simonin, G. Gradwohl, G. Poirier and G. de Murcia, *Nucleic Acids Res.*, 1989, **17**, 4689.

17. G. de Murcia, V. Schreiber, M. Molinete, B. Saulier, O. Poch, M. Masson, C. Niedergang and J. Ménissier-de Murcia , *Mol. Cell. Biochem.*, 1994, **138**, 15.

18. G. de Murcia and J. Ménissier-de Murcia, *Trends Biochem. Sci.*, 1994, **19**, 172.

19. S. Smith, *Trends Biochem. Sci.*, 2001, **26**, 174.

20. E. Babiychuk, P. B. Cottrill, S. Storozhenko, M. Fuangthong, Y. Chen, M. K. O'Farrell, M. Van Montagu, D. Inze D and S. Kushnir, *Plant J.*, 1998, **15**, 635.

21. W. M. Shieh, J. C. Ame, M. V. Wilson, Z. Q. Wang, D. W. Koh, M. K. Jacobson and E. L. Jacobson, *J. Biol. Chem.*, 1998, **273**, 30069.

22. J. C. Ame, V. Rolli, V. Schreiber, C. Niedergang, F. Apiou, P. Decker, S. Muller, T. Hoger, J. M. de Murcia and G. de Murcia, *J. Biol. Chem.*, 1999, **274**, 17860.

23. M. Johansson, *Genomics*, 1999, **57**, 442.

24. V. A. Kickhoefer, A. C. Siva, N. L. Kedersha, E. M. Inman, C. Ruland, M. Streuli and L. H. Rome, 1999, *J. Cell Biol.*, **146**, 917.

25. S. Smith, I. Giriat, A. Schmitt and T. de Lange, *Science*, 1998, **282**, 1484.

26. J. Ménissier-de Murcia, C. Niedergang, C. Trucco, M. Ricoul, B. Dutrillaux, M. Mark, F. J. Oliver, M. Masson, A. Dierich, M. LeMeur, C. Walztinger, P. Chambon P and G. de Murcia, *Proc. Natl. Acad. Sci. USA*, 1997, **94**, 7303.

27. P. G. Kaminker, S. H. Kim, R. D. Taylor, Y. Zebarjadian, W. D. Funk, G. B. Morin, P. Yaswen and J. Campisi, 2001, *J. Biol. Chem.*, **276**, 35891.

28. G. de Murcia, J. C. Ame, C. Spenlehauer, V. Schreiber, F. Dantzer, A. Huber, C. Niedergang, L. Monaco, R. Loury, P. Sassone-Corsi, J. Ménissier-de Murcia, *Int. Med. J. Exp. Clin. Res.*, 2003, **9**, S1-48.

29. L. Tentori, I. Portarena and G. Graziani, *Pharmacol. Res.*, 2002, **45**, 73.

30. F. R. Althaus, H. E. Kleczkowska, M. Malanga, C. R. Muntener, J. M. Pleschke, M. Ebner and B. Auer, *Mol. Cell. Biochem.*, 1999, **193**, 5.

31. I. U. Schraufstatter, P. A. Hyslop, J. H. Jackson and C. G. Cochrane, *J. Clin. Invest.*, 1988, **82**, 1040.

32. K. Uchida, S, Hanai, K. Ishikawa, Y. Ozawa, M. Uchida, T. Sugimura and M. Miwa, *Proc. Natl. Acad. Sci. USA*, 1993, **90**, 3481.

33. R. C. Benjamin and D. M. Gill, *J. Biol. Chem.*, 1980, **255**, 10493.

34. T. Lindahl, M. S. Satoh, G. G. Poirier and A. Klungland, *Trends Biochem. Sci.*, 1995, **20**, 405.

35. S. Tanuma, T. Yagi and G. S. Johnson, *Arch. Biochem. Biophys.*, 1985, **237**, 38.

36. G. Krupitza and P. Cerutti, *Biochemistry*, 1989, **28**, 4054.

37. Y. Ohashi, A. Itaya, Y. Tanaka, K. Yoshihara, T. Kamiya and A. Matsukage, *Biochem. Biophys. Res. Commun.*, 1986, **140**, 666.

38. K. Yoshihara, A. Itaya, Y. Tanaka, Y. Ohashi, K. Ito, H. Teraoka, K. Tsukada, A. Matsukage and T. Kamiya, *Biochem. Biophys. Res. Commun.*, 1985, **128**, 61.

39. R. Alvarez-Gonzalez, G. Pacheo-Rodriguez and H. Mendoza-Alvarez, *Mol. Cell. Biochem.*, 1994, **138**, 33.

40. R. J. Griffin, N. J. Curtin, D. R. Newell, B. T. Golding, B. W. Durkacz and A. H. Calvert, *Biochimie.*, 1995, **77**, 408.

41. G. Keith, J. Desgres and G. de Murcia, *Anal. Biochem.*, 1990, **191**, 309.

42. G. de Murcia, A. Huletsky, D. Lamarre, A. Gaudreau, J. Pouyet, M. Daune and G. G. Poirier, *J. Biol. Chem.*, 1986, **261**, 7011.

43. C. M. Whitacre, H. Hashimoto, M. L. Tsai, S. Chatterjee, S. J. Berger and N. A. Berger, *Cancer Res.*, 1995, **55**, 3697.

44. L. Davidovic, M. Vodenicharov, E. B. Affar and G. G. Poirier, *Exp. Cell Res.*, 2001, **268**, 7.

45. K. Hatekayama, Y. Nemoto, Y. Ueda and O. Hayashi, *J. Biol. Chem.*, 1986, **261**, 14902.

46. T. Shimokawa, M. Masutani, S. Nagasawa, T. Nozaki, N. Ikota, Y. Aoki, H. Nakagama and T. Sugimura, *J. Biochem.*, 1999, **126**, 748.

47. P. Zahradka and K. Ebisuzaki, *Eur. J. Biochem.*, 1982, **127**, 579.

48. J. Zhang and J.-H. Li, *Drugs of the Future*, 2002, **27**, 371.

49. A. Ludwig, B. Behnke, J. Holtlund and H. Hilz, *J. Biol. Chem.*, 1988, **263**, 6993.

50. Z.-Q. Wang, B. Auer, L. Stingl, H. Berghammer, D. Haidacher, M. Schweiger and E. Wagner, *Genes Dev.*, 1995, **9**, 509.

51. C. Trucco, F. J. Oliver, G. de Murcia and J. Menissier-de Murcia, *Nucleic Acids Res.*, 1998, **26**, 2644.

52. S. Chatterjee, M. F. Cheng, D. Trivedi, S. J. Petzold and N. A. Berger, *Cancer Commun.*, 1989, **1**, 389.

53. M. Masson, C. Niedergang, V. Schreiber, S. Muller, J. Ménissier-de Murcia and G. de Murcia, *Mol. Cell Biol.*, 1998, **18**, 3563.

54. S. Chatterjee, S. J. Berger and N. A. Berger, *Mol. Cell. Biochem.*, 1999, **193**, 23.

55. N. A. Berger, *Radiat. Res.*, 1985, **101**, 4.

56. S. I. Tanuma, T. Enomoto and M. A. Yamada, *Exp. Cell Res.*, 1978, **117**, 421.

57. Y. Kanai, S. Tanuma and T. Sugimura, *Proc. Natl. Acad. Sci. USA*, 1981, **78**, 2801.

58. Y. Leduc, J. J. Lawrence, G. de Murcia and G. G. Poirier, *Biochim. Biophys. Acta.*, 1988, **968**, 275.

59. C. M. Simbulan-Rosenthal, D. S. Rosenthal, H. Hilz, R. Hickey, L. Malkas, N. Applegren, Y. Wu, G. Bers and M. E. Smulson, *Biochemistry*, 1996, **35**, 11622.

60. F. Dantzer, H. P. Nasheuer, J. L. Vonesch, G. de Murcia and J. Ménissier-de Murcia, *Nucleic Acids Res.*, 1998, **26**, 1891.

61. D. D'Amours, S. Desnoyers, I. D'Silva and G. G. Poirier, *Biochem. J.*, 1999, **342**, 249.

62. G. E. Francis, D. A. Gray, J. J. Berney, M. A. Wing, J. E. Guimaraes and A. V. Hoffbrand, *Blood*, 1983, **62**, 1055.

63. M. Bhatia, J. B. Kirkland and K. A. Meckling-Gill, *Cell Growth Differ.*, 1996, **7**, 91.

64. A. Frechette, A. Huletsky, R. J. Aubin, G. de Murcia, P. Mandel, A. Lord, G. Grondin, G. G. Poirier, *Can. J. Biochem. Cell Biol.*, 1985, **63**, 764.

65. C. M. Simbulan-Rosenthal, D. H. Ly, D. S. Rosenthal, G. Konopka, R. Luo, Z. Q. Wang, P. G. Schultz and M. E. Smulson, *Proc. Natl. Acad. Sci. USA*, 2000, **97**, 11274.

66. B. Zingarelli, A. L. Salzman and C. Szabo, *Circ. Res.*, 1998, **83**, 85.

67. F. J. Oliver, J. Ménissier-de Murcia, C. Nacci, P. Decker, R. Andriantsitohaina, S. Muller, G. de la Rubia, J. C. Stoclet and G. de Murcia, *Eur. Mol. Biol. Organ. J.*, 1999, **18**, 4446.

68. M. Uchida, S. Hanai, N. Uematsu, K. Sawamoto, H. Okano, M. Miwa and K. Uchida, *J. Biol. Chem.*, 2001, **277**, 6696.

69. P. Pacher, J. G. Mabley, F. G. Soriano, L. Liaudet and C. Szabo, *Int. J. Mol. Med.*, 2002, **9**, 659.

70. H. C. Ha, K. Juluri, Y Zhou, S Leung, M. Hermankova and S. H. Snyder, *Proc. Natl. Acad. Sci. USA*, 2001, **98**, 3364.

71. H. C. Ha and S. H. Snyder, *Neurobiol Dis.*, 2000, **7**, 225.

72. J. L. Sims, S. J. Berger and N. A. Berger, *Biochemistry*, 1983, **22**, 5188.

73. C. Szabo and V. L. Dawson, *Trends Pharmacol. Sci.*, 1998, **19**, 287.

74. N. A. Berger, J. L. Sims, D. M. Catino, S. J. Berger, In *ADP-ribosylation, DNA repair and Cancer,* eds. M. Miwa, O. Hayaishi, S. Shall, M. Smulson and T. Sugimura, Japan Sci. Press, Tokyo, 1983.

75. S. Coppola, C. Nosseri, V. Maresca and L. Ghibelli, *Exp. Cell Res.*, 1995, **221**, 462.

76. M. Leist, B. Single, A. F. Castoldi, S. Kuhnle and P. Nicotera, *J. Exp. Med.*, 1997, **185**, 1481.

77. Y. A. Lazebnik, S. H. Kaufmann, S. Desnoyers, G. G. Poirier and W. C. Earnshaw, *Nature*, 1994, **371**, 346.

78. D. D'Amours, F. R. Sallmann, V. M. Dixit and G. G. Poirier, *J. Cell Sci.*, 2001, **114**, 3771.

79. C. Richter, M. Schweizer, A. Cossarizza and C. Franceschi, *FEBS Lett.*, 1996, **378**, 107.

80. E. Bonfoco, D. Krainc, M. Ankarcrona, P. Nicotera and S. A. Lipton, *Proc. Natl. Acad. Sci. USA*, 1995, **92**, 7162.

81. A. A. Pieper, A. Verma, J. Zhang and S. H. Snyder, *Trends Pharmacol. Sci.*, 1999, **20**, 171.

82. D. J. Hearse and R. Bolli, *Cardiovasc. Res.*, 1992, **26**, 101.

83. C. Szabo, *Shock*, 1996, **6**, 79.

84. B. Zingarelli, S. Cuzzocrea, Z. Zsengeller, A. L. Salzman and C. Szabo, *Cardiovasc. Res.*, 1997, 36, 205.

85. L. Liaudet, E. Szabo, L. Timashpolsky, L. Virag, A. Cziraki and C. Szabo, *Br. J. Pharmacol.*, 2001, **133**, 1424.

86. N. Wayman, M. C. McDonald, A. S. Thompson, M. D. Threadgill and C. Thiemermann, *Eur. J. Pharmacol.*, 2001, **430**, 93.

87. C. Thiemermann, J. Bowes, F. P. Myint and J. R. Vane, *Proc. Natl. Acad. Sci. USA*, 1997, **94**, 679.

88. J. Bowes, H. Ruetten, P. A. Martorana, H. Stockhausen and C. Thiemermann, *Eur. J. Pharmacol.*, 1998, **359**, 143.

89. R. Faro, Y. Toyoda, J. McCully, P. Jagtap, E. Szabo, L. Virag, C. Bianchi, S. Levitsky and C. Szabo, *Ann. Thorac. Surg.*, 2002, **73**, 575.

90. J. Zhang, V. L. Dawson, T. M. Dawson and S. H. Snyder, *Science*, 1994, **263**, 687.

91. M. J. Eliasson, K. Sampei, A. S. Mandir, P. D. Hurn, R. J. Traystman, J. Bao, A. Pieper, Z. Q. Wang, T. M. Dawson and S. H. Snyder, *Nat. Med.*, 1997, **3**, 1089.

92. A. Y. Sun and J. S. Cheng, *Zhongguo Yao Li Xue Bao*, 1998, **19**, 104.

93. K. Takahashi, J. H. Greenberg, P. Jackson, K. Maclin and J. Zhang, *J. Cereb. Blood Flow Metab.*, 1997, **17**, 1137.

94. G. Abdelkarim, K. Gertz, C. Harms, J, Katchanov, U. Dirnagl, C. Szabo and M. Endres, *Int. J. Mol. Med.*, 2001, **7**, 255.

95. S. Cuzzocrea, B. Zingarelli, G. Costantino, A. Szabo, A. L. Salzman, A. P. Caputi and C. Szabo, *Br. J. Pharmacol.*, 1997, **121**, 1065.

96. E. Mazzon, L. Dugo, S. A. De, J. H. Li, A. P. Caputi, J. Zhang and S. Cuzzocrea, *Shock*, 2002, **17**, 222.

97. P. Jagtap, F. G. Soriano, L. Virag, L. Liaudet, J. Mabley, E. Szabo, G. Hasko, A. Marton, C. B. Lorigados and F. Gallyas, *Crit. Care Med.*, 2002, **30**, 1071.

98. H. Mota-Filipe, B. Sepodes, M. McDonald, S. Cuzzocrea, R. Pinto and C. Thiemermann, *Med. Sci. Monit.*, 2002, **8**, BR444.

99. D. R. Martin, A. J. P. Lewington, M. R. Hammerman and B. J. Padanilam, *Am. J. Physiol. Regulatory Integrative Comp. Physiol.*, 2000, **279**, R1834.

100. T. T. Lam, *Res. Commun. Mol. Pathol. Pharmacol.*, 1997, **95**, 241.

101. G. Szabo, S. Bahrle, N. Stumpf, K. Sonnenberg, E. Szabo, P. Pacher, T. Csont, R. Schulz, T. J. Dengler and L. Liaudet, *Circ. Res.*, 2002, **90**, 100.

102. A. Szabo, P. Hake, A. L. Salzman and C. Szabo, *Shock*, 1998, **10**, 347.

103. M. C. McDonald, H. Mota-Filipe, J. A. Wright, M. Abdelrahman, M. D. Threadgill, A. S. Thompson and C. Thiemermann, *Br. J. Pharmacol.*, 2000, **130**, 843.

104. H. Yamamoto and H. Okamoto, *Biochem. Biophys. Res. Commun.*, 1980, **95**, 474.

105. Y. Uchigata, H. Yamamoto, A. Kawamura and H. Okamoto, *J. Biol. Chem.*, 1982, **257**, 6084.

106. P. Masiello, T. L. Cubeddu, G. Frosina and E. Bergamini, *Diabetologia*, 1985, **28**, 683.

107. R. Miesel, M. Kurpisz and H. Kroger, *Inflammation*, 1995, **19**, 379.

108. H. B. Jijon, T. Churchill, D. Malfair, A. Wessler, L. D. Jewell, H. G. Parsons and K. L. Madsen, *Am. J. Physiol. Gastrointest. Liver Physiol.*, 2000, **279**, G641.

109. S. I. Said, H. I. Berisha and H. Pakbaz, *Proc. Natl. Acad. Sci. USA*, 1996, **93**, 4688.

110. L. Liaudet, P. Pacher, L. Virag, F. G. Soriano, G. Hasko and C. Szabo, *Am. J. Respir. Crit. Care Med.*, 2002, **165**, 372.

111. S. Cuzzocrea, M. C. McDonald, E. Mazzon, L. Dugo, I. Serraino, M. D. Threadgill, A. P. Caputi and C. Thiemermann, *Biochem. Pharmacol.*, 2002, **63**, 293.

112. A. Szabo, A. L. Salzman and C. Szabo, *Life Sci.*, 1998, **63**, 2133.

113. R. H. Goldfarb, A. Marton, E. Szabo, L. Virag, D. Glock, R. McCarthy, J. E. Parillo and C. Szabo, *Crit. Care Med.*, 2002, **30**, 974.

114. N. Nduka, C. J. Skidmore and S. Shall, *Eur. J. Biochem.*, 1980, **105**, 525.

115. D. Weltin, V. Holl, J. W. Hyun, P. Dufour, J. Marchal and P. Bischoff, *Int. J. Radiat. Biol.*, 1997, **72**, 685.

116. S. Boulton, L. C. Pemberton, J. K. Porteous, N. J. Curtin, R. J. Griffin, B. T. Golding and B. W. Durkacz, *Br. J. Cancer*, 1995, **72**, 849.

117. P. Pacher, L. Liaudet, P. Bai, L. Virag, J. G. Mabley, G. Haskó and C. Szabó, *J. Pharmacol. Exp. Ther.*, 2002, **300**, 862.

118. I. Racz, K. Tory, F. Gallyas, Z. Berente, E. Osz, L. Jaszlits, S. Bernath, B. Sumegi, G. Rabloczky and P. Literati-Nagy, *Biochem. Pharmacol.*, 2002, **63**, 1099.

119. J. A. Gaken, M. Tavassoli, S. U. Gan, S. Vallian, I. Giddings, D. C. Darling, J. Galea-Lauri, M. G. Thomas, H. Abedi and V. Schreiber, *J. Virol.*, 1996, **70**, 3992.

120. G. Furlini, M. C. Re and M. La Placa, *Microbiologica*, 1991, **14**, 141.

121. G. A. Cole, G. Bauer, E. Kirsten, J. Mendeleyev, P. I. Bauer, K. G. Buki, A. Hakam and E. Kun, *Biochem. Biophys. Res. Commun.*, 1991, **180**, 504.

122. I. I. Krasil'nikov, L. B. Kalnina, M. N. Korneeva, D. N. Nosik, A. I. Zlobin, V. G. Vladimirov and D. K. L'vov, *Vopr. Virusol.*, 1991, **36**, 216.

123. C. Cosi, F. Colpaert, W. Koek, A. Degryse and M. Marien, *Brain Res.*, 1996, **729**, 264.

124. S. Love, R. Barber and G. K. Wilcock, *Brain*, 1999, **122**, 247.

125. F. G. Soriano, P. Pacher, J. Mabley, L. Liaudet and C. Szabo, *Circ. Res.*, 2001, **89**, 684.

126. H. Kroger, A. Dietrich, M. Ohde, R. Lange, W. Ehrlich and M. Kurpisz, *Gen. Pharmacol.*, 1997, **28**, 257.

127. B. Farkas, M. Magyarlaki, B. Csete, J. Nemeth, G. Rabloczky, S. Bernath, P. Literati-Nagy and B. Sümegi, *Biochem. Pharmacol.*, 2002, **63**, 921.

128. R. B. Elliott and H. P. Chase, *Diabetologia*, 1991, **34**, 362.

129. C. Conde, M. Mark, F. J. Oliver, A. Huber, G. de Murcia and J. Ménissier-de Murcia, *Eur. Mol. Biol. Organ J.*, 2001, **20**, 3535.

130. S. Shall, In *DNA Repair and its Inhibition*, eds. A. Collins, C. S. Downes and R. T. Johnson, 143, IRL Press, Oxford, 1981.

131. J. B. Clark, G. M. Ferris and S. Pinder, *Biochem. Biophys. Acta.*, 1971, **282**, 82.

132. S. Shall, *Biochem.*, 1975, **77**, 2.

133. M. Banasik and K. Ueda, *J. Enzyme Inhibition*, 1999, **14**, 239.

134. M. R. Purnell and W. J. D. Whish, *Biochem. J.*, 1980, **185**, 775.

135. R. J. Griffin, L. C. Pemberton, D. Rhodes, C. Bleasdale, K. Bowman, A. H. Calvert, N. J. Curtin, B. W. Durkacz, D. R. Newell, J. K. Porteous and B. T. Golding, *Anti-Cancer Drug Design*, 1995, **10**, 507.

136. M. Banasik, H. Komura, M. Shimoyama and K. Ueda, *J. Biol. Chem.*, 1992, **267**, 1569.

137. J. L. Sims, G. W. Sikorski, D. M. Catino, S. J. Berger and N. A. Berger, *Biochemistry*, 1982, **21**, 1813.

138. M. J. Suto, W. R. Turner, C. M. Arundel-Suto, L. M. Werbel and J. S. Sebolt-Leopold, *Anti-Cancer Drug Design*, 1991, **7**, 107.

139. P. Sestili, G. Spadoni, C. Balsamini, I. Scovassi, F. Cattabeni, E. Duranti, O. Cantoni, D. Huggins, C. Thomson, *J. Cancer Res. Clin. Oncol.*, 1990, **116**, 615.

140. O. Cantoni, P. Sestilli, G. Spadoni, C. Balsamini, L. Cucchiaini and F. Cattabeni, *Biochem. Int.*, 1987, **15**, 329.

141. A. Ruf, G. de Murcia and G. E. Schulz, *Biochemistry*, 1998, **37**, 3893.

142. G. Costantino, A. Macchiarulo, E. Camaioni and R. Pellicciari, *J. Med. Chem.*, 2001, **44**, 3786.

143. A. Ruf, J. M. de Murcia, G. M. de Murcia and G. E. Schulz, *Proc. Natl. Acad. Sci. USA*, 1996, **93**, 7481.

144. K. Takahashi, A. A. Pieper, S. E Croul, J. Zhang, S. H. Snyder and J. H. Greenberg, *Brain Res.*, 1999, **829**, 46.

145. V. Burkart, Z. Q. Wang, J. Radons, B. Heller, Z. Herceg, L. Stingl, E. F. Wagner and H. Kolb, *Nat. Med.*, 1999, **5**, 314.

146. C. Szabo, B. Zingarelli, M. O'Connor and A. L. Salzman, *Proc. Natl. Acad. Sci. USA*, 1996, **93**, 1753.

147. E. Mazzon, I. Serraino, J. H. Li, L. Dugo, A. P. Caputi, J. Zhang and S. Cuzzocrea, *Eur. J. Pharmacol.*, 2001, **415**, 85.

148. A. W. White, R. Almassy, A. H. Calvert, N. J. Curtin, R. J. Griffin, Z. Hostomsky, K. Maegley, D. R. Newell, S. Srinivasan and B. T. Golding, *J. Med. Chem.*, 2000, **43**, 4084.

149. R. J. Griffin, S. Srinivasan, K. Bowman, A. H. Calvert, N. J. Curtin, D. R. Newell, L. C. Pemberton and B. T. Golding, *J. Med. Chem.*, 1998, **41**, 5247.

150. KuDOS Pharmaceuticals Ltd., WO 02/36576, 2002.

151. S. Stacie, C. Koch, L. H. Thoresen, J. G. Tikhe, K. A. Maegley, R. J. Almassy, J. Li, X.-H. Yu, S. E. Zook, R. A. Kumf, C. Zhang, T. J. Boritzki, R. N. Mansour, K. E. Zhang, A. Ekker, C. R. Calabrese, N. J. Curtin, S. Kyle, H. D. Thomas, L.-Z. Wang, A. H. Calvert, B. T. Golding, R. J. Griffin, D. R. Newell, S. E. Webber and Z. Hostomsky, *J. Med. Chem.*, 2002, **45**, 4961.

152. D. J. Skalitzky, J. T. Marakovits, K. A. Maegley, A. Ekker, X.-H. Yu, Z. Hostomsky, S. E. Webber, B. W. Eastman, R. J. Almassy, J. Li, N. J. Curtin, D. R. Newell, A. H. Calvert, R. J. Griffin and B. T. Golding, *J. Med. Chem.*, 2003, **46**, 210.

153. D. Ferraris, R. P. Ficco, D. Dain, M. Ginski, S. Lautar, K. Lee-Wisdom, S. Liang, Q. Lin, M. X. C. Lu, L. Morgan, B. Thomas, L. R. Williams, J. Zhang, Y. Zhou and V. J. Kalish, *Bioorg. Med. Chem.*, 2003, **11**, 3695.

154. A. Chiarugi, E. Meli, M. Calvani, R. Picca, R. Baronti, E. Camaioni, G. Costantino, M. Marinozzi, D. E. Pellegrini-Giampietro, R. Pellicciari and F. Moroni, *J. Pharmacol. Exp. Ther.*, 2003, **305**, 943.

155. K. Buki, P. Bauer, J. Mendeleyev, A. Hakam and E. Kun, *FEBS Lett.*, 1991, **290**, 181.

156. P. K. Chatterjee, B. E. Chatterjee, H. Pedersen, A. Sivarajah, M. C. McDonald, H. Mota-Filipe, P. A. J. Brown, K. N. Stewart, S. Cuzzocrea, M. D. Threadgill and C. Thiemermann, *Kidney Int.*, 2004, **65**, 499.

157. A. E. Shinkwin, W. J. D. Whish and M. D. Threadgill, *Bioorg. Med. Chem.*, 1999, **7**, 297.

158. C. Y. Watson, W. J. D. Whish and M. D. Threadgill, *Bioorg. Med. Chem.*, 1998, **6**, 721.

159. I. Parveen I, D. P. Naughton, W. J. D. Whish and M. D. Threadgill, *Bioorg. Med. Chem. Lett.*, 1999, **9**, 2031.

160. S. Ferrer, D. P. Naughton and M. D. Threadgill, *Tetrahedron*, 2003, **59**, 3437.

161. S. Ferrer, D. P. Naughton and M. D. Threadgill, *Tetrahedron*, 2003, **59**, 3445.

162. H. Nogami, *J. Pharm. Soc. Japan*, 1941, **61**, 46.

163. J. L. Warnell and R. L. Shriner, *J. Am. Chem. Soc.*, 1957, **79**, 3165.

164. J. P. Brown, A. Robertson, W. B. Whalley and N. J. Cartwright, *J. Chem. Soc.*, 1949, 867.

165. H. A. Dieck and R. F. Heck, *J. Organomet. Chem.*, 1975, **93**, 259.

166. A. O. King, N. Okukado and E. Negishi, *J. Chem. Soc., Chem. Commun.*, 1977, 683.

167. K. Sonogashira, Y. Tohda and N. Hagihara, *Tetrahedron Lett.*, 1975, 4467.

168. K. Sonogashira, In *metal-catalysed cross-coupling reactions*, eds. F. Diederich and P. J. Stang, Wiley-VCH, Weinheim, 1998.

169. P. J. Culhane, *Organic Syntheses*, 1967, Collect. Vol. 1, 125.

170. J. M. Swan and D. St. C. Black, In *Organometallic in Organic Synthesis*, eds. R. P. Bell, N. N. Greenwood and R. O. C. Norman, Chapman and Hall, London, 1974.

171. E. Negishi, *Acc. Chem. Res.*, 1982, **15**, 340.

172. J. E. Baldwin, *J. Chem. Soc., Chem. Commun.*, 1976, 734.

173. R. D. Stephens and C. E. Castro, *J. Org. Chem.*, 1963, **28**, 3313.

174. C. E. Castro, E. J. Gaughan and D. C. Owsley, *J. Org. Chem.*, 1966, **31**, 4071.

175. W. B. Austin, N. Bilow, W. J. Kelleghan and K. S. Y. Lau, *J. Org. Chem.*, 1981, **46**, 2280.

176. C. C. Bond and M. Hooper, *J. Chem. Soc.*, 1969, 2453.

177. R. F. Heck and J. P. Nolley, *J. Org. Chem.*, 1972, **37**, 2320.

178. S. M. Wong, B. Shah, P. Shah, I. C. Butt, E. C. Y. Woon, J. A. Wright, A. S. Thompson, C. Upton and M. D. Threadgill, *Tetrahedron Lett.*, 2002, **43**, 2299.

179. S. Hanessian and E. Moralioglu, *Can. J. Chem.*, 1972, **50**, 233.

180. W. R. H. Hurtley, *J. Chem. Soc.*, 1929, 1870.

181. K. A. Cirigottis, E. Ritchie and W. C. Taylor, *Austral. J. Chem.*, 1974, **27**, 2209.

182. A. Bruggink and A. McKillop, *Tetrahedron*, 1975, **31**, 2607.

183. T. Sakamoto, M. An-Naka, Y. Kondo and H. Yamanaka, *Chem. Pharm. Bull.*, 1986, **34**, 2754.

184. Y. Ogawa, M. Maruno and T. Wakamatsu, *Heterocycles*, 1995, **41**, 2587.

185. H. Sashida and A. Kawamukai, *Synthesis*, 1999, **7**, 1145.

186. H. Y. Liao and C. H. Cheng, *J. Org. Chem.*, 1995, **60**, 3711.

187. D. Villemin and D. Goussu, *Heterocycles*, 1989, **29**, 1255.

188. M. Kimura, I. Waki, Y. Deguchi, K. Amemiya and T. Maeda, *Chem. Pharm. Bull.*, 1983, **31**, 1277.

189. N. Yoneda, S. Matsuoka, N. Miyaura, T. Fukuhara and A. Suzuki, *Bull. Chem. Soc. Jpn.*, 1990, **63**, 2124.

190. A. E. Shinkwin, PhD thesis, 1997.

191. I. D. Rae, *Can. J. Chem.*, 1986, **46**, 2589.

192. K. Seno, S. Hagishita, T. Sato and K. Kuriyama, *J. Chem. Soc., Perkin Trans. 1*, 1984, 2013.

193. T. Nagasaka and Y. Koseki, *J. Org. Chem.*, 1998, **63**, 6797.

194. R. C. Larock and L. W. Harrison, *J. Am. Chem. Soc.*, 1984, **106**, 4218.

195. A. Bogert, *J. Amer. Chem. Soc.*, 1927, **49**, 1320.

196. D. C. Iffland and H. Siegel, *J. Am. Chem. Soc.*, 1958, **80**, 1947.

197. F. Houben, *Chem.Ber.*, 1931, **64**, 2636.

198. D. E. Ames, *J. Chem. Soc., Perkin Trans. 1*, 1973, 2818.

199. C. Arnone, G. Consiglio, V. Frenna and D. Spinelli, *J. Org. Chem.*, 1997, **62**, 3093.

200. S. Takahashi, Y. Kuroyama, K. Sonogashira and N. Hagihara, *Synthesis*, 1980, **8**, 627.

201. A. Alberti, G. F. Pedulli and F. Ciminale, *Tetrahedron*, 1982, **38**, 3605.

202. W. Eaborn, *J. Organomet. Chem.*, 1964, **2**, 95.

203. J. Carran, R. Waschbuesch, A. Marinetti and P. Savignac, *Synthesis*, 1996, **12**, 1494.

204. J. Morris, D. Wishka and G. Donn, *Synthesis*, 1994, **10**, 43.

205. A. Carpita, R. Rossi and C. A. Veracini, *Tetrahedron*, 1985, **41**, 1919.

206. Y. Takahashi and Y. Zasshi, *Chem. Abstr.*, 1979, **90**, 6486.

207. H. F. Chow, C. W. Wan, K. H. Low and Y. Y. Yeung, *J. Org. Chem.*, 2001, **66**, 1910.

208. M. J. Haddadin, *Tetrahedron*, 1976, **32**, 719.

209. E. V. Tretyakov, D. W. Knight and S. F. Vasilevsky, *J. Chem. Soc., Perkin Trans. 1*, 1999, **24**, 3713.

210. G. Maerkl, H. Hauptmann and A. Merz, *J. Organomet. Chem.*, 1983, **249**, 335.

211. S. Levine, *J. Amer. Chem. Soc.*, 1950, 1678.

212. D. R. Bryant and C. R. Hauser, *J. Org. Chem.* **1961**, *27*, 694.

213. C. J. Kowalski and R. E. Reddy, *J. Org. Chem.*, 1992, **57**, 7194.

214. M. Tercel, M. A. Gieseg, W. A. Denny and W. R. Wilson, *J. Org. Chem.*, 1999, **64**, 5946.

215. A. H. Fauq, F. Hong, B. Cusack, B. M. Tyler, P. P. Yuan and E. Richelson, *Tetrahedron Asymmetry*, 1998, **23**, 4127.

216. B. C. Soderberg and J. A. Shriver, *J. Org. Chem.,* 1997, **62**, 5838.

217. C. A. Grob and O. Weissbach, *Helv. Chim. Acta*, 1961, **44**, 1736.

218. S. Pivsa-Art, T. Satoh, Y. Kawamura, M. Miura and M. Nomura, *Bull. Chem. Soc. Jpn.*, 1998, **71**, 467.

219. Y. Aoyagi, A. Inoue, I. Koizumi, R. Hashimoto, K. Tokunaga, K. Gohma, J. Komatsu, K. Sekine, A. Miyafuji and A. Ohta, *Heterocycles*, 1992, **33**, 257.

220. A. A. Morton and D. Bannerman, *J. Am. Chem. Soc.*, 1945, **67**, 1503.

221. E. Negishi, A. O. King and Nobuhisa O, *J. Org. Chem.*, 1977, **42**, 1821.

222. K. J. Dillon, G. C. M. Smith and N. M. B. Martin, *J. Biomol. Screening*, 2003, **8**, 347.

223. W. Eaborn, *J. Organomet. Chem.*, 1964, **2**, 95.

224. J. Salauen, *J. Org. Chem.*, 1977, **42**, 28.

225. R. Schumacher, *Liebigs Ann.*, 1997, 521.

Appendix

X-ray crystallography of 3-(4-methylphenyl)-5-nitroisocoumarin **(103)**.

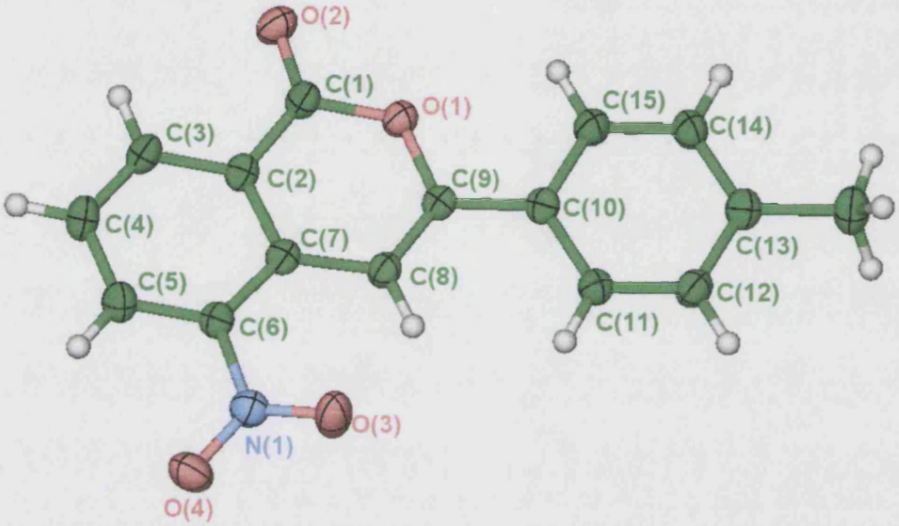

X-ray crystallography data for 3-(4-methylphenyl)-5-nitroisocoumarin **(103)**.

Identification code	Compound **(103)**
Empirical formula	$C_{16}H_{11}NO_4$
Formula weight	281.26
Temperature	293(2) K
Wavelength	0.71073 Å
Crystal system	Monoclinic
Space group	$P2_1/n$
Unit cell dimensions	a = 5.8870(2)Å $\alpha = 90^\circ$ b = 12.0270(3)Å $\beta = 96.8020(10)^\circ$ c = 18.4880(7)Å $\gamma = 90^\circ$
Volume	1299.79(7) $Å^3$
Z	4
Density (calculated)	1.437 Mg/m^3
Absorption coefficient	0.105 mm^{-1}
F(000)	584
Crystal size	0.40 x 0.13 x 0.08 mm
Theta range for data collection	3.53 to 27.45°
Index ranges	-7<=h<=7; -13<=k<=15; -23<=l<=23
Reflections collected	13240
Independent reflections	2964 [R(int) = 0.0686]
Reflections observed (>2 σ)	1523
Data Completeness	0.996
Max. and min. transmission	0.9922 and 0.9593
Refinement method	Full-matrix least-squares on F^2
Data / restraints / parameters	2964 / 0 / 192
Goodness-of-fit on F^2	0.950
Final R indices [I>2 σ (I)]	$R_1 = 0.0548$ $wR_2 = 0.1228$
R indices (all data)	$R_1 = 0.1295$ $wR_2 = 0.1617$
Largest diff. peak and hole	0.300 and -0.279 $eÅ^{-3}$

Table 22. *Crystal data and structure refinement for (103).*

Atom	x	y	z	U (eq)
O(1)	3993(2)	3632(1)	860(1)	60(1)
O(2)	2944(3)	1897(1)	668(1)	73(1)
O(3)	11238(3)	4273(1)	2604(1)	96(1)
O(4)	13723(3)	2966(1)	2636(1)	82(1)
N(1)	11802(3)	3325(2)	2456(1)	63(1)
C(1)	4402(3)	2506(2)	942(1)	55(1)
C(2)	6543(3)	2182(2)	1368(1)	52(1)
C(3)	6962(4)	1055(2)	1481(1)	61(1)
C(4)	8922(4)	690(2)	1880(1)	66(1)
C(5)	10498(4)	1458(2)	2177(1)	61(1)
C(6)	10079(3)	2574(2)	2083(1)	52(1)
C(7)	8094(3)	2998(2)	1673(1)	50(1)
C(8)	7528(3)	4137(2)	1522(1)	52(1)
C(9)	5543(3)	4426(2)	1129(1)	51(1)
C(10)	4726(3)	5554(2)	952(1)	51(1)
C(11)	6099(3)	6479(2)	1123(1)	59(1)
C(12)	5291(3)	7536(2)	961(1)	63(1)
C(13)	3096(4)	7722(2)	620(1)	59(1)
C(14)	1755(4)	6803(2)	440(1)	63(1)
C(15)	2541(4)	5742(2)	603(1)	61(1)
C(16)	2208(4)	8881(2)	452(1)	76(1)

Table 23. *Atomic coordinates ($Å^2$ x 10^4) and equivalent isotropic displacement parameters ($Å^2$ x 10^3) for* ***(103)****. U (eq) is defined as one third of the trace of the orthogonalized Uij tensor.*

O(1)-C(9)	1.373(2)	O(1)-C(1)	1.380(3)
O(2)-C(1)	1.195(2)	O(3)-N(1)	1.228(2)
O(4)-N(1)	1.219(2)	N(1)-C(6)	1.468(3)
C(1)-C(2)	1.458(3)	C(2)-C(3)	1.388(3)
C(2)-C(7)	1.412(3)	C(3)-C(4)	1.366(3)
C(4)-C(5)	1.377(3)	C(5)-C(6)	1.371(3)
C(6)-C(7)	1.412(3)	C(7)-C(8)	1.429(3)
C(8)-C(9)	1.347(3)	C(9)-C(10)	1.463(3)
C(10)-C(11)	1.389(3)	C(10)-C(15)	1.387(3)
C(11)-C(12)	1.378(3)	C(12)-C(13)	1.388(3)
C(13)-C(14)	1.377(3)	C(13)-C(16)	1.507(3)
C(14)-C(15)	1.378(3)		
C(9)-O(1)-C(1)	122.92(15)	O(4)-N(1)-O(3)	122.35(18)
O(4)-N(1)-C(6)	118.50(19)	O(3)-N(1)-C(6)	119.07(17)
O(2)-C(1)-O(1)	116.63(18)	O(2)-C(1)-C(2)	126.6(2)
O(1)-C(1)-C(2)	116.74(18)	C(3)-C(2)-C(7)	121.55(19)
C(3)-C(2)-C(1)	118.00(19)	C(7)-C(2)-C(1)	120.41(18)
C(4)-C(3)-C(2)	121.3(2)	C(3)-C(4)-C(5)	119.0(2)
C(6)-C(5)-C(4)	120.2(2)	C(5)-C(6)-C(7)	123.16(19)
C(5)-C(6)-N(1)	116.04(18)	C(7)-C(6)-N(1)	120.78(19)
C(2)-C(7)-C(6)	114.71(19)	C(2)-C(7)-C(8)	117.64(18)
C(6)-C(7)-C(8)	127.63(19)	C(9)-C(8)-C(7)	121.34(18)
C(8)-C(9)-O(1)	120.83(17)	C(8)-C(9)-C(10)	126.97(18)
O(1)-C(9)-C(10)	112.18(16)	C(11)-C(10)-C(15)	117.26(18)
C(11)-C(10)-C(9)	121.61(18)	C(15)-C(10)-C(9)	121.13(18)
C(12)-C(11)-C(10)	120.85(19)	C(11)-C(12)-C(13)	121.8(2)
C(14)-C(13)-C(12)	117.17(19)	C(14)-C(13)-C(16)	121.2(2)
C(12)-C(13)-C(16)	121.6(2)	C(13)-C(14)-C(15)	121.5(2)
C(14)-C(15)-C(10)	121.40(19)		

Table 24. *Bond angles [°] and bond lengths [Å] (in parentheses) for* ***(103)****.*

Atom	U11	U22	U33	U23	U13	U12
O(1)	58(1)	50(1)	70(1)	1(1)	-4(1)	-4(1)
O(2)	70(1)	57(1)	89(1)	-2(1)	-9(1)	-15(1)
O(3)	90(1)	57(1)	130(2)	-16(1)	-35(1)	4(1)
O(4)	56(1)	88(1)	98(1)	-9(1)	-4(1)	6(1)
N(1)	58(1)	63(1)	66(1)	1(1)	-2(1)	-1(1)
C(1)	61(1)	45(1)	59(1)	1(1)	6(1)	-3(1)
C(2)	61(1)	46(1)	49(1)	1(1)	9(1)	0(1)
C(3)	73(1)	44(1)	64(1)	-2(1)	6(1)	-7(1)
C(4)	85(2)	46(1)	68(1)	5(1)	8(1)	7(1)
C(5)	67(1)	54(2)	62(1)	3(1)	4(1)	7(1)
C(6)	56(1)	49(1)	52(1)	-1(1)	7(1)	0(1)
C(7)	55(1)	47(1)	47(1)	-1(1)	11(1)	-1(1)
C(8)	56(1)	44(1)	56(1)	-3(1)	3(1)	-2(1)
C(9)	54(1)	47(1)	52(1)	-1(1)	7(1)	-2(1)
C(10)	56(1)	49(1)	48(1)	1(1)	7(1)	1(1)
C(11)	55(1)	52(1)	67(1)	5(1)	-1(1)	2(1)
C(12)	66(1)	52(2)	69(1)	0(1)	1(1)	-5(1)
C(13)	71(1)	55(2)	53(1)	-1(1)	8(1)	5(1)
C(14)	59(1)	56(2)	73(1)	0(1)	-4(1)	6(1)
C(15)	59(1)	52(1)	70(1)	-2(1)	-3(1)	-3(1)
C(16)	93(2)	53(2)	80(2)	-3(1)	-2(1)	12(1)

Table 25. *Anisotropic displacement parameters ($Å^2$ x 10^3) for* ***(103)****.*

Atom	x	y	z	U(eq)
H(3)	5887	540	1282	73
H(4)	9188	-67	1949	79
H(5)	11852	1220	2442	73
H(8)	8551	4689	1699	63
H(11)	7582	6383	1350	71
H(12)	6243	8141	1085	75
H(14)	284	6899	203	76
H(15)	1586	5139	477	74
H(16A)	819	8841	124	114
H(16B)	3329	9299	231	114
H(16C)	1910	9239	895	114

Table 26. *Hydrogen coordinates (x 10^4) and isotropic displacement parameters ($Å^2$ x 10^3) for* ***(103)****.*

Publications

M. D. Threadgill, J. M. Berry, S. Ferrer, I. Parveen, A. E. Shinkwin and E. C. Y. Woon. 5-aminoisoquinolin-1-one and other water-soluble PARP inhibitors. *Int. Med. J. Exp. Clin. Res.*, 2003, **9**, S1-71.

S.-M. Wong, B. Shah, P. Shah, I. C. Butt, E. C. Y. Woon, J. A. Wright, A. S. Thompson, C. Upton and M. D. Threadgill. A new synthesis of "push-pull" naphthalenes by condensation of nitro-2-methylbenzoate esters with dimethylacetamide dimethyl acetal. *Tetrahedron Lett.*, 2002, **43**, 2299.

MEDICAL SCIENCE
M * O * N * I * T * O * R
International Medical Journal for Experimental and Clinical Research

Volume 9 Supplement 1

Poly (ADP-Ribose) Polymerases
as Novel Therapeutic Targets

PARP-2003 is endorsed by the European Shock Society
and the Academy of Sciences of Lisboa

Abstracts of PARP-2003

Guest Editor/Chairman:
Professor Chris Thiemermann (United Kingdom)

May 2nd–5th, 2003
The Marriott Hotel
Lisbon, Portugal

69 Systemic administration of the PARP-1 inhibitor GPI 15427 increases the anti-tumor activity of temozolomide against metastatic melanoma

Tentori L[1], Leonetti C[2], Scarsella M[2], d'Amati G[3], Xu W[4], Kalish V[4], Zhang J[4], Graziani G[1]

[1] Department of Neuroscience, University of Rome 'Tor Vergata', Italy
[2] Experimental Preclinical Laboratory, Regina Elena Institute for Cancer Research, Italy
[3] Department of Experimental Medicine and Pathology, University of Rome 'La Sapienza'; Rome, Italy
[4] Guilford Pharmaceuticals Inc., Baltimore, MD, USA

key words: PARP-1 inhibitor • anticancer therapy • temozolomide • melanoma

We previously demonstrated that the antitumor activity of temozolomide (TMZ) can be enhanced at the CNS site by intracerebral injection of a PARP-1 inhibitor that does not permeate the blood-brain barrier [1]. TMZ is an anticancer agent with promising activity against metastatic melanoma [2,3]. Here we tested whether systemic administration of GPI 15427, a novel PARP inhibitor capable of crossing the blood-brain barrier, could enhance the anti-tumor efficacy of TMZ against melanoma involving the CNS site. The efficacy of drug treatment was also tested against lung metastases.

Murine B16 melanoma cells were injected intracranially in syngeneic mice. Animals were treated for three days with TMZ (100 mg/kg, i.p.) ± GPI 15427 (1 mg/mouse, i.v.) when neoplastic infiltration of the brain tissue was evident in histological sections. Administration of GPI 15427 shortly before TMZ significantly increased life-span of tumor-bearing mice with respect to untreated controls, or to groups treated with either GPI 15427 or TMZ only ($P<0.0001$). The increase in survival detected in the group treated with the drug combination was accompanied by a marked reduction of tumor infiltration in the brain, as evidenced by histological studies.

GPI 15427 also enhanced the anti-metastatic activity of TMZ. In fact, the number of pulmonary metastases obtained after iv injection of B16 cells was significantly lower in mice treated with GPI 15427+TMZ than in those receiving TMZ only ($P=0.004$).

In conclusion, these data indicate that systemic administration of GPI 15427 induces significant enhancement of TMZ anti-tumor activity against melanoma, even at the CNS site.

References:

1. *Tentori L, Leonetti C, Scarsella M et al: Combined treatment with temozolomide and poly(ADP-ribose) polymerase inhibitor enhances survival of mice bearing hematologic malignancy at the central nervous system site. Blood, 2002; 99: 2241-44*
2. *Antonadou D, Paraskevaidis M, Sarris G et al: Throuvalas Phase II randomized trial of temozolomide and concurrent radiotherapy in patients with brain metastases. J Clin Oncol, 2002; 20: 3644-50*
3. *Biasco G, Pantaleo MA, Casadei S: Treatment of brain metastases of malignant melanoma with temozolomide. N Engl J Med, 2001; 345: 621-2*

70 PARP and myocardial ischaemia-reperfusion injury

Thiemermann C

William Harvey Research Institute, London, UK,
email: c.thiemermann@qmul.ac.uk

key words: heart • infarction • 5-AIQ • reperfusion injury • cardiac ischemia • ischaemia

There is now good evidence that inhibitors of PARP activity reduce the tissue injury caused by regional myocardial ischemia and reperfusion. For instance, various, chemically distinct inhibitors of PARP activity [including 3-aminobenzamide (3-AB) and 1, 5-dihydroxyisoquinoline (ISO)] reduce the infarct size caused by ischaemia-reperfusion injury of the rabbit heart *in vivo*. In addition, 3-AB and ISO also reduce the infarct size caused by regional myocardial ischaemia and reperfusion in the heart of the rat *in vivo* and *in vitro*. Moreover, ISO reduces the contractile dysfunction, the fall in high-energy phosphates caused by global myocardial ischemia and reperfusion in the rat heart. Exposure of human cardiac myoblasts *in vitro* results in an increase in PARP activity, and secondary cell death. Inhibition of this increase in PARP activity reduces the impairment in mitochondrial respiration as well as the associated cell death caused by these reactive oxygen species. The tissue injury caused by coronary artery occlusion and reperfusion in PARP-1 knock out mice is substantially reduced (when compared to their wild-type litter mates). Potent, water-soluble inhibitors of PARP activity (including 5-aminoisoquinolinone, PJ-34 and others) cause a substantial reduction in myocardial infarct size in the rat *in vivo*. Taken together, these findings support the view that (1) the excessive activation of PARP contributes to myocardial reperfusion injury, and (2) potent, water-soluble inhibitors of PARP activity may be useful in conditions associated with acute myocardial ischemia and reperfusion. These conditions may include acute myocardial infarction, coronary angioplasty, cardiac transplantation and bypass heart surgery.

References:

1. *Thiemermann C et al: Proc Natl Acad Sci USA, 1997; 94: 679-683*

71 5-Aminoisoquinolin-1-one and other water-soluble PARP inhibitors

Threadgill MD, Berry JM, Ferrer S, Parveen I, Shinkwin AE, Woon ECY

Department of Pharmacy & Pharmacology, University of Bath, UK,
email: prsmdt@bath.ac.uk

key words: 5-Aminoisoquinolin-1-one • thieno [3,4-c]pyridin-4(5H)-one • prodrug • solubility • reperfusion

Inhibitors of the activity of PARP have applications in the treatment of many disease states. Most of the known inhibitors of PARP mimic the nicotinamide of the substrate NAD^+. The consensus pharmacophore for PARP inhibitors is a primary or secondary benzamide with N–H conformationally constrained *anti* to the carbonyl-arene bond. However, this can also be considered as a 'pharmacophore' for insolubility in water. In this presentation, the results of our work on extending this pharmacophore into heterocyclyl carboxamides, into more water-soluble inhibitors and into potential prodrugs will be outlined. For example, 5-substituted isoquinolin-1-ones and 2, 8-substituted quinazolin-4-ones are known [1,2] to be potent inhibitors of PARP; we have shown [3] that the analogous thieno [3,4-*c*]pyridin-4(5H)-ones and thieno [3,4-*d*]pyrimidin-4(3H)-ones are also strongly active. New synthetic routes to 5-aminoisoquinolin-1-one (5-AIQ) have been developed [4], making this inhibitor more readily available. 5-AIQ shows IC_{50} = 250 nM aga-

inst PARP activity in a broken nuclear preparation; its corresponding IC_{50} against a mono-ADP-ribosyl transferase (diphtheria toxin) is 80 μM, making 5-AIQ highly selective for PARP. This compound is highly water-soluble as its hydrochloride, making it suitable for rapid i.v. administration. 5-AIQ protects against organ damage in a rat model of haemorrhagic shock at the remarkably low dose of 30 $\mu g \cdot Kg^{-1}$. It is similarly active *in vivo* in models of myocardial infarction and acute lung inflammation. Potential bioreductively activated prodrugs of this and other isoquinolin-1-ones have been synthesised [5,6] and are shown to release drug rapidly in experimental systems; these include 2-(2-nitroimidazol-5-ylmethyl)isoquinolin-1-ones and 1, 2-dimethyl-3-(isoquinolin-1-yloxymethyl)-5-methoxyindole-4, 7-diones. Further developments from these leads are under active research.

References:

1. *Suto MJ, Turner WR et al: Anti-Cancer Drug Design, 1991; 7: 107*
2. *Griffin RJ, Pemberton LC et al: Anti-Cancer Drug Design, 1995; 10: 507*
3. *Shinkwin AE, Whish WJD, Threadgill MD: Bioorg Med Chem, 1999; 7: 297*
4. *McDonald MC, Mota-Filipe H, Wright JA et al: Br J Pharmacol, 2000; 130: 843*
5. *Parveen I, Naughton DP et al: Bioorg Med Chem Lett, 1999; 9: 2031*
6. *Ferrer S, Naughton DP, Parveen I et al: J Chem Soc Perkin Trans, 2002; 1: 335*

72 Niacin deficiency enhances spontaneous and nitrosourea-induced micronuclei in rat bone marrow

Toxopeus LA, Kirkland JB

Department of Human Biology and Nutritional Sciences, University of Guelph, ON, N1G2W1 Canada, email: ltoxopeu@uoguelph.ca

key words: niacin deficiency • NAD^+ • ethylnitrosourea (ENU) • micronuclei (MN)

Niacin deficiency in rats decreases bone marrow NAD^+, impairing PARP function. Using the micronucleus (MN) assay, this study examined altered dietary niacin status on genomic stability in rats. Weanling male Long-Evans rats were fed niacin deficient (ND), or pair-fed niacin replete (PF) diet for 3 weeks. Bone marrow MN frequency in polychromatic erythrocytes (MN-PCEs) was increased significantly (4.4-fold) by deficiency alone. As the decrease in marrow NAD^+ levels was dramatic (80%), the model was extended to include adolescent rats, using 2 diets which cause moderate and mild deficiencies. ND rats with a moderate decrease in marrow NAD^+ (55%), showed a significant increase in MN-PCE (1.9-fold). However, ND rats with a mild decrease in NAD^+ (25%) did not have a significantly enhanced MN-PCE frequency (1.2-fold). These experiments have identified the range of marrow NAD^+ levels that lead to this type of genomic instability. To further characterize the interaction between niacin status and MN formation, ethylnitrosourea (ENU) treatment (30 mg/kg) was used to induce DNA damage. ND, in the weanling model, caused a dramatic increase (3.6-fold) in ENU-induced MN-PCEs (likely clastogenic in nature). This study emphasizes the importance of niacin in the maintenance of genomic stability in rats. We are working on identification of aneugenic versus clastogenic MN to help define the mechanisms by which ND increases genomic instability. Other data from our laboratory using comet analysis suggests that clastogenicity will not account for the large increase in genomic instability due to ND alone.

Supported by the National Cancer Institute of Canada.

73 Regulation of microglial functions by PARP-1 – a target for therapeutic interventions?

Ullrich O

Department of Cell- and Neurobiology, Institute of Anatomy, Medical Faculty (Charité), Humboldt-University Berlin, Schumannstr. 20/21, 10098 Berlin, Germany, email: oliver.ullrich@charite.de

key words: neuroinflammation • microglia • cytokines • integrins

During the last decade of neurobiological research, it has become evident that inflammatory pathways in the CNS, involving a network of non-neuronal and neuronal cells, are important contributors to the onset and progress of several major neurodegenerative diseases [1]. One major component of inflammatory neuronal damage is the transformation of microglia cells into activated immunoeffector cells and their migration towards the sites of injury, where they produce large amounts of toxic cytokines and oxygen radicals [2]. During this transformation, PARP-1 is highly activated and enables microglia cells to cope with oxidative challenges, in particular by upregulating the proteasomal degradation of damaged nuclear proteins [3]. Besides the initiation of intracellular defense pathways, PARP-1-dependent signalling is also involved in regulating specific functions of activated microglia: It regulates the expression of the integrin CD11a through interaction with the translocated NF-κB and therefore strongly controls migration into the regions of neuronal injury [4]. Furthermore, it enhances the production of the proinflammatory cytokine TNF-alpha and of the antiinflammatory endocannabinoid 2-AG, which in turn downregulates the release of nitric oxide. We are therefore considering PARP-1 to be a multiple player in the concert of neuroinflammation, in which therapeutic interventions directed against PARP-1 would affect both neuronal and non-neuronal components. Downregulation of PARP-1 specifically in microglia almost completely abrogates microglial migration and prevents neurons from secondary damage. This renders PARP-1 a target for therapeutic strategies in neurodegenerative diseases, in which pathological microglia activation and migration play a major role.

Supported by the DFG, SFB 507/C6 and the Friedrich-Althoff-Program

References:

1. *Floyd RA et al: Free Radic Biol Med, 1999; 26: 1346-1355*
2. *Mabuchi T et al: Stroke, 2000; 31(7): 1735-1743*
3. *McGeer PL et al: Brain Res Rev, 1995; 21: 195-218*
4. *Ullrich O et al: FASEB J, 2001; 15: 1460-1462*
5. *Ullrich O et al: Nature Cell Biol, 2001; 3: 1035-1042*

74 Competition and co-operation of PARP-1 and DNA-PK in the repair of DNA strand breaks

Veuger SJ, Curtin NJ, Calvert AH, Newell DR, Griffin RJ, Smith GCM, Hostomsky Z, Durkacz BW

Northern Institute for Cancer Research, Medical School, University of Newcastle Upon Tyne, NE2 4HH, UK, email: S.J.Veuger@ncl.ac.uk

key words: PARP-1 • DNA-PK • DNA repair

Cells deficient in poly(ADP-ribose) polymerase (PARP-1) or DNA-dependent protein kinase (DNA-PK) are highly radiosensitive. Potent, specific inhibitors of PARP-1 (AG14361) and DNA-PK (NU7026) developed in collaboration with KuDOS Pharmaceuticals (UK) and Agouron/Pfizer GRD (CA), respectively, are radiosensitizers when used alone and in combination [1]. To fully exploit the potential of PARP-1 and DNA-PK inhi-

Pergamon

Tetrahedron Letters 43 (2002) 2299–2302

TETRAHEDRON LETTERS

A new synthesis of 'push–pull' naphthalenes by condensation of nitro-2-methylbenzoate esters with dimethylacetamide dimethyl acetal

See-Mun Wong, Bhavini Shah, Priyal Shah, Ian C. Butt, Esther C. Y. Woon, James A. Wright, Andrew S. Thompson, Christopher Upton and Michael D. Threadgill*

Department of Pharmacy & Pharmacology, University of Bath, Bath BA2 7AY, UK

Received 2 January 2002; revised 21 January 2002; accepted 30 January 2002

Abstract—Whereas condensation of 2-methyl-3-nitrobenzoate esters with dimethylformamide dimethyl acetal gives 5-nitroisocoumarin, analogous condensation with dimethylacetamide dimethyl acetal proceeds via a different route, affording 1-methoxy-3-dimethylamino-5-nitronaphthalene in good yield. Extension of the reaction to other naphthalenes with this novel 'push–pull' substitution motif has been explored. A deuterium labelling study revealed that equilibration of the alkoxy groups in the reaction mixture took place before the final carbocyclisation.

Most syntheses of polysubstituted naphthalenes involve modification and substitution of a preformed bicyclic naphthalene core, with a few employing construction of the rings with the substituents already attached to the acyclic or monocyclic precursors. Examples of the latter ring-closure routes include Diels–Alder cyclisations of dienes with benzoquinones,[1,2] acid-catalysed cyclisations of phenylethylidenemalononitriles to 2-cyanonaphthyl-1-amines[3] and base-catalysed cyclisation of 2-allyl-*N*,*N*-dialkylbenzamides to naphth-1-ols.[4] However, these routes are not generally amenable to synthesis of substituted alkoxy- and amino-naphthalenes. We report here a new synthesis of novel polysubstituted naphthalenes, which bear the 'push–pull' motif of electron-withdrawing substituents on one ring and electron-donating substituents on the other.

We[5,6] and others[7] have previously reported that condensation of methyl 2-methyl-3-nitrobenzoate **1a** with dimethylformamide dimethyl acetal (dimethoxymethyl dimethylamine, DMFDMA) gives the enamine **2** (Scheme 1). Treatment of this crude enamine with silica gel provides sufficient acid catalysis to hydrolyse the enamine and cyclise the intermediate enol to the isocoumarin **3**. In an initial attempt to explore the scope and mechanism of this reaction, the isopropyl ester **1b**[8] was treated similarly with DMFDMA; the condensation followed a similar path but the cyclisation with silica gel was much slower and gave lower yields of **3** (Scheme 1). This observation is consistent with steric obstruction by the bulky isopropyl group during cyclisation.

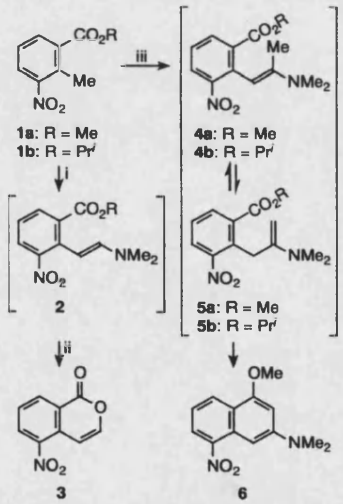

Scheme 1. Reactions of 2-methyl-3-nitrobenzoate esters with orthoamides. *Reagents and conditions*: (i) $HC(OMe)_2NMe_2$, DMF, 150°C, 16 h, 53%; (ii) SiO_2, EtOAc; (iii) $MeC(OMe)_2NMe_2$, $MeCONMe_2$, 150°C, 16 h, 77%.

* Corresponding author. Tel.: +44-1225-826840; fax: +44-1225-826114; e-mail: m.d.threadgill@bath.ac.uk

0040-4039/02/$ - see front matter
PII: S0040-4039(02)00228-9

In contrast, when the ester **1a** was treated with dimethylacetamide dimethyl acetal (1,1-dimethoxyethyl dimethylamine, DMADMA),[9] none of the expected 3-methyl-5-nitroisocoumarin was formed. The sole isolable product was a deep red solid, formed in high yield. The strong colour suggested that it was not an isocoumarin (most 5-nitroisocoumarins are pale yellow); this was borne out by the lack of a carbonyl absorption in the IR spectrum.[9] The ^{1}H NMR spectrum[9] showed five aromatic protons, together with signals for NMe_2 and OMe. One of the aromatic proton signals was shifted markedly upfield at δ 6.48, corresponding to a location between the electron-donating NMe_2 and OMe groups. These data, together with the mass spectrum, allowed the assignment of the naphthalene structure **6** to the condensation product. The locations of the NMe_2 and OMe substituents were confirmed by a NOESY spectrum, which showed NOE connectivity between OMe and the 2-H (δ 6.48, d, J=2.3 Hz) and between NMe_2 and the 2-H and 4-H (δ 7.37, d, J=2.3 Hz). The deep red colour is a consequence of the 'push–pull' substitution pattern of the naphthalene chromophore. Compounds with a nitro group at one end of a conjugated system and an amine at the other are often deeply coloured, ranging from simple 2-nitroethenamines[10] to laser dyes and dark red 1-nitro-7-aminonaphthalenes.[11–14] For this unprecedented synthesis of the naphthalene ring system, we propose the course of reaction shown in Scheme 1. Initial condensation with the DMADMA gives the enamine **4**, by analogy with the identified intermediate enamine **2** for the sequence employing DMFDMA. Whereas the C–H enamine **2** has no opportunity for further reaction under the conditions, the C–Me enamine **4** can tautomerise to the alternative enamine **5**, presumably via an iminium species. This second enamine **5** then provides a nucleophilic carbon correctly located to attack the ester carbonyl. It is noteworthy that water is the sole leaving group in the condensation of the enamine with the ester (giving **6**); no 3-dimethylamino-5-nitronaphth-1-ol was obtained (through loss of methanol).

A short study revealed aspects of the mechanism, generality and limitations of this new synthesis of substituted naphthalenes. Firstly, condensation of the isopropyl ester **1b**[8] with DMADMA gave the methoxynaphthalene **6** as the sole naphthalene product (Scheme 1); no isopropoxynaphthalene was evident in the crude product mixture. This observation suggests either that the mechanism of the reaction is complex and involves intramolecular transfer of a methoxy group in an intermediate or that there is an equilibrium exchange of alkoxy groups ($Pr^iO \leftrightarrow MeO$) between the ester and the orthoamide before the final ring-closure. The complete absence of isopropoxynaphthalenes is consistent with the latter, since it is likely that ring-closure with the isopropyl ester **5b** will be much slower than that with the methyl ester **5a**, owing to the greater steric bulk of the Pr^iO; this steric retardation of ring-closure is analogous to that observed in the formation of the isocoumarin **3** from **1b**. Secondly, to select between these two alternative mechanisms (intramolecular MeO transfer and ester exchange), an isotopic competition experiment was performed (Scheme 2). 2-Methyl-3-nitrobenzoic acid **7** was converted to its trideuteromethyl (CD_3) ester **8**[15] in 88% yield. This isotopomer was then treated with DMADMA in which the methoxy groups were all OCH_3, under the standard reaction conditions. Mass spectroscopic and NMR analysis of the product **9** showed that the ratio of OCD_3 to OCH_3 corresponded to the ratio of OCD_3 (in **8**) to OCH_3 (in DMADMA) in the reaction mixture. Thus, as there is virtually no difference between the steric requirements of CD_3 and CH_3, the mechanism must involve full equilibration of the alkoxy groups between the ester and the orthoamide before final ring-closure. Hence, introduction of alternative alkoxy groups at position-1 of the naphthalene in this new condensation will require other appropriate orthoamides.

Scheme 3 shows three further studies on the generality of the reaction. Treatment of methyl 2-methyl-5-nitrobenzoate **10**[16] with DMADMA under the standard reaction conditions gave the corresponding 1-methoxy-3-dimethylamino-7-nitronaphthalene **11**.[17] In contrast, similar treatment of the 3,5-dinitro analogue **12**,[18] in which the arylmethyl group is further activated, gave only degradation products. To explore an alternative approach to activating the arylmethyl further and, simultaneously, to introduce a 4-substituent into the naphthalene, methyl 2-benzyl-3-nitrobenzoate **16** was synthesised. 3-Nitrophthalic acid **14** was decarboxylated/mercurated with $Hg(OAc)_2$ and the intermediate aryl-Hg compound was treated with iodine to give 2-iodo-3-nitrobenzoic acid, by the method of Seno et al.;[19] this was converted to its methyl ester **15**. Negishi coupling with benzyl zinc bromide/DIBAL-H/$Pd(PPh_3)_2Cl_2$ then afforded the novel 2-benzylbenzoate ester **16** in moderate yield.[20] However, this failed to afford the target 4-phenylnaphthalene **17** on treatment with DMADMA.

In this letter, we report a novel method for the synthesis of substituted naphthalenes by treatment of nitro-2-methylbenzoate esters with dimethylacetamide dimethyl acetal (DMADMA), together with early studies on its

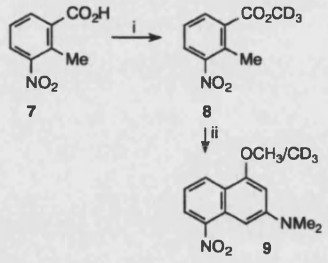

Scheme 2. Studies on the source of the naphthalene 1-substituent. *Reagents and conditions*: (i) CD_3OD, H_2SO_4, reflux, 72 h; (iii) $MeC(OCH_3)_2NMe_2$ (3 equiv.), $MeCONMe_2$, 150°C, 16 h.

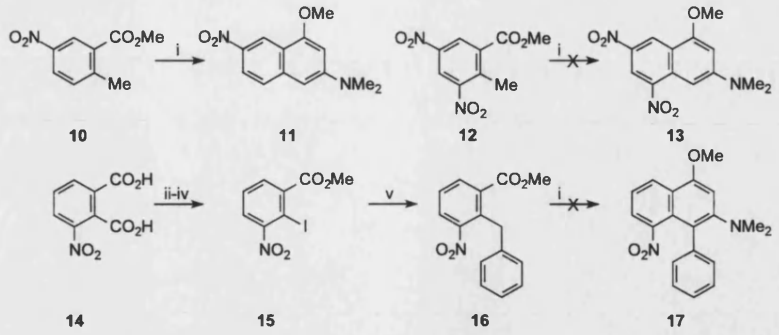

Scheme 3. Synthesis of 1-methoxy-3-dimethylamino-7-nitronaphthalene **11** and preliminary exploration of the limitations of the naphthalene-forming condensation reaction. *Reagents and conditions*: (i) $MeC(OMe)_2NMe_2$, $MeCONMe_2$, 150°C, 16 h, 5.3%; (ii) $Hg(OAc)_2$, aq. NaOH (10%), reflux, 3 days; (iii) I_2, aq. NaOH (3.4%), reflux, 16 h; (iv) MeOH, H_2SO_4, 62% from **14**; (v) $PhCH_2ZnBr$, $Bu^t{}_2AlH$, $Pd(PPh_3)_2Cl_2$, THF, 45°C, 72 h, 32%.

mechanism and generality. This condensation has considerable potential for construction of 'push-pull'-substituted polycyclic arenes. The results of a more comprehensive study on this reaction will be published later.

Acknowledgements

We thank Mr. R. R. Hartell and Mr. D. J. Wood for the NMR spectra and Mr. C. Cryer for the mass spectra. J.A.W. held a Research Studentship from the Department of Pharmacy & Pharmacology, University of Bath. Part of this work was carried out by S.-M.W., B.S., P.S. and I.C.B. as an Undergraduate Research Project for the MPharm degree.

References

1. Bailey, A. S.; Shuttleworth, A. J. *J. Chem. Soc. C* **1968**, 1115.
2. House, H. O.; Koepsell, D. G.; Campbell, W. J. *J. Org. Chem.* **1972**, *37*, 1003.
3. Sepiol, J. J.; Wilamowski, J. *Tetrahedron Lett.* **2001**, *42*, 5287.
4. Sibi, M. P.; Dankwart, J. W.; Snieckus, V. *J. Org. Chem.* **1986**, *51*, 271.
5. McDonald, M. C.; Mota-Filipe, H.; Wright, J. A.; Abdelrahman, M.; Threadgill, M. D.; Thompson, A. S.; Thiemermann, C. *Br. J. Pharmacol.* **2000**, *130*, 843.
6. Parveen, I.; Naughton, D. P.; Whish, W. J. D.; Threadgill, M. D. *Bioorg. Med. Chem. Lett.* **1999**, *9*, 2031.
7. Somei, M.; Karasawa, Y.; Shoda, T.; Kaneko, C. *Chem. Pharm. Bull.* **1981**, *29*, 249.
8. Rohr, O. US Patent 4048217, **1997**.
9. **Synthesis of 6**. Ester **1a** (1.01 g, 5.2 mmol) was heated at 150°C with $MeC(OMe)_2NMe_2$ (2.5 g, 18.8 mmol) in $MeCONMe_2$ (6 mL) for 16 h. Evaporation and chromatography (hexane/EtOAc, 10:1) gave **6** (990 mg, 77%) as dark red needles; mp 123–124°C; IR ν_{max} 1522, 1343 cm^{-1}; NMR ($CDCl_3$) δ_H 3.13 (6H, s, NMe_2), 4.00 (3H, s, OMe), 6.48 (1H, d, J=2.3 Hz, 2-H), 7.11 (1H, dd, J=8.2, 7.8 Hz, 7-H), 7.37 (1H, d, J=2.3 Hz, 4-H), 8.24 (1H, dd, J=7.8, 1.2 Hz, 8-H), 8.37 (1H, dd, J=8.2, 1.2 Hz, 6-H); MS (EI) m/z 246 (M). Found: C, 63.4; H, 5.72; N, 11.4. $C_{13}H_{14}N_2O_3$ requires C, 63.41; H, 5.69; N, 11.38%.
10. Gate, E. N.; Meek, M. A.; Schwalbe, C. H.; Stevens, M. F. G.; Threadgill, M. D. *J. Chem. Soc., Perkin Trans. 2* **1985**, 251.
11. Schurman, J. V.; Becker, E. I. *J. Org. Chem.* **1953**, *18*, 211.
12. Friedländer, P.; Szymanski, S. *Chem. Ber.* **1892**, *25*, 2076.
13. Machida, M.; Bando, M.; Migata, Y.; Machida, M. I.; Kanaoka, Y. *Chem. Pharm. Bull.* **1976**, *24*, 3045.
14. Gould, R. G.; Jacobs, W. A. *J. Biol. Chem.* **1939**, *130*, 407.
15. **Data for 8**: Mp 62–65°C; IR (KBr) ν_{max} 2186, 1724, 1524, 1363 cm^{-1}; NMR ($(CD_3)_2SO$) δ_H 2.40 (3H, s, Me), 7.56 (1H, dd, J=8.2, 7.8 Hz, 5-H), 8.00 (1H, d, J=7.8 Hz, 6-H), 8.04 (1H, d, J=8.2 Hz, 4-H). Found: C, 54.4; H, 4.59; N, 7.05. $C_9H_6D_3NO_4$ requires C, 54.5; H, 4.54; N, 7.07%.
16. Phadnis, A. P.; Nanda, B.; Patwardhan, S. A.; Gupta, A. S. *Indian J. Chem. B* **1984**, *23*, 1098.
17. **Data for 11**: Dark red needles; mp 172–174°C; NMR ($CDCl_3$) δ_H 3.15 (6H, s, NMe_2), 4.03 (3H, s, OMe), 6.52 (1H, brs, 2-H), 6.56 (1H, brs, 4-H), 7.54 (1H, d, J=9.5 Hz, 5-H), 8.08 (1H, dd, J=9.5, 2.6 Hz, 6-H), 9.00 (1H, d, J=2.6 Hz, 8-H); δ_C 40.5, 55.5, 95.1, 98.3, 117.0, 120.4, 120.6, 126.0, 138.7, 141.0, 151.8, 158.0; MS (EI) m/z 246.0998 (M) ($C_{13}H_{14}N_2O_3$ requires 246.1004). Found: C, 63.2; H, 5.80; N, 11.2. $C_{13}H_{14}N_2O_3$ requires C, 63.41; H, 5.69; N, 11.38%.
18. Racine, S. *Liebigs Ann. Chem.* **1887**, *239*, 71.
19. Seno, K.; Hagishita, S.; Sato, T.; Kuriyama, K. *J. Chem. Soc., Perkin Trans. 1* **1984**, 2012.
20. **Synthesis of 16**. Compound **15** (2.5 g, 8.1 mmol) and benzyl zinc bromide (0.5 M in THF, 24.5 mL, 12.2 mmol) in dry THF (30 mL) were added to $Pd(PPh_3)_2Cl_2$ (330

mg, 500 μmol) and Bu^i_2AlH (1.0 M in hexane, 1.0 mL, 1.0 mmol) in dry THF (15 mL) under Ar and the mixture was stirred for 72 h at 45°C. Extraction ($CHCl_3$), evaporation and chromatography (hexane/EtOAc, 9:1) gave **16** (700 mg, 32%) as a yellow oil: IR (film) ν_{max} 1731, 1532, 1362 cm^{-1}; NMR ($CDCl_3$) δ_H 3.77 (3H, s, Me), 4.52 (2H, s, CH_2), 7.02 (2H, d, $J=7.4$ Hz, Ph 2,6-H_2), 7.14 (1H, t, $J=7.4$ Hz, Ph 4-H), 7.21 (2H, t, $J=7.4$ Hz, Ph 3,5-H_2), 7.42 (1H, t, $J=7.8$ Hz, 5-H), 7.81 (1H, dd, $J=7.8$, 1.6 Hz, 6-H), 7.95 (1H, dd, $J=7.8$, 1.6 Hz, 4-H); MS (FAB) m/z 272.0921 (M+H) ($C_{15}H_{14}NO_4$ requires 272.0923).